Synthesis and Structure-Property Relationships of Polysaccharide-Based Block Copolymers and Hydrogels

Junyi Chen

Dissertation submitted to the faculty of the Virginia Polytechnic Institute and State University in partial fulfillment of the requirements for the degree of

Doctor of Philosophy

In

Chemistry

Kevin Edgar, Chair

John Matson

Guoliang Liu

Judy Riffle

December 17, 2019

Blacksburg, VA

Keywords: cellulose ether, dextran, block copolymer, *in situ* forming hydrogel, self-healing, injection, thermal-induced property.

Synthesis and Structure-Property Relationships of Polysaccharide-Based Block Copolymers and Hydrogels

Junyi Chen

Abstract

Polysaccharides are known as among the most abundant natural polymers on the Earth. As this class of material is usually renewable, biodegradable, biocompatible in many contexts and environmentally friendly, it is of great interest to use these benign polymers to design and prepare materials, especially for applications with green and biomedical purposes. In this dissertation we will discuss novel pathways to two different types of polysaccharide-based materials: block copolymers and hydrogels.

Block copolymers are composed of two or even more covalent bonded polymer blocks that have quite distinct properties. Synthesis of polysaccharide-based block copolymers is an attractive and challenging research topic, opening up promising application potential and requiring advances in polysaccharide regio- and chemoselectivity. Herein, we report two independent approaches to prepare these interesting and potential useful materials. In one approach, trimethyl cellulose was modified regiospecifically at the reducing end anomeric carbon to create an ω-unsaturated alkyl acetal by solvolysis with an ω-unsaturated alcohol. Then, olefin cross-metathesis, a known versatile and mild tool for polysaccharide chemical modification, was used to couple the trimethyl cellulose block with various polymer blocks containing acrylates. To demonstrate the method, trimethyl cellulose-*b*-poly(tetrahydrofuran), cellulose-*b*-poly(ethylene glycol), and cellulose-*b*-poly(lactic acid) were synthesized by this coupling strategy. In another approach, we introduced a simple and novel method to prepare dextran-based block copolymers. In this strategy, *N*-bromosuccinimide (NBS)/triphenyl phosphine (PPh_3) was chosen to regioselectively brominate

the only primary alcohol of linear unbranched dextran. The resulting dextran, bearing a terminal C-6 bromide, was coupled with several amine terminated polymers via S_N2 substitution to obtain block copolymers, including dextran-*b*-polystyrene, dextran-*b*-poly(N-isopropylacrylamide) and dextran-*b*-poly(ethylene glycol). Dextran-*b*-poly(*N*-isopropylacrylamide) exhibits thermally-induced micellization as revealed by dynamic light scattering, forming micelles with 155 nm diameter at 40 °C. Dextran-*b*-polystyrene film was analyzed by small angle X-ray scattering, suggesting the existence of microphase separation.

This dissertation also introduces a novel, simple and effective strategy to prepare polysaccharide-based hydrogels. Hydrogels are typically crosslinked hydrophilic polymers that have high water affinity and no longer dissolve in water. Polysaccharide-based hydrogels are of great interest to for biomedical applications due to their benefits including biocompatibility, polyfunctionality, and biodegradability. Recently the Edgar group has discovered that chemoselective oxidation of oligo(hydroxypropyl)-substituted polysaccharides impairs ketone groups at the termini of the oligo(hydroxypropyl) side chains. These ketones can condense with amines to form imines, leading hydrogel formation., Based on this concept, we prepared oxidized hydroxypropyl polysaccharide/chitosan hydrogels. This class of all-polysaccharide hydrogels exhibits a series of interesting properties such as tunable moduli (300 Pa to 13 kPa), self-healing, injectability, and high swelling ratios. To further explore imine-crosslinked hydrogels, we designed thermally responsive hydrogels by using a Jeffamine, a polyethylene oxide-*b*-polypropylene oxide-*b*-polyethylene oxide triblock copolymer with two terminal amines. As the Jeffamine has a lower critical solution temperature, oxidized hydroxypropyl cellulose/Jeffamine hydrogels display moduli that are tunable by controlling the temperature.

Synthesis and Structure-Property Relationships of Polysaccharide-Based Block Copolymers and Hydrogels

Junyi Chen

General Audience Abstract

Polysaccharide are natural polymers that are among the most abundant polymers on Earth. It is greatly in society's interest to extend the scope of their applications, due to the benign nature of polysaccharides. This dissertation mainly focuses on two polysaccharides: cellulose and dextran. Cellulose is a long linear polymer of linked glucose molecules. As cellulose is sustainable, biodegradable, non-toxic, affordable and accessable for chemical modification, it is a suitable polymer for biomedical and environmentally friendly application. Dextran is also a polymer chain made up only of glucose but connected with each other differently from cellulose by, bacterial fermentation, and it may be lightly branched. It is biocompatible in many situations and is biodegradable both *in vivo* and in the environment, thus it has been investigated for drug delivery and many other medical applications. Using these two polysaccharides, we designed and prepared two quite different classes of materials: block copolymers and hydrogels.

Block copolymers consist of two or more different types of polymer blocks connected by strong covalent bonds. As block copolymerization enables construction of a single polymer comprising segments with distinct properties, it is appealing to synthesize a block copolymer which preserves the properties of natural polymers coupled to very different polymers, such as polyolefins (e.g. the polyethylene that is used for milk bottles). In order to prepare polysaccharide-based block copolymers, we developed two different synthetic routes to end-functionalize methyl cellulose and dextran , and these resulting products were used to prepare two independent series of polysaccharide-based block copolymers via combination (in other words, sticking the

polysaccharide and, e.g., the polyethylene together end to end). This study confirms the feasibility of this method to make methyl cellulose-based and dextran-based block copolymers. We expect these classes of materials will have significant potential in applications including drug delivery, as compatibilizers for polymer blends of materials that otherwise cannot be mixed (polyolefin/polysaccharide), membrane and adhesive.

Hydrogels are crosslinked polymer networks with high water affinity, and they have been heavily investigated in the field of tissue engineering, drug delivery, agriculture and 3D printing. Polysaccharide-based hydrogels are attractive materials for these applications because they are biocompatible, biodegradable and have polyfunctionality. However, any use of toxic small molecules to crosslink the hydrogels diminishes their usefulness in biomedical applications. In this work, we demonstrate a simple, green and efficient method for preparation of all-polysaccharide-based hydrogels. The starting materials, oxidized hydroxypropylpolysaccharide, were simply prepared by using household bleach (NaOCl) as the oxidation reagent. We discovered that oxidized hydroxypropyl polysaccharides readily form hydrogels with hydrophilic amine-containing polymers like chitosan (a natural polysaccharide that comes from shells of crustaceans like crabs or shrimp) and Jeffamines, affording interesting properties including tunable stiffness, self-healing, injectability, and responsiveness to acidity and temperature. We expect that this new class of hydrogel will be very promising for biomedical-related applications.

Dedication

To my dear mother.

Acknowledgements

I am deeply grateful to my advisor Dr. Kevin Edgar for his patience, invaluable insight and guidance throughout my graduate school years. He provides a comfortable research environment and gave me the freedom to study things that I wanted to explore. I know these things are rare for graduate school and I deeply appreciate them. I will not have gotten where I am without Dr. Edgar.

I want to thank my committee members, Dr. John Matson, Dr. Guoliang Liu and Dr. Judy Riffle for guiding my research work. I would like to give a special thanks to Dr. Matson for many insightful suggestions and assistance to my research. I would also like to thank Dr. Charles Frazier and Dr. Ann Norris for helping me with the hydrogel project. I also would like to thank Dr. Maren Roman for improving my presentation skills.

I would like to thank Dr. Ruoran Zhang, Dr. Xueyan Zheng, Dr. Xiangtao Meng, Dr. Cigdem Arca, Dr. Yifan Dong, Dr. Shu Liu, Chengzhe Gao, Brittany Nichols, Diana Novo, Yang Zhou and Stella Petrova for their support and creating a comfortable lab atmosphere. It's has been my great pleasure to work and study with them in the Edgar lab for these years. I also would like to thank my colleagues in Chemistry Department and SBIO who helped me in many ways.

At last I want to thank my family, especially my parents, fiancé and aunt. Because of your love and unequivocal support, I have been able to fully concentrate on my research work during graduate school years.

Attribution

Several colleagues have assisted in data collection for the chapters in this dissertation.

Dr. Kevin Edgar was the principal investigator and primary contributor to all the projects included in this dissertation.

Chapter 2 Literature review

Dr. John Matson, Dr. Guoliang Liu and Dr. Judy Riffle helped to edit and review the manuscript.

Chapter 3 Synthesis of polysaccharide-based block copolymers via olefin cross-metathesis.

Dr. Hiroshi Kamitakahara at Kyoto University proposed the methyl cellulose end-functionalization via solvolysis and served as co-author.

Mr. Ryan Carrazzone at Virginia Tech helped with the SEC analysis.

Chapter 4 Regioselective bromination of the dextran non-reducing end creates a pathway to dextran-based block copolymers.

Dr. Robert Moore at Virginia Tech helped to review the manuscript and served as co-author.

Mr. Glenn Spiering at Virginia Tech contributed the SAXS analysis of dextran-based block copolymers and served as co-author.

Dr. Charles Carfagna at Virginia Tech helped with the aqueous SEC analysis.

Chapter 5 All-polysaccharide, self-healing injectable hydrogels based on chitosan and oxidized hydroxypropyl polysaccharides.

Dr. Charles Frazier at Virginia Tech helped to design the rheological experiment and review the manuscript. He also served as a co-author for this paper.

Dr. Ann Norris at Virginia Tech assisted the rheological experiment and served as co-author.

Dong Guo at Virginia Tech helped with the SEC analysis.

Chapter 6 Thermo responsive *in situ* forming hydrogel, oxidized hydroxyl propyl cellulose/ Jeffamine.

Mr. Abdulaziz Alali as a REU student helped with the hydrogel drug releasing experiment.

Table of Contents

Chapter 1: Research Introduction

Cellulose, a homopolymer of glucose with the structure 4→)β-D-Glc*p*(→1, is one of the most abundant natural polysaccharides. Industries and researchers prepare cellulose derivatives to improve processability and modulate properties to application requirements. These cellulose derivatives are sustainable, biodegradable, and their modified properties usually allow high performance and the potential to replace traditional polymers like polyolefins.

Block copolymers, consisting of building blocks with distinct properties, even those that are thermodynamically incompatible, are of great interest for various applications including capacitors, separation membranes, and compatibilizers. It is extremely attractive to design and prepare polysaccharide-based block copolymers since this class of material has potential to combine benign polysaccharides with, e.g., traditional polyolefins. However, only a limited number of studies report the preparation of polysaccharide-based block copolymers, as it is challenging to end-functionalize polysaccharides. Past studies of polysaccharide block copolymers discovered a distinguishable reactive site: the anomeric carbon at the reducing end, that is in the aldehyde oxidation state. Due to the distinct reactivity of the reducing end anomeric position, which is a hemiacetal in equilibrium with an aldehyde, several approaches were developed to modify the reducing end of polysaccharide. In one approach, 1-glycosyl bromides were synthesized by reaction with HBr. Reductive amination is another frequently used method to convert the reducing end aldehyde into an amine. Chapter 2 will introduce several pathways to end functionalize polysaccharides and different strategies for preparing their block copolymers. Moreover, the properties of these block copolymers such like micellization and self-assembly are also discussed.

In Chapter 3, inspired by the work reported by Kamitakahara[1], we introduced a novel pathway to append olefin groups to the trimethyl cellulose reducing end via solvolysis with ω-unsaturated

alcohols. The resulting product, trimethyl cellulose functionalized with a Type 1 reactive olefin at the reducing end, serves as an efficient substrate in the cross-metathesis reaction with Hoveyda-Grubbs' 2nd generation catalyst, readily coupling with small molecules and polymers bearing a Grubbs Type II olefin. A series of block copolymers, including trimethyl cellulose-*b*-polyethylene oxide, trimethyl cellulose-*b*-polylactic acid and trimethyl cellulose-*b*-poly(tetrahydrofuran) were prepared by this cross-metathesis coupling approach. This method has the potential to be applied to a broad range of polysaccharide derivatives.

For linear dextran, the anomeric carbon at the reducing end of the polysaccharide chain is not the only distinctive reactive site. In Chapter 4, we designed a unique method to prepare dextran-based block copolymers. In this study, *N*-bromosuccinimide (NBS)/triphenyl phosphine (PPh_3) were used to regio-selectively brominate the sole primary alcohol of linear, unbranched dextran, at C-6 of the non-reducing end monosaccharide. The resulting dextran bearing a terminal bromide was coupled with several amine-terminated polymers via S_N2 substitution, and the resulting block copolymers including dextran-*b*-poly(N-isopropylacrylamide), dextran-*b*-poly(ethylene glycol), and dextran-*b*-polystyrene were fully characterized, confirming the formation of block copolymers. This class of polysaccharide block copolymers exhibits various interesting and potential useful properties. Dextran-*b*-poly(N-isopropylacrylamide) displays thermally-induced micellization as revealed by dynamic light scattering, forming micelles (155 nm diameter) upon heating above the lower critical solution temperature (33 °C). We also discovered the existence of microphase separation of dextran-*b*-polystyrene by using small angle X-ray scattering.

Polysaccharides such as cellulose, dextran, hyaluronic acid and their derivatives have been heavily investigated as hydrogel materials due to their benign natures including biocompatibility, biodegradability, and accessibility for further chemical modification. Thus, this class of hydrogel

is of great interest to biomedical applications, including tissue engineering, drug delivery and wound dressings. However, use of polysaccharide-based hydrogels may be limited by toxic small molecule crosslinkers. Herein, in Chapter 5, we report a simple, green and efficient strategy for preparation of polysaccharide *in situ* forming hydrogels. Oxidized oligo(hydroxypropyl)-substituted polysaccharides, which were prepared by chemoselective oxidation using sodium hypochlorite, were used as the hydrogel component. We discovered this oxidation can impart ketone groups at the termini of oligo(hydroxypropyl) chains, and the resulting ketones are readily to form imine linkages with amines from amine-containing polymers. Chitosan, a natural polysaccharide with free primary amine groups, was selected as the other hydrogel component due to its low toxicity, bioadhesion, biodegradability, and biocompatibility toward many tissues. By combining the oxidized hydroxypropyl polysaccharides with chitosan, we prepared two different hydrogels, oxidized hydroxypropyl cellulose-chitosan and oxidized hydroxypropyl dextran-chitosan. This class of hydrogel exhibits several interesting properties including high swelling ratio, injectability and tunable modulus (300 Pa to 13 kPa) by controlling the degree of substitution of the ketone group. Furthermore, due to the imine linkages, the crosslinks, are dynamic covalent bonds which can form and cleave reversibly. Therefore the hydrogels demonstrated self-healing properties which were revealed by both rheometry and macroscopic experiments.

As we discovered that oxidized hydroxypropyl polysaccharides are promising materials for *in situ* forming hydrogel preparation, it was of great interest to further explore and extend the scope of this class of hydrogel. In Chapter 6, we introduced a novel thermally responsive, *in situ* forming hydrogel: oxidized hydroxypropyl cellulose/Jeffamine hydrogel. Jeffamine is a biocompatible polyethylene oxide-*b*-polypropylene oxide-*b*-polyethylene oxide triblock copolymer with two amines at its termini, which exhibits lower critical solution temperature behavior and thus displays

temperature-responsive properties. By using Jeffamine as the hydrogel component, thermal responsiveness was successfully introduced to the imine crosslinked oxidized hydroxypropyl cellulose-based hydrogel. Revealed by rheological experiment, the storage modulus (G') of hydrogel can be tuned by controlling the temperature and molecular weight of Jeffamine, covering the range from 3 kPa to 21 kPa. This hydrogel also displays self-healing due to the reversible imine linkages. Moreover, the microstructure, swelling ratio, and drug release properties of the hydrogel were also investigated in this work.

Chapter 7 summarizes all the studies included in this dissertation and proposes several promising future studies. We expect these studies will afford novel pathways for designing and preparation of various polysaccharide-based block copolymers and hydrogels, greatly enhancing the application potential of these nature polymers.

1.1 References

(1) Nakagawa, A.; Fenn, D.; Koschella, A.; Heinze, T.; Kamitakahara, H. Synthesis of Diblock Methylcellulose Derivatives with Regioselective Functionalization Patterns. *J. Polym. Sci. Part A Polym. Chem.* **2011**, *49* (23), 4964–4976. https://doi.org/10.1002/pola.24952.

Chapter 2: Literature review

2.1 Synthesis and characterization of polysaccharide-based block copolymers

2.1.1 Introduction

Polysaccharides are polymeric carbohydrates which consist of monosaccharides connected by ketal or acetal linkages. Polysaccharides play critical roles in nature. For example, cellulose, a linear polysaccharide, gives strength and flexibility to the cell wall in plants. Starch and glucans are two polysaccharide classes that serve as food storage polymers in plants and animals. Glycosaminoglycans, polysaccharides that exist in mammalian tissues, have roles in many key natural processes including cell adhesion. The huge abundance of polysaccharides makes them desirable materials for applications. Thanks to advances in synthetic methodologies, we can design highly controlled and well-defined polysaccharide macromolecular structures. In the following two paragraphs, we briefly introduce cellulose and dextran, which are heavily discussed in this review.

Cellulose is a homopolymer (→4-β-D-Glcp-1→) with no substituents and no branches in nature. It is one of the most abundant natural polymers on earth. Along with its huge abundance, cellulose is relatively low cost and it has potential to replace petroleum-based polymer products. Application of unmodified cellulose is limited because of its strong polarity. Cellulose has essentially no solubility in water or organic solvents. As hydrogen bonds exist between cellulose chains, its theoretical glass transition temperature is above its decomposition temperature, making it impossible to melt process. Substitution reactions of the 2, 3, 6 hydroxyl groups on cellulose (for example, esterification[1], sulfation[2] and etherification[3]) can dramatically improve its solubility in organic solvents. Several processing methods like solution spinning and extrusion can be applied to the modified cellulose. All the references discussed in this review start from modified cellulose derivatives.

Dextran is an (α-1$\rightarrow$6) glucan which may have branches at the 2, 3, or 4 positions. It has useful biomedical properties including water solubility, biodegradability, and biocompatibility in some medical applications including infusion[4]. Dextran has relatively high solubility in various polar aprotic solvents, which broadens the range of reaction choices.

Design, synthesis and characterization of copolymers have been important topics in the polymer field for a long time. Different types of polymer chains or segments are connected covalently, and specific properties can thus be obtained. One of the most common phenomena for copolymers, especially for block copolymers, is phase separation. Phase separation could lead to several different copolymer morphology patterns (cubic, hexagonal cylindrical, bicontinuous gyroid, and lamellar). Each morphology pattern has its advantage in particular applications. Due to the huge interest in polysaccharide materials, it is an interesting topic to build polysaccharide copolymers with practical morphologies.

Graft copolymerization is a convenient and well-developed method of polysaccharide derivative property modification. In contrast, relatively few attempts at synthesis of polysaccharide-based block copolymers have been reported. It is difficult to selectively functionalize the polysaccharide chain ends. Compared to graft copolymers, block copolymers preserve the linear backbone structure of the original polysaccharide derivative. Furthermore, block copolymers usually have more well-defined nanostructures than those of graft copolymers. Polysaccharide block copolymers have tremendous application potential, inspiring efforts to overcome the synthetic challenges.

Two synthesis approaches characterize the literature to date. One is end-to-end coupling between polysaccharide chains and other polymer chains. The other one is preparing a polysaccharide-

based macroinitiator which can initiate polymerization at the reducing end. These two methods are discussed in the following sections.

2.1.2 Polymerization of synthetic blocks from polysaccharide macroinitiator

2.1.2.1 ATRP polysaccharide macroinitiator

Atom transfer radical polymerization (ATRP) was developed by Matyjaszewski[5, 6]. ATRP is a useful and practical method to prepare polymers with controlled molecular weight, polydispersity, and architecture.

Haddleton et al. reported the first synthesis of polysaccharide block copolymers by ATRP[7]. Fully acetylated maltoheptaoses with hydroxyl groups at the reducing end were used as the starting materials. 2-Bromo-2-methylpropionyl bromide was attached to the reducing end by a condensation reaction to form an ATRP initiator (shown in Scheme 1).

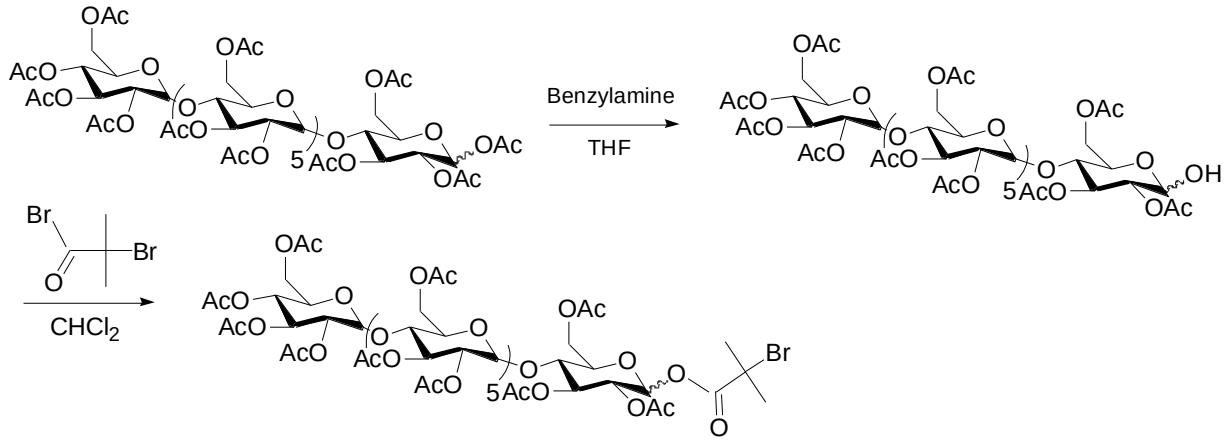

Scheme 1. Synthesis of maltoheptaose-based ATRP initiator[7]

Styrene and methyl acrylate were separately used as monomers to conduct ATRP. Two types of diblock copolymers, acetylated maltoheptaose-polystyrene and acetylated maltoheptaose-polymethylacrylate, were synthesized. The highlight of this study was the high efficiency of the ATRP initiator. This was shown by a linear relationship between monomer conversion and M_n of

the polymer block. The polydispersity of polymer blocks was narrow (PDI < 1.2) which was further evidence for the high efficiency of the initiator. The limitation of this study was the short length of the maltoheptaose-based initiator, limiting the contribution of the polysaccharide block to copolymer properties.

Yagi et al. reported the synthesis of a cellulose-polystyrene diblock copolymer by ATRP polymerization.[8] Microcrystalline cellulose was used as the starting material and was hydrolyzed to synthesize cellulose with different DPs (20 and 50). The cellulose chains with terminal formyl groups reacted with 2-chloroacetamide in a DMAc/LiCl system (shown in Scheme 2). The functionalized cellulose chain plays the role of macroinitiator. ATRP was conducted with CuCl, pentamethyldiethylenetriamine (PMDETA), styrene, and macroinitiator in a DMAc/LiCl system. Acetylation and carbanilation were applied to the cellulose-polystyrene diblock copolymer to improve its solubility in organic solvents. The structure of the cellulose-polystyrene diblock copolymer was determined by NMR and SEC. The author found that the diblock copolymer could improve compatibility of a cellulose/PS blend. According to optical microscope images (shown in Figure 1), phase separation of cellulose and PS was suppressed by the cellulose-PS diblock copolymer. However, the compatibility was still limited; diameters of the PS phases were still fairly large. Additionally, the efficiency of the macroinitiators was low. This study showed that as polysaccharide ATRP initiator DP rose, efficiency of the initiation step of polymerization declined.

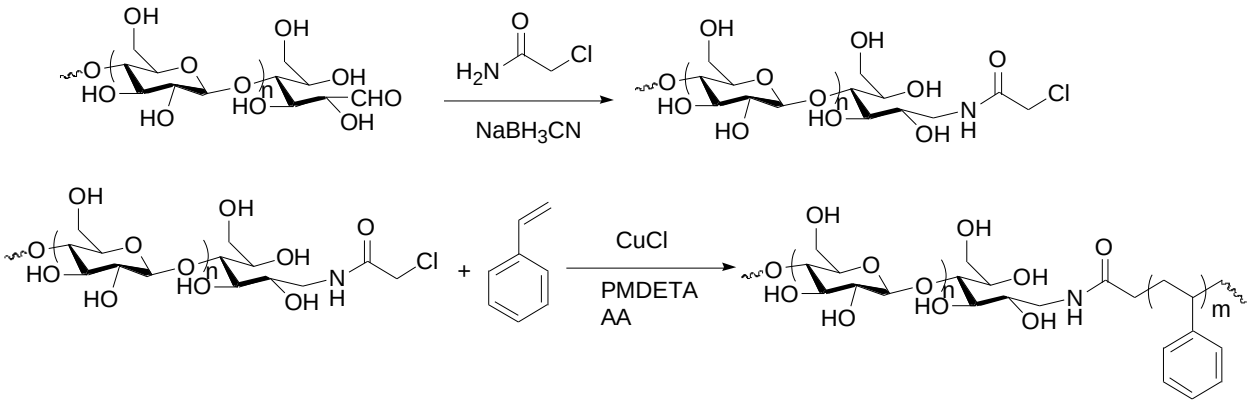

Scheme 2. Synthesis of cellulose-polystyrene diblock copolymer[8].

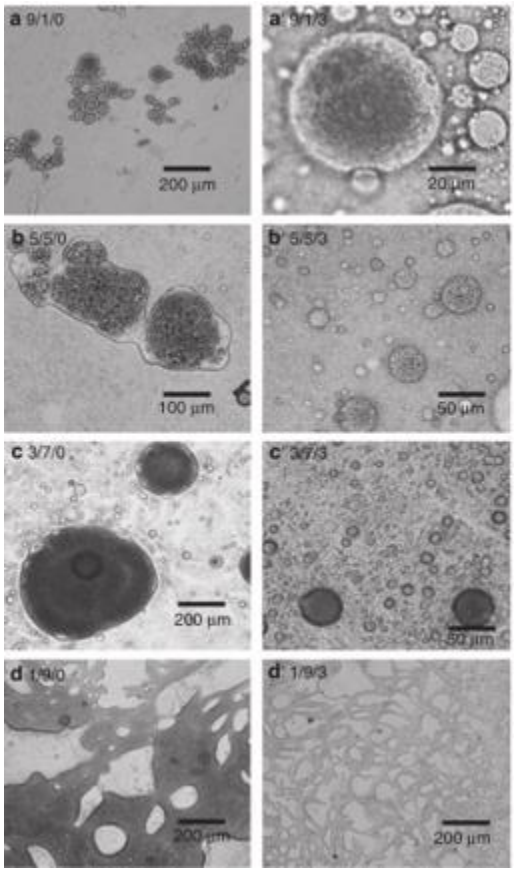

Figure 1. Micrographs of cellulose/PS/Cellulose. The component weight ratios are (a) 9/1/0, (a') 9/1/3, (b) 5/5/0, (b') 5/5/3, (c) 3/7/0, (c') 3/7/3, (d) 1/9/0 and (d') 1/9/3.[8]

Gnanou et al. reported the first dextran-based ATRP macroinitiator for the synthesis of a dextran-polystyrene diblock copolymer.[9] Dextran with M_n 6600 g mol^{-1} was chosen as the starting material. Unlike cellulose, dextran is composed of α-D-glucopyranose with (1-6) linkages and may have a partially branched structure[10]. The author used the terminal anomeric aldehyde from dextran to react with an amine functionalized ATRP initiator by reductive amination (shown in Scheme 3). Before carrying out ATRP, the dextran macroinitiators were fully silylated to make them soluble in organic solvents[11]. Next, ATRP of the silylated dextran macroinitiator and styrene was conducted in toluene by using CuBr/PMDETA as the catalyst. Based on the symmetrical curve shape from SEC, the author concluded that the ATRP initiators worked efficiently. To study the amphiphilic properties of dextran-polystyrene diblock copolymers, the block copolymer was desilylated under acidic conditions. DLS and TEM detected micelle-like phases (diameter 50 nm) in dextran-polystyrene diblock copolymer aqueous solution. Furthermore, the author found that morphologies of the diblock copolymers strongly depended on the component ratio. For example, a diblock copolymer with 87% polystyrene content exhibited a vesicular morphology as shown by TEM and DLS. A highlight of this study was the apparently high efficiency of ATRP initiation, especially for the medium size dextran-based initiator (6000 g/mol). However, the study did not provide quantitative ATRP initiation efficiency results.

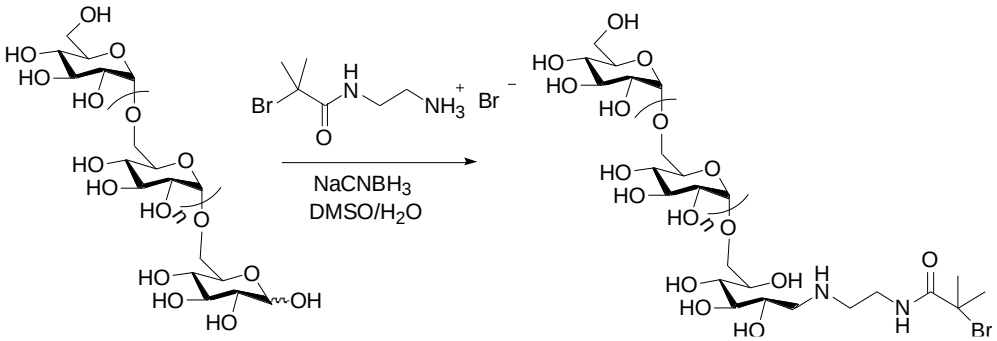

Scheme 3. Synthesis of dextran based ATRP initiator

Ramon et al. proposed a synthetic route to building dextran-*b*-PDMAEMA diblock copolymers[12]. Dextran was selected as the starting block for its good water solubility. Varying molecular weight dextran polymer chains (3 kDa, 6 kDa, and 40 kDa) were synthesized by citric acid-catalyzed dextran degradation. Synthesis of the dextran ATRP initiator is illustrated in Scheme 4. In this case, oxime chemistry was more efficient than the reductive amination of Borsali[5]. ATRP reactions of PDMAEMA were conducted with dextran macroinitiators, Cu and ligands (HMTETA, PMDETA or Me_6TREN) in DMSO solution in a glove box. Conversion was monitored by ^{1}H NMR. The author found that the macroinitiators with short dextran blocks had relatively high initiator efficiency (73%). Furthermore, Cu(II) also slightly increased macroinitiator efficiency. Product purification took advantage of the LCST behavior of PDMAEMA. Unreacted macroinitiators were removed from dextran-PDMAEMA by dialysis in water at pH 11 at 40 °C (above the cloud point of PDMAEMA). Nevertheless, the diblock copolymer was partly lost during dialysis. The interpolyelectrolyte complex (IPEC) of dextran-PDMAEMA and sodium poly(styrene sulfonate) (PSS) was studied, with IPEC assembly characterized by DLS and TEM. The results illustrated that diblock copolymers with dextran DP 36 were insufficient to prevent aggregation of the formed nanoassemblies, while nanoassemblies became stable against aggregation when dextran DP reached 86. The authors showed that dextran-based ATRP initiators with high DP displayed lower initiation efficiency, studies from Müller[12] and Borsali[9] made the same observation. The low efficiency could be due to the steric demands of larger initiators. At the same time, a sufficiently long dextran block was a prerequisite to stabilize the phase structure of diblock copolymer.

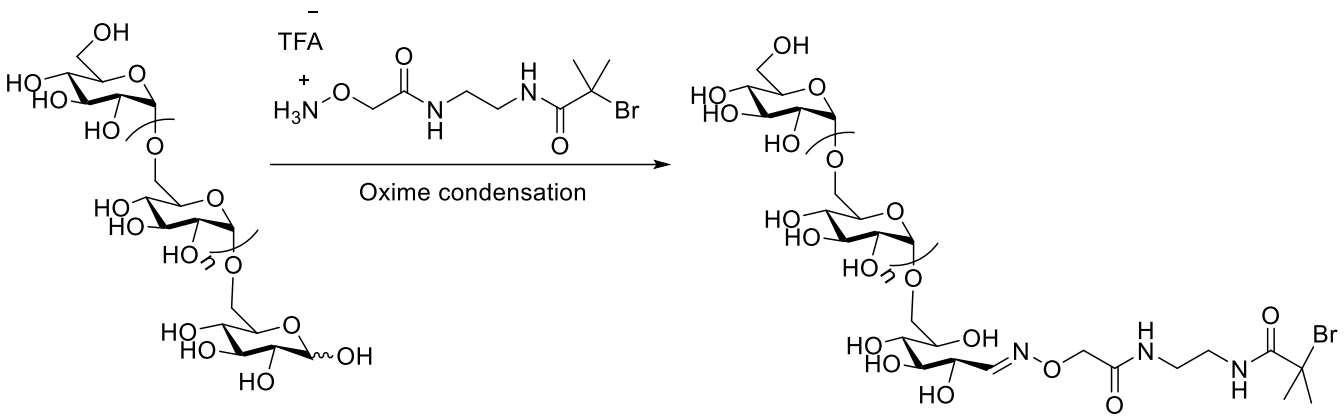

Scheme 4. Synthesis of dextran based ATRP initiator[8]

2.1.2.2 Nitroxide mediated-living radical polymerization

Nitroxide-mediated living radical polymerization is a controlled and living radical polymerization. It is a useful for design of complex, well-defined, and functional macromolecules[13].

Kakuchi et al. proposed the application of nitroxide-mediated-living radical polymerization for the synthesis of β-cyclodextrin-polystyrene diblock copolymer[14]. 2,2,6,6-Tetramethylpiperidinyloxy (TEMPO)-substituted β-cyclodextrins were synthesized via amidation of 6-amino-6-deoxy-β-cyclodextrin by using 4-[1'-(2'',2''6'',6''-tetramethyl-1''-piperidinyloxy)- ethyl] benzoic acid, DCC, and Et_3N in DMF. The macroinitiators were acetylated for use in nitroxide-mediated polymerization (NMP) of styrene (molar ratio: styrene/initiator = 200). By SEC the diblock product showed a molecular weight of 11400 g/mol with a narrow PDI (1.1).

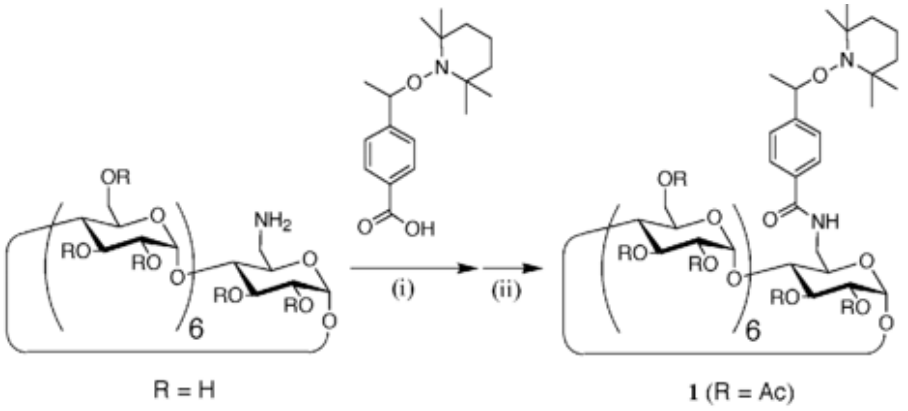

Figure 2. Synthesis of β-cyclodextrin based initiator.[12] (i) Coupling reaction using DCC in DMF in the presence of HBT and Et_3N; (ii) Acetylation using Ac_2O in pyridine

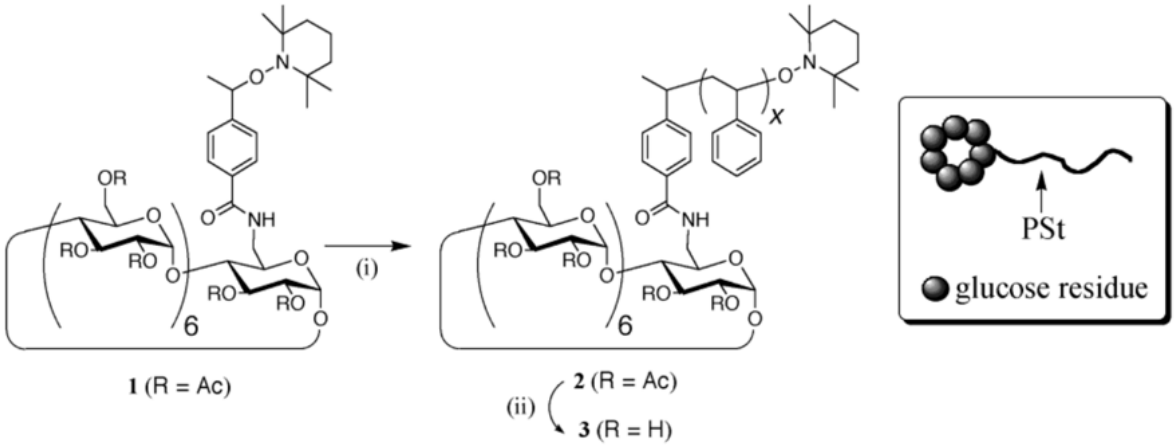

Figure 3. (i) Polymerization of styrene (ii) Deacetylation[15]

Later, the authors used the same synthetic method to end functionalize a polystyrene polymer chain by using glucose, maltose, maltotriose, maltotetraose, maltopentaose, and maltohexaose. The diblock products had controlled molecular weights and narrow dispersities (1.1). Based on static laser light scattering, the diblock copolymer formed polymeric reverse micelles in toluene which had saccharide-cores and polystyrene shells.[14] The study showed that a low DP polysaccharide can

initiate polymerization efficiently. Additionally, though the β-CD block was small, the β-cyclodextrin-polystyrene diblock copolymers could form micelles in aqueous solution.

2.1.2.3 Reversible addition-fragmentation chain transfer

Reversible addition-fragmentation chain transfer (RAFT) is a living free-radical polymerization. RAFT can be used across a broad range of reaction conditions and monomers. The chain transfer agent, usually in the form of a thiocarbonyl thiol compound, controls the radical concentration in the polymerization system. As a result, RAFT provides polymer products with well-controlled molecular weights and narrow polydispersities[15].

Bernard et al. reported synthesis of a dextran-polyvinyl acetate copolymer by emulsion polymerization[16]. Polysaccharide-based block copolymers exhibit potential as emulsifying agents which can stabilize latex particles effectively. In this study, propargyl groups were introduced to reducing ends of dextran chains by reductive amination with propargylamine. Then xanthate moieties were used to end functionalize dextran by Huisgen's 1,3-dipolar cycloaddition (shown in Scheme 5). The conversion of this step was low (30%), possibly due to undesired interaction between copper and dextran. The functionalized dextran played a role as macro RAFT agent in surfactant-free emulsion polymerization of vinyl acetate. This emulsion polymerization gave *in situ* formed amphiphilic dextran-polyvinylacetate diblock copolymers. In early stage of the RAFT polymerization, the macro RAFT agents improved the size and size-distribution of latexes. The latexes also had high solid content (27%). This work showed that the amphiphilic properties of polysaccharide-based RAFT agents gave them advantages over conventional RAFT agents in some specific cases like emulsion polymerization.

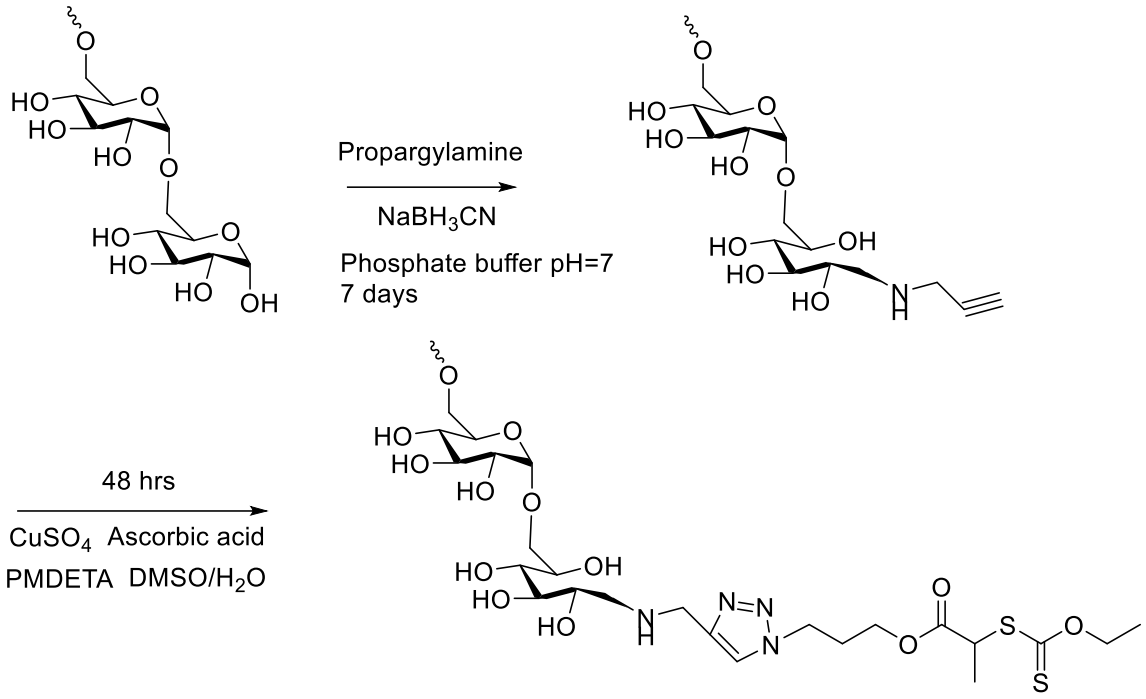

Scheme 5. Selective end-functionalization of dextran by a xanthate[16]

2.1.3. End-to-End coupling strategy

End-to-end coupling between polysaccharides and other polymer blocks is a practical synthetic strategy for medium and short polymer chains. Several coupling techniques have been applied to polysaccharide-based block copolymer synthesis.

2.1.3.1 Selective Reductive Amidation

In most polysaccharide end functionalization studies, selective reductive amination in the presence of sodium cyanoborohydride has been used to target the aldehyde groups at reducing ends of polysaccharide chains. This synthetic strategy was first developed by Borch et al.[17]. Yalpani first applied selective reductive amination to dextran end-functionality[18].

Slaghek et al. reported the synthesis of polystyrene-polysaccharide diblock copolymers by using reductive amination[19]. Dextrans and maltodextrins with different molecular weights were used as polysaccharide blocks. The commercially available polystyrene block was amine-terminated (M_w

12,300 Da, PDI = 1.02). Reductive amination ($NaBH_3CN$) between polysaccharide blocks and amine-terminated polystyrene blocks were performed in DMF (Scheme 6). The reaction was slow (7 d, 60 °C), but afforded copolymers by precipitation in water with 75-95 wt% yields. To achieve high reaction conversion, large excesses (50-100 eqs) of polysaccharides were added. Molecular weights of polysaccharide blocks varied from 180 Da to 6000 Da. The author attempted to use dextrans with M_w 9500 Da in the coupling step, but this was unsuccessful due to low conversion. In interfacial pressure measurements (water/air), the results showed that the diblock copolymer exhibited amphiphilic properties. There were two shortcomings of this method; the long reaction time, and the need for great excesses of polysaccharide blocks to achieve moderate conversion.

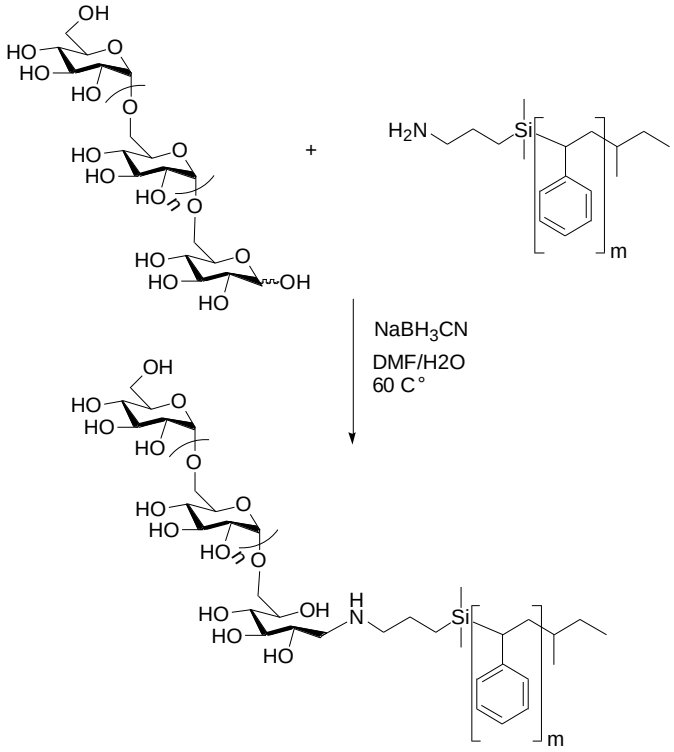

Scheme 6. Synthesis of diblock copolymer of dextran-polystyrene[19]

Winnik reported the synthesis of dextran-poly(ethylene glycol) diblock copolymers[20]. The aldehyde groups at dextran reducing ends were oxidized to give dextran-lactone by using I_2 and

KOH[21]. In the coupling step, the aminolysis between MeO-PEG-NH_2[22] and dextran-lactone was performed in DMSO (product structure is shown in Scheme 7). To achieve high reaction conversions, large excesses of MeO-PEG-NH_2 blocks were added and long reaction time was applied. Yields were low (30 wt% for dextran$_{40}$-PEG$_{140}$). Then the diblock copolymers were converted to polyanions by carboxymethylation (DS = 1.8)[23]. Dynamic light scattering (DLS) was used to detect the pH-dependent properties of aqueous carboxymethyldextran-PEG diblock copolymers. The diblock copolymer formed micelles with R_H (radius of micelle) = 100 nm and unimodal size distribution. Increasing the pH of the solution could lead to decreased micelle R_H. When pH was above 9, the DLS signal from micelles was weak, indicating that under basic conditions the carboxylate groups caused reduction in interchain and intrachain hydrogen bonding interactions of the block copolymer.

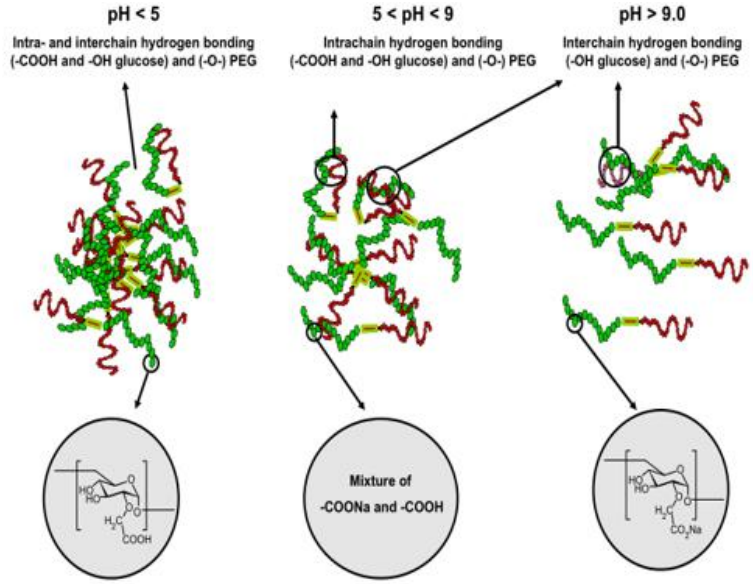

Figure 4. Pictorial representation of the assemblies formed in aqueous solutions of CMD-ACMD-PEG block copolymer at various pH values and illustration of the intra and inter-chain H-bond interactions likely to occur in acidic, neutral and alkaline polymer solutions[23].

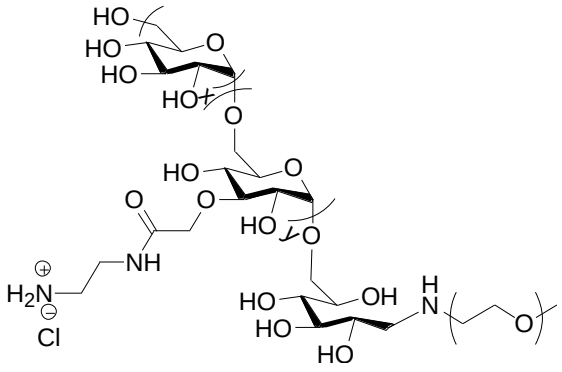

Scheme 7. Structure of CMD-ACMD-PEG block copolymer[23].

Zhang et al. reported synthesis of dextran-poly(ε-caprolactone) diblock copolymers[24]. The poly(ε-caprolactone) blocks were synthesized by ring opening polymerization using ε-caprolactone monomers. Then the poly(ε-caprolactone) blocks were end-capped with acryloyl groups in presence of acryloyl chloride in anhydrous DMF. Amine functionalization of dextran (M_n = 3700g/mol) blocks was carried out in aqueous sodium borate solution with sodium cyanoborohydride and ethylenediamine. This reaction took 8 days at 60 °C. Coupling of these two blocks was performed by Michael reaction, conducted in DMSO in the presence of hydroquinone and p-toluene sulfonic acid. DLS and fluorometry were used to investigate amphiphilic properties of the diblock copolymers in aqueous solution. Micelles with 50 nm diameter were observed, with fairly low critical micelle concentration (0.06 mg/ml).

2.1.3.2 Azide-alkyne Huisgen Cycloaddition

The azide-alkyne Huisgen cycloaddition is a 1,3-dipolar cycloaddition between an alkyne and an azide to give a 1,2,3-triazole, also called a click reaction. This click reaction is high yielding, wide in scope, and the byproduct can be easily removed[25]. These factors make azide-alkyne Huisgen cycloaddition a suitable reaction for polysaccharide modification[26], including end-to-end coupling

of polysaccharide block copolymers. This click coupling strategy also takes advantage of selective reductive amination to introduce azide and alkyne groups at reducing ends of polysaccharide chains.

Kamitakahara reported the synthesis of diblock copolymers with cellulose derivatives[27]. Cellulose triacetate (CTA) was synthesized as the starting material. A glycosyl bromide group was introduced at C1 via reaction with HBr, bromide was displaced by azide, and the azide was hydrogenated to an amine. The amine group at the terminal C1 could react with a polymer functionalized by an acyl chloride to form a cellulose copolymer. The macromonomer used by Kamitakahara in the polymer block was Oligoamide-15 (Scheme 8) with terminal azide and acyl chloride functionalities. One advantage was that the length of polymer block could be tunable; length of the Oligoamide-15 (polymer block) could be controlled by condensation between amine and aryl chloride group. At the same time, the polydispersity of poly(Oligoamide-15) was narrow. Mass spectroscopy confirmed the narrow molecular weight distribution of the Oligoamide-15 chain. Dynamic thermal analysis showed that three transitions occurred during copolymer heating; glass transition (T_g), crystallization (T_c), and melting (T_m) contributed by the CTA block. One interesting phenomenon was that the T_c and T_g of copolymer were independent of the length of poly(Oligoamide-15). The T_g and T_m of the diblock copolymer increased with increasing length of the cellulose triacetate (CTA) block. By DSC, T_g, T_c and T_m of the diblock copolymer were observed. Moreover, XRD also proved the existence of crystalline phases and an annealing process could improve the quality of the crystalline phase. However, there was no direct evidence to show phase separation between CTA and poly(Oligoamide-15) blocks. Further morphology study could help illuminate the phase structure of the diblock copolymer.

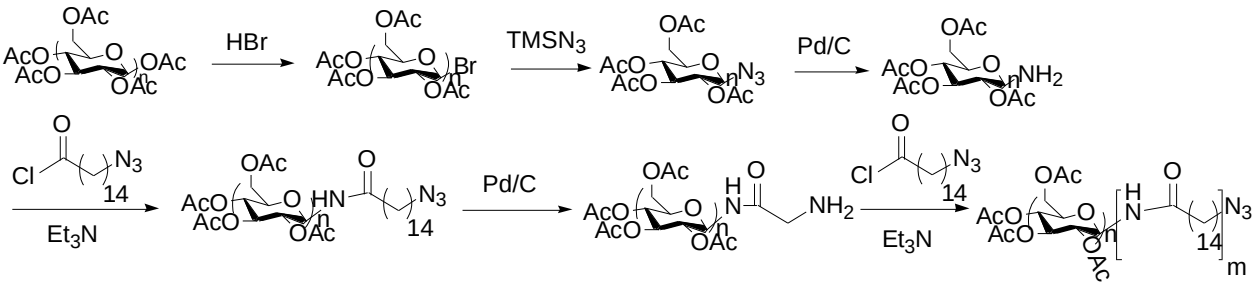

Scheme 8. Synthetic route to cellulose triacetate-block-oligoamide-15 diblock copolymer[28]

Kamitakahara et al. proposed another way to synthesize polysaccharide-based diblock copolymer by Huisgen 1,3-dipolar cycloaddition[29]. Two families of polysaccharide-based diblock copolymers were synthesized. One was cellobiose-2,3,6-tri-*O*-methyl cellulose and the other was cellulose-2,3,6-tri-O-methyl-cellulose diblock copolymers. The highlight of this paper was that alkyne groups were introduced to the non-reducing C-4 positions of 2,3,6-tri-*O*-methyl cellulose. In most studies about polysaccharide derivative diblock copolymers, end-functionalization was performed at the reducing end of the polysaccharide chain[28]. Propargyl groups were introduced to the non-reducing ends of 2,3,6-tri-*O*-methyl cellulose chains by using 3-bromopropyne in the presence of NaH in DMF. Regioselective introduction of propargyl groups was enabled by sulfuric acid-catalyzed methanolysis of trimethyl cellulose (TMC), which generated free 4-OH groups only at the terminal monosaccharides on the non-reducing ends of the TMC chains. Fully acrylated cellobiose and acrylated cellulose (DP = 7) were end-functionalized at reducing ends with azide groups by using trimethylsilyl azide[30, 31]. In the coupling step, copper(I) was used as the catalyst in the presence of sodium ascorbate and PMDETA (Scheme 9). Acetyl groups of diblock copolymer were removed by using NaOMe in MeOH and THF. Then the diblock copolymer in 2 wt% aqueous solution showed thermoreversible gelation properties which were supported by DSC analysis.

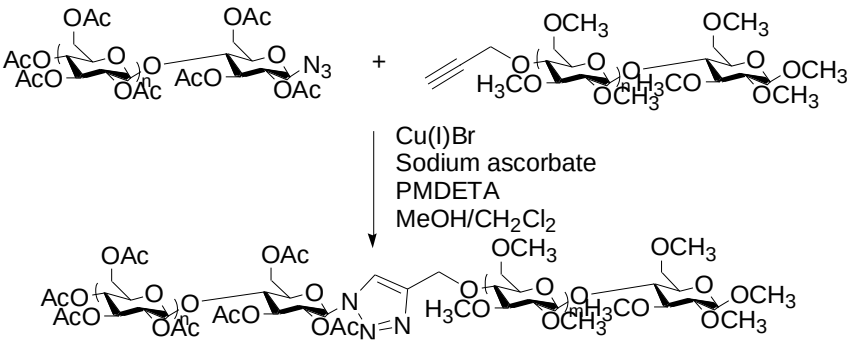

Scheme 9. Synthesis of triacetate cellulose-methyl cellulose diblock copolymer[31]

Halila et al. reported synthesis of an acetylated maltoheptaose-maltoheptaose diblock copolymer through end-to-end connection by click reaction[32]. Alkyne was introduced to maltoheptaose (DP=7), prepared by ring-opening of β-CD, at the reducing end by reaction of maltoheptaose with propargylamine. Then acetylation was carried out by reaction with acetic anhydride in pyridine. The other maltoheptaoses (DP=7) with azide groups were synthesized by reaction of maltoheptaoses with sodium azide 2-chloroimidazolinium and Et_3N. Finally, these two maltoheptaose blocks were connected by click reaction with sodium ascorbate and copper (II) sulfate (60% yield). Self-assembly properties of maltoheptaose based block copolymers in deionized water were studied by DLS, TEM and AFM, showing that the block copolymer formed spherical micelles with approximately 35 nm diameter (Figure 5). The maltoheptaose based block copolymer was degraded using glucoamylase enzyme. All of these properties made them promising biocompatible and biodegradable nanocarriers.

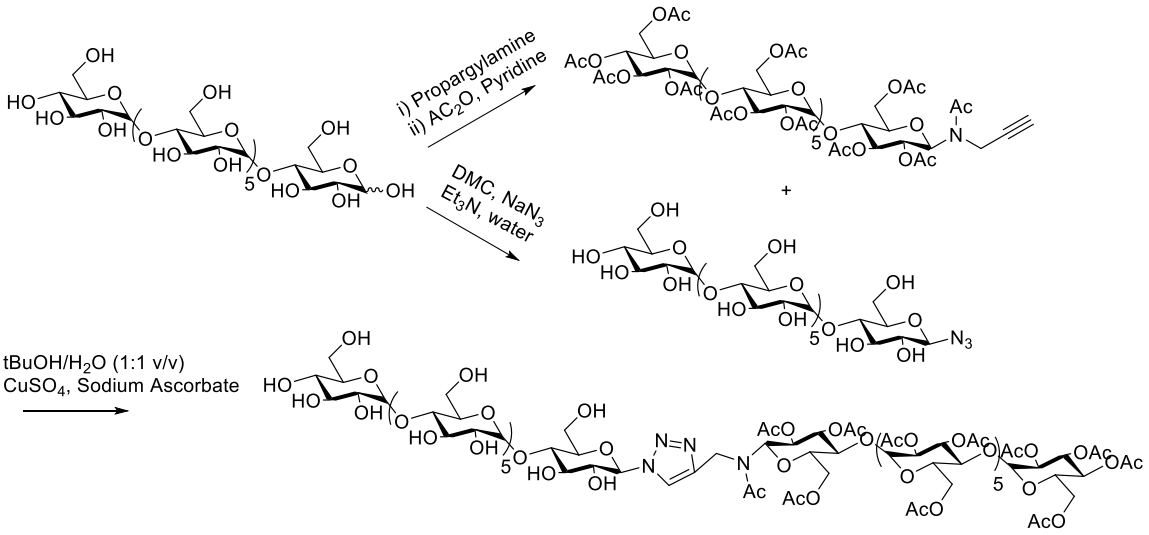

Scheme 10. Synthesis route to acetylated maltoheptaose-*b*-maltoheptaose block copolymers

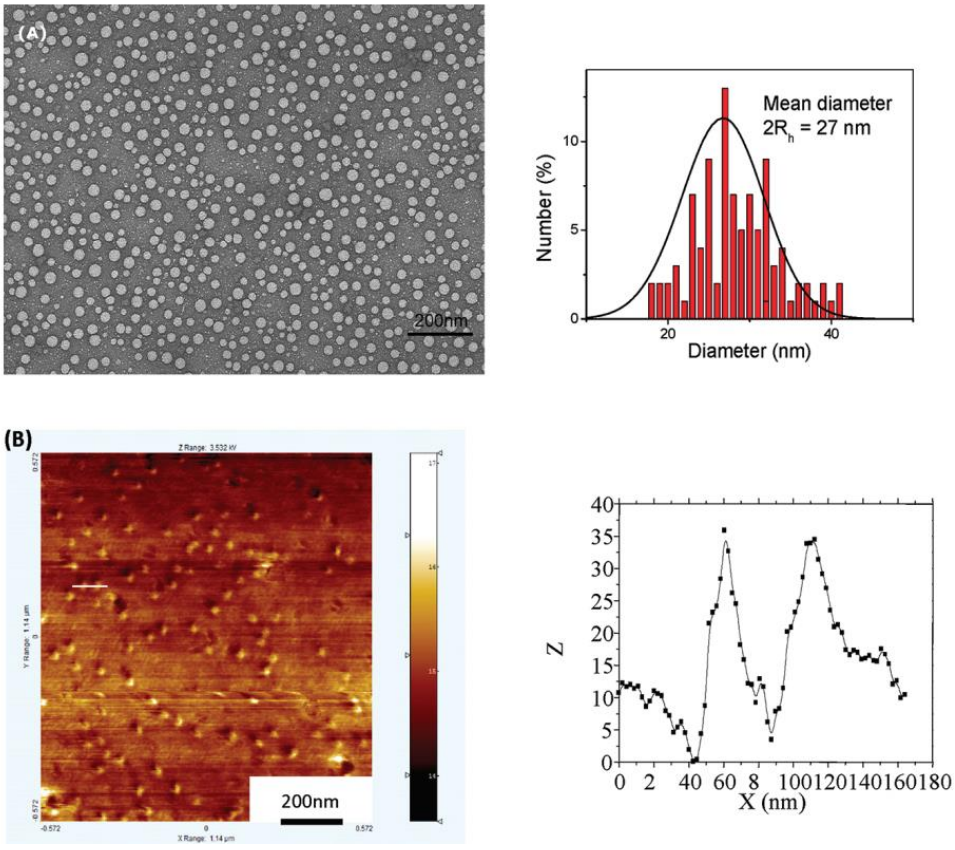

Figure 5. (A) Transmission electron micrograph with size distribution (B) tapping mode AFM phase images with sectional analysis of Mal_7-$AcMal_7$ micelles[32]

Lecommandoux et al. reported synthesis of a polysaccharide-polypeptide diblock copolymer[33] in order to mimic glycoproteins. They began by introducing alkyne groups at the reducing end of dextrans (M_n=6600 g/mol, PDI: 1.35) by reductive amination with propargylamine[34]. Then, the polypeptide block poly(γ-benzyl ι–glutamate) (PBLG) (DP = 59) was end-functionalized with an azide group by using 1-azido-3-aminopropane to initiate polymerization of γ-benzyl ι–glutamate N-carboxylic anhydride. Finally, these two blocks were quantitatively coupled by Cu catalyzed click reaction. Diblock copolymers could be simply purified from the reaction mixture by dialyzing the solution medium against water. Purification of block copolymers from their polymeric precursors, especially after being prepared by condensation reactions, can be problematic due to the potential difficulties in polymer/polymer separation. The amphiphilic properties of the diblock copolymer were studied by DLS in water, showing that the micelles had hydrodynamic radius (R_H) of 45 nm with a narrow polydispersity (σ = 0.20). Moreover, both TEM and SANS analysis indicate that the dextran-*b*-PBLG has a vesicle-like structure with a membrane thickness of ca. 20 nm. The micelle morphology of the diblock copolymer was promising for drug-delivery.

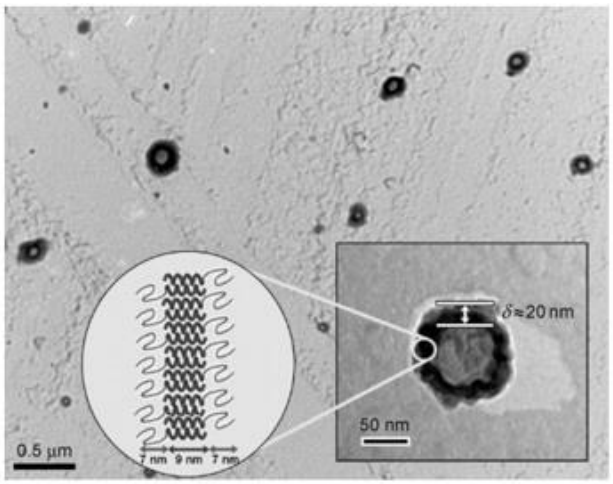

Figure 6. TEM image of dried dispersion of dextran-PBLG diblock copolymer.[33]

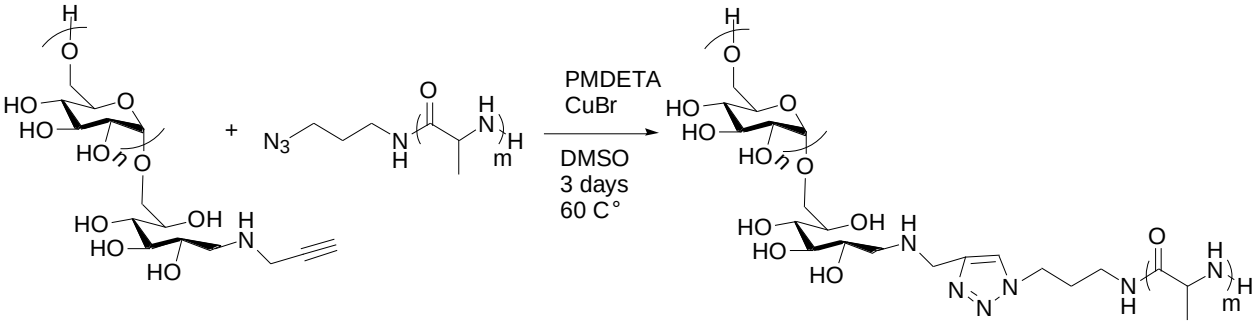

Scheme 11. Synthesis of dextran-polypeptide block copolymer.[33]

The authors applied the same strategy to the synthesis of hyaluronan (HA)-poly(γ-benzyl glutamate) diblock copolymer[35]. The purpose of switching dextran to HA blocks was that HA could target cancer-related protein receptors. The hydrophilic HA block had DP = 10 and PDI = 1.4. The hydrophobic poly(γ-benzyl glutamate) block had DP = 23 with PDI = 1.1. These two blocks were connected by Huisgen 1,3-dipolar cycloaddition. HA-poly(γ-benzyl glutamate) diblock copolymer micelles were characterized by DLS, SANS, and TEM. DLS showed that the hydrodynamic radius of micelles was 220 nm with a narrow polydispersity(σ = 0.08). The thickness of the membrane was 9.3 nm as measured by SANS and TEM (Figure 7); the author described the thickness of diblock copolymer as at least two times that of other liposomes. As a result, they predicted that the diblock copolymer would have better colloidal stability than other liposomes. Doxorubicin was selected for drug loading because of its fluorescent properties, achieving 12 wt % loading with ca. 50% encapsulation efficiency.

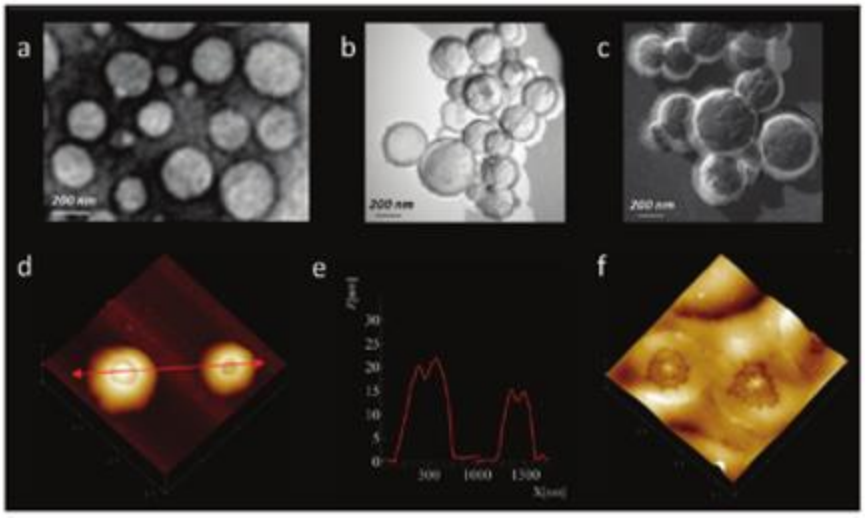

Figure 7. TEM and AFM images of PBLG-HYA diblock copolymer.[35]

Borsali reported synthesis of thermoresponsive maltoheptaose-poly(N-isopropylacrylamide)[36]. Maltoheptaose with DP 7 was end-functionalized by reductive amination with propargylamine. Then N-propargyl maltoheptaosylamine was selectively N-acetylated by using acetic anhydride in MeOH. Poly(N-isopropylacrylamide) (PNIPAM) with terminal azide groups was synthesized by ATRP using an azide functionalized initiator. PNIPAMs with DPs 28, 45, 119 and 220 were used in the coupling reaction. Azide functionalized PNIPAM and alkyne-functionalized maltoheptaose were condensed by click reaction. Self-assembly properties of diblock copolymers were characterized by DLS in aqueous solution below and above cloud point temperature (T_{cp}). DLS results showed weak scattered intensities below T_{cp}, reflecting little aggregation of the diblock copolymer. Above the $T_{cp,}$ DLS results showed that the R_h of maltoheptaose-$PNIPAM_{220}$ diblock copolymers was 144 nm. TEM (90 °C) showed vesicular morphologies, supporting the DLS results (Figure 8).

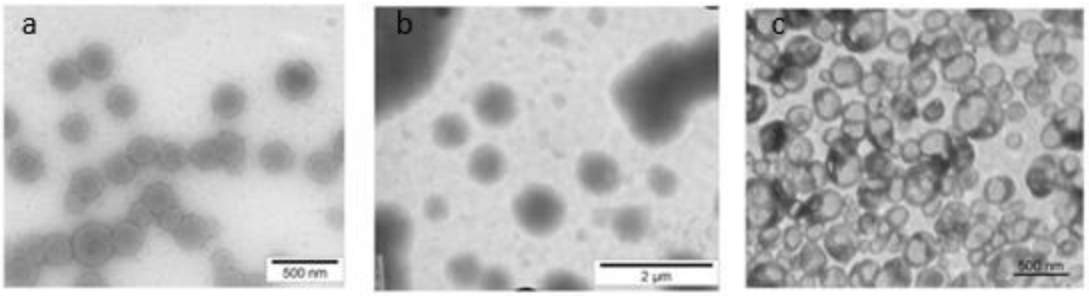

Figure 8. (a) TEM imagine of a dried dispersion of Mal_7-$PNIPAM_{220}$ at 90 °C, (b) TEM image of a dried dispersion of N_3-$PNIPAM_{220}$ at 90 °C, (c) TEM image of dried dispersion of Mal_7-$PNIPAM_{119}$ at 90 °C[36].

Kim reported synthesis of a cellulose block copolymer in 1976[37]. Cellulose hydroxyls were substituted by acetyl or methyl groups. The substituted cellulose was degraded in acetic acid and water to an oligomer containing a reactive hydroxyl at the reducing end, with DP ca. 20-30. The substituted cellulose oligomer could react with a difunctional polymer chain or difunctional monomer to give a cellulose block copolymer. As this cellulose block copolymer was designed to be biodegradable, the cellulose substituents needed to be removed from the cellulose block copolymer. Thus a cellulose acetate block was deacetylated by sodium methoxide. The molecular weight of the deacetylated product was not reported, but noticeable degradation of cellulose copolymer was reported upon exposure to enzymes (enzyme type was not mentioned in the paper).

2.1.4 Summary

Polysaccharide-based block copolymer syntheses can be organized into two strategic categories; end-to-end coupling, and polysaccharide macroinitiator methods. One similarity between these two strategies is that both of them take advantage of the high reactivity of reducing ends to introduce functionality or to couple another polymer block. Most studies in this field are limited to synthesis of diblock copolymers because it is difficult to selectively modify at the non-reducing

end. My research goal is to develop a synthetic route to cellulose-based triblock copolymers. Functionalities will be introduced to both reducing and non-reducing ends of cellulose derivatives. End to end coupling strategy by cross metathesis will be applied to attach polymer blocks to each end of cellulose derivatives chains. I expect cross metathesis to be a synthetic strategy that is highly efficient, with rapid reaction rates, and high conversion.

2.2 Polysaccharide-based *in situ* forming hydrogels

2.2.1 Introduction

Hydrogels are hydrophilic polymer crosslinking networks capable of absorbing great amounts of water[38]. In the 1960s, hydrogels were first used in contact lenses. Since then, application of hydrogels has increased tremendously in a broad range of fields, especially for biomedical[39] and pharmaceutical[40] related applications. Natural polymers like polysaccharides are important building blocks for hydrogel preparation due to their generally benign natures including biocompatibility in many situations and towards many tissues, and biodegradability. In recent decades, hydrogel research studies have shifted from implantable to injectable hydrogels that enable gel formation at the desired injection site[41]. *In situ* hydrogels are particularly attractive for this purpose as they are usually injectable and can be introduced to the targeted location by minimally invasive procedures. This class of hydrogel can be prepared by several strategies, such as UV-induced crosslinking, creating non-reversible covalent linkages, and using reversible physical or chemical interactions to create the polymer networks. Due to the inherent benefits of polysaccharides and their versatile potential for chemical modifications, it is of great interest to prepare *in situ* forming polysaccharide hydrogels and use them in tissue engineering, drug delivery, and cell delivery. In the following sections, we will introduce several reported strategies for preparing interesting and useful polysaccharide-based hydrogels.

2.2.2 Chemically crosslinked *in situ* forming hydrogels

In situ forming hydrogels can be divided into two categories: irradiation-induced and self-assembled systems. Photo-crosslinked hydrogels are formed *in situ* but are not self-gelling. In contrast, the crosslinking of self-assembling hydrogel is spontaneous or occurs upon exposure to certain triggers like temperature and pH.

2.2.2.1 Photo-crosslinked hydrogels

In situ photopolymerization and photocrosslinking have been investigated in biomedical applications for many years. This class of materials was used in various microfabrications like photolithography, micro molding, and bioprinting. Azido-chitosan is one of the cell-seeding hydrogels that is used in UV lithography, first reported by Langer[42]. The study discussed the synthesis of photocrosslinkable chitosan and its utility in fabricating a cell-seeded (human hepatoblastoma cell) hydrogel microstructure. 4-Azidobenzoic acid was appended to chitosan through amidation thus introducing the capability for photo-induced crosslinking. This hydrogel is expected to be a promising platform for implantable bioartificial organs. The UV-crosslinkable azido-chitosan was also reported as a scaffold for bone tissue engineering[43]. Zhou[44] reported a water soluble, photo-crosslinkable and injectable chitosan for cell-laden microgels. The chitosan was chemoselectively N-acylated using methacrylic anhydride, and the resulting chitosan was readily cured within 60s *in vivo*. However, photocrosslinkable hydrogels are limited to microgels as UV light cannot pass through thick hydrogel layer[45]. In addition, UV irradiation also cause issues like cytotoxicity of some photosensitizers[46].

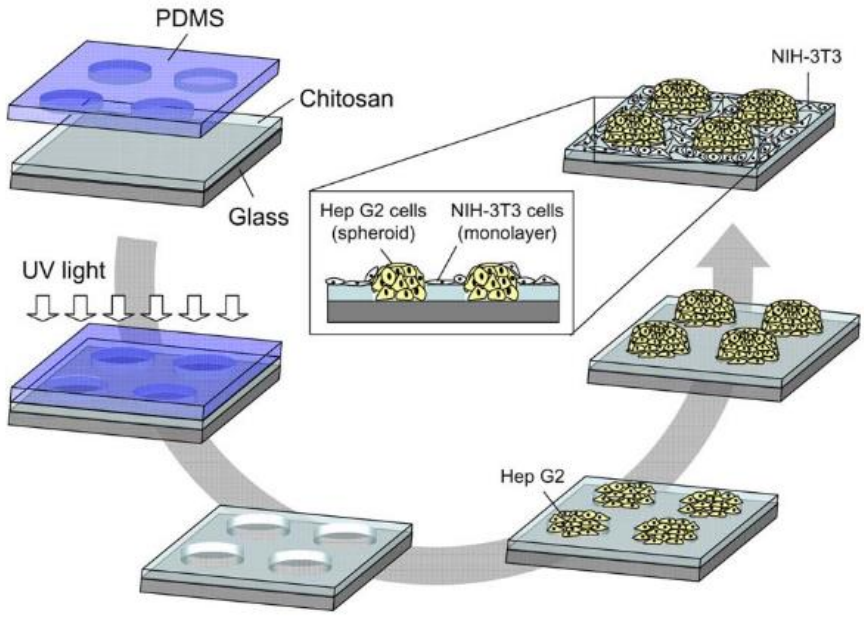

Figure 9. Schematic of fabrication of Hep G2 cells using micromolding technology with photocrosslinkable chitosan hydrogel.[42]

2.2.2.2 Hydrogels prepared by Schiff base chemistry

In situ forming hydrogels can be prepared by Schiff base reactions between an amine and an aldehyde or ketone, without using small molecule crosslinkers. The imine bond is dynamic and covalent, and can form spontaneously without the need for a catalyst[47]. This dynamic nature favors self-healing, and is a reason that imine crosslinked hydrogels have proved attractive. Bloodgood[48] reported preparation of imine-based hydrogels from polysaccharides utilizing sodium periodate to cleave vicinal diols, thereby creating ring-opened dialdehydes. The excess aldehyde groups within the hydrogel can be used for conjugating drugs that possess appropriate chemical moieties. Hyaluronic acid[49], dextran[46], chondroitin sulfate[50] and chitosan have been oxidized to prepare hydrogels via this approach. This oxidation changes the relatively rigid native polysaccharide backbone, imparts flexibility, and introduces chemical instability due to the excess new formed aldehyde groups and the acidic protons alpha to the aldehydes. As a result, such structural changes

result in serious degradation of the polysaccharide, and inferior mechanical properties. Functionalization of the polysaccharide with ketones is an alternative route for preparing Schiff base-crosslinked polysaccharide hydrogels. Mao[51] reported preparation of a hydrogel by using cellulose acetoacetate, which can form hydrogels by reaction of its ketone groups with chitosan. The gelation time and physical performances of these hydrogels rely on the ratio of the ketone/aldehyde and amines. Moreover, due to the reversible linkages, the imine crosslinked hydrogel usually exhibits self-healing and injectability, affording potential for biomedical applications.

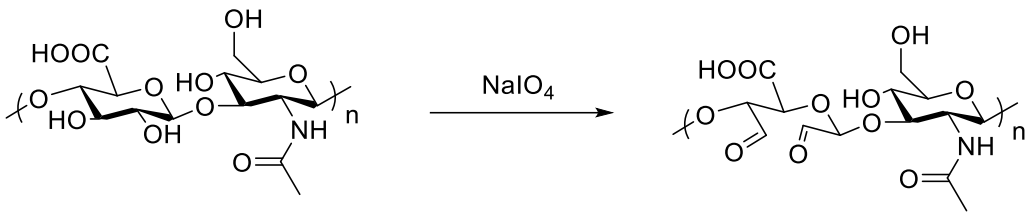

Scheme 12. Sodium periodate oxidation of hyaluronic acid[49].

2.2.2.3 Hydrogels prepared by Michael addition

Michael addition is a nucleophilic addition that typically involves reaction between thiols or amines and α,β-unsaturated carbonyl groups[52]. The Michael reaction frequently displays high reactivity and selectivity under physiological conditions, often without involving toxic compounds and with no side products. Therefore, Michael additions have been intensively investigated in the field of injectable hydrogels for biomedical applications. Polysaccharides like hyaluronic acid[53] and heparin[54] were functionalized with thiols, vinyl sulfones, or aminoethyl methacrylate to prepare substrates for creating hydrogels. Cells and drugs can be loaded to the hydrogel by simply mixing with the precursor solution. Extracel™ is a typical hydrogel crosslinked by Michael addition between a thiol appended carboxymethyl hyaluronic acid and diacrylated PEG[55]. The

hydrogel gelation can be modulated by pH and concentration of the polysaccharide solutions. Due to the many benefits of Michael addition crosslinked hydrogels, this class of materials has been applied to tissue engineering[56], drug delivery[57] and bioadhesion[24].

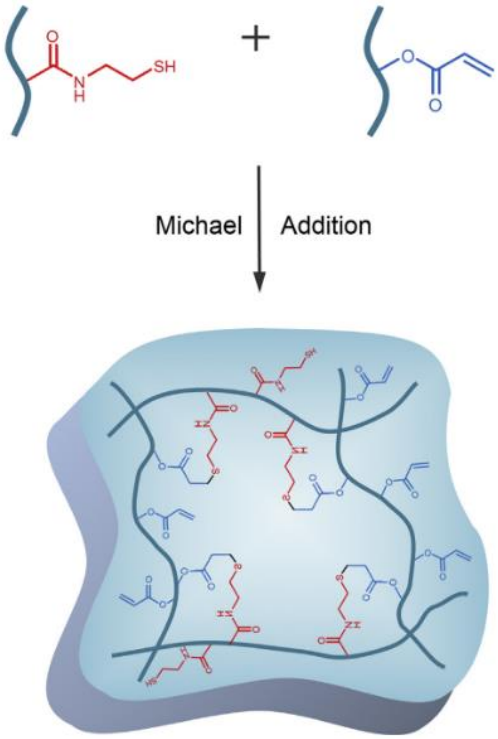

Figure 10. Illustration of heparin-based *in situ* forming hydrogel by using Michael addition.[58]

2.2.3 Electrostatic interaction crosslinked *in situ* forming hydrogel

2.2.3.1 Alginate-base hydrogels

Alginate is a natural anionic polysaccharide that is frequently used in the pharmaceutical applications. Like many ionic polysaccharides, alginate can form hydrogels by interaction with multivalent cations including Mg^{2+}, Ca^{2+}, and Ba^{2+}. This class of hydrogels, some of which are employed in FDA[59] approved medical products, have been widely used in cell encapsulation, drug delivery, and tissue engineering. The mechanical performance and gelation time of alginate hydrogels can be controlled by tuning the concentration and the type of cation. Ma[60] reported that

the rate of alginate hydrogel formation was increased with increasing concentration of $CaCO_3$ and $CaSO_4$. The study also reports that hydrogel mechanical properties are affected by the alginate concentration, molecular weight, and the ratio of glucuronic acid to mannuronic acid. However, as divalent ionic crosslinks can be destroyed by ion exchange with monovalent ions in body fluids, the cation crosslinked alginate hydrogels are not stable in the human body[61]. Moreover, alginate hydrogels display poor cell adhesion and require proper purification due to their inherent compositions. To improve hydrogel stability, additional functionality such as methacrylate groups was appended to alginate to provide another, stable crosslinking mechanism. In addition, appropriately purified alginate hydrogels can be successfully used in biomedical related applications.

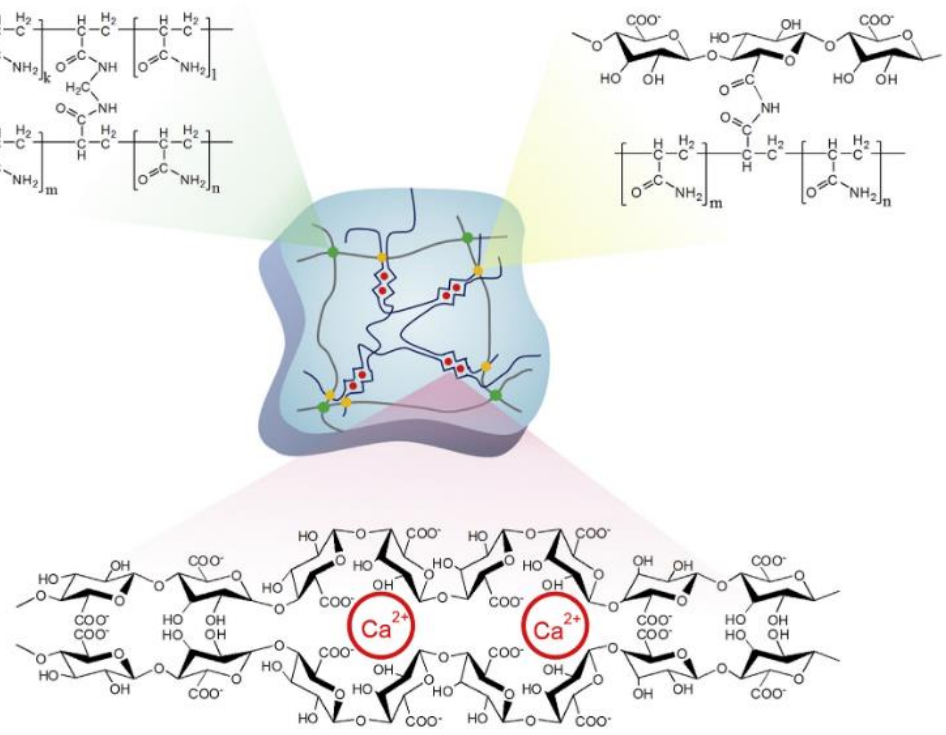

Figure 11. Illustration of alginate-based *in situ* forming hydrogel using ionic interactions and covalent linkages.[62]

2.2.3.2 Chitosan-based hydrogels

Chitosan is considered a desirable candidate polymer for hydrogel preparation by many investigators. Chitosan have features including inherent free amines, biocompatibility towards many tissues, and biodegradability *in vivo* and in the environment. Chitosan readily forms hydrogel complexes with anionic polymers via electrostatic interaction[63]. Polyol salts that have a single anionic head such like sorbitol-, glycerol-, and fructose- salt derivatives are used to prepare pH and temperature responsive hydrogels with chitosan[64, 65]. Hydrogel formation occurred not only due to electrostatic interactions, but due also to hydrogen bonding and hydrophobic interactions between polyol and chitosan. The gelation of this class of hydrogel can be controlled by temperature and pH, and thus hydrogel formation can be triggered at specific and desired conditions. Therefore, cells or drugs can be simply entrapped with the hydrogel precursor solution before injection, providing a practical approach for drug delivery and cell encapsulation.

2.2.4 Conclusion

We summarized a series of polysaccharide-based *in situ* forming hydrogels that have been applied to the biomedical field, including tissue engineering, drug delivery and cell encapsulation. Polysaccharide-based hydrogels display advantages and limitations in terms of biomedical application. Chemically crosslinked hydrogels exhibit great mechanical properties, but *in vivo* utility has been restricted by its possible cytotoxicity of the reactive crosslinkers. On the other hand, physically crosslinked hydrogels exhibit benign natures for biomedical applications due to the absence of reactive and potentially toxic crosslinkers. However, due to the poor durability of hydrogel physical interactions in the body, the physically crosslinked hydrogels exhibit instability and poor mechanical properties. Overall, this class of hydrogel demonstrates tunable properties, biocompatibility under some conditions, biodegradability and injectability, making them important and promising materials for biomedical applications.

2.3 REFERENCES

(1) Edgar, K. J.; Buchanan, C. M.; Debenham, J. S.; Rundquist, P. A.; Seiler, B. D.; Shelton, M. C.; Tindall, D. Advances in Cellulose Ester Performance and Application. *Prog. Polym. Sci.* **2001**, *26* (9), 1605–1688. https://doi.org/10.1016/S0079-6700(01)00027-2.

(2) Zhang, R.; Edgar, K. J. Properties, Chemistry, and Applications of the Bioactive Polysaccharide Curdlan. *Biomacromolecules* **2014**, *15* (4), 1079–1096. https://doi.org/10.1021/bm500038g.

(3) Fox, S. C.; Li, B.; Xu, D.; Edgar, K. J. Regioselective Esterification and Etherification of Cellulose - A Review. *Biomacromolecules* **2011**, *12*, 1956–1972. https://doi.org/10.1021/bm200260d.

(4) Mattox, K. L.; Maningas, P. A.; Moore, E. E.; Mateer, J. R.; Marx, J. A.; Aprahamian, C.; Burch, J. M.; Pepe, P. E. Prehospital Hypertonic Saline/Dextran Infusion for Post-Traumatic Hypotension. The U.S.A. Multicenter Trial. *Ann. Surg.* **1991**, *213* (5), 482–491. https://doi.org/10.1097/00000658-199105000-00014.

(5) Wang, J.-S.; Matyjaszewski, K. Controlled/"Living" Radical Polymerization. Atom Transfer Radical Polymerization in the Presence of Transition-Metal Complexes. *J. Am. Chem. Soc.* **1995**, *117* (20), 5614–5615. https://doi.org/10.1021/ja00125a035.

(6) Wang, J.-S.; Matyjaszewski, K. Controlled/"Living" Radical Polymerization. Halogen Atom Transfer Radical Polymerization Promoted by a Cu(I)/Cu(II) Redox Process. *Macromolecules* **1995**, *28* (23), 7901–7910. https://doi.org/10.1021/ma00127a042.

(7) and, D. M. H.; Ohno, K. Well-Defined Oligosaccharide-Terminated Polymers from Living Radical Polymerization. **2000**. https://doi.org/10.1021/BM005531U.

(8) Yagi, S.; Kasuya, N.; Fukuda, K. Synthesis and Characterization of Cellulose-b-Polystyrene. *Polym. J.* **2010**, *42* (4), 342–348. https://doi.org/10.1038/pj.2009.342.

(9) Houga, C.; Meins, J.-F. Le; Borsali, R.; Taton, D.; Gnanou, Y. Synthesis of ATRP-Induced Dextran-b-Polystyrene Diblock Copolymers and Preliminary Investigation of Their Self-Assembly in Water. *Chem. Commun.* **2007**, *0* (29), 3063. https://doi.org/10.1039/b706248f.

(10) Heinze, T.; Liebert, T.; Heublein, B.; Hornig, S. Functional Polymers Based on Dextran. In *Polysaccharides II*; Springer Berlin Heidelberg, 2006; pp 199–291. https://doi.org/10.1007/12_100.

(11) Isabelle Ydens, †; Delphine Rutot, †; Philippe Degée, †; Jean-Luc Six, ‡; Edith Dellacherie, ‡ and; Philippe Dubois*, †. Controlled Synthesis of Poly(ε-Caprolactone)-Grafted Dextran Copolymers as Potential Environmentally Friendly Surfactants. **2000**. https://doi.org/10.1021/MA0002803.

(12) Novoa-Carballal, R.; Pfaff, A.; Müller, A. H. E. Interpolyelectrolyte Complexes with a Polysaccharide Corona from Dextran-Block-PDMAEMA Diblock Copolymers. *Polym. Chem.* **2013**, *4* (7), 2278. https://doi.org/10.1039/c3py21088j.

(13) Nicolas, J.; Guillaneuf, Y.; Lefay, C.; Bertin, D.; Gigmes, D.; Charleux, B. Nitroxide-Mediated Polymerization. *Prog. Polym. Sci.* **2013**, *38* (1), 63–235. https://doi.org/10.1016/J.PROGPOLYMSCI.2012.06.002.

(14) Narumi, A.; Miura, Y.; Otsuka, I.; Yamane, S.; Kitajyo, Y.; Satoh, T.; Hirao, A.; Kaneko, N.; Kaga, H.; Kakuchi, T. End-Functionalization of Polystyrene by Malto-Oligosaccharide Generating Aggregation-Tunable Polymeric Reverse Micelle. *J. Polym. Sci. Part A Polym. Chem.* **2006**, *44* (16), 4864–4879. https://doi.org/10.1002/pola.21582.

(15) John Chiefari; Y. K. (Bill) Chong; Frances Ercole; Julia Krstina; Justine Jeffery; Tam P. T. Le; Roshan T. A. Mayadunne; Gordon F. Meijs; Catherine L. Moad; Graeme Moad, *; et al. Living Free-Radical Polymerization by Reversible Addition−Fragmentation Chain Transfer: The RAFT Process. **1998**. https://doi.org/10.1021/MA9804951.

(16) Bernard, J.; Save, M.; Arathoon, B.; Charleux, B. Preparation of a Xanthate-Terminated Dextran by Click Chemistry: Application to the Synthesis of Polysaccharide-Coated Nanoparticles via Surfactant-Freeab Initio Emulsion Polymerization of Vinyl Acetate. *J. Polym. Sci. Part A Polym. Chem.* **2008**, *46* (8), 2845–2857. https://doi.org/10.1002/pola.22618.

(17) Borch, R. F.; Bernstein, M. D.; Durst, H. D. Cyanohydridoborate Anion as a Selective Reducing Agent. *J. Am. Chem. Soc.* **1971**, *93* (12), 2897–2904. https://doi.org/10.1021/ja00741a013.

(18) Yalpani, M.; Brooks, D. E. Selective Chemical Modifications of Dextran. *J. Polym. Sci. Polym. Chem. Ed.* **1985**, *23* (5), 1395–1405. https://doi.org/10.1002/pol.1985.170230513.

(19) W. T. E. Bosker, *,†; K. Ágoston, ‡; M. A. Cohen Stuart, †; W. Norde, †; J. W. Timmermans, ‡ and; Slaghek§, T. M. Synthesis and Interfacial Behavior of Polystyrene−Polysaccharide Diblock Copolymers. **2003**. https://doi.org/10.1021/MA020925U.

(20) Hernandez, O. S.; Soliman, G. M.; Winnik, F. M. Synthesis, Reactivity, and PH-Responsive Assembly of New Double Hydrophilic Block Copolymers of Carboxymethyldextran and Poly(Ethylene Glycol). *Polymer (Guildf).* **2007**, *48* (4), 921–930. https://doi.org/10.1016/J.POLYMER.2006.12.036.

(21) Zhang, T.; Marchant, R. E. Novel Polysaccharide Surfactants: Synthesis of Model Compounds and Dextran-Based Surfactants. *Macromolecules* **1994**, *27* (25), 7302–7308. https://doi.org/10.1021/ma00103a011.

(22) Olga Aronov, †; Aviva T. Horowitz, ‡; Alberto Gabizon, ‡ and; Dan Gibson*, †,§. Folate-Targeted PEG as a Potential Carrier for Carboplatin Analogs. Synthesis and in Vitro Studies. **2003**. https://doi.org/10.1021/BC025642L.

(23) Huynh, R.; Chaubet, F.; Jozefonvicz, J. Anticoagulant Properties of Dextranmethylcarboxylate Benzylamide Sulfate (DMCBSu); a New Generation of Bioactive Functionalized Dextran.

Carbohydr. Res. **2001**, *332* (1), 75–83. https://doi.org/10.1016/S0008-6215(01)00066-0.

(24) Liu, Y.; Shu, X. Z.; Prestwich, G. D. Reduced Postoperative Intra-Abdominal Adhesions Using Carbylan-SX, a Semisynthetic Glycosaminoglycan Hydrogel. *Fertil. Steril.* **2007**, *87* (4), 940–948. https://doi.org/10.1016/J.FERTNSTERT.2006.07.1532.

(25) Kolb, H. C.; Finn, M. G.; Sharpless, K. B. Click Chemistry: Diverse Chemical Function from a Few Good Reactions. *Angew. Chemie Int. Ed.* **2001**, *40* (11), 2004–2021. https://doi.org/10.1002/1521-3773(20010601)40:11<2004::AID-ANIE2004>3.0.CO;2-5.

(26) Meng, X.; Edgar, K. J. "Click" Reactions in Polysaccharide Modification. *Prog. Polym. Sci.* **2016**, *53*, 52–85. https://doi.org/10.1016/J.PROGPOLYMSCI.2015.07.006.

(27) Kamitakahara, H.; Enomoto, Y.; Hasegawa, C.; Nakatsubo, F. Synthesis of Diblock Copolymers With Cellulose Derivatives. 2. Characterization and Thermal Properties of Cellulose Triacetate-Block-Oligoamide-15. *Cellulose* **2005**, *12* (5), 527–541. https://doi.org/10.1007/s10570-005-7135-3.

(28) Nakagawa, A.; Fenn, D.; Koschella, A.; Heinze, T.; Kamitakahara, H. Synthesis of Diblock Methylcellulose Derivatives with Regioselective Functionalization Patterns. *J. Polym. Sci. Part A Polym. Chem.* **2011**, *49* (23), 4964–4976. https://doi.org/10.1002/pola.24952.

(29) Nakagawa, A.; Kamitakahara, H.; Takano, T. Synthesis and Thermoreversible Gelation of Diblock Methylcellulose Analogues via Huisgen 1,3-Dipolar Cycloaddition. *Cellulose* **2012**, *19* (4), 1315–1326. https://doi.org/10.1007/s10570-012-9703-7.

(30) Györgydeák, Z.; Szilágyi, L.; Paulsen, H. Synthesis, Structure and Reactions of Glycosyl Azides. *J. Carbohydr. Chem.* **1993**, *12* (2), 139–163. https://doi.org/10.1080/07328309308021266.

(31) Kamitakahara, H.; Nakatsubo, F.; Klemm, D. Block Co-Oligomers of Tri-O-Methylated and Unmodified Cello-Oligosaccharides as Model Compounds for Methylcellulose and Its

Dissolution/Gelation Behavior. *Cellulose* **2006**, *13* (4), 375–392. https://doi.org/10.1007/s10570-005-9003-6.

(32) de Medeiros Modolon, S.; Otsuka, I.; Fort, S.; Minatti, E.; Borsali, R.; Halila, S. Sweet Block Copolymer Nanoparticles: Preparation and Self-Assembly of Fully Oligosaccharide-Based Amphiphile. *Biomacromolecules* **2012**, *13* (4), 1129–1135. https://doi.org/10.1021/bm3000138.

(33) Schatz, C.; Louguet, S.; Le Meins, J.-F.; Lecommandoux, S. Polysaccharide- *Block* -Polypeptide Copolymer Vesicles: Towards Synthetic Viral Capsids. *Angew. Chemie Int. Ed.* **2009**, *48* (14), 2572–2575. https://doi.org/10.1002/anie.200805895.

(34) Mullarkey, C. J.; Edelstein, D.; Brownlee, M. Free Radical Generation by Early Glycation Products: A Mechanism for Accelerated Atherogenesis in Diabetes. *Biochem. Biophys. Res. Commun.* **1990**, *173* (3), 932–939. https://doi.org/10.1016/S0006-291X(05)80875-7.

(35) Upadhyay, K. K.; Meins, J.-F. Le; Misra, A.; Voisin, P.; Bouchaud, V.; Ibarboure, E.; Schatz, C.; Lecommandoux, S. Biomimetic Doxorubicin Loaded Polymersomes from Hyaluronan- *Block* -Poly(γ-Benzyl Glutamate) Copolymers. *Biomacromolecules* **2009**, *10* (10), 2802–2808. https://doi.org/10.1021/bm9006419.

(36) Otsuka, I.; Fuchise, K.; Halila, S.; Fort, S.; Aissou, K.; Pignot-Paintrand, I.; Chen, Y.; Narumi, A.; Kakuchi, T.; Borsali, R. Thermoresponsive Vesicular Morphologies Obtained by Self-Assemblies of Hybrid Oligosaccharide- *Block* -Poly(*N* -Isopropylacrylamide) Copolymer Systems. *Langmuir* **2010**, *26* (4), 2325–2332. https://doi.org/10.1021/la902743y.

(37) Kim, S.; Stannett, V. T.; Gilbert, R. D. Biodegradable Cellulose Block Copolymers. *J. Macromol. Sci. Part A - Chem.* **1976**, *10* (4), 671–679. https://doi.org/10.1080/00222337608061209.

(38) Peppas, N. A.; Bures, P.; Leobandung, W.; Ichikawa, H. Hydrogels in Pharmaceutical Formulations. *Eur. J. Pharm. Biopharm.* **2000**, *50* (1), 27–46. https://doi.org/10.1016/S0939-

6411(00)00090-4.

(39) Hoffman, A. S. Hydrogels for Biomedical Applications. *Adv. Drug Deliv. Rev.* **2002**, *54* (1), 3–12. https://doi.org/10.1016/S0169-409X(01)00239-3.

(40) Peppas, N. A. Hydrogels and Drug Delivery. *Curr. Opin. Colloid Interface Sci.* **1997**, *2* (5), 531–537. https://doi.org/10.1016/S1359-0294(97)80103-3.

(41) Hatefi, A.; Amsden, B. Biodegradable Injectable in Situ Forming Drug Delivery Systems. *J. Control. Release* **2002**, *80* (1–3), 9–28. https://doi.org/10.1016/S0168-3659(02)00008-1.

(42) Fukuda, J.; Khademhosseini, A.; Yeo, Y.; Yang, X.; Yeh, J.; Eng, G.; Blumling, J.; Wang, C.-F.; Kohane, D. S.; Langer, R. Micromolding of Photocrosslinkable Chitosan Hydrogel for Spheroid Microarray and Co-Cultures. *Biomaterials* **2006**, *27* (30), 5259–5267. https://doi.org/10.1016/j.biomaterials.2006.05.044.

(43) Tsai, W.-B.; Chen, Y.-R.; Liu, H.-L.; Lai, J.-Y. Fabrication of UV-Crosslinked Chitosan Scaffolds with Conjugation of RGD Peptides for Bone Tissue Engineering. *Carbohydr. Polym.* **2011**, *85* (1), 129–137. https://doi.org/10.1016/j.carbpol.2011.02.003.

(44) Li, B.; Wang, L.; Xu, F.; Gang, X.; Demirci, U.; Wei, D.; Li, Y.; Feng, Y.; Jia, D.; Zhou, Y. Hydrosoluble, UV-Crosslinkable and Injectable Chitosan for Patterned Cell-Laden Microgel and Rapid Transdermal Curing Hydrogel in Vivo. *Acta Biomater.* **2015**, *22*, 59–69. https://doi.org/10.1016/J.ACTBIO.2015.04.026.

(45) Ruel-Gariépy, E.; Leroux, J.-C. In Situ-Forming Hydrogels—Review of Temperature-Sensitive Systems. *Eur. J. Pharm. Biopharm.* **2004**, *58* (2), 409–426. https://doi.org/10.1016/j.ejpb.2004.03.019.

(46) Maia, J.; Ferreira, L.; Carvalho, R.; Ramos, M. A.; Gil, M. H. Synthesis and Characterization of New Injectable and Degradable Dextran-Based Hydrogels. *Polymer (Guildf).* **2005**, *46* (23), 9604–

9614. https://doi.org/10.1016/J.POLYMER.2005.07.089.

(47) Wang, T.; Turhan, M.; Gunasekaran, S. Polym. Int. Selected Properties of PH-sensitive, Biodegradable Chitosan–Poly (Vinyl Alcohol) Hydrogel. **2004**, *53* (7), 911–918.

(48) Woodward, M. P.; Young Jr, W. W.; Bloodgood, R. A. J. immunol. methods. Detection of Monoclonal Antibodies Specific for Carbohydrate Epitopes Using Periodate Oxidation. **1985**, *78* (1), 143–153.

(49) Tan, H.; Chu, C. R.; Payne, K. A.; Marra, K. G. Injectable in Situ Forming Biodegradable Chitosan–Hyaluronic Acid Based Hydrogels for Cartilage Tissue Engineering. *Biomaterials* **2009**, *30* (13), 2499–2506. https://doi.org/10.1016/J.BIOMATERIALS.2008.12.080.

(50) Wang, D.-A.; Varghese, S.; Sharma, B.; Strehin, I.; Fermanian, S.; Gorham, J.; Fairbrother, D. H.; Cascio, B.; Elisseeff, J. H. Multifunctional Chondroitin Sulphate for Cartilage Tissue–Biomaterial Integration. *Nat. Mater.* **2007**, *6* (5), 385–392. https://doi.org/10.1038/nmat1890.

(51) Liu, H.; Sui, X.; Xu, H.; Zhang, L.; Zhong, Y.; Mao, Z. Self-Healing Polysaccharide Hydrogel Based on Dynamic Covalent Enamine Bonds. *Macromol. Mater. Eng.* **2016**, *301* (6), 725–732. https://doi.org/10.1002/mame.201600042.

(52) Nair, D. P.; Podgórski, M.; Chatani, S.; Gong, T.; Xi, W.; Fenoli, C. R.; Bowman, C. N. The Thiol-Michael Addition Click Reaction: A Powerful and Widely Used Tool in Materials Chemistry. *Chem. Mater.* **2014**, *26* (1), 724–744. https://doi.org/10.1021/cm402180t.

(53) Zheng Shu, X.; Liu, Y.; Palumbo, F. S.; Luo, Y.; Prestwich, G. D. In Situ Crosslinkable Hyaluronan Hydrogels for Tissue Engineering. *Biomaterials* **2004**, *25* (7–8), 1339–1348. https://doi.org/10.1016/J.BIOMATERIALS.2003.08.014.

(54) Giyoong Tae, *,†; Yang-Jung Kim, †; Won-Il Choi, †; Mihye Kim, †; Patrick S. Stayton, ‡ and; Hoffman‡, A. S. Formation of a Novel Heparin-Based Hydrogel in the Presence of Heparin-

Binding Biomolecules. **2007**. https://doi.org/10.1021/BM0701189.

(55) Burdick, J. A.; Prestwich, G. D. %J A. materials. Hyaluronic Acid Hydrogels for Biomedical Applications. **2011**, *23* (12), H41–H56.

(56) Shu, X. Z.; Liu, Y.; Palumbo, F.; Prestwich, G. D. Disulfide-Crosslinked Hyaluronan-Gelatin Hydrogel Films: A Covalent Mimic of the Extracellular Matrix for in Vitro Cell Growth. *Biomaterials* **2003**, *24* (21), 3825–3834. https://doi.org/10.1016/S0142-9612(03)00267-9.

(57) Cai, S.; Liu, Y.; Zheng Shu, X.; Prestwich, G. D. Injectable Glycosaminoglycan Hydrogels for Controlled Release of Human Basic Fibroblast Growth Factor. *Biomaterials* **2005**, *26* (30), 6054–6067. https://doi.org/10.1016/J.BIOMATERIALS.2005.03.012.

(58) Kim, M.; Lee, J. Y.; Jones, C. N.; Revzin, A.; Tae, G. Heparin-Based Hydrogel as a Matrix for Encapsulation and Cultivation of Primary Hepatocytes. *Biomaterials* **2010**, *31* (13), 3596–3603. https://doi.org/10.1016/J.BIOMATERIALS.2010.01.068.

(59) Lee, K. Y.; Mooney, D. J. Alginate: Properties and Biomedical Applications. *Prog. Polym. Sci.* **2012**, *37* (1), 106–126. https://doi.org/10.1016/J.PROGPOLYMSCI.2011.06.003.

(60) Kuo, C. K.; Ma, P. X. Ionically Crosslinked Alginate Hydrogels as Scaffolds for Tissue Engineering: Part 1. Structure, Gelation Rate and Mechanical Properties. *Biomaterials* **2001**, *22* (6), 511–521. https://doi.org/10.1016/S0142-9612(00)00201-5.

(61) Donati, I.; Asaro, F.; Paoletti, S. Experimental Evidence of Counterion Affinity in Alginates: The Case of Nongelling Ion Mg^{2+}. *J. Phys. Chem. B* **2009**, *113* (39), 12877–12886. https://doi.org/10.1021/jp902912m.

(62) Sun, J.-Y.; Zhao, X.; Illeperuma, W. R. K.; Chaudhuri, O.; Oh, K. H.; Mooney, D. J.; Vlassak, J. J.; Suo, Z. Highly Stretchable and Tough Hydrogels. *Nature* **2012**, *489* (7414), 133–136. https://doi.org/10.1038/nature11409.

(63) Berger, J.; Reist, M.; Mayer, J. .; Felt, O.; Gurny, R. Structure and Interactions in Chitosan Hydrogels Formed by Complexation or Aggregation for Biomedical Applications. *Eur. J. Pharm. Biopharm.* **2004**, *57* (1), 35–52. https://doi.org/10.1016/S0939-6411(03)00160-7.

(64) Molinaro, G.; Leroux, J.-C.; Damas, J.; Adam, A. Biocompatibility of Thermosensitive Chitosan-Based Hydrogels: An in Vivo Experimental Approach to Injectable Biomaterials. *Biomaterials* **2002**, *23* (13), 2717–2722. https://doi.org/10.1016/S0142-9612(02)00004-2.

(65) Wei, Z.; Yang, J. H.; Liu, Z. Q.; Xu, F.; Zhou, J. X.; Zrínyi, M.; Osada, Y.; Chen, Y. M. Novel Biocompatible Polysaccharide-based Self-healing Hydrogel. *Adv. Funct.* **2015**, *25* (9), 1352–1359.

Chapter 3: Synthesis of polysaccharide-based block copolymers via olefin cross-metathesis

(Published in *Carbohydrate polymers*, **2020**, 115530,
https://doi.org/10.1016/J.CARBPOL.2019.115530)

Junyi Chen[a], Hiroshi Kamitakahara[b], and Kevin J. Edgar[c, d]

[a]Department of Chemistry, Virginia Tech, Blacksburg, VA 24061, United States

[b]Graduate School of Agriculture, Kyoto University, Kyoto, Japan

[c]Department of Sustainable Biomaterials, Virginia Tech, Blacksburg, VA 24061, United States

[d]Macromolecules Innovation Institute, Virginia Tech, Blacksburg, VA 24061, United States

3.1 Abstract

Polysaccharide-based copolymers with brush-like, graft architectures have been prepared by many investigators. In contrast, it is challenging to prepare linear polysaccharide-based block copolymers. Only a few approaches have been reported for preparation of such architectures, despite the clear application potential of renewable-based linear block copolymers. The challenging nature of regioselective polysaccharide end-group functionalization has impeded their preparation. Herein we report a different, flexible approach to linear block copolymers, demonstrated for derivatives of renewable, natural cellulose. To illustrate this approach, trimethyl cellulose-*b*-poly(ethylene glycol), trimethyl cellulose-*b*-poly(tetrahydrofuran) and trimethyl cellulose-*b*-poly(lactic acid) were synthesized by a coupling strategy. Trimethyl cellulose was functionalized regiospecifically at the reducing end anomeric carbon to create an ω-unsaturated alkyl acetal by solvolysis of trimethyl cellulose with an ω-unsaturated alcohol. Subsequently, mild and versatile olefin cross-metathesis was used to couple efficiently (100% conversion) the trimethyl cellulose block with a series of acrylate derivatives, including acrylated polymer blocks. The targeted block co-polymeric structures were confirmed by nuclear magnetic resonance (NMR)

spectroscopy, and the degree of polymerization was relatively well-preserved during the coupling step, as shown by size exclusion chromatography (SEC). The results confirm that this new solvolysis/cross-metathesis method is a promising approach to polysaccharide-based linear AB, and likely ABC, block copolymers.

3.2 Introduction

Cellulose, a homopolymer of glucose with the structure 4→)β-D-Glc*p*(→1, is among the most abundant natural polysaccharides. Researchers and industries prepare cellulose derivatives in order to enhance processability (solution and/or thermal) and tailor properties to application needs. These derivatives are renewable-based, in some cases are biodegradable[1], and their modified properties (vs. cellulose) frequently permit high performance and the potential to replace petroleum-based polymers in a wide variety of applications[2]. On the other hand, the breadth of commercially available cellulose derivatives is constrained by the poor solubility and low reactivity of cellulose itself. Available cellulose esters and ethers do range in properties (for example, from water-soluble ethers like carboxymethyl cellulose, to cellulose esters like cellulose acetate butyrates that have some solubility in non-polar organic solvents), but that range is circumscribed by the limits of the synthetic chemistry. As cellulose derivatives have linear, high degree of polymerization (DP) backbones, they should be good candidates for block copolymer synthesis, if and only if regioselective end modification can be accomplished.

Investigators often design block copolymer materials comprising building blocks that have quite distinct properties, even blocks that are thermodynamically incompatible. Block copolymer structure-property relationships are heavily influenced by block incompatibility effects; such incompatibility can afford morphology that may uniquely enable practical applications.[3] Polysaccharide backbones are stiff, broad (more ribbon-like than linear) and generally hydrophilic,

properties which distinguish them from hydrophobic, flexible, highly entangled polyolefins. Thus polysaccharide-*b*-polyolefin block copolymers would be predicted to undergo microphase separation, which could generate morphologies leading to high performance in applications including compatibilizers[4], capacitors[5], batteries[6], and separation membranes[7].

Currently, no polysaccharide-based block copolymers are commercially available, and relatively few synthetic approaches to such copolymers have been described. Synthesis of ditelechelic polymers based on natural polysaccharides is inherently difficult, since polysaccharides are multifunctional, and therefore are difficult to end-functionalize selectively. Reactivity differences between polysaccharide hydroxyl groups are relatively small, and discrimination between them is further impaired by the strong reaction conditions that are often necessary due to the influence of the sterically bulky and often rigid polysaccharide chain.

Past studies of polysaccharide block copolymers have typically exploited a potentially unique and distinguishable reactive site; the anomeric carbon (C1) of the reducing end monosaccharide of the chain, that is in the aldehyde oxidation state. Since the reducing end anomeric position is a hemiacetal in equilibrium with a ring-opened aldehyde, its reactivity is distinct from that of every other position along the polymer, and researchers have taken advantage of this fact. One approach has been conversion to a 1-glycosyl bromide by reaction with HBr, analogous to small molecule glycosylation reactions[8]. In another approach, reductive amination (e.g. with $NaBH_3CN$ as reducing agent) is used to convert the reducing end aldehyde into an amine[9], with concomitant ring opening of the former reducing end glucose. Kamitakahara reported application of Huisgen click chemistry to synthesis of diblock cellulosic copolymers[10]. Synthesis of a glycosyl bromide of cellulose by reaction with HBr, followed by bromide displacement by azide, affords a cellulose ester segment activated at the reducing end with a C-1 azide group. Then they reacted this azide

with an ω-alkyne segment using copper-catalyzed Huisgen click chemistry[11] to make diblock copolymers containing linking triazole rings[12].

Olefin cross-metathesis (CM), introduced primarily by the Grubbs group[13], is a highly efficient synthetic tool that has been intensively applied in polymerization chemistry[14, 15]. Recently, the Edgar group reported that olefin CM is a highly effective method for polysaccharide modification. Cellulose derivatives to which ω-unsaturated side chains had been appended as "handles", using relatively conventional chemistry, were successfully reacted with a series of CM partners including acrylic acid, acrylates, and acrylamides by employing the Hoveyda–Grubbs 2nd generation ruthenium complex catalyst. These studies showed that CM is mild, fast, functional group-tolerant, efficient (with high yields and conversions), and selective for synthesis of cellulose derivatives with brush architectures. Those brushes may bear a diverse set of functional groups16, 17, 18.

Initial explorations of some metathesis chemistries have been reported for preparation of non-polysaccharide based block copolymers. An important, illustrative example is the work reported by Meier19, where his group used an interesting acyclic diene metathesis and olefin cross-metathesis (ADMET) approach to synthesize a diblock copolymer. Meier reacted an acrylate-terminated poly(□□hydroxyhexanoic acid) with an aliphatic ester bearing a terminal isolated olefin (undec-1-enyl acrylate, Type I by the Grubbs categorization)13 under ADMET conditions to prepare a block copolymer. A recent study reported a cellulose triacetate-poly(butadiene)-based block copolymer synthesized by ring-opening metathesis that proved to be a remarkable compatibilizer, strongly reducing interfacial energy of such ordinarily incompatible polymers as methyl cellulose and poly(ethylene) and enabling a well-mixed blend that displayed combined useful properties of both polymers.4 There have however been no reports of using CM chemistry as a regio- and chemoselective route to polysaccharide block copolymers. Herein we employ a

coupling strategy to build diblock copolymers via olefin CM. We hypothesize that solvolysis of a polysaccharide or derivative with an □-unsaturated alcohol will afford a suitable, reactive substrate for olefin CM. We further hypothesize that reaction of this polysaccharide, functionalized with a Type 1 reactive olefin regiospecifically at the reducing end, with another polymer segment bearing a Grubbs Type II olefin20 will therefore create a diblock copolymer. We investigate solvolysis of trimethyl cellulose with a terminally unsaturated alkanol, determining its suitability for synthesis of derivatives with a single exposed, reactive 4-hydroxyl in the non-reducing end monosaccharide, and an □-olefin-bearing substituent (Grubbs Type I) at the anomeric position of the reducing end monosaccharide. Clearly these two functional groups would have orthogonal reactivity, and lend themselves to elaboration to block copolymer structures like A-B, A-B-C, A-B-A, and even more complex architectures. We investigate reaction of the solvolysis products with various acrylates via olefin CM to confirm that the olefin appended to the reducing end of trimethyl cellulose has the necessary CM reactivity. Finally, we describe efforts to carry out CM with model polymers bearing Grubbs Type II olefins, for example an acrylated polyethylene glycol, in order to prove the copolymer synthesis concept by synthesizing AB diblock copolymers including (PEG)-b-(trimethyl cellulose), trimethyl cellulose-b-PTHF, and trimethyl cellulose-b-PLA, in order to test the scope of this approach and to further explore the properties of this class of materials. This is a preliminary synthetic study to prove the practicality of this approach, and iron out issues of reactivity, purification, and other key aspects, towards realizing the potential of sustainable-based block copolymers in a wide variety of applications which may include use as polymer compatibilizers, surfactants, emulsifiers, membranes, in drug delivery systems, and many others.

3.3 Experimental section

3.3.1 Abbreviations

TMC refers to trimethyl cellulose. TMC-Cn refers to trimethyl cellulose with terminal ω-unsaturated alkyl substituent, where "n" denotes the length of the terminally unsaturated chain. For example, TMC-C3 refers to the allyl glycoside of TMC, while TMC-C5 refers to its 1-pent-4-enyl glycoside. Polymers are abbreviated as PEG (polyethylene glycol), PTHF (poly(tetrahydrofuran)), and PLA (poly(L-lactide)). Block copolymer abbreviations include TMC-*b*-PEG for TMC–PEG diblock copolymer, TMC-*b*-PTHF for TMC-PTHF diblock copolymer, and TMC-*b*-PLA for TMC–PLA diblock copolymer.

3.3.2 Materials

Methyl cellulose (DS(methyl) = 1.96, determined by ^{1}H NMR; approximate molecular weight 40,000 g/mol, provided by Sigma Aldrich) was purchased from Sigma Aldrich. Sodium hydride (95%), methyl iodide (MeI), methanesulfonic acid, allyl alcohol, anhydrous tetrahydrofuran (THF), acrylic acid (AA), methyl acrylate (MA), poly(ethylene glycol) methyl ether acrylate (PEGMEA) (M_n 480 g/mol, DP 9), 2,6-di-tert-butyl-4-methylphenol (BHT), Hoveyda-Grubbs' second generation catalyst, 4-penten-1-ol, acryloyl chloride, acrylate-terminated poly(L-lactide) (M_n 2500 g/mol), polytetrahydrofuran (M_n 2000 g/mol), and triethyl amine were purchased from Sigma-Aldrich. All reagents were used as received without further purification. Dialysis tubing (molecular weight cutoff 3500 Da) was purchased from Fisher Scientific.

3.3.3 Measurements

^{1}H NMR spectra were acquired either on a Bruker Avance II spectrometer operating at 500 MHz or on an Agilent MR4 instrument operating at 400 MHz. All samples were analyzed as solutions in $CDCl_3$ (ca. 10 mg/mL) at 25 °C in standard 5 mm o.d. tubes. ^{13}C NMR spectra were acquired on a Bruker Avance II 500 MHz spectrometer with a minimum of 10,000 scans in $CDCl_3$ (ca. 40

mg/mL). FT-IR spectra were obtained on a Nicolet 8700 instrument using potassium bromide powder as matrix. T_g values were obtained by differential scanning calorimetry (DSC) on a TA Discovery instrument using a modulated DSC (MDSC) method: sample (ca. 5 mg dry powder in Tzero aluminum pan) first equilibrated at −50 °C and then gradually heated to 190 °C with underlying ramp heating rate 5 °C/min and oscillation amplitude ±0.5 °C with oscillation period 60 s. Size exclusion chromatography (SEC) in HPLC-grade THF was carried out at 30 °C and 1 mL/min flow rate on two connected Agilent PLgel Mixed-B columns with a Wyatt Dawn Heleos light scattering detector and a Wyatt Optilab Rex refractive index (RI) detector.

3.3.4 Preparation of trimethyl cellulose (DS = 3.0)

This methylation procedure follows the one described by Kamitakahara *et al.*.[21] To a solution of MC (DS = 1.8, 3.03 g, 0.016 mol) in anhydrous THF (100 mL), NaH (95%, 1.64 g, 0.064 mol, 4.8 equiv per hydroxyl group) was added at 0 °C. The reaction mixture was stirred at 50 °C overnight. Then MeI (4.0 mL, 0.064 mol, 4.8 equiv per hydroxyl group) was added to the solution. The reaction mixture was stirred at 50 °C for 72 h. MeOH (6 mL) was added to the reaction mixture, and then the mixture was poured slowly into water (3.0 L). The precipitates were washed with water three times, then with EtOH twice, centrifuged (12,000 rpm/10 min), and dried in a vacuum oven at 50 °C overnight to give a light yellow powder (2.485 g, 75.5% yield).

^{1}H NMR (400 MHz, $CDCl_3$): 2.95 (t, C2-H), 3.2-3.9 (m, cellulose backbone, C2-OCH_3, C3-OCH_3, C6-OCH_3), 4.33 (d, C1-H). ^{13}C NMR (500 MHz, $CDCl_3$): 58.13 (C6-OCH$_3$), 59.32 (C2-OCH$_3$), 59.52 (C3-OCH$_3$), 69.26 (C6), 73.83 (C5), 76.44 (C4), 82.47 (C2), 84.09 (C3), 102.18 (C1).

3.3.5 General procedure for solvolysis of TMC

Trimethyl cellulose (1.0 g, DS(Me) 3.0, 0.037 mmol) was dissolved in 10 mL $CHCl_3$ and 4-penten-1-ol (2.50 g, 29.03 mmol, about 784 equiv.) or allyl alcohol (2.56 g, 44.08 mmol, about

1190 equiv.). Methanesulfonic acid (0.22 g, 2.28 mmol, about 61 equiv.) was added to catalyze solvolysis. The solution was heated to 50 °C and stirred at that temperature for 2h. The reaction mixture was then cooled and poured slowly into 100 mL isopropanol. The resulting precipitate was isolated by filtration, then washed with 3 x 10 mL acetone to remove residual methanesulfonic acid. The final product was dried in a vacuum oven at 50 °C for 24 h to give a white powder (0.68 g, 68% yield).

^{1}H NMR (400 MHz, $CDCl_3$): 1.15 (m, -$OCH_2C\underline{H}_2CH_2CH=CH_2$), 2.14 (q, -$OCH_2CH_2C\underline{H}_2CH=CH_2$), 3.11 (t, -$OC\underline{H}_2CH_2CH_2CH=CH_2$), 2.95 (t, C2-$\underline{H}$), 3.2-3.9 (m, cellulose backbone, C2-$OC\underline{H}_3$, C3-$OC\underline{H}_3$, C6-$OC\underline{H}_3$), 4.33 (d, C1-$\underline{H}$). 4.92 (d, αC1-$\underline{H}$), 4.94-5.04 (m, -$OCH_2CH_2CH_2CH=C\underline{H}_2$), 5.75-5.86 (m, -$OCH_2CH_2CH_2C\underline{H}=CH_2$). ^{13}C NMR (500 MHz, $CDCl_3$): 28.82 (C6-$OCH_3\underline{C}H_3CH_3CH=CH_2$), 30.52 (C1-$OCH_3CH_3\underline{C}H_3CH=CH_2$), 58.13 (C6-$O\underline{C}H_3$), 59.32 (C2-$O\underline{C}H_3$), 59.52 (C3-$O\underline{C}H_3$), 69.26 (C6), 73.83 (C5), 72.39 73.34 (αC1-$O\underline{C}H_3CH_3CH_3CH=CH_2$, βC1- $O\underline{C}H_3CH_3CH_3CH=CH_2$) 76.44 (C4), 82.47 (C2), 84.09 (C3), 102.18 (C1), 114.97 (C1- $OCH_3CH_3CH_3CH=\underline{C}H_2$), 138.35 (C1- $OCH_3CH_3CH_3\underline{C}H=CH_2$).

3.3.6 General procedure for olefin metathesis of TMC-C5, illustrated with methyl acrylate.

TMC-C5 (0.25 g, 0.032 mmol) was dissolved in 10 mL THF under nitrogen. Hoveyda-Grubbs 2nd generation catalyst (5 mg, 0.008 mmol, 0.25 equiv.) and BHT (10 mg, 0.0454 mmol, 1.41 equiv, antioxidant) were added to the solution, then methyl acrylate (0.260 g, 3.02 mmol, 100 equiv.) was added. After 6 h, the reaction was terminated by adding ethyl vinyl ether at room temperature. The solution was added to acetone (100 mL) to precipitate the product. The product was isolated by filtration, following by washing with excess acetone, then was dried under vacuum for 18 h to give the final product (0.239 g, 0.029 mmol, yield 92%). Similar procedures were employed for olefin

metathesis of TMC-C5 with acrylic acid (0.225 g, 3.12 mmol, 103 equiv., yield 90%) and benzyl acrylate (0.226 g, 1.38 mmol, 46 equiv., yield 87%).

TMC-C5-MA ^{1}H NMR (400 MHz, $CDCl_3$): 1.15 (m, -$OCH_2C\underline{H}_2CH_2CH{=}CHCOOCH_3$), 2.14 (q, -$OCH_2CH_2C\underline{H}_2CH{=}CH_2COOCH_3$), 3.11 (t, -$OC\underline{H}_2CH_2CH_2CH{=}CHCOOCH_3$), 2.95 (t, C2-$\underline{H}$), 3.2-3.9 (m, cellulose backbone, C2-$OC\underline{H}_3$, C3-$OC\underline{H}_3$, C6-$OC\underline{H}_3$), 4.33 (d, C1-$\underline{H}$). 4.92 (d, αC1-$\underline{H}$), 5.82-5.86 (d, -$OCH_2CH_2CH_2CH{=}C\underline{H}COOCH_3$), 6.93-7.02 (m, -$OCH_2CH_2CH_2C\underline{H}{=}CHCOOCH_3$).

3.3.7 Procedure for olefin metathesis of TMC-C5 with PEG methyl ether acrylate, PTHF acrylate, and PLA acrylate

TMC-C5 (0.25 g, 0.032 mmol) was dissolved in 10 mL THF under nitrogen. Hoveyda-Grubbs 2nd generation catalyst (5 mg, 0.00798 mmol, 0.25 equiv.) and BHT (10 mg, 0.0454 mmol, 1.41 equiv.) were added and a green solution was formed, then PEG methyl ether acrylate (0.5 g, 480 g/mol, 1.66 mmol, 51.88 equiv.) was added. After 24 h, the solution displayed a brown color, and the reaction was terminated by adding ethyl vinyl ether. The solution was added to dialysis tubing, dialyzed against ethanol for 24 h, then against deionized (DI) water for 48 h. The final product was obtained by freeze drying (0.17 g, 0.020 mmol, yield 64%). TMC-*b*-PTHF (yield 78%) and TMC-*b*-PLA (yield 72%) were prepared by equivalent procedures. These two block copolymers were purified through dialysis against acetone for 72 h. The solid products were collected by centrifuging (7000 rpm at 25 °C) and dried in vacumn oven at 60 °C for 24 h.

TMC-C5-PEG ^{1}H NMR (400 MHz, $CDCl_3$): 1.15 (m, -$OCH_2C\underline{H}_2CH_2CH{=}CHCOO$-PEG), 2.14 (q, -$OCH_2CH_2C\underline{H}_2CH{=}CH_2COO$-PEG), 3.11 (t, -$OC\underline{H}_2CH_2CH_2CH{=}CHCOO$-PEG), 2.95 (t, C2-$\underline{H}$), 3.20-3.90 (m, cellulose backbone, C2-$OC\underline{H}_3$, C3-$OC\underline{H}_3$, C6-$OC\underline{H}_3$), 3.64 (t, PEG backbone) 4.33

(d, C1-H). 4.92 (d, αC1-H), 5.82-5.86 (d, -$OCH_2CH_2CH_2CH$=C<u>H</u>COO-PEG), 6.93-7.02 (m, -$OCH_2CH_2CH_2C$<u>H</u>=CHCOO-PEG). ^{13}C NMR (500 MHz, $CDCl_3$): 28.82 (C6-OCH_3<u>C</u>H_3CH_3CH=CHCOO-PEG), 30.52 (C1-OCH_3CH_3<u>C</u>H_3CH=CHCOO-PEG), 58.13 (C6-O<u>C</u>H_3), 59.32 (C2-O<u>C</u>H_3), 59.52 (C3-O<u>C</u>H_3), 69.26 (C6), 70.71 (PEG backbone), 73.83 (C5), 72.39 73.34 (αC1- O<u>C</u>$H_3CH_3CH_3CH$=CHCOO-PEG, βC1- O<u>C</u>$H_3CH_3CH_3CH$=CHCOO-PEG) 76.44 (C4), 82.47 (C2), 84.09 (C3), 102.18 (C1), 121.49 (C1- $OCH_3CH_3CH_3CH$=<u>C</u>HCOO-PEG), 148.93 (C1- $OCH_3CH_3CH_3$<u>C</u>H=CHCOO-PEG), 166.29 (C1- $OCH_3CH_3CH_3CH$=CH<u>C</u>OO-PEG).

3.4 Results and discussion

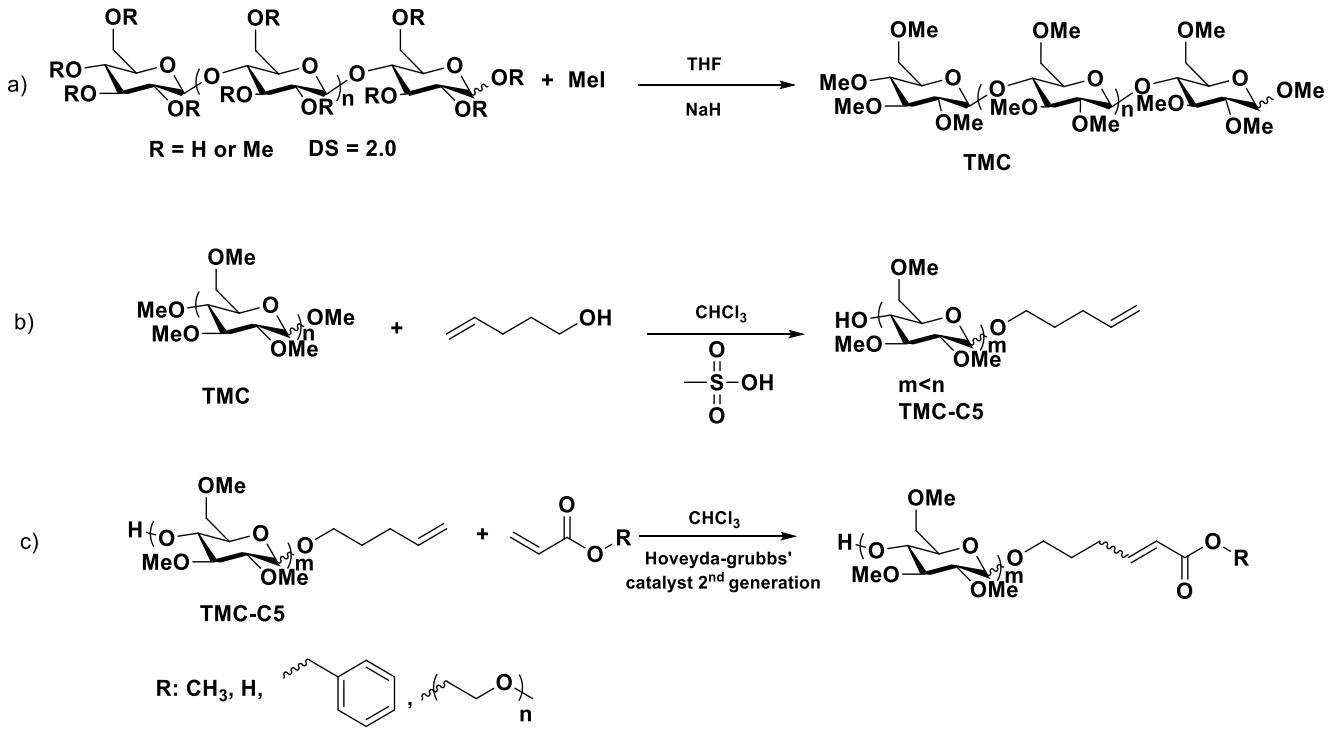

Scheme 1. a) Synthesis of TMC, b) TMC solvolysis product (TMC-C5), c) Olefin cross-metathesis of TMC-C5 with PEG methyl ether.

To explore cellulose-based block copolymers, we synthesized TMC with DS(Me) 3.0 from commercial methyl cellulose. TMC is a suitable substrate to test our synthetic strategy for two

reasons: 1) Solvolysis of persubstituted TMC with an olefin-bearing alcohol should afford heterotelechelic, difunctional polysaccharide derivatives **(Scheme 1)**. Since all 2-, 3-, and 6-oxygens are methylated, these derivatives have only a single exposed reactive C-4 hydroxyl at the non-reducing end, and a substituent bearing a terminal olefin at the reducing end, creating the potential to build a polysaccharide-based ABC triblock copolymer. 2) TMC has excellent solubility in various organic solvents (e.g. $CHCl_3$, CH_2Cl_2, THF). Peralkylation assures that, after solvolysis, the reducing end olefin and the non-reducing end C-4 OH will be the only two, orthogonal reactive sites on the polymer. The good solubility of the TMC block should allow selection from a broad range of reaction conditions for construction of block copolymers.

We investigated etherification of methyl cellulose (DS = 1.8) based on the work of Kamitakahara [21], in which NaH was used as base and MeI was the alkylating reagent. The DS value of TMC was determined to be 3.0 by ^{1}H NMR **(Fig.1)** integration. We emphasize that this permethylation was necessary to preserve the possibility of making ABC triblock copolymers; it would not be necessary if diblock copolymers were targeted.

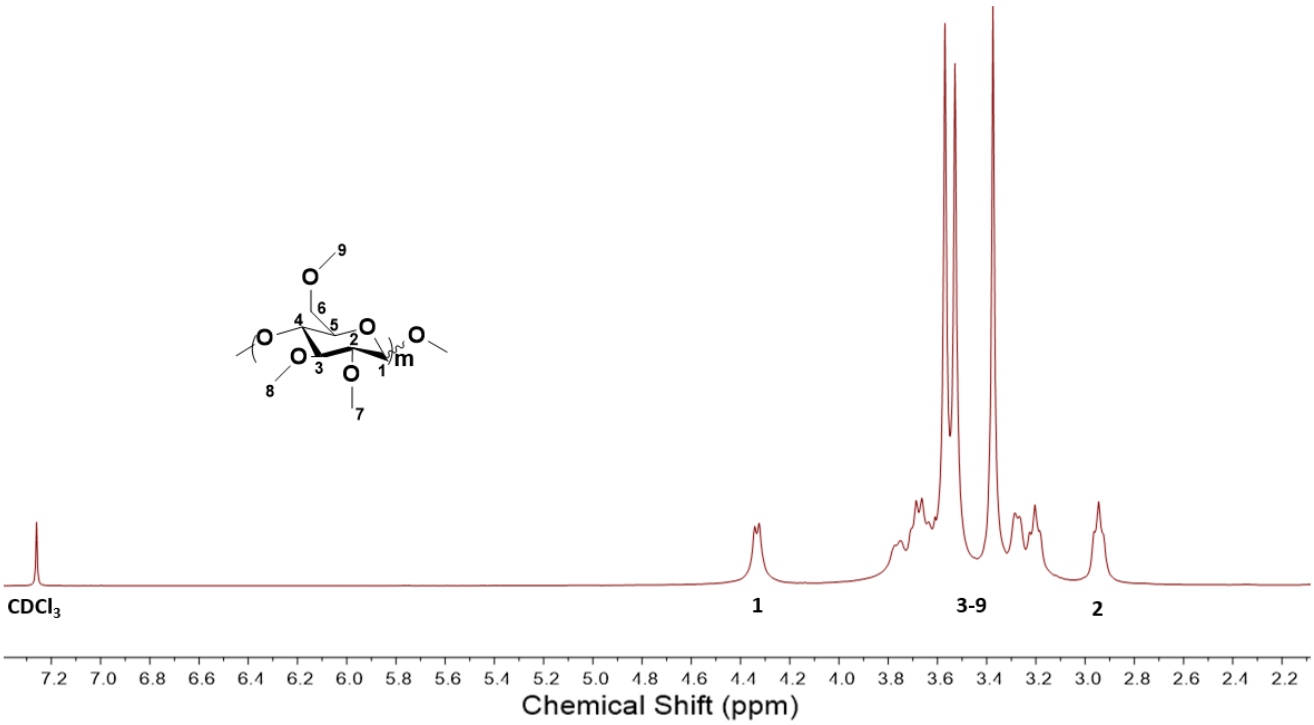

Fig.1 ^{1}H NMR spectrum of TMC.

Initially, we investigated solvolysis as a way to introduce C1 tethers with terminal unsaturation to serve as electron-rich metathesis partners of Type 1 in the Grubbs classification system[13]. In employing solvolysis, we needed to take a number of factors into consideration. The first thing to think about was the selection of acid catalyst, which protonates the C-1 acetal oxygen. We needed to avoid acids which can combine with free hydroxyls (sulfation), or which are difficult to separate from the product. Another factor to consider was the fact that solvolysis inherently degrades the DP of the starting TMC. In order to obtain a solvolysis product with sufficient molecular weight to serve as a useful polymer block, we needed to be able to influence the relative rates of solvolysis and DP loss by understanding the impact of solvolyis reaction conditions. A related process issue is the need for anhydrous conditions, since adventitious water could capture the anomeric cation, thereby causing DP loss without introduction of the needed ω-unsaturated glycosidic substituent. Therefore we sought acid concentration just sufficient to catalyze solvolysis, and optimal reaction

time for high solvolysis conversion while minimizing DP loss. We worked under anhydrous conditions to minimize water competition with the ω-unsaturated alcohol for the anomeric cation.

In this study, we chose methanesulfonic acid as acid catalyst due to its strong acidity (pKa = 2.6), organic solubility, and lack of propensity to combine with (sulfate) the polysaccharide. The result was a suitable procedure (see experimental section) which provided solvolysis product with relatively high molecular weight.

We chose allyl alcohol for solvolysis screening experiments since it is relatively inexpensive, and since we have shown in previous studies that allyl polysaccharide ethers (of the 2-, 3-, and 6-OH groups)[16] do participate in olefin CM chemistry, albeit at modest to moderate conversions. 4-Penten-1-ol was chosen as the unsaturated alcohol for further solvolysis and subsequent CM studies, since pentenyl cellulose ethers have been shown by our group to be reactive, useful CM substrates[16]. Solvolysis at 50 °C in chloroform was sufficient, and products were readily obtained free of acid and excess alcohol by using isopropanol as non-solvent and washing the precipitate with acetone. Initially, we were concerned that quantification of anomeric substitution might be difficult, as signal intensity of the single anomeric substituent could have been insufficient for reliable integration. We were pleased to find that ^{1}H NMR was a capable tool for quantitative analysis of the allyl (TMC-C3) **(Fig. S8)** and pent-4-enyl (TMC-C5) glycosides **(Fig. 2a)**, due to the sharpness of the olefin signals and their clean separation downfield of cellulose backbone resonances. Olefin ^{1}H NMR resonances of TMC-C5 (5.82 (a) and 4.98 (b) ppm, **Fig. 2a**) and TMC-C3 (5.92 (a) and 5.25 (b) ppm, **Fig. S8**) were present in the solvolysis products, indicating that pent-4-enyl and allyl, respectively, were successfully appended to the TMC reducing end. ^{13}C NMR spectroscopy was also useful for establishing identity. For example in the ^{13}C NMR spectrum of TMC-C5 (**Fig. 2b**), olefin resonances at 138 (10, proximal end) and 115 ppm (11,

distal end) were observed, supporting formation of the proposed solvolysis product. To our knowledge this is the first time that a polysaccharide derivative has been regioselectively solvolized at the reducing end C1 to afford an alkenyl glycoside.

We then explored synthesis of TMC-based diblock copolymers using these ω-unsaturated alkyl glycoside intermediates. The Edgar group has successfully applied olefin CM to polysaccharide backbone modifications, in which cellulose ethers[15,16,22,23] and esters[14,17,24] with ω-unsaturated side chains were coupled with a series of CM partners catalyzed by the Hoveyda–Grubbs 2nd generation Ru catalyst[14, 16]. We have synthesized a variety of useful brush-like, side-chain functionalized cellulose derivatives with diverse functional end groups by this mild, selective, frequently quantitative method. We realized that this highly efficient method for polysaccharide post-modification might be a promising entrée into block copolymers, by utilizing the reducing end ω-olefinic glycosidic substituent as metathesis partner. We expected that, as in our previous studies, it would be necessary to use an excess of electron-deficient olefin (Grubbs type II, we employed ca. 40-fold molar excess relative to glycosidic olefin) in order to completely suppress polysaccharide self-metathesis. We tested the hypothesis that these derivatives would undergo clean CM, and that we would be able to detect the single new α,β-unsaturated olefin of the target product by ^{1}H and ^{13}C NMR methods, by using TMC-C3 as polysaccharide CM substrate and methyl acrylate (MA) as type II olefin partner. Initial CM of TMC-C3 was carried out in THF at room temperature using the HGII catalyst. 3,5-Di-tert-4-butylhydroxytoluene (BHT) was added as radical scavenger to prevent the free-radical reactions (γ-hydrogen abstraction and subsequent condensations) to which these α, β- unsaturated CM products are prone[14]. In this polymer – small molecule CM reaction, it was simple to collect the product by precipitation using acetone as a non-solvent, followed by dialysis against ethanol and deionized water. In the case of the short chain

unsaturated glycoside TMC-C3, even at high catalyst levels and long reaction times, we observed modest conversion with MA (30- 40%)[13]. We have previously observed lower conversions in the case of allyl ethers than with longer chain ω-unsaturated ethers[16]. These incomplete conversions may result either from restricted approach angles, due to proximity of the allyl olefin to the cellulose main chain, and/or from the electron-withdrawing effect of the nearby ether oxygen. It is difficult to separate these two possible effects experimentally. We proceeded to study CM of TMC-C5 which has a longer polymethylene spacer between ether oxygen and olefin, and therefore should be less troubled by either steric or electronic effects.

As we hoped, CM of TMC-C5 was highly efficient in THF at room temperature. ^{1}H NMR spectra (**Fig. 2a**) show that CM was complete within 6h, with 100% conversion, determined as described below. We were pleased to be able to confirm and quantify CM conversion by ^{1}H NMR integration (**Fig. 2a**), in spite of the fact that there was only one olefin per polymer molecule. In the starting CM partner, resonances from the TMC-C5 terminal olefin protons (**Fig. 2a**) appeared clearly at 4.98 (b) and 5.82 ppm (a), well separated from the TMC backbone. Upon CM with MA, the product olefin was conjugated with the terminal ester, moving the olefin resonances further downfield (**Fig. 2a**), to 5.75 (d) and 6.92 ppm (c). Comparing the ^{1}H NMR spectra of TMC-C5 and TMC-C5-MA, we observed that the starting olefin resonances had disappeared entirely, indicating (within the limitations of ^{1}H NMR detection) complete conversion to the targeted CM product. The CM product olefin signals indicated the E configuration, consistent with previous polysaccharide CM studies from our lab and with studies by others using non-polysaccharide substrates[14, 16] (it must of course be noted that we have consistently observed E:Z ratios of > 10:1 in previous polysaccharide side chain CM studies; it is quite likely that the minor Z olefin resonances are present, but too weak to observe). The resonance at 4.89 ppm was assigned to the

anomeric hydrogen atom at the reducing end, and its shift indicated predominant β-linkage to the 5-carboxypent-4-ene moiety[25], established during the solvolysis reaction. ^{13}C NMR spectra of TMC-C5 and TMC-MA provided additional support to the hypothesis of clean and complete CM. Saturated olefin carbon resonances 11 and 10 at 114.9 and 138.4 ppm in TMC-C5 shifted downfield upon conjugation in the TMC-C5-MA product, as expected, to 121.49 (11) and 148.93 ppm (10), respectively **(Fig. 2b)**. We also used CM with MA to briefly explore flexibility with regard to reaction solvent, finding that CH_2Cl_2 and $CHCl_3$ as solvents also afforded 100% conversion to TMC-C5-MA.

Encouraged by these selective, high-conversion results, we briefly examined the scope of CM of TMC-C5 with regard to olefin partner. Benzyl acrylate reacts efficiently with TMC-C5 under conditions similar to those for MA. ^1H NMR **(Fig. S3)** confirmed that CM with benzyl acrylate was successful, with 100% conversion (yield 92%), as all olefin resonances from TMC-C5 disappeared, and the expected product aromatic reasonances were evident. Under identical reaction conditions, CM with acrylic acid also reached 100% conversion (yield 89%) (**Fig. S4**).

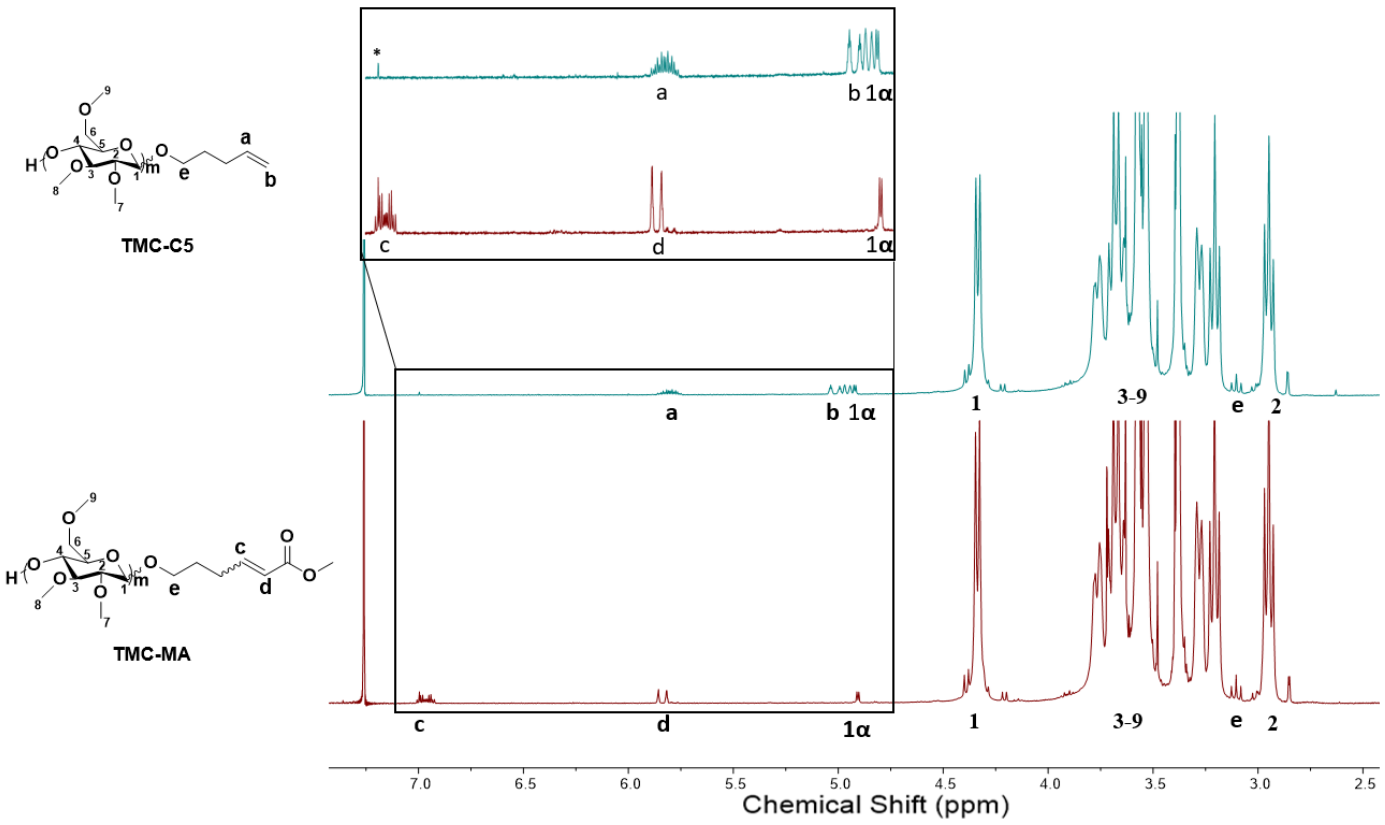

Fig.2a ^{1}H NMR spectra of TMC-C5 and TMC-MA. (*$CDCl_3$ spinning side band)

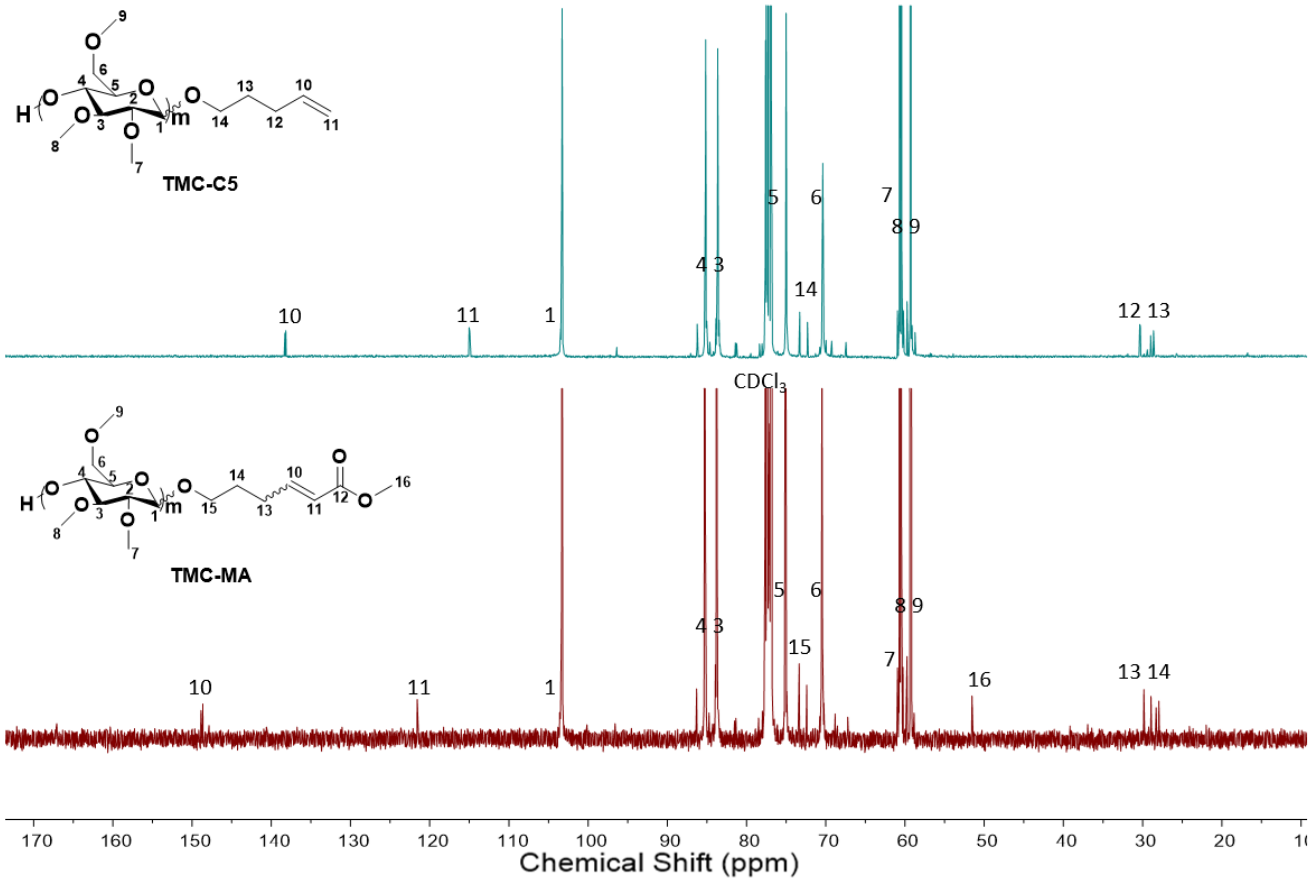

Fig. 2b ^{13}C NMR spectra of TMC-C5 and TMC-MA.

After successful CM of TMC-C5 with the series of small molecule acrylates, we investigated synthesis of a TMC-*b*-PEG diblock copolymer. Compared to small molecule acrylates, CM of poly(ethylene glycol) methyl ether acrylate (M_n = 480 g mol^{-1}) with TMC-C5 was slower, taking 16 h to reach 95% conversion, and 24 h to reach 100% conversion. Reaction conversion was determined by comparing the integrals of initial isolated olefin resonances with those of newly formed conjugated olefins. The relatively long reaction time could be caused by the steric demands of both the cellulose derivative and the PEG acrylate, combined with the fact that with both polymers in solution, viscosity is increased, reducing diffusion rates of the reagents.

A key issue in this polymer – polymer CM reaction was how to cleanly isolate the diblock copolymer product. At the end of CM, the crude reaction mixture contained the desired TMC-*b*-PEG diblock copolymer, BHT, catalyst, and a substantial amount (ca. 39-fold) of excess, unreacted PEGMEA; there is of course also the possibility of unreacted TMC-C5 if conditions are used in which conversion is incomplete. Initially, block copolymer products were purified by dialysis against EtOH and water. We were unsatisfied with this method, however, since it was lengthy, might be incapable of quantitative separation of desired copolymer from some starting polymers, and since catalyst residues could not be fully removed in this way. Therefore, we designed another workup procedure, in which TMC-*b*-PEG diblock copolymer was purified and isolated by precipitation with acetone, followed by centrifugation. Precipitation effectively removed the unreacted PEGMEA and other reagents. Centrifugation limits the loss of the diblock copolymer product during workup. CM conversion was determined by ^{1}H NMR **(Fig. 3)**, which clearly showed the disappearance of isolated olefin resonances, and appearance of conjugated olefin resonance, indicating complete conversion (after 24 h reaction time) as observed with the small molecule acrylates. Appearance of resonances at 3.62 ppm assigned to the methylenes of the PEG backbone also supported the proposed product structure, and the absence of PEG acrylate olefin resonances at 5.57, 5.86 and 6.13 ppm **(Fig. S1)** supported the hypothesis that the excess PEG acrylate was removed completely. ^{13}C NMR spectroscopy provided additional evidence for successful formation of the TMC-*b*-PEG diblock copolymer. After CM, the ester carbonyl (13) resonance moved from 172.4 **(Fig. S2)** to 166.6 ppm. Olefin resonances 10 (138.4 ppm) and 11 (114.9 ppm) shifted downfield to 15 (149.1 ppm) and 14 (121.9 ppm) due to conjugation with the ester. Also, a new resonance appeared at 70.7 ppm, which was assigned to the PEG backbone

methylenes (12). Overall, the hypothesized chemical structure of the TMC-*b*-PEG diblock copolymer was confirmed by its ^{1}H and ^{13}C NMR spectra.

Having demonstrated the concept of CM of TMC-C5 as a pathway to diblock copolymers, we wished to explore its scope and its utility for connecting more diverse blocks. Polymers with terminal acrylate esters were hypothesized as effective CM partners in this coupling strategy. To test the hypothesis, acrylate terminated PTHF (2000 g/mol) and acrylate terminated PLA (2500 g/mol) were employed with TMC-C5, using a CM process directly analogous to that used to make TMC-*b*-PEG. Product structure and reaction conversion were determined by ^{1}H NMR spectroscopy. By comparing integrals of initial olefin resonances with those of new formed conjugated olefin resonances, we found that both coupling reactions reached nearly 100% conversion, affording the desired diblock copolymers, TMC-*b*-PTHF **(Fig. S9)** and TMC-*b*-PLA (Fig S10). These block copolymers were also characterized by FT-IR. For TMC-*b*-PLA (Fig 5), a distinctive absorbance at 1765 cm^{-1} was observed and assigned as an ester C=O stretch from PLA blocks (**Fig S12**), supporting the formation of TMC-*b*-PLA. Interpretation of TMC-*b*-PEG and TMC-*b*-PTHF FT-IR spectra was complicated by the fact that blocks PEG, PTHF and TMC all contain similar chemical entities, thus their absorbances overlap with each other. The TMC-*b*-PTHF was also analyzed by Diffusion ordered spectroscopy (DOSY) NMR. According to Fig.S16, PTHF and TMC blocks exhibited the same diffusion coefficient of 1.65×10^{-10} m^2 s^{-1}, reveals the formation of block copolymers.

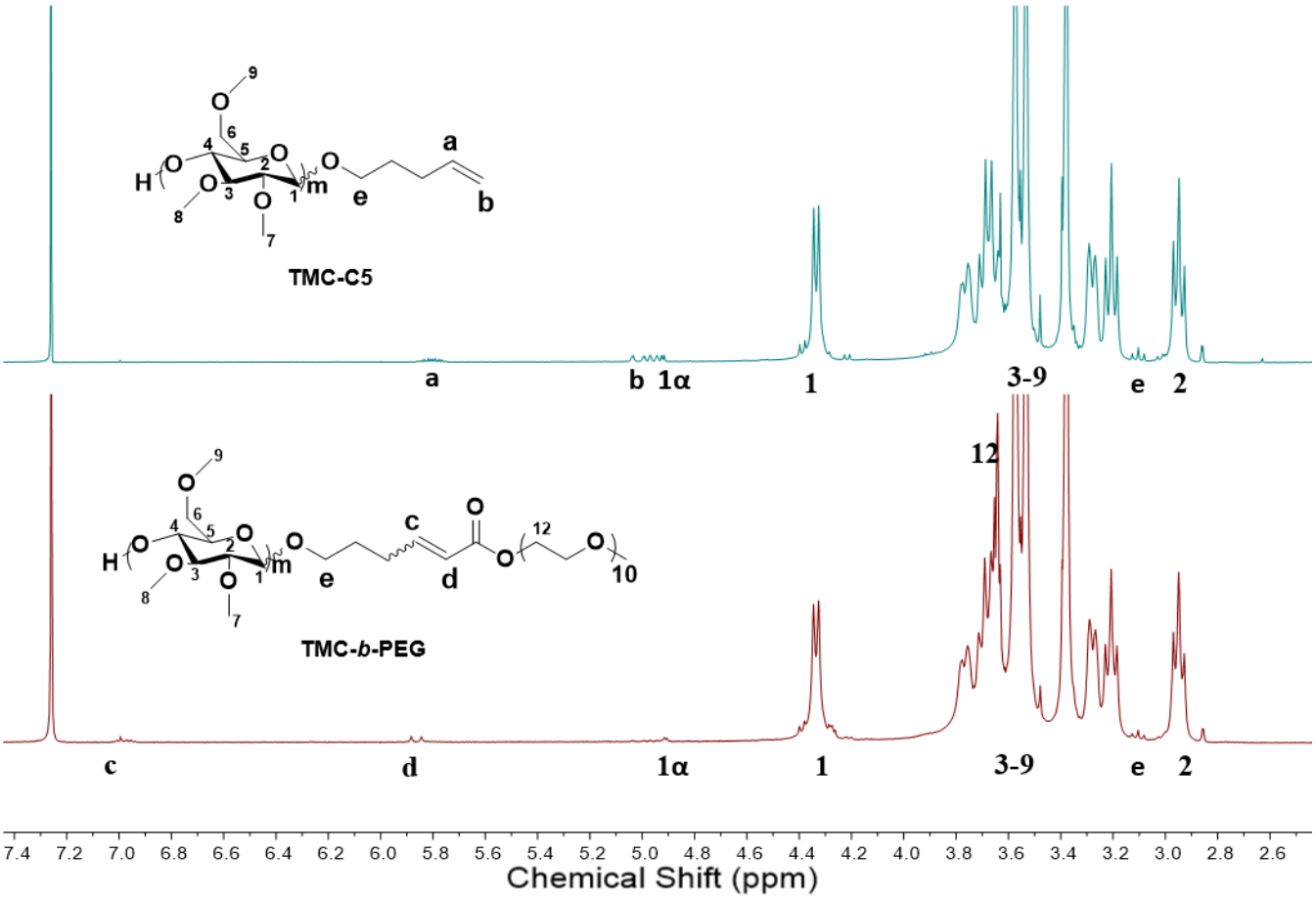

Fig 3. ^{1}H NMR spectra of TMC-C5 and TMC-*b*-PEG diblock copolymer

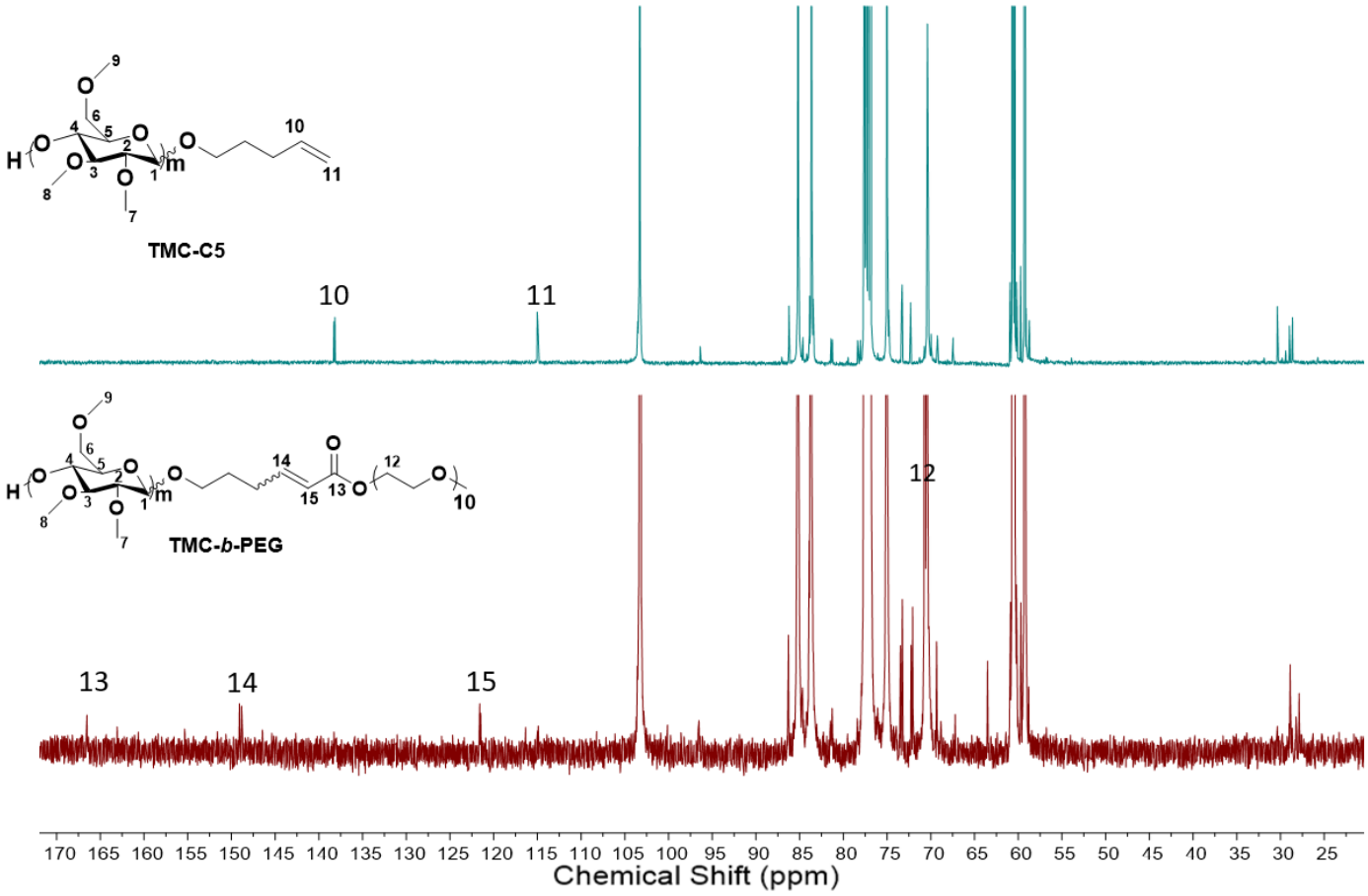

Fig 4. ^{13}C NMR spectra of TMC-C5 and TMC-*b*-PEG.

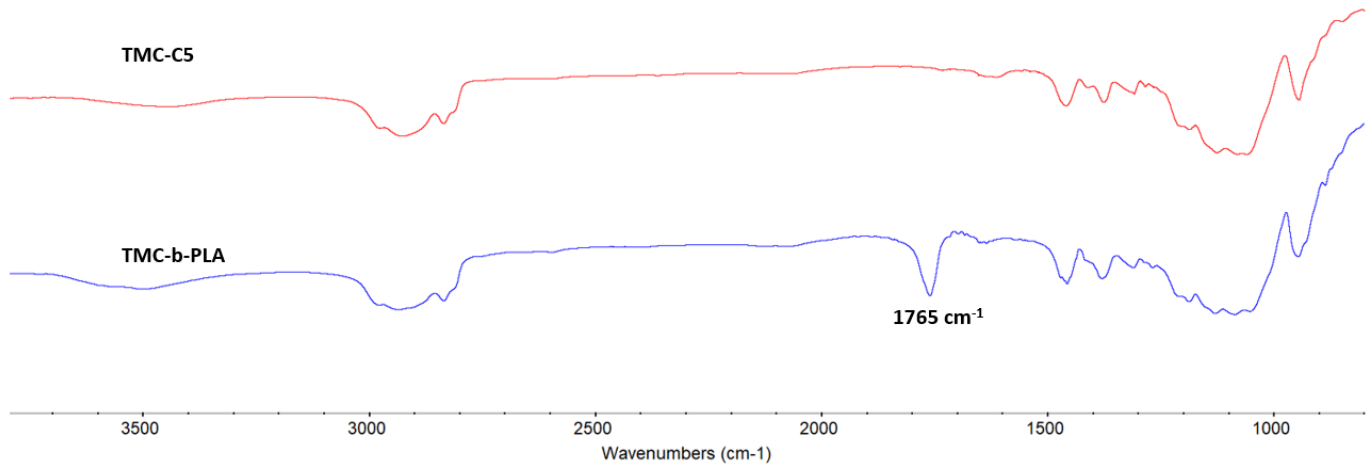

Fig 5. FT-IR spectra of TMC-C5 (red) and TMC-*b*-PLA (blue).

SEC was used to quantify changes in degree of polymerization (DP) during solvolysis and CM reactions (**Table 1**). Due to alkaline peeling during the permethylation reaction[26], the DP of TMC is approximately 37% lower than that of the starting methyl cellulose. The solvolysis mechanism also dictates that DP decreases significantly during that reaction, as reflected in the roughly 70% decrease in M_n observed, from ca. 27K g/mol (TMC) to 7600 g/mol for TMC-C5. The subsequent CM reaction, with its mild conditions and absence of acidic or basic catalysts, preserved DP. In the case of poly(ethylene glycol) methyl ether acrylate, the M_n of TMC-*b*-PEG increased to 9100 g/mol after CM, roughly as expected based upon the molecular weight of the added PEG block.

Samples	M_n (g/mol)	DP	PDI
Methyl cellulose	~40,000*	~211.6	
TMC	27,100	132.8	4.6
TMC-C5	7600	37.2	1.89
TMC-*b*-PEG	9100		1.72
TMC-*b*-PTHF	9700		1.79
TMC-*b*-PLA	10500		1.68

*Provided by manufacturer (determined by viscosity)

Table 1. SEC analyses of methyl cellulose, TMC, TMC-C5,TMC-*b*-PEG, TMC-*b*-PTHF, TMC-*b*-PLA.

It was of great interest to study the thermal properties of the block copolymers available by the new CM approach. Microphase separation of the blocks of this copolymer, differing significantly in polarity as they do, are expected to lead to various morphologies. These structures may offer novel thermal properties that are not observed in the homopolymers[27]. Some cellulose derivatives have broad thermal transitions due to their heterogeneity (of properties like DP and position of

substitution, for example), at times making it difficult to quantify important transitions like the glass transition temperature (T_g). TMC is a homopolymer, so variations of position and extent of substitution should not be an issue, but distribution of DP values will be. Modulated DSC is effective at separating irreversible thermal transitions (like melting) from reversible transitions (like T_g), and can frequently improve the resolution and clarity of DSC transitions of polysaccharide derivatives[28]. Therefore, modulated DSC was used to analyze the thermal behavior of TMC, TMC-C5, and TMC-*b*-PEG. TMC exhibits a sharp glass transition around 110 °C. The solvolysis product TMC-C5 has reduced molecular weight for the reasons already noted. Partly as a result, TMC-C5 shows a lower glass transition (T_g = 97 °C) than that observed for TMC (the small amount of pentyl group present may also contribute some internal plasticization[29]). On the other hand, the TMC-*b*-PEG diblock copolymer is expected to exhibit quite different thermal properties compared to its precursors. The separate thermal properties of each block might be observed, if they occupy separate domains. Plasticization of the stiff (TMC) block by the flexible block (PEG) might also be observed. In the event, the modulated DSC thermogram (Fig. S5) of the TMC-*b*-PEG copolymer revealed an endothermic transition at about 51 °C, close to the T_m (52 °C) of PEG homopolymer (Fig. S7), and thus assigned to melting of the PEG block. No clear glass transition was observed in the total heat trace (Fig. S5). As PEG is a known plasticizer for cellulose ethers[30], it is likely that the PEG block acted as a plasticizer for the TMC block, thereby reducing its glass transition temperature (82 °C) in the TMC-*b*-PEG copolymer. In order to test this hypothesis, we analyzed the block copolymer reversing heat flow, thereby removing interference by non-reversing transitions such as melting. Fig. S6 shows a clear T_g of the TMC block at 54 °C, confirming that the failure to observe any T_g in the total heat flow trace resulted from overlap with the PEG block melt transition.

We sought to determine whether microphase separation was occurring by SAXS experiments using TMC-*b*-PEG, TMC-*b*-PLA and TMC-*b*-PTHF thin films, prepared by casting from chloroform solution. However, light scattering from micro domains was not observed in SAXS profiles of these films. The absence of microphase separation is probably due to a high degree of phase mixing, which is likely caused by a combination of strong A-B interactions and low molecular weights of these block copolymers, as both χ (Flory parameter characterizing A-B interactions) and degree of polymerization are key parameters relevant to microphase separation[3]. We will seek in future work to prepare block copolymers in which DP of each segment is further maximized and in which χ differences are also maximized.

3.5 Conclusions

We have successfully demonstrated the concept of olefin cross-metathesis as a coupling strategy for diblock copolymer synthesis by preparation of TMC-*b*-PEG. Trimethyl cellulose derivatives bearing ω-unsaturated alkyl glycoside substituents, regiospecifically substituted at the reducing end anomeric (C1) position, were prepared by solvolysis with allyl alcohol and pent-4-en-ol. Reaction conditions were identified that provided reasonable DP preservation and high conversion to the alkenyl glycoside (vs. competing hydrolysis at the anomeric position), providing an alkenyl polyglycoside reaction partner with block DP ca. 35. Due to issues that may include narrow approach angles and olefin electron deficiency, TMC-C3 only gave limited CM conversion (similar to results we have observed in other allyl polysaccharide CM reactions[16]). On the other hand, TMC-C5 was a highly efficient CM substrate. A series of small molecule and polymeric Grubbs Type II olefins was reacted with TMC-C5 to give CM products in 100% conversions, as confirmed by multiple techniques including ^{1}H and ^{13}C NMR spectroscopy. The TMC-C5 metathesis products have a single exposed 4-OH group at the non-reducing end, set up perfectly

to append another polymer block. We are investigating these diblock polymers as intermediates to A-B-C triblock copolymers by several different methods, and will describe the results of this work in the near future.

This is the first introduction of an ω-olefin substituent only to the reducing end anomeric position (C-1 OH) of a polysaccharide, and the first time that such a substituent was successfully elaborated by olefin cross-metathesis. This method should be applicable to most other polysaccharides as well. It creates pathways towards polysaccharide-based block copolymers, and end-functional polysaccharide derivatives. It should be noted that we used trimethyl cellulose in this work so that all secondary hydroxyls would be substituted prior to solvolysis, providing a product with only the single exposed hydroxyl at the non-reducing end 4-OH (as a by-product of the solvolysis). We did so to preserve the possibility of selective synthesis of a triblock copolymer. However, if a diblock copolymer is desired, and if the alkenyl polyglycoside has desired solubility in useful metathesis solvents, ***native polysaccharides*** or less than fully substituted ether derivatives (or any other substituent where the attachment to the polysaccharide is stable during the solvolysis reaction) may also be used as solvolysis substrates, leading to diblock copolymers via olefin CM.

This exploratory study also highlighted some potential limitations. In the solvolysis reaction, only partial control of trimethyl cellulose molecular weight is possible, since acid-catalyzed solvolysis and resulting chain cleavage is random, so can occur at any 1→4 anomeric linkage. Purification of block copolymer products can be another issue, particularly when reacting the alkenyl polyglycoside with another polymer. Separation of one polymer from another (or from two others; potentially both residual, unreacted starting cellulose derivative, and the inevitable excess metathesis substrate) can be a challenge. We observed that precipitation is a viable option in some cases. However, it can be difficult to find a solvent which solvates excess CM partners, and not

the diblock copolymer product. Dialysis is a useful purification method for separating low molecular weight polymers from high molecular weight copolymer products. However, dialysis may not be useful for efficiently removing high molecular weight polymers, nor for separating copolymer products from reagent polymers of similar molecular weight. Selection of the partners to facilitate clean separation is key. Our future studies will focus on how to address these issues and synthesize high molecular weight di- and triblock copolymers.

3.6 Acknowledgment.

We thank the Departments of Chemistry and of Sustainable Biomaterials, and the Institute for Critical Technologies and Applied Science (ICTAS) at Virginia Tech for facility support. We thank the National Science Foundation for partial support of this work through grant DMR-1308276. We also thank Ryan Carrazzone and Glenn Spiering at Virginia Tech for performing SEC and SAXS analyses.

3.7 References

1. Buchanan, C. M.; Gardner, R. M.; Komarek, R. J., *J. Appl. Polym. Sci.,* 1993, **47** (10), 1709-1719.

2. Edgar, K. J.; Buchanan, C. M.; Debenham, J. S.; Rundquist, P. A.; Seiler, B. D.; Shelton, M. C.; Tindall, D., *Prog. Polym. Sci.,* 2001, **26** (9), 1605-1688.

3. Leibler, L., *Macromolecules,* 1980, **13** (6), 1602-1617.

4. Arrington, K. J.; Haag IV, J. V.; French, E. V.; Murayama, M.; Edgar, K. J.; Matson, J. B., *ACS Macro lett.* 2019**,** 8, 447-453.

5. Black, C.; Guarini, K.; Milkove, K.; Baker, S.; Russell, T.; Tuominen, M., *Appl. Phys. Lett.,* 2001**, 79** (3), 409-411.

6. Xiao, Q.; Wang, X.; Li, W.; Li, Z.; Zhang, T.; Zhang, H., *J. Memb. Sci.,* 2009, **334** (1), 117-122.

7. Car, A.; Stropnik, C.; Yave, W.; Peinemann, K.-V., *J. Memb. Sci.,* 2008, **307** (1), 88-95.

8. Mezger, T.; Cantow, H. J., *Macromol. Rapid Commun.,* 1983**, 4** (5), 313-320.

9. Yalpani, M.; Brooks, D. E., *J. Polym. Sci. A.,* 1985, **23** (5), 1395-1405.

10. Kamitakahara, H.; Suhara, R., *Carbohydr. Polym.,* 2016, **151**, 88-95.

11. Rostovtsev, V. V.; Green, L. G.; Fokin, V. V.; Sharpless, K. B., *Angew. Chem. Int. Ed.,* 2002, **41** (14), 2596-2599.

12. Opsteen, J. A.; van Hest, J. C., *Chem. Commun.* 2005, (1), 57-59.

13. Chatterjee, A. K.; Choi, T.-L.; Sanders, D. P.; Grubbs, R. H., *J. Am. Chem. Soc.,* 2003, **125** (37), 11360-11370.

14. Meng, X.; Matson, J. B.; Edgar, K. J., *Biomacromolecules,* 2013, **15** (1), 177-187.

15. Dong, Y.; Matson, J. B.; Edgar, K. J., *Biomacromolecules,* 2017, **18**(6),1661-1676.

16. Dong, Y.; Edgar, K. J., *Polym. Chem.,* 2015**, 6** (20), 3816-3827.

17. Meng, X.; Matson, J. B.; Edgar, K. J., *Polym. Chem.,* 2014, **5** (24), 7021-7033.

18. Dong, Y.; Novo, D. C.; Mosquera-Giraldo, L. I.; Taylor, L. S.; Edgar, K. J., *Carbohydr. Polym.,* 2019.

19. de Espinosa, L. M.; Meier, *Chem. Commun.* 2011, **47** (6), 1908-1910.

20. Scherman, O. A.; Rutenberg, I. M.; Grubbs, R. H., *J. Am. Chem. Soc.,* 2003, **125** (28), 8515-8522.

21. Nakagawa, A.; Kamitakahara, H.; Takano, T., *Carbohydr. Res.,* 2011, **346** (13), 1671-1683.

22. Dong, Y.; Mosquera-Giraldo, L. I.; Taylor, L. S.; Edgar, K. J., *Biomacromolecules,* 2016, **17** (2), 454-465.

23. Dong, Y.; Mosquera-Giraldo, L. I.; Troutman, J.; Skogstad, B.; Taylor, L. S.; Edgar, K. J., *Polym. Chem.,* 2016, **7** (30), 4953-4963.

24. Meng, X.; Edgar, K. J., *Carbohydr. Polym*., 2015, **132**, 565-573.

25. Nakagawa, A.; Fenn, D.; Koschella, A.; Heinze, T.; Kamitakahara, H., *J. Polym. Sci. A,* 2011, **49** (23), 4964-4976.

26. Knill, C. J.; Kennedy, J. F., *Carbohydr. Polym.,* 2003, **51** (3), 281-300.

27. Ohta, T.; Kawasaki, K. J., *Macromolecules,* 1986, **19** (10), 2621-2632.

28. Marks, J. A.; Wegiel, L. A.; Taylor, L. S.; Edgar, K. J., *J. Pharm. Sci.,* 2014, **103** (9), 2871-2883.

29. Edgar, K. J.; Pecorini, T. J.; Glasser, W. G., Long-chain cellulose esters: preparation, properties, and perspective. ACS Publications: 1998.

30. Entwistle, C.; Rowe, R. J., *J. Pharm. Pharmacol.,* 1979, **31** (1), 269-272.

Chapter 4: Regioselective bromination of the dextran non-reducing end creates a pathway to dextran-based block copolymers

Junyi Chen[a], Glenn Spiering[a], Robert B. Moore[a, b], and Kevin J. Edgar[b, c]

[a]Department of Chemistry, Virginia Tech, Blacksburg, VA 24061, USA

[b]Macromolecules Innovation Institute, Virginia Tech, Blacksburg, VA 24061, USA

[c]Department of Sustainable Biomaterials, Virginia Tech, Blacksburg, VA 24061, USA

4.1 Abstract

Preparation of polysaccharide-based block copolymers with linear architectures is an important goal, opening up clear application potential and requiring significant advances in polysaccharide regio- and chemoselectivity. Due to the difficulty of selective polysaccharide end-group functionalization, only a few successful approaches to polysaccharide-based linear block copolymers have been reported. Herein we report a simple approach to prepare dextran-based block copolymers. Reaction with *N*-bromosuccinimide (NBS)/triphenyl phosphine (PPh_3) regioselectively brominates the sole primary alcohol of linear, unbranched dextran (which is an α-1-6 linked homopolymer of glucose) at C-6 of the non-reducing end monosaccharide. The resulting dextran, monofunctionalized with a terminal C-6 bromide, was coupled with various amine terminated polymers to prepare block copolymers, including dextran-*b*-poly(ethylene glycol), dextran-*b*-polystyrene, and dextran-*b*-poly(*N*-isopropylacrylamide). These linear block copolymers were characterized by nuclear magnetic resonance spectroscopy (NMR), Fourier-transform infrared spectroscopy (FTIR) and size exclusion chromatography (SEC). These renewable-based block copolymers, prepared in two selective, high-yielding steps from native linear dextran, exhibit various interesting properties. Dextran-*b*-poly(*N*-isopropylacrylamide) undergoes thermally-induced micellization as revealed by dynamic light scattering (DLS), forming

micelles (155 nm diameter) upon exceeding the lower critical solution temperature (LCST) of poly(*N*-isopropylacrylamide) (33 °C). We also observed microphase separation in dextran-*b*-polystyrene by using small angle X-ray scattering (SAXS). Overall, this methodology provides a new, highly chemo- and regioselective, versatile route to diverse dextran-based block copolymers with useful properties, enabling drug delivery, compatibilization, and other applications.

4.2 Introduction

Block copolymers, comprising two or more different polymer blocks connected covalently, may have valuable properties. Block copolymerization enables construction of single polymer molecules comprising structurally distinct segments; the homopolymers corresponding to the segments in many cases may be thermodynamically incompatible. These block copolymers can be designed to take on various microstructures, including microphase separated domains, that enable practical applications[1]. Unlike polyolefins, which are typically hydrophobic and flexible, affording the propensity for chain entanglement, polysaccharide backbones are ribbon-like, generally hydrophilic, and prone to self-association due to their abundance of hydroxyl groups (capable of both hydrogen bond donation and acceptance). Thus hypothetical polysaccharide-*b*-polyolefin block copolymers might be prone to microphase formation, which could generate morphologies that enable high performance in applications ranging from compatibilizers[2], to batteries[3], to separation membranes[4].

Dextrans are homopolymers of glucose, typically obtained by bacterial fermentation[5], that may be branched (with α-linked glucose chains) from any of the secondary alcohol groups[6]; location and extent of branching depends in part on bacterial species. Linear, unbranched dextran (-6→α-D-Glc*p*→1-), has great utility in biomedical applications. It is biocompatible in many situations[7], is biodegradable both *in vivo*[8] and in the environment, and thus has been widely utilized in medicine,

including in infusion[9], for drug delivery[10], and in hydrogels . Dextran has solubility in both water and polar aprotic solvents (e.g. DMSO), such that it can be more readily chemically modified than cellulose. Moreover, dextran is commercially available in a wide range of molecular weights (5000 – 1,000,000 Daltons) with relatively narrow polydispersities, enhancing potential for investigating structure-property relationships of block copolymers.

No polysaccharide-based block copolymers are commercially available, and only a few synthetic routes to polysaccharide-based block copolymers have been reported. It is difficult to prepare mono- or dichelic polysaccharide derivatives, since polysaccharides contain many sites of similar reactivity; three secondary alcohols (2-, 3-, and 4-OH) per monosaccharide in the case of linear dextran. Previous attempts to prepare polysaccharide-based block copolymers have exploited a potentially unique and distinguishable reactive site; the anomeric carbon (C-1) of the reducing end monosaccharide, the only carbon in the molecule in the aldehyde oxidation state. The reducing end anomeric position is in equilibrium between cyclic hemiacetal and acyclic aldehyde, and the aldehyde isomer can be uniquely captured by reagents vs. all other dextran sites. Based on this reactivity, researchers have developed several methods to end-functionalize polysaccharides, including conversion to a 1-glycosyl bromide by reaction with HBr[11,12], solvolysis with ω-unsaturated alcohol[13], and reductive amination[14].

Inspired by dextran's renewable nature, biomedical utility (it is frequently used for intravenous infusions of various types in the clinic[5]), and ready availability, several investigators have reported synthesis of dextran-based block copolymers by taking advantage of reducing end anomeric positions. Indeed, essentially all syntheses of polysaccharide-based block copolymers take advantage of the unique reactivity of the reducing end C1 in its aldehyde oxidation state[2,15,16]. These approaches can be categorized into two different strategies, end-to-end coupling and

polymerization of synthetic blocks from polysaccharide macroinitiators. Borsali et al. reported preparation of a dextran-based atom-transfer radical polymerization (ATRP) initiator by reductive amination, and elaboration of the macroinitiator by ATRP to a dextran-*b*-polystyrene[17]. Reductive amination has also been used to prepare block copolymers based on dextran and other polysaccharides by coupling strategies. The terminal anomeric aldehyde, e.g. from dextran, has been condensed with amine-terminal polymers to prepare block copolymers, including dextran-*b*-poly(ethylene glycol)[18], dextran-*b*-polystyrene[19] and dextran-*b*-poly(ε-caprolactone). There have however been no techniques reported for elaborating block copolymers by regio- and chemoselective reactions of the ***dextran non-reducing end*** (nor of any other polysaccharide's reducing end).

Due to the fact that its backbone comprises α-1→6 linkages, each dextran chain has one and only one primary alcohol at C-6 of its non-reducing end monosaccharide. We realized that this dextran architecture affords an unusual, previously unexploited way to end-functionalize the polymer, since primary alcohols can be modified with specificity unavailable to other polysaccharide positions[20] (discrimination between secondary alcohol groups being especially difficult)[21 22 23] . Bromination with a combination of triphenylphosphine (PPh_3) and *N*-bromosuccinimide (NBS), as discovered by Furuhata[24], is a highly selective method for regioselective halogenation at the C-6 positions of cellulose[25], curdlan[26], and many other polysaccharides. NBS/PPh_3 bromination of dextran has not been reported. Recently, chemo- and regioselective chlorination of polysaccharide primary alcohols (methanesulfonyl chloride/*N*, *N*-dimethyl formamide) has also been reported[27].

The Edgar group has previously reported exploitation of Furuhata bromination and its exquisite selectivity to permit synthesis of comb-like polysaccharide derivatives substituted with complete selectivity at C-6[28,29]. In the case of curdlan, for example, 6-bromo-6-deoxycurdlan and its 2, 4-O-

diesters were coupled with a series of alkyl amines[26] to afford 6-amino-6-deoxycurdlans with complete regioselectivity. Similar methodology provided C-6 cationic, anionic, and zwitterionic derivatives of cellulose[25,30,31]. We realized that such monofunctionalization of linear, unbranched dextran in a single location in the entire polymer, with a good leaving group like bromide, could provide ready access to block copolymers by coupling with amine-terminal polymers via bromide displacement.

Hence, we hypothesized that NBS/PPh_3 would brominate dextran with complete regio- and chemoselectivity only at the C-6 of the non-reducing end glucose (one bromine per polymer molecule). We further hypothesized that displacement of this bromide by a polymer containing a terminal amine group would be an efficient, effective, rapid, broadly useful strategy for constructing dextran-based block copolymers. In order to test our hypotheses and exploit the potential application of this class of material, we designed and sought to prepare three distinctive block copolymers: dextran-*b*-PEG, dextran-*b*-polystyrene and dextran-*b*-poly(*N*-isopropylacrylamide). Polyethylene glycol (PEG) is a hydrophilic polymer, extensively used in biomedical applications due to its low toxicity[32] and ability to sterically screen particles[33]. Many PEG-based polymers and systems are already part of formulations approved for internal consumption by the Food and Drug Administration[32,34]. In this study, a dextran-*b*-PEG was prepared to demonstrate the feasibility of the synthetic route. We selected poly(*N*-isopropylacrylamide) (PNIPA) as a building block due to its special thermal behavior in aqueous media. PNIPA undergoes an unusual macromolecular transition from a hydrophilic to a hydrophobic structure upon heating at or above its LCST (ca. 33°C)[35]. Because of this thermally-induced phase transition near body temperature (ca. 37°C), many studies use PNIPA building blocks as either cores or shells in designing thermoresponsive micelles[36]. To extend the scope of

thermoresponsive polymeric micelles based on PNIPA and explore the potential applications of its copolymers with hydrophilic dextran, we employed the condensation method to attempt synthesis of dextran-*b*-PNIPA. Finally, we wished to prepare dextran-*b*-polystyrene by a similar strategy to explore block copolymer morphology in a case where there would be an excellent chance of block incompatibility and microphase separation. Polystyrene is quite hydrophobic, in contrast with hydrophilic dextran, thus we anticipated interesting phase behavior from the putative dextran-*b*-polystyrene. We report herein a preliminary study to prove the principle of this proposed synthetic approach, which if successful would afford several interesting dextran-based block copolymers with potential in a wide variety of applications including as surfactants, membranes, polymer compatibilizers, components of drug delivery systems, and many others.

4.3 Experimental section

4.3.1 Abbreviations

PEG refers to polyethylene glycol. PNIPA refers to poly(*N*-isopropylacrylamide). Dex-Br refers to dextran with a 6-bromo-6-deoxyglucose as its non-reducing terminal monosaccharide. PS refers to polystyrene. DP refers to degree of polymerization.

4.3.2 Materials

Dextran from *Leuconostoc mesenteroides* (M_n 10,100 g/mol, determined by aqueous SEC), amine terminated PEG (M_n 2900 g/mol) amine terminated polystyrene (M_n 5000 g/mol, provided by manufacturer), amine terminated PNIPA (M_n 1500 g/mol, provided by manufacturer) and sodium iodide were from Sigma Aldrich. Lithium bromide (laboratory grade) was from Fisher. Dimethyl sulfoxide (DMSO, HPLC grade, Fisher) was stored over 4 Å molecular sieves. Triphenylphosphine (Ph_3P, 99%) was from Acros. Regenerated cellulose dialysis tubing (MWCO

3500 g/mol) was from Fisher. Deionized water was prepared using an ROpure ST reverse osmosis/tank system.

4.3.3 Measurements

^{1}H and ^{13}C NMR spectra were obtained on a Bruker Avance II 500 MHz spectrometer, employing 64 and 15,000 scans, respectively, in DMSO-d^6 or D_2O at room temperature or 50 °C. Infrared spectroscopic analyses of samples as pressed KBr pellets (1 mg sample/100 mg KBr) were performed on a Thermo Electron Nicolet 8700 instrument using 64 scans and 4 cm^{-1} resolution. Molecular weights were measured on a Waters Breeze Aqueous Size-Exclusion Chromatograph using Agilent aquagel-OH columns and in conjunction with a Waters 2414 refractive index detector and Wyatt miniDawn Treos MALS. Polymers were dissolved in deionized water (1 mg/mL) and the solutions were filtered through a 0.45 μm PTFE filter. SEC experiments were conducted at 30 ° C in HPLC grade H_2O with a flow rate of 1 mL/min. Small angle X-ray scattering (SAXS) experiments were performed using a Rigaku S-Max 3000 3 pinhole SAXS system, equipped with a rotating anode emitting X-rays with a wavelength of 0.154 nm (Cu Kα). The sample-to-detector distance was 1600 mm for SAXS, and the q-range was calibrated using a silver behenate standard. Two-dimensional SAXS patterns were obtained using a 2D multiwire, proportional counting, gas-filled detector, with an exposure time of 2 h. SAXS data were corrected for sample thickness and transmission and were put on an absolute scale by correction using a glassy carbon standard from the Advanced Photon Source (APS). All SAXS data were analyzed using the SAXSGUI software package to obtain radially integrated SAXS intensity versus the scattering vector q, where $q = (4\pi/\lambda)\sin(\theta)$, θ is one half of the scattering angle and λ is the X-ray wavelength. Dynamic light scattering (DLS) experiments were performed at 25 °C and 40 °C using a Malvern Zetasizer Nano-ZS instrument using 1 mg/mL polymer aqueous solutions. The

hydrodynamic diameter and PDI were measured in a quartz cuvette. After 5 min equilibration, data was recorded for 120 s. Polymer thermal properties were obtained by differential scanning calorimetry (DSC) on a TA Discovery instrument using a modulated (MDSC) method: sample (ca. 5 mg dry powder in Tzero aluminum pan) was analyzed with underlying ramp heating rate 5 °C/min and oscillation amplitude ± 0.5 °C with oscillation period 60 s. The solubility parameters of homopolymers and block copolymers were calculated based on the work reported by Fedors[37].

4.3.4 General procedure for dextran bromination

PPh_3 (1.35 g, 5.15 mmol, 100 equiv.) was dissolved in 10 mL of dry DMSO, and a second solution was prepared containing NBS (0.91 g, 5.15 mmol 100 equiv.) in an additional 10 mL of dry DMSO. In a separate flask, dextran (520 mg) was dissolved in 50 mL DMSO. Subsequently, the Ph_3P solution was added dropwise to the 50 mL dextran solution, followed by dropwise addition of the NBS solution. This solution was heated to 70 °C under N_2. After 4 h, the product was precipitated by adding the reaction solution to 500 mL acetone, then the solid product was collected by centrifuge (8000 rpm, 25 °C) and washed with excess acetone twice. The resulting solid was dried overnight in a vacuum oven at 50 °C to give a white powder (495.6 mg, 4.91 mmol, yield 95.3%).

^{1}H NMR (400 MHz, $CDCl_3$): δ 3.35 – 4.05, (m, dextran backbone, Br-C<u>H</u>$_2$-), δ 4.80 (d, C1-<u>H</u>).

^{13}C NMR (500 MHz, D_2O): δ 100 (dextran C1), δ 60-74 (dextran C2-C6), δ 26 (-<u>CH</u>$_2$-Br).

4.3.5 Condensation of Dex-Br with allyl amine

Dex-Br (500 mg, 0.05 mmol) was dissolved in 20 mL of DMSO in a 100 mL flask. Allyl amine (89 mg, 1.56 mmol, 30 equiv.) and NaI (233 mg, 1.56 mmol, 30 equiv.) were added. The mixture was heated to 40 °C and stirred at that temperature for 24 h. The homogeneous solution was cooled to room temperature and added to 200 mL acetone to precipitate the product. The resulting solid was redissolved in 10 mL DMSO and precipitated in 100 mL acetone. This reprecipitation was

repeated twice more. The product was dried in vacuum oven at 60 °C for 24 h. Finally, the product was collected as a white powder (Dex-NAllyl, 486 mg, 0.049 mmol yield 97.2%).

^{1}H NMR (400 MHz, $CDCl_3$): δ 3.35 – 4.05, (m, dextran backbone), δ 4.80 (d, C1-H), δ 5.45 (d, -CH=CH_2), δ 5.95 (m, -CH_2-CH=CH_2).

^{13}C NMR (500 MHz, D_2O): δ 136 (-CH_2-CH=CH_2), δ 121 (-CH_2-CH=CH_2), δ 100 (dextran C1), δ 60-74 (dextran C2-C6), δ 41 (-CH_2-NH-)

4.3.6 Preparation of Dextran-*b*-PEG

Dex-Br (500 mg, 0.05 mmol) was dissolved in 20 mL DMSO in a 100 mL flask. PEG-amine (450 mg, 0.15 mmol, 3 equiv.) and NaI (100 mg, 0.66 mmol, 13.4 equiv.) were added. The mixture was heated to 80 °C and stirred at that temperature for 48 h. The homogeneous solution was cooled to room temperature and added to 200 mL acetone to precipitate the product. The resulting solid was redissolved in 10 mL DMSO and precipitated in 100 mL acetone followed by washing with excess acetone. After that, the collected solid product was transferred to 3500 g/mol MWCO dialysis tubing (prewet with water) that was placed in a beaker containing 1L of DI water. The mixture was dialyzed for three days during which the DI water was replaced 3 times, and the solution was freeze-dried to give white powder product (567 mg, 0.043 mmol, yield 87.2%).

^{1}H NMR (400 MHz, D_2O): δ 3.35 – 4.05, (m, dextran backbone), δ 3.52 (t, PEG backbone), δ 4.80 (d, C1-H).

^{13}C NMR (500 MHz, D_2O): δ 100 (dextran C1), δ 60-74 (dextran C2-C6, PEG)

4.3.7 Preparation of Dextran-*b*-PNIPA

Dex-Br (500 mg, 0.05 mmol) was dissolved in 20 mL of DMSO in a 100 mL flask. PNIPA-amine (234 mg, 0.16 mmol, 3 equiv.) and NaI (100 mg, 0.66 mmol, 13.4 equiv.) were added. The mixture

was heated to 80 °C and stirred at that temperature for 48 h. The homogeneous solution was cooled to room temperature and was added to 200 mL acetone to precipitate the product. The resulting white solid was redissolved in 10 mL DMSO and precipitated in 100 mL acetone. This reprecipitation was repeated twice, then the collected solid product was transferred to 3500 g/mol MWCO dialysis tubing (prewet with water) that was placed in a beaker containing 1L of deionized water. The mixture was dialyzed for three days during which the deionized water was replaced 3 times, and the solution was freeze-dried to give a white powder product (537 mg, 0.047 mmol, 93.0% yield).

^{1}H NMR (400 MHz, $CDCl_3$): δ 1.13, [d, -CO-NH-CH-($C\underline{H}_3$)$_2$], δ 1.65, (d, PNIPA backbone), δ 2.04, (t, PNIPA backbone), δ 3.35 – 4.05, (m, dextran backbone), δ 4.80 (d, C1-$\underline{H}$).

^{13}C NMR (500 MHz, D_2O): δ 153 (C=O), δ 100 (dextran C1), δ 60–74 [dextran C2-C6, (-CH_2-$\underline{C}$H-)], δ 42 (-$\underline{C}$H-(CH_3)$_2$), δ 22 (-CH_3).

4.3.8 Preparation of dextran-*b*-PS diblock copolymer

Dex-Br (500 mg, 0.05 mmol) was dissolved in 20 mL of DMSO in a 100 mL flask. Polystyrene-amine (750 mg, 0.16 mmol, 3 equiv.) and NaI (100 mg, 0.66 mmol, 13.4 equiv.) were added. The mixture was heated to 80 °C and stirred at that temperature for 48 h. The homogeneous solution was cooled to room temperature and was added to 200 mL acetone to precipitate the product. The resulting solid was redissolved in 10 mL DMSO and precipitated in 100 mL acetone. This reprecipitation was repeated twice, followed by washing with excess acetone. After that, the product was dried in a vacuum oven at 60 °C for 24 h. Finally, the product was collected as a white powder (623 mg, 0.04 mmol, 81.9% yield).

^{1}H NMR (400 MHz, $CDCl_3$): δ 1.16 – 1.86, (m, polystyrene backbone), δ 3.05–5.15, (m, dextran backbone), δ 3.35 – 4.05, (m, dextran backbone), δ 6.51 (m, aromatic protons), δ 7.03 (m, aromatic protons).

^{13}C NMR (500 MHz, DMSO): δ 125-145 (-$\underline{C}_6H_5$), δ 100 (dextran C1), δ 60–74 [dextran C2-C6, (-CH_2-$\underline{C}$H-)], δ 44 (-$\underline{C}$H-CH_2-), δ 40 (-CH-$\underline{C}H_2$-).

4.3.9 Preparation of dextran-*b*-PS solvent-cast films

Dextran-*b*-PS (100 mg) was dissolved in 2 mL DMSO. Then the polymer solution was added into a Teflon mold and allowed to evaporate for 14 days at room temperature in the presence of a desiccant. Subsequently, the solvent casting sample was dried in a vacuum oven at 60 °C for 48 h to remove the rest of the DMSO. At last, the resulting polymer film was taken from the mold, ready for SAXS analysis. Films of dextran, Dex-Br, Dextran-*b*-PNIPA and Dextran-*b*-PEG were also prepared similarly.

4.4 Results and discussion

As the linear dextran backbone consists of α–1-6 glycosidic linkages, each dextran polymer chain only has one primary alcohol at its non-reducing end. Our first task was to confirm our hypothesis that this single, terminal primary alcohol, chemically distinct from other hydroxyl groups along the chain, could be cleanly converted to 6-Br by Furuhata bromination (Scheme 1). We selected reaction conditions similar to those in previous work where we were preparing brush-like structures from cellulose and other polysaccharides, employing NBS as bromination reagent and PPh_3 as promoter in DMSO solvent[26,31,38] Given the extremely low concentration of primary alcohols, 100 equiv. each of NBS and PPh_3 were added to increase the likelihood of collisions leading to desired reactions. The reaction product was purified by dialysis against water and collected by freeze-drying. Confirmation of conversion to Dex-Br was challenging, as for example

it was difficult to detect the new alkyl bromide by FT-IR due to the low bromide content (0.7 wt % at full conversion); for the same reason elemental analysis would not have been sufficiently informative. By ^{1}H NMR spectroscopy the resonances of protons adjacent to terminal bromides overlapped with resonances from the dextran backbone, and thus could not be clearly identified and quantified.

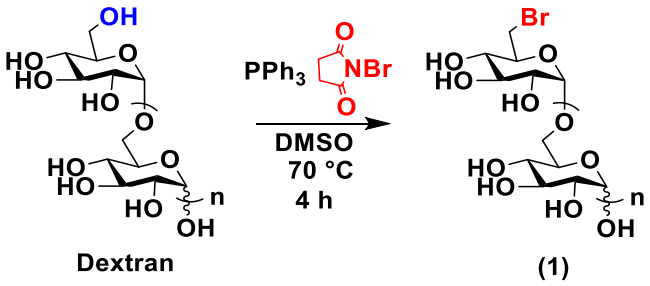

Scheme 1. NBS/PPh_3 bromination of dextran

To circumvent this issue, it was more revealing to characterize the products of subsequent amine displacement. To get an idea of the coupling conditions that would be required, we employed the small molecule allyl amine in initial experiments. We added NaI (30 equiv.) to the Dex-Br solution in order to generate a certain concentration of the more reactive alkyl iodide *in situ*[39]. Condensation with Dex-Br was carried out in a 0.078 mol L^{-1} solution of allyl amine at 40 °C for 24 h (Scheme 2). By-product HBr was neutralized by the excess of allyl amine. In this polymer-small molecule reaction, it was simple to collect the product through precipitation by using acetone as a non-solvent, followed by reprecipitation. After workup and drying, excess unreacted allyl amine, which has a low boiling point (55 °C) and excellent solubility in acetone, was fully removed. The resulting product was analyzed by ^{1}H NMR spectroscopy. As shown in Fig.1, new vinyl proton resonances appeared at 5.95 ppm (b) and 5.43 ppm (a), indicating that allyl groups were appended to dextran. This result supports our hypothesis that amine alkylation of Dex-Br is a promising

approach for block copolymer synthesis. Furthermore, it also illustrates that NBS bromination successfully end-functionalizes dextran. It should be noted that the allyl amine condensation product, with its vinyl substituent solely at the non-reducing end C6, could be a model macroinitiator for other new polysaccharide block copolymer families.

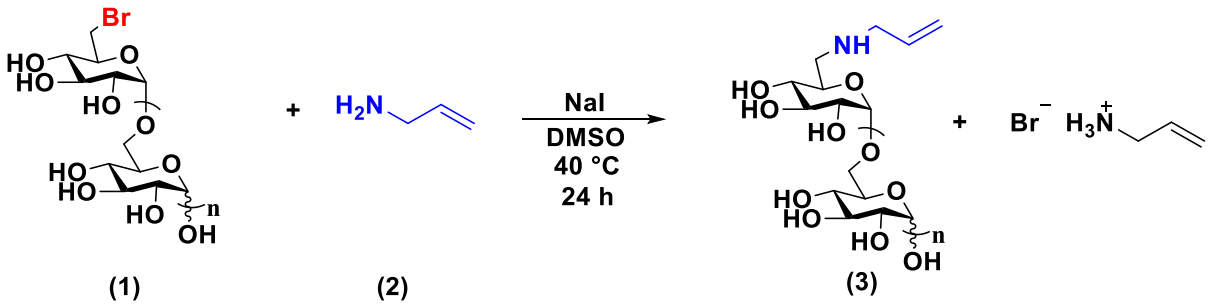

Scheme 2. Condensation of Dex-Br **(1)** with allyl amine

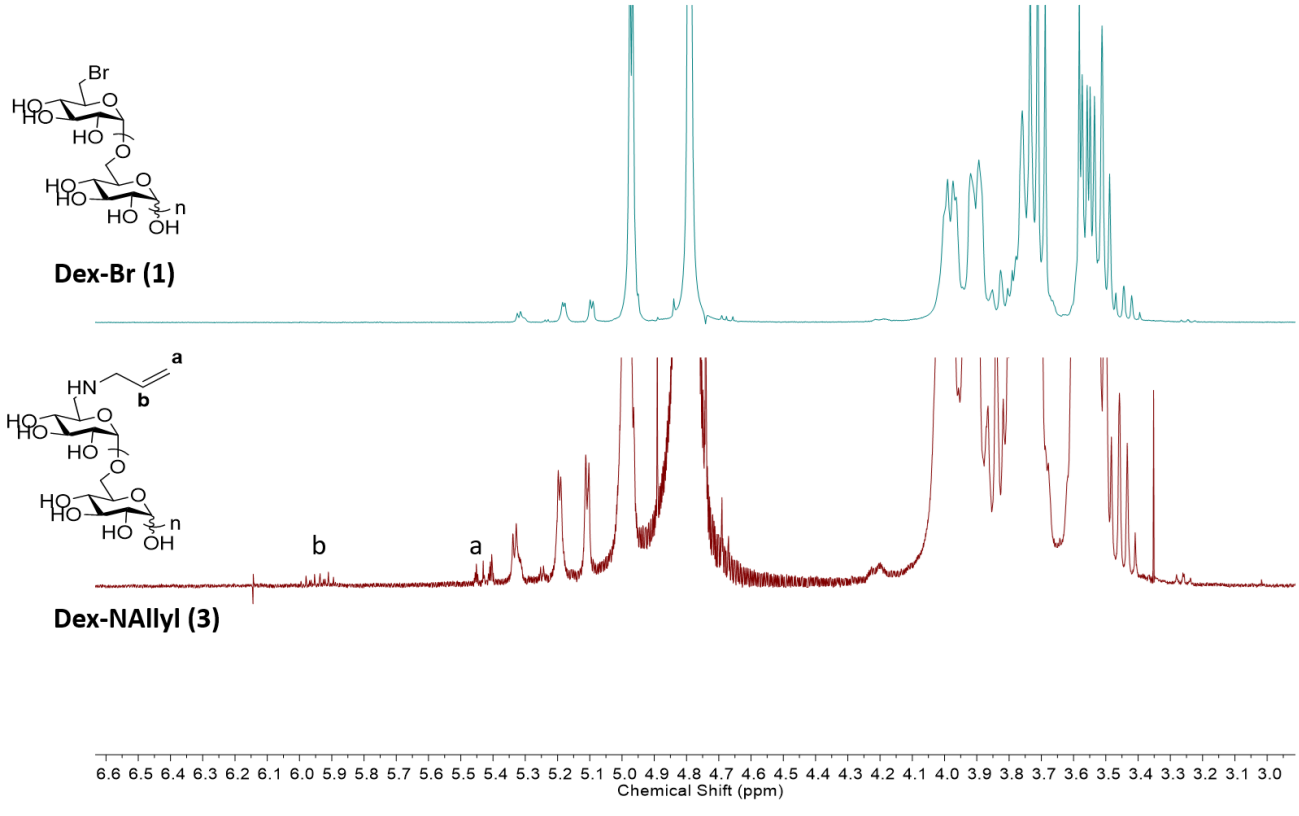

Figure 1. ^{1}H NMR spectra of Dex-Br **(1)** and Dex-NAllyl **(3)**

Having confirmed selective C-6 bromination by NBS/PPh_3, and subsequent bromide displacement by a small molecule amine, we took the next step by attempting condensation with the macromolecule PEG-amine (DP 120, primary amine terminated on one end and capped as a methyl ether at the other end). As a flexible, primary amine, we felt that PEG-amine was a good test case and would afford an interesting block copolymer if successful. We used a moderate excess of PEG-amine (3 equiv) and found that a relatively long reaction time (48 h) was required for best results, unsurprising given the low concentration of bromide end groups, the expected slower diffusion of a polymeric amine, and the higher solution viscosity that results from the presence of multiple polymers in solution.

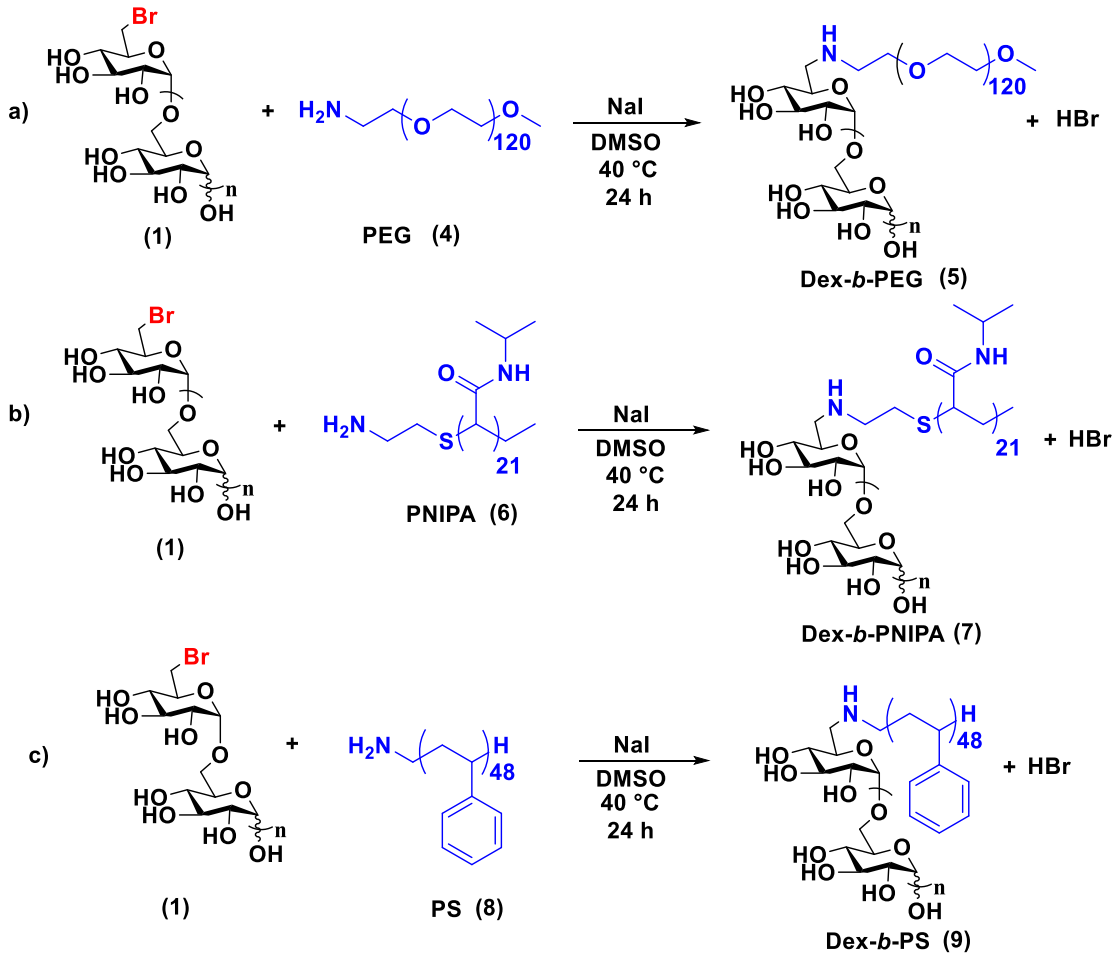

Scheme 3. Syntheses of a) Dextran-*b*-PEG **(5)**, b) Dextran-*b*-PNIPA **(7)** and c) Dextran-*b*-PS **(9)**

A key issue in this polymer-polymer amine displacement reaction was how to cleanly isolate the diblock copolymer product from the reaction mixture. At the end of the condensation, the crude DMSO reaction solution contains desired Dextran-*b*-PEG diblock copolymer, unreacted PEG-amine, the HBr salt of PEG-amine, and NaI. If the reaction did not go to completion, there could also be residual Dex-Br polymer. For the diblock copolymers made herein, we found that acetone was an effective non-solvent. Therefore precipitation into acetone afforded the desired product in partly purified form. Subsequent dialysis of the product against deionized water was also effective, since excess unreacted PEG-amine can pass through the dialysis tubing used with its 3500 g/mol

cut-off. This workup procedure efficiently removes residual excess polymeric amine starting material and limits the loss of the block copolymer, affording good yields (83-87%) of pure products.

The purified Dextran-*b*-PEG product was analyzed by ^{1}H-NMR spectroscopy. As shown in Fig. 1, we observe resonances from the PEG methylenes and the dextran glucose ring non-anomeric protons at 3.69 ppm and 3.0 – 4.0 ppm respectively. To further confirm formation of Dextran-*b*-PEG, we need to prove that these two distinct blocks are covalently bonded. However, the blocks are connected by only a single C-N bond per molecule, and it is difficult to distinguish and quantify by ^{1}H NMR spectroscopy as the CH-N protons are few and their resonances overlap with those of the dextran backbone. More definitive evidence was sought to confirm the diblock architecture of Dextran-*b*-PEG.

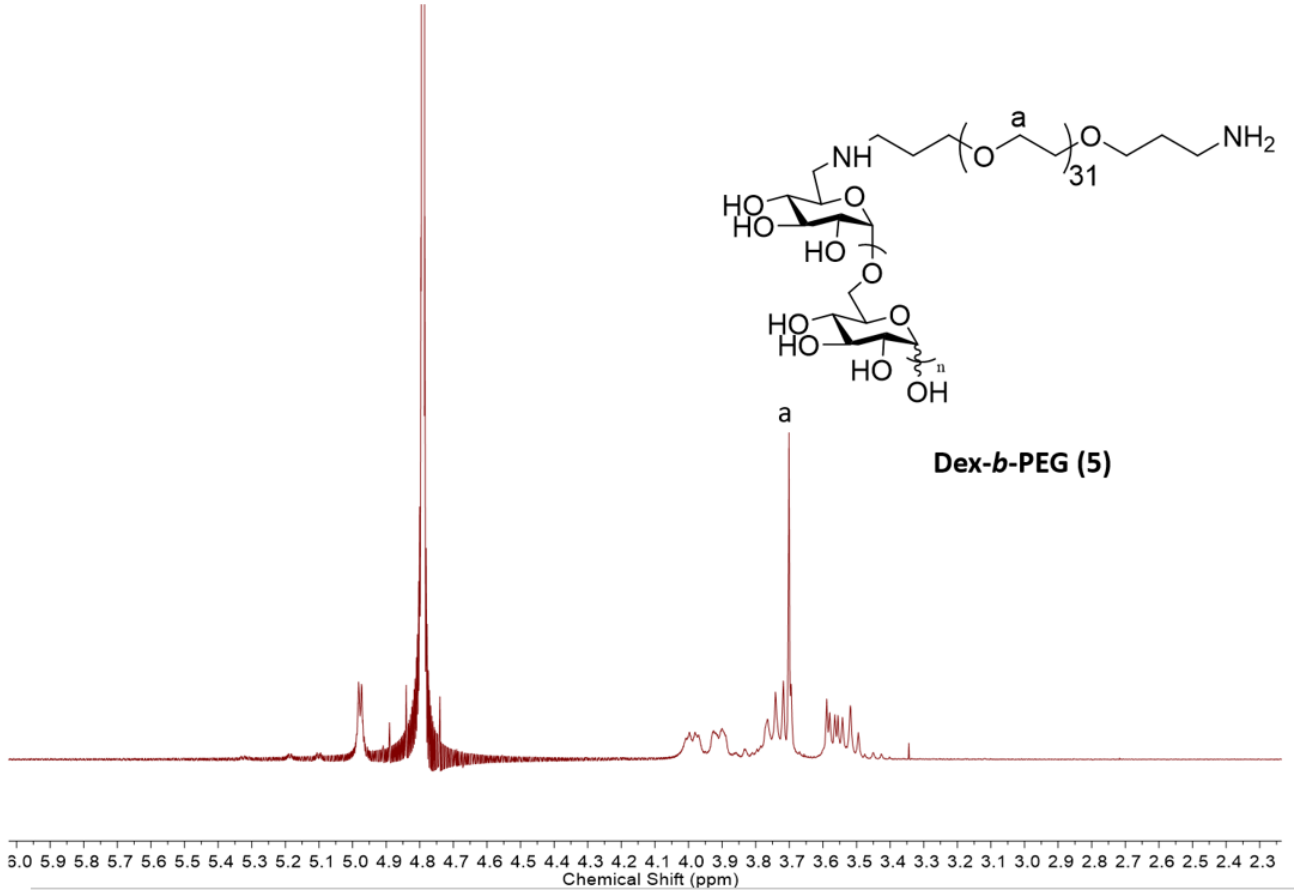

Figure 2. ^{1}H NMR spectrum of dextran-*b*-PEG **(5)** diblock copolymer.

We turned to SEC to provide evidence about the structure and purity of the purported Dextran-*b*-PEG. As dextran and PEG are both water soluble, it was unsurprising that the condensation product also exhibited excellent water solubility. We therefore performed SEC in water vs. starting Dex-Br and starting PEG-amine. Fig. 3 displays aqueous SEC elution traces of Dextran-*b*-PEG (red) and Dex-Br (black). The longer SEC retention time of the product is consistent with the higher molecular weight expected for the Dextran-*b*-PEG condensation product. There is too much overlap between peaks from the starting Dex-Br and the product to be certain of the absence of Dex-Br, but its absence is indicated by ^{13}C NMR spectroscopy results (Fig. S13). However, SEC can confirm the absence of PEG-amine from the product (Fig. S1). In combination with the PEG

methylene protons observed in the ^{1}H NMR spectrum, this is powerful evidence that the targeted Dextran-*b*-PEG copolymer has been obtained. The number average molecular weights of block copolymers and their starting materials were also analyzed using a multi-angle light scattering (MALS) detector. As shown in Table 1, the M_n value of Dextran-*b*-PEG as measured by aqueous SEC was 10,900 g/mol, suggesting the formation of the proposed diblock structure. However, the M_n values of these block copolymers are below theoretical, (ca. 12,400 based on adding M_n values of Dextran-Br and PEG-amine, and subtracting HBr) which may be the result of a small amount of dextran degradation during the amine condensation reaction (catalyzed by the amine-HBr salt)). Overall, SEC data are consistent with the hypothesis that the proposed diblock copolymer Dextran-*b*-PEG has been successfully obtained.

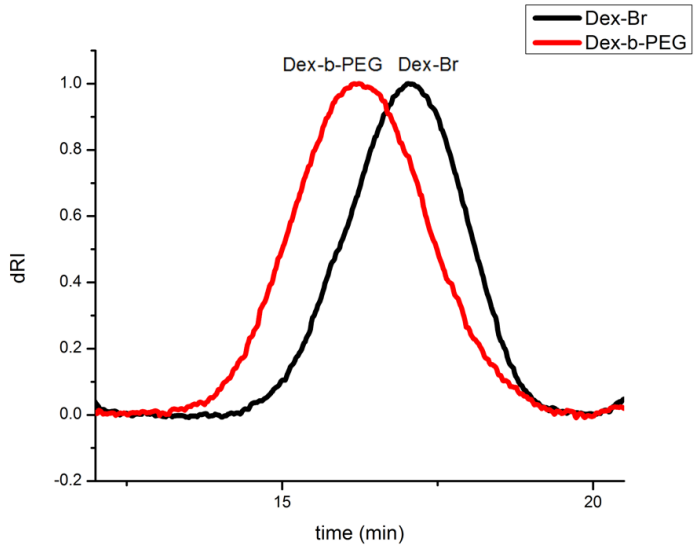

Figure 3. SEC chromatograms of Dex-Br **(1)** and Dextran-*b*-PEG **(5)**.

Encouraged by the successful condensation and diblock copolymer formation between PEG-amine and Dex-Br, we examined the scope of bromide displacement with regard to amine-terminated polymers. PNIPA-amine and PS-amine were chosen as alkylation partners to couple with Dex-Br. These diblock copolymers were prepared by methods analogous to those used for PEG-amine, by condensation of 3 equiv. of amine (PNIPA-amine; 2500 g/mol, PS-amine; 5000 g/mol) with Dex-Br at 80 °C in DMSO containing NaI. The key block copolymer purifications were effected by precipitation and reprecipitation with acetone, which was a poor solvent for the products and a good solvent for both PNIPA and PS. After dialysis and lyophilization, purified Dextran-*b*-PNIPA and Dextran-*b*-PS were analyzed by ^{1}H NMR spectroscopy. Resonances at 1.14, 1.58 and 2.00 ppm, contributed by the PNIPA backbone, support the formation of Dextran-*b*-PNIPA (Fig S2). The SEC elution profile (Fig S3) also supports the proposed diblock structure, as the expected molecular weight increase is seen after the coupling step. For Dextran-*b*-PS, we observed PS resonances at 7.03, 6.55 (protons from aromatic ring), 1.78 and 1.43 ppm (protons from -C$\underline{H}_2$-C$\underline{H}$-) in its ^{1}H NMR spectrum (Fig. S4), suggesting that product has the targeted block copolymer structure. Dextran-*b*-PNIPA was also analyzed by diffusion ordered spectroscopy (DOSY) NMR.[40] In a DOSY spectrum, covalently bonded polymer blocks would be expected have the same diffusion coefficient, while those that are not covalently linked should be seen to diffuse at different rates due to their significant structural and molecular weight

differences. As seen in Fig. S12, dextran and PNIPA blocks exhibited the same diffusion coefficient (4.36×10^{-10} m^2 s^{-1}), providing further support for the postulated diblock architecture.

Table 1. Aqueous SEC analyses of polymers and block copolymers

Samples	M_n (g/mol)*	Đ*
Dextran	10,100	1.32
Dextran-Br **(1)**	9600	1.31
Dextran-*b*-PEG **(5)**	10,900	1.37
Dextran-*b*-PNIPA **(9)**	10,300	1.36
PEG-amine **(4)**	2900	1.16

* M_n and Đ were measured by SEC with MALS.

While Dextran-*b*-PEG is a diblock copolymer comprising two hydrophilic blocks, and PEG is often a polymeric plasticizer for polysaccharide derivatives[41], Dextran-*b*-PNIPA and Dextran-*b*-PS each combine two blocks that differ significantly in properties, potentially leading to more interesting diblock copolymer properties. Dextran-*b*-PS with its hydrophilic dextran and hydrophobic PS blocks was thought to be the most likely of the copolymers prepared to demonstrate interesting morphology arising from microphase separation.

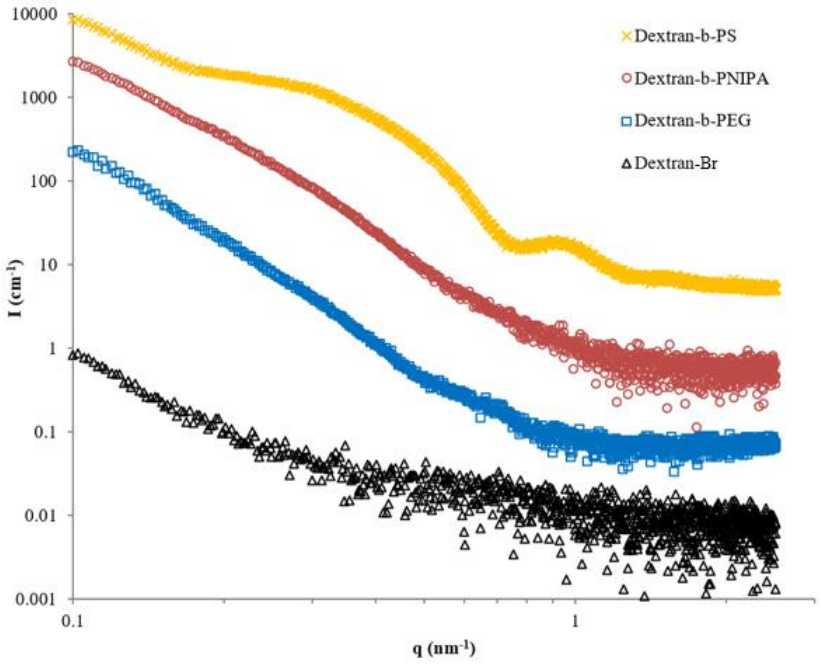

Figure 4. SAXS (Cu Kα) profile of Dextran-*b*-PS **(9)**, Dextran-*b*-PNIPA **(7)**, Dextran-*b*-PEG **(5)** and Dextran-Br **(1)** thin films. (Plots are vertically shifted for clarity)

To explore the morphologies of the dextran-based diblock copolymers, thin films of Dextran-*b*-PS, Dextran-*b*-PNIPA, Dextran-*b*-PEG, and dextran were prepared and investigated by SAXS. The SAXS profiles of Dextran-*b*-PS, Dextran-*b*-PNIPA, Dextran-*b*-PEG, and dextran are shown in Figure 4. The dextran homopolymer is expected to be amorphous and acts as an experimental control. As expected, the scattering profile for dextran is featureless. In contrast, the Dextran-*b*-PS exhibits two broad scattering features, around 0.41 nm^{-1} and 0.92 nm^{-1}, characteristic of a weakly-ordered phase separated morphology. Based on the composition of this block copolymer, it is reasonable to anticipate a typical hexagonally packed cylindrical morphology; however, the lack of order precludes a definitive structural assignment. For the more polar Dextran-*b*-PNIPA and Dextran-*b*-PEG block copolymers, excess scattering at low q is observed, but little evidence of phase ordering exists for these systems. The presence of weakly-ordered domains in the Dextran-

b-PS system suggests that thermodynamic immiscibility between the PS and dextran blocks drives phase development. With increased polarity of the PNIPA and PEG blocks, the driving force for phase separation is significantly reduced. This consideration is consistent with the solubility parameter difference between dextran and PS, which is larger than those between dextran and PEG, and dextran and PNIPA (Tables S1 and S2).[42–45] As the square of the solubility parameter difference is proportional to the Flory interaction parameter χ, the driving force for phase separation between the two blocks of dextran/PEG and dextran/PNIPA, may be insufficient to drive significant microphase separation.

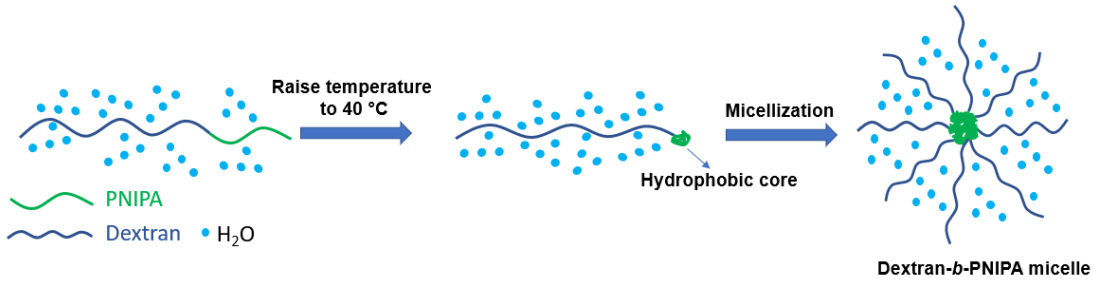

Figure 5. Micellization of Dextran-*b*-PNIPA **(7)**

Having prepared dextran-*b*-PNIPA, we explored whether the copolymer would display thermoresponsive behavior similar to that of PNIPA itself. As a copolymer of two water soluble blocks, dextran-*b*-PNIPA predictably and readily dissolved in water at room temperature. We prepared a 1 mg/mL aqueous solution of dextran-*b*-PNIPA, and analyzed its thermoresponsive behavior by DLS; Figure 5 illustrates the predicted thermoresponsive behavior. Figure 6 shows distributions of hydrodynamic radii (R_h) of Dextran-*b*-PNIPA in water at 25 °C and 40 °C. At 25 °C, the size distribution was monomodal. The average 4.4 nm Rh was consistent with a single diblock copolymer chain[46]. When the temperature was raised to 40 °C, above the LCST of PNIPA, the size distribution showed a single Rh peak at 85 nm. This higher diameter and the monomodal

distribution indicated formation of well-defined micelles. We hypothesize that the core of these micelles was formed through temperature-induced phase transition of PNIPA above its LCST (33 °C), whereas the corona comprised hydrophilic dextran blocks. To further confirm this hypothesis, the temperature was cooled to 25 °C and the Rh peak at 85 nm disappeared (Fig. S5), indicating disappearance of micelles. We postulate that the mechanism for these observations was that once temperature was reduced below the LCST, PNIPA blocks regained water solubility, destroying the core-corona architecture, and leading to dissolution of the diblock copolymer. In a control experiment, 1 mg/mL PNIPA-amine aqueous solution was studied in the same manner. PNIPA-amine also exhibits a single Rh at 25 °C, with 11 nm diameter consistent with single, solvated PNIPA-amine chains (Fig. S6). When the temperature was increased to 40 °C, as shown in Figure 6, a single peak with a 1600 nm Rh appeared, indicating that PNIPA amine formed large aggregates above its LCST. This control experiment reveals that the dextran block plays an important role in preventing PNIPA blocks from forming large aggregates. Taken together, these experiments show that Dextran-*b*-PNIPA micelles can be simply prepared by heating an aqueous solution of Dextran-*b*-PNIPA above the LCST of PNIPA, **without the need for organic solvents**. Moreover, the micellization of Dextran-*b*-PNIPA was observed to be complete within 5 min, which is relatively rapid compared to other thermally responsive polymers[47]. This appears to be the first report of synthesis and evaluation of a thermally responsive polysaccharide/PNIPA micelle.

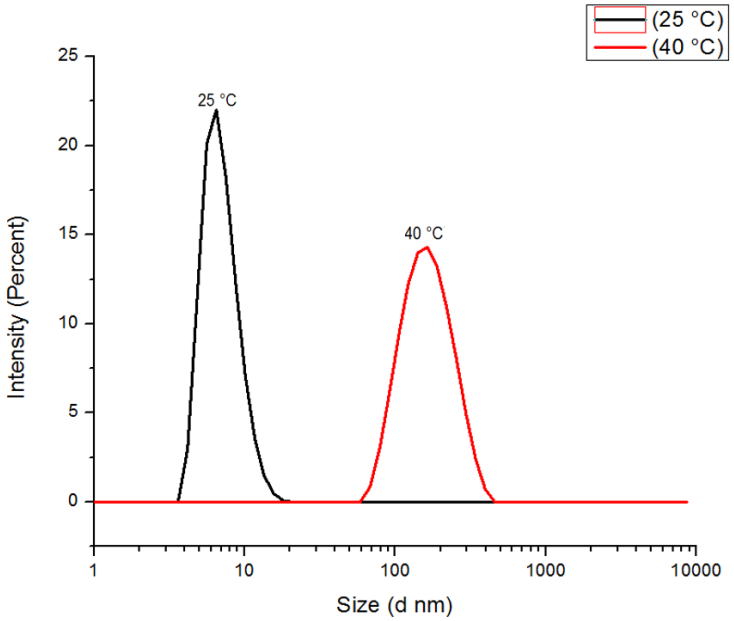

Figure 6. Size distribution by intensity of Dextran-*b*-PNIPA **(7)** vs. temperature

4.5 Conclusions

We have successfully demonstrated the concept of NBS bromination as an end-functionalization method for dextran at its non-reducing end, and the resulting regio- and chemoselectively substituted 6-bromo-6-deoxy-dextran was proven to be an effective substrate for block copolymer synthesis by direct condensation. This is the first time that a bromide was introduced only to the non-reducing end C-6 of dextran, and the first time that such a substituent was successfully elaborated by S_N2 displacement chemistry. This creates a simple, two-step pathway from native linear dextran via end-functional dextran derivatives to dextran-based block copolymers.

Three different block copolymers, Dextran-*b*-PEG, Dextran-*b*-PNIPA and Dextran-*b*-PS, were prepared through this coupling strategy, in which Dex-Br was reacted with amine-bearing polymers by bromide displacement. The structures of these block copolymers were confirmed by multiple techniques including ^{1}H and ^{13}C NMR spectroscopy, DOSY NMR, aqueous SEC, and FT-IR spectroscopy. The morphology of Dextran-*b*-PS was characterized by SAXS, which

suggested the existence of microphase separation, induced by thermodynamic incompatibility between the two distinct blocks. The thermal responsiveness of Dextran-*b*-PNIPA was investigated by DLS in dilute aqueous solution. This hydrophilic-amphiphilic block copolymer formed micelles with an average diameter of 170 nm at 37 °C, induced by the LCST behavior of the PNIPA block. The small micelle size and prevention of aggregation by the dextran block, as well as the ability, provided by the dextran block, to prepare micelles without the need for organic solvent, are noteworthy and potentially valuable characteristics of these new polysaccharide-based block copolymers.

These dextran block copolymers still have their C-1 anomeric positions intact, which suggests the possibility of further regioselective modification at the reducing end. Thus, these diblock copolymers may also be promising intermediates for A-B-C and A-B-A triblock copolymer synthesis. We are investigating and will describe in future reports the potential of these simply prepared, partly renewable-based, AB block copolymers for interesting and valuable applications.

4.6 Acknowledgments

We thank the Departments of Chemistry and of Sustainable Biomaterials, and the Institute for Critical Technologies and Applied Science (ICTAS) at Virginia Tech for facility support. We thank the National Science Foundation for partial support of this work through award DMR-1308276. We also thank Charles Carfagna and Rui Zhang at Virginia Tech for performing aqueous SEC and DOSY NMR analyses.

4.7 References

(1) Leibler, L. Theory of Microphase Separation in Block Copolymers. *Macromolecules* **1980**, *13* (6), 1602–1617. https://doi.org/10.1021/ma60078a047.

(2) Arrington, K. J.; Haag IV, J. V.; French, E. V.; Murayama, M.; Edgar, K. J.; Matson, J. B. Toughening Cellulose: Compatibilizing Polybutadiene and Cellulose Triacetate Blends. *ACS Macro Lett.* **2019**, *8* (4), 447–453. https://doi.org/10.1021/acsmacrolett.9b00136.

(3) Xiao, Q.; Wang, X.; Li, W.; Li, Z.; Zhang, T.; Zhang, H. Macroporous Polymer Electrolytes Based on PVDF/PEO-b-PMMA Block Copolymer Blends for Rechargeable Lithium Ion Battery. *J. Memb. Sci.* **2009**. https://doi.org/10.1016/j.memsci.2009.02.018.

(4) Car, A.; Stropnik, C.; Yave, W.; Peinemann, K. V. PEG Modified Poly(Amide-b-Ethylene Oxide) Membranes for CO2 Separation. *J. Memb. Sci.* **2008**. https://doi.org/10.1016/j.memsci.2007.09.023.

(5) Heinze, T.; Liebert, T.; Heublein, B.; Hornig, S. Functional Polymers Based on Dextran. In *Polysaccharides Ii*; Springer, 2006; pp 199–291.

(6) Kasaai, M. R. Dilute Solution Properties and Degree of Chain Branching for Dextran. *Carbohydr. Polym.* **2012**. https://doi.org/10.1016/j.carbpol.2011.12.012.

(7) Williams, D. F. There Is No Such Thing as a Biocompatible Material. *Biomaterials.* **2014**, *35* (38), 10009–10014.

(8) Jin, R.; Hiemstra, C.; Zhong, Z.; Feijen, J. Enzyme-Mediated Fast in Situ Formation of Hydrogels from Dextran–Tyramine Conjugates. *Biomaterials* **2007**, *28* (18), 2791–2800. https://doi.org/10.1016/J.BIOMATERIALS.2007.02.032.

(9) Koutroubakis, I. E.; Oustamanolakis, P.; Karakoidas, C.; Mantzaris, G. J.; Kouroumalis, E. A. Safety and Efficacy of Total-Dose Infusion of Low Molecular Weight Iron Dextran for Iron

Deficiency Anemia in Patients with Inflammatory Bowel Disease. *Dig. Dis. Sci.* **2010**, *55* (8), 2327–2331. https://doi.org/10.1007/s10620-009-1022-y.

(10) Varshosaz, J. Dextran Conjugates in Drug Delivery. *Expert Opin. Drug Deliv.* **2012**, *9* (5), 509–523. https://doi.org/10.1517/17425247.2012.673580.

(11) Mezger, T.; Cantow, H.-J. Cellulose Containing Block Copolymers. 4. Cellulose Triester Macroinitiators. *Angew. Makromol. Chemie* **1983**, *116* (1), 13–27. https://doi.org/10.1002/apmc.1983.051160102.

(12) De Oliveira, W.; Classer, W. G. Novel Cellulose Derivatives. II. Synthesis and Characteristics of Mono-Functional Cellulose Propionate Segments. *Cellulose* **1994**, *1* (1), 77–86. https://doi.org/10.1007/BF00818800.

(13) Chen, J.; Kamitakahara, H.; Edgar, K. J. Synthesis of Polysaccharide-Based Block Copolymers via Olefin Cross-Metathesis. *Carbohydr. Polym.* **2019**, 115530. https://doi.org/10.1016/J.CARBPOL.2019.115530.

(14) Yalpani, M.; Brooks, D. E. Selective Chemical Modifications of Dextran. *J. Polym. Sci. Polym. Chem. Ed.* **1985**, *23* (5), 1395–1405. https://doi.org/10.1002/pol.1985.170230513.

(15) Oliveira, W. de; Glasser, W. G. Multiphase Materials with Lignin: 13. Block Copolymers with Cellulose Propionate. *Polymer (Guildf).* **1994**, *35* (9), 1977–1985. https://doi.org/10.1016/0032-3861(94)90991-1.

(16) Yamagami, M.; Kamitakahara, H.; Yoshinaga, A.; Takano, T. Thermo-Reversible Supramolecular Hydrogels of Trehalose-Type Diblock Methylcellulose Analogues. *Carbohydr. Polym.* **2018**, *183*, 110–122. https://doi.org/10.1016/J.CARBPOL.2017.12.006.

(17) Houga, C.; Meins, J.-F. Le; Borsali, R.; Taton, D.; Gnanou, Y. Synthesis of ATRP-Induced Dextran-b-Polystyrene Diblock Copolymers and Preliminary Investigation of Their Self-Assembly in Water. *Chem. Commun.* **2007**, *0* (29), 3063. https://doi.org/10.1039/b706248f.

(18) Hernandez, O. S.; Soliman, G. M.; Winnik, F. M. Synthesis, Reactivity, and PH-Responsive Assembly of New Double Hydrophilic Block Copolymers of Carboxymethyldextran and Poly(Ethylene Glycol). *Polymer (Guildf).* **2007**, *48* (4), 921–930. https://doi.org/10.1016/J.POLYMER.2006.12.036.

(19) Bosker, W. T. E.; Agoston, K.; Cohen Stuart, M. A.; Norde, W.; Timmermans, J. W.; Slaghek, T. M. %J M. Synthesis and Interfacial Behavior of Polystyrene− Polysaccharide Diblock Copolymers. **2003**, *36* (6), 1982–1987.

(20) Fox, S. C.; Li, B.; Xu, D.; Edgar, K. J. Regioselective Esterification and Etherification of Cellulose - A Review. *Biomacromolecules* **2011**, *12*, 1956–1972. https://doi.org/10.1021/bm200260d.

(21) Fox, S. C.; Edgar, K. J. Synthesis of Regioselectively Brominated Cellulose Esters and 6-Cyano-6-Deoxycellulose Esters. *Cellulose* **2011**, *18* (5), 1305–1314. https://doi.org/10.1007/s10570-011-9574-3.

(22) Pereira, J. M.; Mahoney, M.; Edgar, K. J. Synthesis of Amphiphilic 6-Carboxypullulan Ethers. *Carbohydr. Polym.* **2014**, *100*, 65–73. https://doi.org/10.1016/J.CARBPOL.2012.12.029.

(23) Xu, D.; Voiges, K.; Elder, T.; Mischnick, P.; Edgar, K. J. Regioselective Synthesis of Cellulose Ester Homopolymers. *Biomacromolecules* **2012**, *13* (7), 2195–2201. https://doi.org/10.1021/bm3006209.

(24) Furuhata, K.; Koganei, K.; Chang, H.-S.; Aoki, N.; Sakamoto, M. Dissolution of Cellulose in Lithium Bromide-Organic Solvent Systems and Homogeneous Bromination of Cellulose with N-Bromosuccinimide-Triphenylphosphine in Lithium Bromide-N,N-Dimethylacetamide. *Carbohydr. Res.* **1992**, *230* (1), 165–177. https://doi.org/10.1016/S0008-6215(00)90519-6.

(25) Liu, S.; Liu, J.; Esker, A. R.; Edgar, K. J. An Efficient, Regioselective Pathway to Cationic and Zwitterionic *N* -Heterocyclic Cellulose Ionomers. *Biomacromolecules* **2016**, *17* (2), 503–513. https://doi.org/10.1021/acs.biomac.5b01416.

(26) Zhang, R.; Edgar, K. J. Synthesis of Curdlan Derivatives Regioselectively Modified at C-6: O-(N)-Acylated 6-Amino-6-Deoxycurdlan. *Carbohydr. Polym.* **2014**, *105* (0), 161–168. https://doi.org/http://dx.doi.org/10.1016/j.carbpol.2014.01.045.

(27) Gao, C.; Liu, S.; Edgar, K. J. Regioselective Chlorination of Cellulose Esters by Methanesulfonyl Chloride. *Carbohydr. Polym.* **2018**, *193*, 108–118. https://doi.org/10.1016/J.CARBPOL.2018.03.093.

(28) Marks, J. A.; Fox, S. C.; Edgar, K. J. Cellulosic Polyelectrolytes: Synthetic Pathways to Regioselectively Substituted Ammonium and Phosphonium Derivatives. *Cellulose* **2016**, *23* (3), 1687–1704. https://doi.org/10.1007/s10570-016-0929-7.

(29) Pereira, J. M.; Edgar, K. J. Regioselective Synthesis of 6-Amino- and 6-Amido-6-Deoxypullulans. *Cellulose* **2014**, *21* (4), 2379–2396. https://doi.org/10.1007/s10570-014-0259-6.

(30) Liu, S.; Edgar, K. J. Water-Soluble Co-Polyelectrolytes by Selective Modification of Cellulose Esters. *Carbohydr. Polym.* **2017**, *162*, 1–9. https://doi.org/10.1016/j.carbpol.2017.01.008.

(31) Liu, S.; Gao, C.; Mosquera-Giraldo, L. I.; Taylor, L. S.; Edgar, K. J. Selective Synthesis of Curdlan ω-Carboxyamides by Staudinger Ylide Nucleophilic Ring-Opening. *Carbohydr. Polym.* **2018**. https://doi.org/10.1016/j.carbpol.2018.02.074.

(32) Li, B. Q.; Dong, X.; Fang, S. H.; Gao, J. Y.; Yang, G. Q.; Zhao, H. Systemic Toxicity and Toxicokinetics of a High Dose of Polyethylene Glycol 400 in Dogs Following Intravenous Injection. *Drug Chem. Toxicol.* **2011**, *34*, 208–212. https://doi.org/10.3109/01480545.2010.500292.

(33) Zámbó, D.; Radnóczi, G. Z.; Deák, A. Preparation of Compact Nanoparticle Clusters from Polyethylene Glycol-Coated Gold Nanoparticles by Fine-Tuning Colloidal Interactions. *Langmuir* **2015**, *31*, 2662–2668. https://doi.org/10.1021/la504600j.

(34) Ishida, T.; Atobe, K.; Wang, X.; Kiwada, H. Accelerated Blood Clearance of PEGylated Liposomes upon Repeated Injections: Effect of Doxorubicin-Encapsulation and High-Dose First Injection. *J. Control. Release* **2006**, *115*, 251–258. https://doi.org/10.1016/j.jconrel.2006.08.017.

(35) Schild, H. G. Poly(N-Isopropylacrylamide): Experiment, Theory and Application. *Prog. Polym. Sci.* **1992**, *17* (2), 163–249. https://doi.org/10.1016/0079-6700(92)90023-R.

(36) Qin, S.; Geng, Y.; Discher, D. E.; Yang, S. Temperature-Controlled Assembly and Release from Polymer Vesicles of Poly(Ethylene Oxide)-Block- Poly(N-Isopropylacrylamide). *Adv. Mater.* **2006**, *18* (21), 2905–2909. https://doi.org/10.1002/adma.200601019.

(37) Fedors, R. F. A Method for Estimating Both the Solubility Parameters and Molar Volumes of Liquids. *Polym. Eng. Sci.* **1974**, *14* (2), 147–154. https://doi.org/10.1002/pen.760140211.

(38) Gao, C.; Edgar, K. J. Efficient Synthesis of Glycosaminoglycan Analogs. *Biomacromolecules* **2019**, *20* (2), 608–617. https://doi.org/10.1021/acs.biomac.8b01150.

(39) Finkelstein, H. Darstellung Organischer Jodide Aus Den Entsprechenden Bromiden Und Chloriden. *Berichte der Dtsch. Chem. Gesellschaft* **1910**, *43* (2), 1528–1532. https://doi.org/10.1002/cber.19100430257.

(40) Bakkour, Y.; Darcos, V.; Li, S.; Coudane, J. Diffusion Ordered Spectroscopy (DOSY) as a Powerful Tool for Amphiphilic Block Copolymer Characterization and for Critical Micelle Concentration (CMC) Determination. *Polym. Chem.* **2012**, *3* (8), 2006. https://doi.org/10.1039/c2py20054f.

(41) Smits, A. L. M.; Kruiskamp, P. H.; Van Soest, J. J. G.; Vliegenthart, J. F. G. Interaction between Dry Starch and Plasticisers Glycerol or Ethylene Glycol, Measured by Differential Scanning Calorimetry and Solid State NMR Spectroscopy. *Carbohydr. Polym.* **2003**, *53*, 409–416. https://doi.org/10.1016/S0144-8617(03)00119-X.

(42) Güner, A. The Algorithmic Calculations of Solubility Parameter for the Determination of Interactions in Dextran/Certain Polar Solvent Systems. *Eur. Polym. J.* **2004**, *40* (7), 1587–1594. https://doi.org/10.1016/J.EURPOLYMJ.2003.10.030.

(43) Mieczkowski, R. The Determination of the Solubility Parameter Components of Polystyrene by Partial Specific Volume Measurements. *Eur. Polym. J.* **1988**, *24* (12), 1185–1189. https://doi.org/10.1016/0014-3057(88)90109-7.

(44) Adamska, K.; Voelkel, A. Hansen Solubility Parameters for Polyethylene Glycols by Inverse Gas Chromatography. *J. Chromatogr. A* **2006**, *1132* (1–2), 260–267. https://doi.org/10.1016/j.chroma.2006.07.066.

(45) Yagi, Y.; Inomata, H.; Saito, S. Solubility Parameter of an N-Isopropylacrylamide Gel. *Macromolecules* **1992**, *25* (11), 2997–2998. https://doi.org/10.1021/ma00037a034.

(46) Wangqing Zhang; Linqi Shi, *; Kai Wu, A.; An, Y. Thermoresponsive Micellization of Poly(Ethylene Glycol)-b-Poly(N-Isopropylacrylamide) in Water. **2005**. https://doi.org/10.1021/MA0509199.

(47) Wei, H.; Cheng, S.-X.; Zhang, X.-Z.; Zhuo, R.-X. Thermo-Sensitive Polymeric Micelles Based on Poly(N-Isopropylacrylamide) as Drug Carriers. *Prog. Polym. Sci.* **2009**, *34* (9), 893–910. https://doi.org/10.1016/J.PROGPOLYMSCI.2009.05.002.

Chapter 5: All-polysaccharide, self-healing injectable hydrogels based on chitosan and oxidized hydroxypropyl polysaccharides

Junyi Chen[a], Brittany L. B. Nichols[a], Ann M. Norris[b, c], Charles E. Frazier[b, c], and Kevin J. Edgar[b, c]

[a]Department of Chemistry, Virginia Tech, Blacksburg, VA 24061, United States

[b]Department of Sustainable Biomaterials, Virginia Tech, Blacksburg, VA 24061, United States

[c]Macromolecules Innovation Institute, Virginia Tech, Blacksburg, VA 24061, United States

5.1 Abstract

Polysaccharide-based hydrogels are attractive materials for biomedical applications for reasons that include their polyfunctionality, generally benign nature, and biodegradability. However, use of polysaccharide-based hydrogels may be limited by toxicity arising from small molecule crosslinkers, or may involve undesired chemical modification[1].

Here, we report a green, simple, efficient strategy for preparation of polysaccharide-based, *in situ* forming hydrogels. The Edgar group reports in the accompanying manuscript that chemoselective oxidation of oligo(hydroxypropyl)-substituted polysaccharides introduces ketone groups at the termini of the oligo(hydroxypropyl) chains[2]. Amine containing moieties can condense with ketones to form imines. The imine linkage is dynamic in the presence of water, providing the potential for self-healing[3] , injectability[4], and pH responsiveness[5].

In this work, we designed and prepared two different types of hydrogels, oxidized hydroxypropyl cellulose/chitosan (OX-HPC-Chitosan) and oxidized hydroxypropyl dextran/chitosan (OX-HPD-Chitosan), each crosslinked by imine bonds. The mechanical properties of these hydrogels were characterized by rheometry, revealing that hydrogel storage modulus could be tuned from 300 Pa to 13 kPa by controlling the degree of substitution (DS) of ketone groups. Rheological characterization also illustrated the rapid self-healing property of these all-polysaccharide

hydrogels. Moreover, these hydrogels exhibited high swelling rates and facile injectability. Therefore, this work reveals a potential strategy for construction of hydrogels that require no small molecule crosslinkers, and are therefore highly attractive for biomedical, agricultural, controlled release, and other applications.

5.2 Introduction

Hydrogels, which are useful components both in natural and manufactured products, are typically polymers with high water affinity that have been crosslinked to create an entity that has such high molecular weight that it can no longer dissolve in water, but retains high water affinity[6]. Polysaccharide-based hydrogels are prominent in biomedical applications[7], due to the fact that they are frequently biocompatible with living tissues in the desired application mode and circumstance[8], they have high water swelling ratios, and high permeability to metabolites and nutrients[9]. As a result, polysaccharides including cellulose[10], chitosan[11], alginic acid[12], hyaluronic acid[13], dextran[14], and their derivatives are frequently investigated as hydrogel components.

In situ forming hydrogels have advantages for biomedical applications vs. preformed hydrogels[15]. An *in situ* forming hydrogel is likely to be injectable in the liquid state, then can transition to the gel state at the site of application. This class of hydrogel has been exploited in drug delivery, tissue engineering, and surgical sealant applications[16]. In the clinic, *in situ* forming hydrogels can be injected at the disease site with great precision, enhancing efficacy and reducing off-target effects[15]. A recent study described an *in situ* forming hydrogel that allows for self-healing, closely resembling the extracellular matrix (ECM) which provides a complex cellular environment[17]. Self-healing behavior of hydrogels can be very important, enabling their use in biological systems where they may be subjected to stress (e.g., in joints) as well as for non-biological applications (e.g. personal care or agriculture) where self-healing to a continuous film or gel could be

functionally important. Moreover, *in vivo* degradability of hydrogels helps to ensure a dynamic biomimetic environment that permits cells to live and function[18]. Since many, perhaps most hydrogel applications create the opportunity for human contact of one type or another, it is absolutely crucial that the hydrogel and all of its components are benign in nature.

In view of this partial list of hydrogel performance criteria, hydrogel design and polymer selection are key. Chitosan has been viewed as a desirable candidate polymer by many investigators[19, 20]. It has many features useful in hydrogel formation; it has free amines, unusual among natural polysaccharides and their readily obtained derivatives. It exhibits biocompatibility towards many tissues, is biodegradable *in vivo* and in the environment (though biodegradation rate decreases as DS(Ac) decreases[21]), has low toxicity[22], is bioadhesive, has limited immunogenicity, and has bacteriostatic and hemostatic properties[23]. Furthermore, chitosan can readily dissolve in mildly acidic (e.g. aqueous HOAc) aqueous solution, a relatively benign system for hydrogel preparation[24]. Dextran is another promising natural polysaccharide for biomedical applications. It is biocompatible in many situations (for example, it is commonly part of intravenous fluids administered to patients, in part to maintain osmotic balance), and is biodegradable both *in vivo* and in the environment. Dextran can be more readily chemically modified than cellulose[25], due to its good solubility in water and in certain polar organic solvents. Dextran is metabolized in humans by amylase enzymes, being cleared through the kidney once molecular weight is reduced to ca. 30K g/mol[15], which is a critical feature for biomedical applications[26]. Cellulose ethers have also been frequently used to prepare hydrogels. Hydroxypropyl cellulose (HPC), a water soluble cellulose ether, is used in pharmaceutical fields including lubricants for artificial tears, and binders in tablets[27]. HPC hydrogels have been of particular interest because of the thermally responsive

nature of HPC solutions[28]. Herein we will exploit these polysaccharides in an attempt to prepare all-polysaccharide hydrogels.

Currently, self-healing hydrogels can be prepared by different strategies which include dynamic covalent[29,30] and non-covalent linkages[31]. Redox-responsive disulfide bonds[32], Diels-Alder cycloadditions[33], and acylhydrazone bond formation[34] are all dynamic chemistries which have been exploited for preparing self-healing hydrogels. However, these hydrogel formation methods typically involve either difunctional small molecule reagents, or appending reactive and/or complex reactive moieties to each polysaccharide partner. Small molecule difunctional reagents are often toxic and are unlikely to react completely in the viscous environment of the forming hydrogel. It is virtually impossible to extract such an unreacted reagent quantitatively from a hydrogel. Appending complex and reactive moieties to polysaccharides can be difficult, expensive, less than perfectly selective, and may impart its own toxicity concerns.

Imine bonds between amine and either aldehyde or ketone groups are dynamic and covalent, and can form spontaneously without the need for a catalyst[35]. This dynamic nature supports self-healing, and is one reason that imine bond-based hydrogels have proved attractive. However, most current methods to form imine-based hydrogels from polysaccharides utilize sodium periodate[36, 37] to cleave vicinal diols and create ring-opened dialdehydes. This oxidation destroys relatively rigid pyran rings, imparts much greater flexibility, and introduces chemical instability due to reactive aldehyde groups and the more acidic protons alpha to the aldehydes. In turn, these structural changes can result in serious degradation of polysaccharide degree of polymerization (DP), and inferior mechanical properties. Functionalization of the polysaccharide with ketone groups is an alternative approach to prepare imine bond-based hydrogels. Mao[38] reported preparation of this class of hydrogel by using cellulose acetoacetate[39], which can readily form

hydrogels with chitosan. However, synthesis of cellulose acetoacetate most efficiently involves diketene, which is highly reactive and whose shipping is therefore restricted, in addition to being a volatile, powerful lachrymator. Alternative methods of acetoacetylation employ more expensive reagents (e.g. *t*-butyl acetoacetate[40] or diketene-acetone adduct[41]), higher temperatures, and may require expensive cellulose solvents (e.g. ionic liquids), limiting the utility of polysaccharide acetoacetates in hydrogels. Ketones can also be appended to polysaccharides by attaching levulinoyl moieties. However, reaction with an appropriate levulinoyl synthon is more difficult in polysaccharide chemistry than it is in small molecule carbohydrate chemistry, and tends to be an inefficient process[42].

Oligo(hydroxypropyl)-substituted polysaccharides such as hydroxypropyl cellulose (HPC), hydroxypropyl methyl cellulose, and hydroxypropyl methyl cellulose acetate succinate are important commercial polymers in fields such as personal care, drug delivery, and food formulation. They are synthesized by ring opening of propylene oxide by a polysaccharide hydroxyl, typically in the presence of a strong base like sodium hydroxide[43]. This creates an oligo(hydroxypropyl) substituent with a single, secondary alcohol at the chain terminal hydroxypropyl group. We describe in the accompanying manuscript that this secondary alcohol can be oxidized selectively. Our process uses the remarkably simple procedure of exposing the polymer to household bleach (sodium hypochlorite, NaOCl) in water at room temperature. This chemistry has been known for some time for simple small molecule secondary alcohols thanks to the pioneering work of Stevens[44], but had never before been applied to polysaccharide chemistry (where many seemingly simple small molecule chemistries founder, due to the restricted mobility and approach angles, and strong hydrogen bonding of polysaccharides). This discovery showed that the terminal secondary alcohols from HPC and other oligo(hydroxypropyl)-substituted

polysaccharides can be selectively oxidized to terminal ketone groups. It is exciting to contemplate the possibility that these ketones could readily combine with amine-substituted polysaccharides to afford imine bond crosslinked hydrogels. Compared to sodium periodate oxidation and other polysaccharide functionalization approaches, this sodium hypochlorite oxidation of hydroxypropyl end groups to ketones is attractive because of its simplicity, economy, and mild nature. It is particularly important that this route promises to prepare ketone-containing polysaccharides without loss of the fundamental, rigid polysaccharide structure, and the properties resulting therefrom.

We hypothesize that oxidized hydroxypropyl cellulose (OX-HPC) and oxidized hydroxypropyl dextran (OX-HPD), prepared from the corresponding hydroxypropyl polysaccharides by NaOCl oxidation, will readily form hydrogels with chitosan. The crosslinking reaction, by formation of imine bonds, is reversible, generating only water as a co-product[45]. We further hypothesize that this novel type of hydrogel will be remarkably dynamic, hydrolyzing, reforming, and self-healing in water. Herein, we report our initial tests of these hypotheses by investigating processes for preparation of such hydrogels, characterizing the products, and testing critical properties.

5.3 Materials and Methods

5.3.1 Materials

HPC (Mn 100,000 g/mol, degree of substitution (DS) (hydroxypropyl) = 2.2, molar substitution (MS) (hydroxypropyl) = 4.4)[46], and propylene oxide 99% were purchased from Acros Organics. Sodium hypochlorite aqueous solution (11-15% available chlorine) was purchased from Alfa Aesar. Dextran from *Leuconostoc mesenteroides* (Mn = 40,000 g/mol), chitosan (medium molecular weight, 75% deacetylated), and phosphate buffered saline tablets (pH 7.4) were all purchased from Sigma-Aldrich. Sodium hydroxide, glacial acetic acid, and dialysis tubing (3500

MWCO) were purchased from Fisher Scientific. Deionized water was prepared by a ROpure ST reverse osmosis/tank system.

5.3.2 Measurements

^{1}H NMR spectra were acquired either on a Bruker Avance II spectrometer operating at 500 MHz or on an Agilent MR4 instrument operating at 400 MHz. All samples were analyzed as solutions in D_2O (ca. 10 mg/mL) at 25 °C in standard 5 mm o.d. tubes. ^{13}C NMR spectra were acquired on a Bruker Avance II 500 MHz spectrometer with a minimum of 10,000 scans in D_2O (ca. 40 mg/mL). FT-IR spectra were obtained on a Nicolet 8700 instrument using potassium bromide powder as matrix.

5.3.3 Rheological characterization of hydrogels

All hydrogel samples were characterized rheologically using a TA AR2000 instrument. The test geometry was a 25 mm Peltier plate. Each hydrogel sample, around 100 mg, was uniformly dispensed on the rheometer plate. The test geometry was moved down to the targeted gap height (1.5 mm), and excess hydrogel was removed. In strain sweep experiments, the range of strain was from 0.2% to 200% and the test was conducted at 25 °C at 0.5 Hz. In frequency sweep experiments, frequency range was from 0.1 to 5.0 Hz and the test was conducted at 25 °C at 1% strain. In step strain sweep experiments, strain was alternated between 0.5% and 200% in 4 minute segments with 2 minute gaps after each 200% strain segment. Temperature and frequency were set to be 25 °C and 0.2 Hz respectively.

5.3.4 Synthesis of oxidized hydroxypropyl cellulose (OX-HPC)

HPC oxidation follows a procedure recently developed by the Edgar group[2]. HPC (4.0 g, Mn 100,000 g/mol, DS = 2.2, MS = 4.4, 31.2 mmol terminal secondary hydroxyl groups) was dissolved in 50 mL DI water. Then 50 mL NaOCl aqueous solution (146.6 mmol, 4.7 equiv.) was slowly

added. After that, 5 mL of acetic acid (87.4 mmol, 2.8 equiv.) was added dropwise. The solution was stirred at room temperature for 1 h. Subsequently, the solution was dialyzed in DI water for 48 h. Finally, the purified OX-HPC solution was freeze dried to give 3.85 g product (yield: 96%).

^{1}H NMR (D_2O): δ 1.14 d, [-CH_2-CH(-C$\underline{H}_3$)-O-], δ 2.13 s, (C$\underline{H}_3$-CO-), δ 3.0 – 4.0, m, (HPC backbone), δ 3.0 – 4.2, d, [-C$\underline{H}_2$-CH(-CH_3)-O-] , δ 3.0 – 4.2, t, [-CH_2-C$\underline{H}$(-CH_3)-O-], δ 4.26, s, (-O-C$\underline{H}_2$-CO-)

^{13}C NMR (D_2O): 210 (CH_3-$\underline{C}$O-), 65-105 {cellulose backbone, [-$\underline{C}H_2$-$\underline{C}$H(-CH_3)-O-], (-O-C$\underline{H}_2$-CO-)}s, 25 ($\underline{CH}_3$-CO-), 15 {$\underline{C}H_3$-CH(OH)-, [-CH_2-CH(-$\underline{C}H_3$)-O-]}

5.3.5 Synthesis of hydroxypropyl dextran (HPD)

Synthesis of HPD follows a procedure recently developed by the Edgar group[2]. Dextran (5.0 g, Mn 40,000 g/mol, 30.3 mmol AGU) was dissolved in 100 mL DI water. NaOH (1.71 g, 42.8 mmol, 1.40 equiv.) and propylene oxide (6.13 mL, 90.7 mmol, 2.99 equiv.) were added into the solution separately. The solution was stirred overnight. After the reaction, the solution was purified by dialysis. HPD (6.48 g) was collected by freeze drying (yield: 88%).

^{1}H NMR (D_2O): δ 1.14 d, [-CH_2-CH(-C$\underline{H}_3$)-O-], δ 1.14 d, [C$\underline{H}_3$-CH(OH)-],δ 3.35 – 4.05, m, (dextran backbone), δ 3.35 – 4.05, d, [-C$\underline{H}_2$-CH(-CH_3)-O-]), δ 3.35 – 4.05, t, [-CH_2-C$\underline{H}$(-CH_3)-O-], δ 3.35 – 4.05, s, [-O-C$\underline{H}_2$-CH(OH)-]

^{13}C NMR (D_2O): 100 (dextran C1), 60-82 {(dextran C2-C6), [-$\underline{C}H_2$-$\underline{C}$H(-CH_3)-O-]}, 16 {$\underline{C}H_3$-CH(OH)-, [-CH_2-CH(-$\underline{C}H_3$)-O-]}

5.3.6 Synthesis of oxidized HPD (OX-HPD)

HPD (4.0 g, Mn 58,000 g/mol, DS = 0.52, MS = 4.6, 4.76 mmol terminal secondary hydroxyl groups) was dissolved in 50 mL DI water. Then 30 mL NaOCl aqueous solution (87.6 mmol, 19 equiv.) was slowly added. After that, 3 mL of acetic acid (52.4 mmol, 11 equiv.) was added dropwise. The reaction solution was stirred at room temperature for 1 h. Subsequently, the reaction solution was dialyzed in DI water for 48 hrs. Finally, the purified OX-HPD solution was freeze dried to give 3.56 g product (yield: 89%).

^{1}H NMR (D_2O): δ 1.14 d, [-CH_2-CH(-C$\underline{H}_3$)-O-], δ 1.14 d, [C$\underline{H}_3$-CH(OH)-],δ 3.35 – 4.05, m, (dextran backbone), δ 3.35 – 4.05, d, [-C$\underline{H}_2$-CH(-CH_3)-O-]), δ 3.35 – 4.05, t, [-CH_2-C$\underline{H}$(-CH_3)-O-], δ 3.35 – 4.05, s, (-O-C$\underline{H}_2$-CO-)

^{13}C NMR (D_2O): 178 (CH_3-$\underline{C}$O- , 162 (-O-C$\underline{H}_2$-CO-), 100 (dextran C1), 60-82 {(dextran C2-C6), [-$\underline{C}H_2$-$\underline{C}$H(-CH_3)-O-]}, 19 ($\underline{CH}_3$-CO-) , 16 {$\underline{C}H_3$-CH(OH)-, [-CH_2-CH(-$\underline{C}H_3$)-O-]}

5.3.7 Preparation of OX-HPC-Chitosan hydrogel

Chitosan (1.0 g, 335 kDa viscosity average molecular weight; see procedure for molecular weight determination below) was added to 30 mL DI water. Subsequently, 0.15 mL acetic acid was added to aid chitosan dissolution. In a separate flask, 1.0 g OX-HPC was dissolved in 20 mL DI water. Then the solutions of OX-HPC and chitosan were combined and stirred overnight. At last, the solid product was collected by freeze drying. To prepare hydrogels, 150 mg of this freeze-dried chitosan-OX HPC product was added to 10 mL PBS at room temperature. After 2 h, the chitosan-OX HPC formed a hydrogel and reached its equilibrium swelling.

5.3.8 Preparation of OX-HPD-Chitosan hydrogel

Chitosan (1.0 g, 335 kDa viscosity average molecular weight) was added to 30 mL DI water. Subsequently, 0.15 mL acetic acid was added to help the dissolution of chitosan. In a separate flask, 1.0 g OX-HPD was dissolved in 20 mL DI water. The solutions of OX-HPC and OX-HPD were combined and stirred overnight. Dry, solid product was collected by freeze drying. To prepare hydrogel samples, 500 mg dry chitosan-OX HPC product was added to 20 mL PBS. After 2 h, the chitosan-OX HPD formed a hydrogel and reached its equilibrium swelling.

5.3.9 Measurement of hydrogel swelling ratio (SR)

OX-HPC-Chitosan and OX-HPD-Chitosan solid products were individually lyophilized. Weighed portions of these solid products (ca. 30 mg) were added to 20 mL scintillation vials. Subsequently, 10 mL of pH 7.4 buffered phosphate solution (PBS) was added to each vial. The hydrogel samples were allowed to stand, completely immersed in PBS, for 2 h. Then the excess unabsorbed PBS was removed by glass pipet and each hydrogel sample was weighed again. The swelling ratio was determined by the following equation:

$$SR = \frac{\mathrm{W(wet)} - \mathrm{W(dry)}}{\mathrm{W(dry)}}$$

In which W(wet) represents the weight of hydrogel at equilibrium water absorption, and W(dry) represents the initial weight of dry, solid OX-HPC-Chitosan or OX-HPD-Chitosan.

5.3.10 Viscosity average molecular weight determination of chitosan

This method followed that used in a previous study[47]. Chitosan solution (0.01 g/mL) was prepared using an aqueous solution that was 0.1 M in acetic acid and 0.2 M in NaCl. The resulting chitosan solution was used for viscometric measurements at 25 °C using a Cannon 9721-R59 Ubbelohde

viscometer. The viscosity average molecular weight was determined using the Mark-Houwink equation,

$$[\eta] = KM^a$$

where viscometric constants K, M and a for chitosan in 0.1 M acetic acid-0.2 M NaCl were calculated by Roberts[47].

5.4 Results and discussion

5.4.1 Formation of OX-HPC-Chitosan and OX-HPD-Chitosan hydrogels

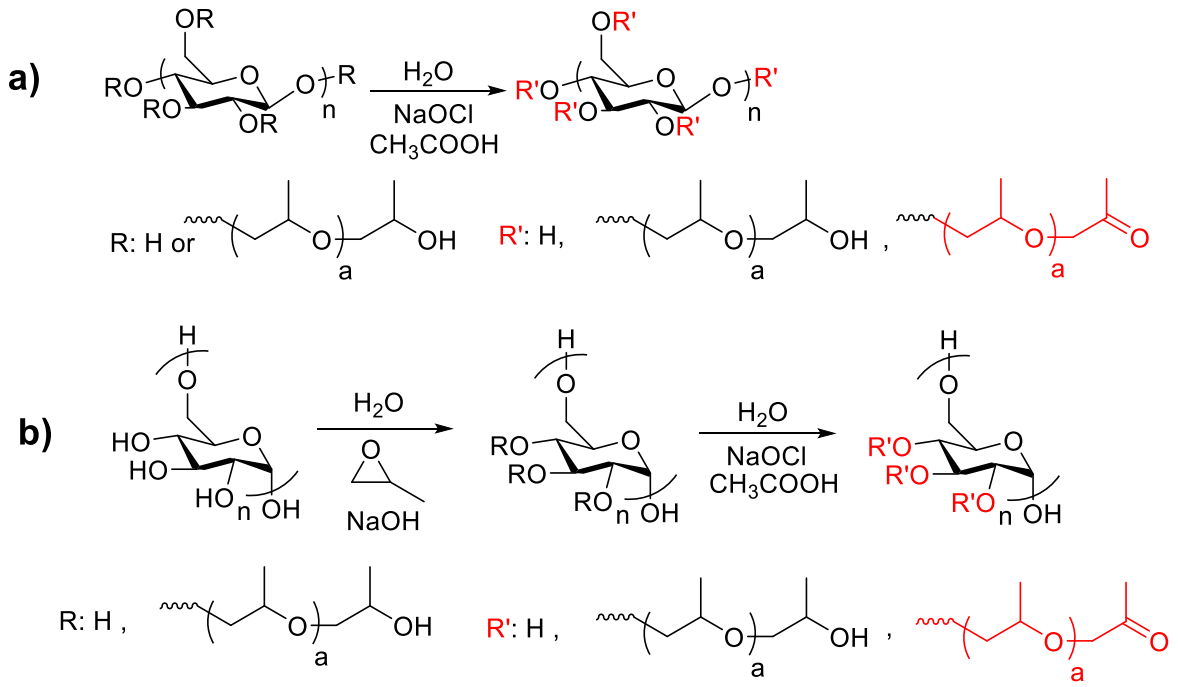

Scheme 1. a) HPC oxidation by sodium hypochlorite. **b)** Synthesis of HPD and its oxidation by sodium hypochlorite.

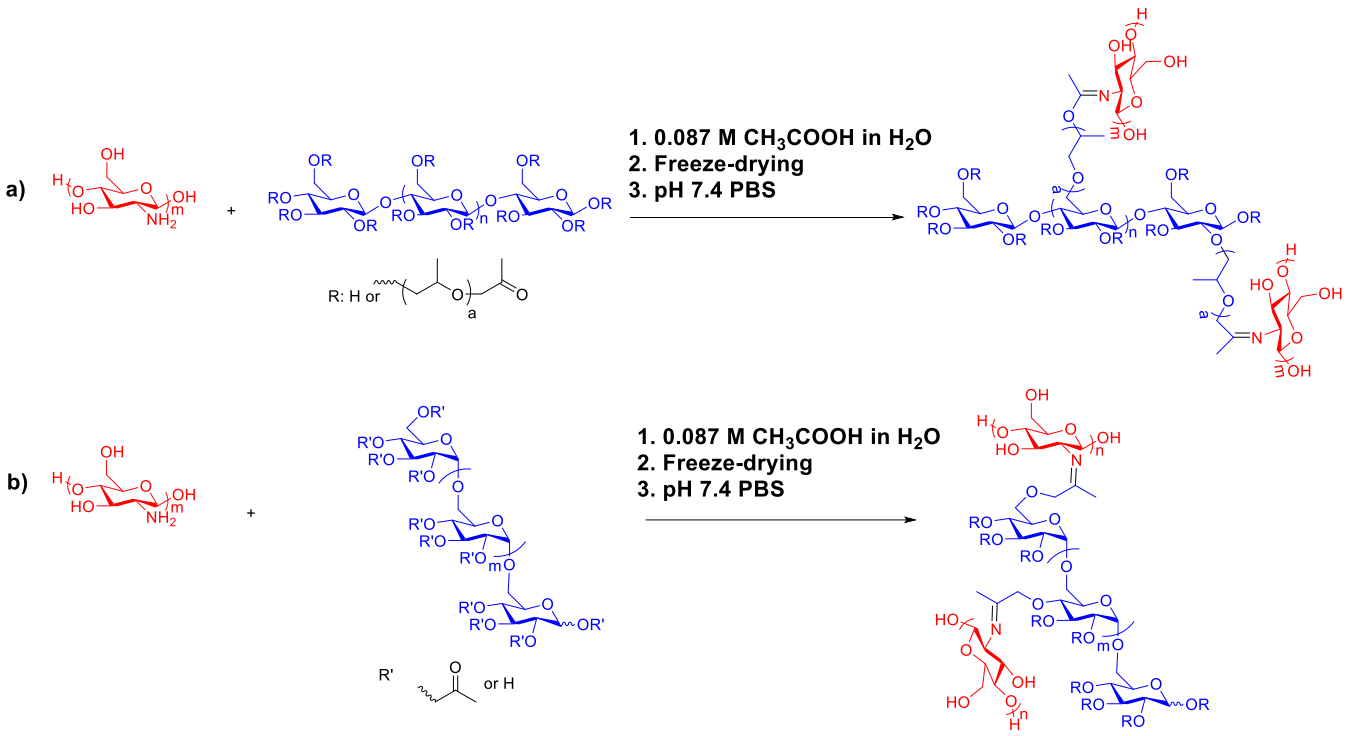

Scheme 2. a) Preparation of OX-HPC-Chitosan hydrogels, **b)** preparation of OX-HPD-Chitosan hydrogels.

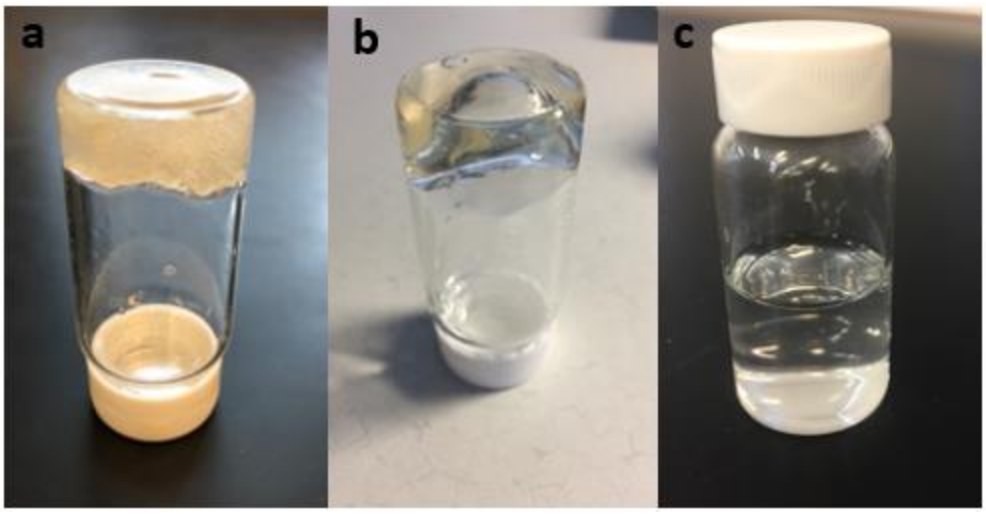

Figure 1. a) OX-HPC-Chitosan hydrogel, **b)** OX-HPD-Chitosan hydrogel, **c)** HPC/Chitosan mixture

In this study, we designed a route to prepare *in situ* forming hydrogels by reacting chitosan with the oxidation products of HPC and HPD (Figure 1), which are both oligo(hydroxypropyl)-substituted polysaccharides. The OX-HPC and OX-HPD were prepared by the chemoselective

oxidation method recently developed by the Edgar group[2]. In this reaction (Scheme 1), the terminal secondary hydroxyl groups of the oligo(hydroxypropyl) chains were oxidized selectively using household bleach (aq. NaOCl) at room temperature to ketones. There are few methods available for introducing ketone groups into polysaccharides (the aforementioned acetoacetylation[38], and attachment of a levulinoyl group[42], are two literature methods that append ketones but also introduce ester linkages simultaneously), and existing methods tend to use reagents that are difficult to handle or access, and/or are expensive and inefficient. In the method described here, we begin with inexpensive, readily available polysaccharide derivatives (commercial in the case of HPC), and subject them to a simple end-group oxidation method that is an economical, green (water solvent, room temperature, NaCl the only co-product), efficient route to ketone-containing polysaccharides. Chemical structures of the oxidized hydroxypropyl polysaccharides were determined using ^{1}H NMR, ^{13}C NMR and FT-IR spectroscopic methods. The ^{1}H NMR spectra of HPC and its oxidation product, OX-HPC are shown in Figure 2. In the ^{1}H NMR spectrum of the starting HPC, the resonance from the methyl protons appears at 1.01 ppm, well separated from the HPC backbone. Upon oxidation, the terminal methyl and methylene resonances shifted to 2.00 and 4.26 ppm respectively, as would be expected for groups flanking the proposed new ketone. Given the measured DS (2.2) and MS (4.4) of oligo(hydroxypropyl) for the HPC employed, the average length of HPC side chains is about two repeat units. Moreover, the total number of methyl protons is constant, so the proton number fraction of downfield, terminal methyls which are adjacent to ketone groups is representative of oxidation conversion. With this information, we can determine the oxidation conversion and the DS(ketone) of OX-HPC by the following equation:

Oxidation conversion: $X = \frac{2a}{a+b} \times 100\%$

Where **a** and **b** are the peak areas of resonances at 2.00 and 1.01 ppm. **X** represents the oxidation conversion. Subsequently, the DS of ketone group in OX-HPC can be calculated by the following equation:

$$\mathrm{DS(ketone)} = X \times DS(hydroxypropyl)$$

where DS of hydroxypropyl groups for the HPC used in this study is 2.2.

^{13}C NMR and FT-IR results provide additional support to the proposed structure of OX-HPC. As observed in ^{13}C NMR spectra of HPC and OX-HPC, resonances at 210 and 25 ppm appeared after the oxidation step, corresponding to the ketone carbonyl carbons and adjacent methyl carbons respectively, thus supporting the formation of ketones. Moreover, in the FT-IR spectrum of OX-HPC (Figure S1), an absorption at 1725 cm^{-1} was observed, assigned as the aliphatic ketone C=O stretch.

To prepare HPD, an unbranched dextran from *Leuconostoc mesenteroides* was reacted with propylene oxide in water with NaOH as catalyst. The isolated, characterized HPD was oxidized in water using NaOCl to give OX-HPD (Scheme 1b). ^{1}H NMR spectra confirm preparation of HPD, and subsequent oxidation to the terminal ketone groups, forming OX-HPD. As shown in Figure 3, the HPD methyl proton resonance a' at 1.14 ppm, from the hydroxypropyl chain termini, partially shifted downfield to 2.15 ppm (a) in the OX-HPD spectrum due to influence of the adjacent carbonyl. In the ^{13}C NMR spectra of HPD and OX-HPD, new methyl (16 ppm) and carbonyl (178 ppm) carbon resonances were observed, supporting the proposed structures. HPD and OX-HPD were also characterized by FTIR. The FTIR absorbance at 1725 cm^{-1} (Figure S2) is assigned as a ketone C=O stretch and supports the postulated oxidation to ketone. Oxidation conversions and DS(ketone) of OX-HPD were calculated by methods similar to those used for OX-HPC.

It is important to note the availability and simplicity of this control element; DS(ketone) is readily controlled by the bleach/HP polysaccharide stoichiometry (and/or by the DS(HP)) (Tables 1 and 2). As we will see, control of DS(ketone) leads directly and simply to control of hydrogel formation and properties.

Table 1. OX-HPC conditions and products

OX-HPC	DS(ketone)	Conversion*	NaOCl Equiv	Oxidation time (min)
1	0.07	3%	0.47	5
2	0.64	29 %	2.69	5
3	0.90	41 %	2.69	40
4	1.12	51 %	14.12	60
5	1.76	80 %	4.70	720
6	1.96	89 %	14.12	1440

* Conversion of secondary alcohol to ketone was measured by ^{1}H NMR.

Table 2. HPD composition, OX-HPD conditions and products

OX-HPD	MS(HP)[2]	DS(HP)[1]	DS(ketone)	Conversion[2]	NaOCl Equiv.
1	2.35	0.28	0.08	28%	2.69
2	2.35	0.28	0.14	50%	3.28
3	2.35	0.28	0.25	89%	19.1
4	4.60	0.52	0.33	63%	8.5
5	4.60	0.52	0.47	90%	19.1

[1] DS(HP) was measured by ^{1}H NMR analysis of peracetylated HPD (Figure S3).

[2] MS(HP) and conversion of secondary alcohol to ketone were measured by ^{1}H NMR.

It was therefore of interest to explore factors that can affect oxidation conversion. Reaction time and equivalents of sodium hypochlorite were found to effect the oxidation degree in rational ways. We used these tools to prepare a series of OX-HPC polymers (Table 1) with different DS(ketone) values in order to investigate the impact of DS(ketone) on hydrogel properties.

There are several reasons for choosing OX-HPC as a reactive polymeric partner to form hydrogels. First, ketone groups on the short side chains of OX-HPC can form imine bonds with the primary

amines in chitosan. Since the ketones are only on the terminal (former) HP unit, they have wider approach angles than would reactive groups on the glucose ring itself. The imine bond is dynamic, able to be cleaved by hydrolysis (reagent water being highly abundant in a hydrogel), reform, and recover under different conditions of stress and pH. We were pleased to learn that after oxidation, despite the increase in hydrophobicity of the polymer caused by loss of hydroxyl groups and concomitant introduction of ketones, the polymer remained soluble in water. This was of course critical for hydrogel formation.

With the keto-substituted HP polysaccharides in hand, the key remaining issue was whether reactivity with chitosan would be sufficiently rapid and complete to result in an extended network, and thus loss of water solubility and hydrogel formation. Our intention to provide hydrogels devoid of toxic, small molecule crosslinkers depended upon confirmation of this aspect of our original hypothesis. Given the water solubility of OX-HPC and OX-HPD, the most straightforward approach to prepare these hydrogels would have been to combine, e.g., an aqueous OX-HPC solution with an aqueous acetic acid solution of chitosan. Unfortunately, combination of these solutions gave a new solution that appeared visually to be clear, and from which no macroscopic hydrogel appeared. We will say more about these initial apparent solutions and their composition in future publications. Clearly this approach was not useful for making macroscopic hydrogels, an initially discouraging result.

Therefore, we explored a slightly different approach. We dissolved OX-HPC and chitosan in pH 5 water, to form a crystal-clear aqueous solution. This solution then was freeze dried, affording a solid, intimate mixture of OX-HPC and chitosan; most if not all of the acetic acid was eliminated during freeze-drying. Addition of this powder to a neutral aqueous medium (pH 7.4 phosphate buffer) then afforded a hydrogel within 1 minute, which was allowed to proceed to form and firm

up over 2 h at room temperature. At neutral pH, chitosan is not highly protonated (chitosan pKa ca. 6)[48]. Thus the imine bond crosslinked OX-HPC/chitosan network was formed readily at neutral pH (Scheme 2).

We had particular interest in dextran-based oxidized hydroxypropyl derivatives, because of our feeling that these hydrogels might have exceptional value in biomedical applications. If the hydrogel is placed inside the body, its components must be able to be cleared from the body in order for the material application to get regulatory approval. While HPC is an excellent starting material for many applications (e.g. formulations of food and orally administered drugs), being inexpensive and relatively non-toxic, humans do not possess cellulase enzymes and thus have limited ability to clear cellulose. Dextran, on the other hand, is slowly degraded in circulation[49] and then lower molecular weight fragments are eliminated through the kidneys, in urine. While there is no guarantee that dextran ethers or the hydrogels prepared therefrom would be biodegradable *in vivo* or in the environment, the fact that polysaccharide etherification tends to be heterogeneous[27] bodes well, we speculate, for leaving some monosaccharides unsubstituted, and therefore as potential starting places for degradative enzymes. Using the OX-HPD prepared as described above, OX-HPD-Chitosan hydrogel was prepared in a manner similar to that used for OX-HPC. The fact that this method works well for OX-HPD/OX-HPC and chitosan-based hydrogels is very promising, since the solid, intimate mixture of polymers can be stored or shipped until the user is ready to prepare the hydrogel by the extremely simple protocol of mixing with water. It is also notable that these hydrogels form at low percent solids; most hydrogels prepared herein had approximately 2.5% solids.

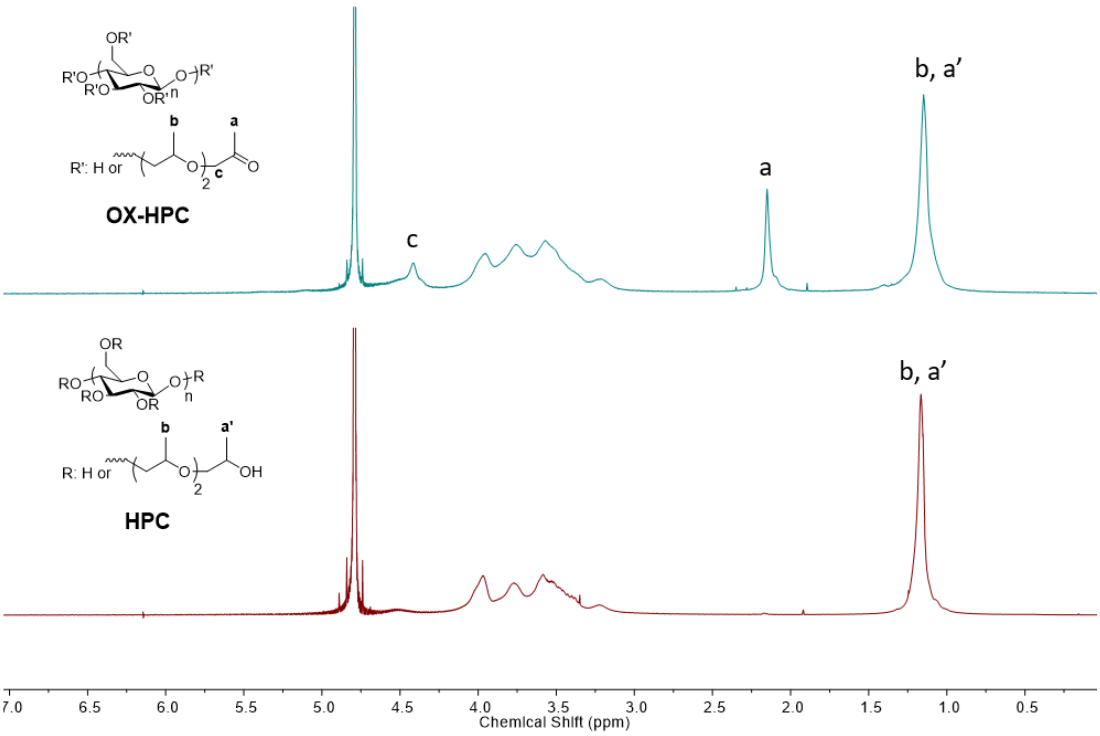

Figure 2. [1]H NMR spectra of HPC and OX-HPC

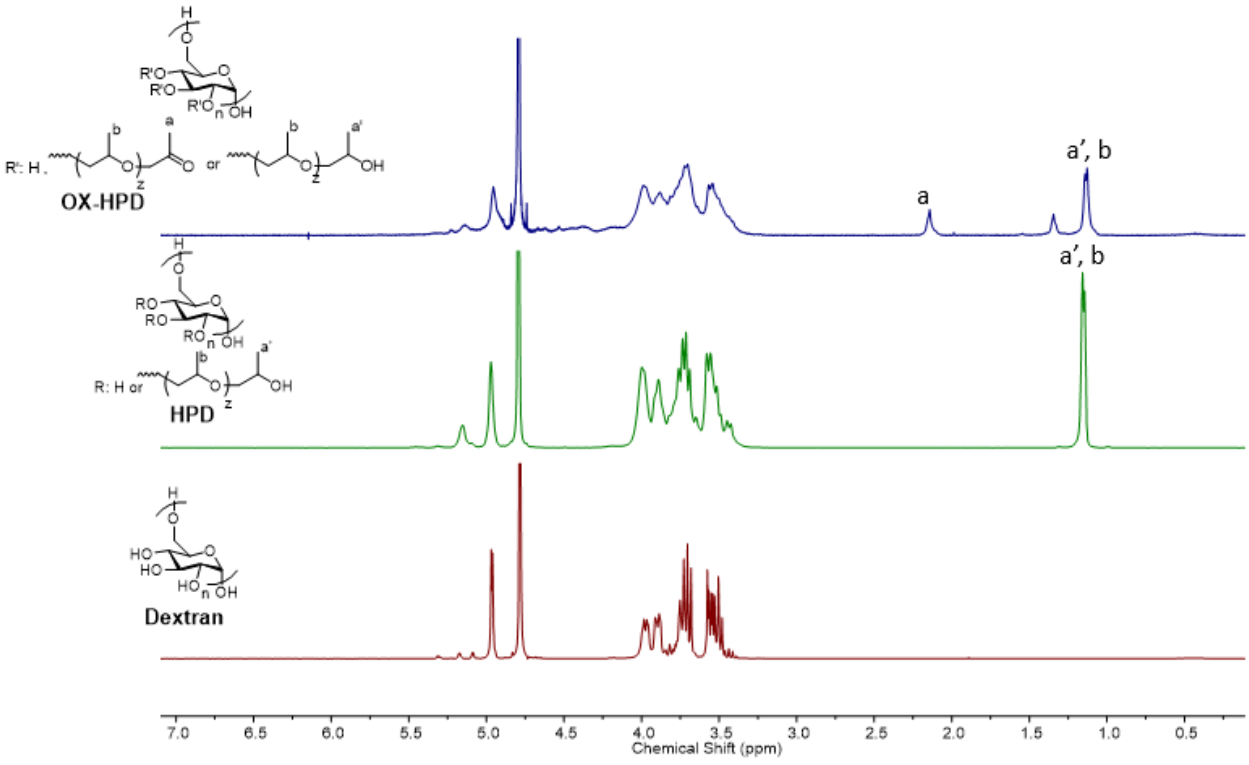

Figure 3. [1]H NMR spectra of dextran, HPD, and OX-HPD

To confirm hydrogel formation, dry OX-HPC-Chitosan and OX-HPD-Chitosan were added to scintillation vials with DI water. These polysaccharide-based materials were allowed to swell for 5 minutes. Then the excess water was decanted off, and the scintillation vials were inverted, placed upon the laboratory bench, and photographed (Figures 1a and 1b). Both OX-HPC-Chitosan and OX-HPD-Chitosan resisted flow, remaining in the former vial "bottom", illustrating hydrogel formation. In contrast, we carried out a control experiment using commercial HPC (not oxidized) and chitosan. The polymers were dissolved together in pH 5 aqueous solution, and this solution was allowed to stir for 24 h. Subsequently, the solution was freeze dried, and the resulting product was added to a vial with excess PBS. As seen in Figure 1c, the HPC/Chitosan mixture dissolved in PBS, and could not form a hydrogel. Properties of OX-HPC-Chitosan and OX-HPD-Chitosan hydrogels were further investigated as follows.

5.4.2 FTIR Spectroscopy

We investigated use of FT-IR spectroscopy as a tool for following gelation kinetics. Unfortunately, the C=N stretching IR absorption of the imine bonds overlapped substantially with the C=O IR absorption of the secondary amide groups from chitosan, and consequently it was not possible to monitor imine bond formation during gelation by ATR or *in situ* FT-IR.

5.4.3 Swelling ratio

The swelling ratio of a hydrogel measures the weight increment due to water absorption. SR is of interest since it influences hydrogel properties such as stiffness, cell encapsulation, and ability to support cell proliferation[50]. We investigated two factors--hydrogel composition (weight ratio of component polymers) and OX-HPC DS(ketone), both of which may impact hydrogel swelling. Swelling ratios were measured gravimetrically (see Experimental section). Hydrogel composition (Table 3) did impact hydrogel swelling ratio. The hydrogel with chitosan/OX-HPC ratio = 1:1

exhibited the lowest SR (35.7); those with either higher or lower chitosan content exhibited greater swelling. These results suggested that the chitosan component may play a more significant role in absorbing water. As chitosan/OX-HPC = 1:1 hydrogel sample has the highest SR, we expect that this composition ratio may have an optimal interpenetrating polymer network with well-defined microstructure, assisting in absorbing water. We also explored the relationship between OX-HPC DS(ketone) and SR. At constant weight ratio of OX-HPC/chitosan, Table 4, the swelling ratio increased slightly with increasing DS(ketone). There are a number of factors at play in these results. Increased oxidation of HPC creates a slightly more hydrophobic polymer by replacing polar OH groups with less polar ketones. At the same time, increased oxidation can enhance crosslinking with chitosan (since weight ratio of chitosan to OX-HPC is kept constant in this experiment, while amine/ketone ratio decreases as oxidation increases). We are inclined to attribute the reduced swelling with greater oxidation to the changes away from the optimum amine/ketone ratio (Table 3), but recognize that these other factors may also have influence. SR values of the OX-HPD-Chitosan hydrogels followed trends similar to these observed for OX-HPC-Chitosan. Overall, both OX-HPC-Chitosan and OX-HPD-Chitosan exhibited high and rationally tunable SR values.

Table 3. SR of OX-HPC-Chitosan hydrogels vs. composition.

Chitosan: OX-HPC[*]	Amine/ketone ratio[#]	SR
3:1	7.60	29 ± 0.7
1:1	2.53	35.7 ± 0.6
1:3	0.84	10.4 ± 0.6

[*] Weight ratio

[#] Calculated based on the mole ratio between chitosan (75 % deacetylated) and OX-HPC with DS (ketone) = 0.48.

Table 4. SR of OX-HPC-Chitosan (1:1) hydrogels with different OX-HPC

Oxidation conversion of OX-HPC*	Amine/ketone ratio#	SR
35%	2.53	35.7 ± 0.5
50%	1.77	31.2 ± 0.7
89%	0.99	28.6 ± 0.6

* Based on HPC DS 2.2

Calculated based on the mole ratio between chitosan (75 % deacetylated) and OX-HPCs.

5.4.4 Rheological properties of OX-HPC-Chitosan and OX-HPD-Chitosan hydrogels

Rheological properties of hydrogels strongly influence their ability to mimic tissues in biomedical applications, or to perform and endure in other applications such as agriculture and personal care. We expect that the physical properties OX-HPC-Chitosan hydrogels and OX-HPD-Chitosan hydrogels will be tunable by controlling various aspects, including DS(HP), degree of oxidation, chitosan DS(Ac), polymer weight ratio, and hydrogel solid content. While control of chitosan DS(Ac) is likely to be a valuable tool for controlling hydrogel physical properties, not every DS(Ac) may be readily available. We have shown herein and elsewhere[2] that the ketone content of OX-HPC and OX-HPD is easily modified by simple NaOCl stoichiometric control. We hypothesize that hydrogel storage modulus should increase with oxidized HP polysaccharide DS(ketone), due to increasing imine crosslink density. Since imine formation in water is dynamic and reversible, increasing DS(ketone) can influence the position of equilibrium in favor of imine formation. To test this hypothesis, we prepared a series of hydrogels using OX-HPC with ketone DS from 0.066 to 1.96. All hydrogel samples were tested at their equilibrium swelling with pH 7.4 PBS. Rheometry was carried out with parallel plate geometry.

To investigate hydrogel behavior vs. frequency, all hydrogel samples were subjected to frequency sweep experiments using 1% strain, selected as a small strain which would be unlikely to destroy hydrogel structure. The example of frequency sweep analysis of OX-HPC-Chitosan (DS(ketone)

= 1.12) is shown in Figure 4a. This frequency sweep displays an equilibrium G' plateau of ca. 5700 Pa, and shows that the hydrogel remains in the gel state within the frequency range studied (0.1-5 Hz). All hydrogel samples remained in the gel state within this frequency range.

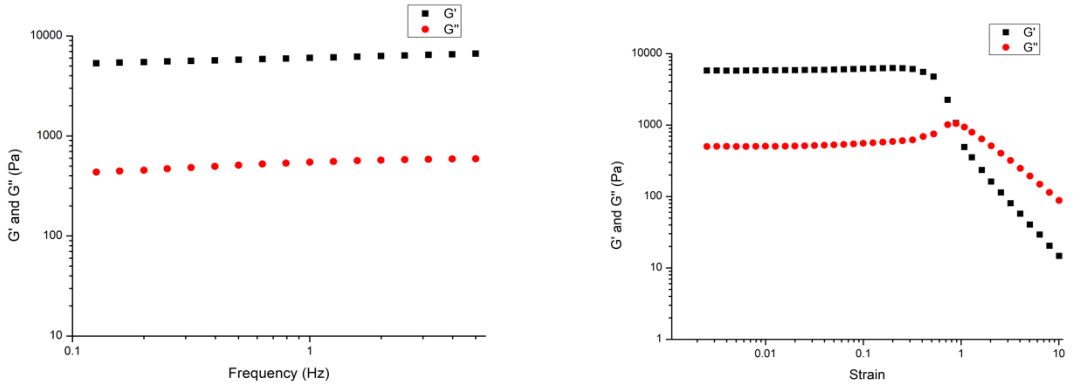

Figure 4. a) Frequency sweep of OX-HPC-Chitosan hydrogel with 1% strain. **b)** Strain sweep of OX-HPC-Chitosan hydrogel with 0.5 Hz frequency.

These hydrogels were further investigated in strain sweep experiments at 0.5 Hz frequency. An example strain sweep experiment using OX-HPC-Chitosan hydrogel (DS(ketone) = 1.12) is shown in Figure 4b. This hydrogel sample exhibited a storage modulus of 5700 Pa, and a linear viscoelastic region limit of 25% strain. This experiment illustrates the existence of crosslinking networks in this hydrogel. Strain sweep data of other OX-HPC-Chitosan hydrogels are listed in Table 5. The data clearly indicate the responsiveness of hydrogel storage modulus to DS(ketone), with modulus increasing from 300 Pa to 13 kPa as DS(ketone) is increased from 0.066 to 1.98. This confirms our hypothesis that hydrogel modulus should increase with increasing DS(ketone), due to increasing crosslink density. At the same time, as shown in Table 5, the maximum strain limits of hydrogel samples decrease with increasing ketone ratio of OX-HPC, which suggests that the crosslinking density effects the extensional property of the hydrogel as would be expected by theory. A highly crosslinked hydrogel network has limited potential for polymer chain movement, which leads to poor ability to respond without failure upon application of increased strain. In

contrast, a relatively lightly crosslinked hydrogel network offers possibilities for polymer chain movement, thus the hydrogel has better extensional properties. It is encouraging that this hydrogel preparation method presents multiple strategies for designing hydrogels with the desired range of mechanical properties, including the readily executed strategy of adjusting DS(ketone) by simple manipulation of NaOCl stoichiometry in the oxidation reaction. This provides tools for, in one example, matching tissue properties in biomedical applications.

Table 5. Mechanical properties of OX-HPC-Chitosan hydrogels vs. DS(ketone)

OX-HPC-Chitosan	DS(ketone)	G' (Pa)*	G'' (Pa)*	Maximum strain
1	0.07	300	80	0.71
2	0.64	2800	210	0.50
3	0.90	3900	290	0.31
4	1.12	5900	280	0.25
5	1.76	9300	410	0.10
6	1.96	13100	530	0.09

* G' and G'' were measured at 1% strain with 0.5 Hz frequency

OX-HPD-Chitosan hydrogels were investigated in a similar manner. OX-HPD with different ketone contents were synthesized to prepare a series of OX-HPD-Chitosan hydrogels. Fig.5b shows the strain sweep results for an OX-HPD-Chitosan hydrogel. This hydrogel exhibited a storage modulus of 9100 Pa, and a linear viscoelastic region limit of 20% strain, which is comparable to the properties of OX-HPC-Chitosan hydrogel. It is interesting that the difference in linkages and polymer shape between cellulose (rigid rod) and dextran (random coil) do not more strongly impact the mechanical behavior of the resulting hydrogels.

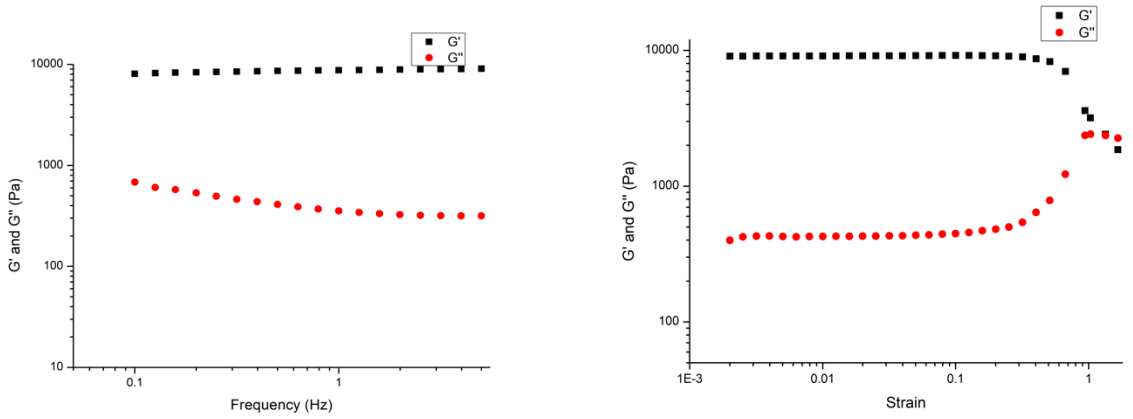

Figure 5. a) Frequency sweep of OX-HPD-Chitosan hydrogel with 1% strain. **b)** Strain sweep of OX-HPD-Chitosan hydrogel with 0.5 Hz frequency.

5.4.5 Self-healing and injectability

The Schiff base linkages of the OX-HPC-chitosan and OX-HPD-Chitosan hydrogels are dynamic, reversibly breaking and reforming in the presence of water (which comprises the great majority of the hydrogel by weight, and even more so on a molar basis); hydrolysis and imine bond reformation are in equilibrium in this system. These reversible processes have led investigators to explore imine crosslinked hydrogels as self-healing materials [31]. Application of external stress can drive facile imine bond hydrolysis rather than the far more energy-consuming breakage of chitosan or OX-HP polysaccharide backbone C-C or C-O sigma bonds, thereby greatly enhancing self-healing. We therefore hypothesized that both OX-HPC-Chitosan and OX-HPD-Chitosan would exhibit self-healing properties. To test this hypothesis macroscopically, a hydrogel disk was prepared by exposing a freeze-dried intimate mixture of chitosan and OX-HPC to pH 7.4 phosphate buffer. Then the hydrogel disk was sliced into two pieces, and those pieces were placed in physical contact with each other, with no applied pressure. Within 1 h, the boundary between two hydrogel pieces was obscure. Gradually, the two hydrogel pieces merged into a single piece, we believe due to reformation of imine bonds between the two halves. The self-healed disc was strong enough to hold its own weight upon picking up with tweezers within 90 minutes (Figure 6).

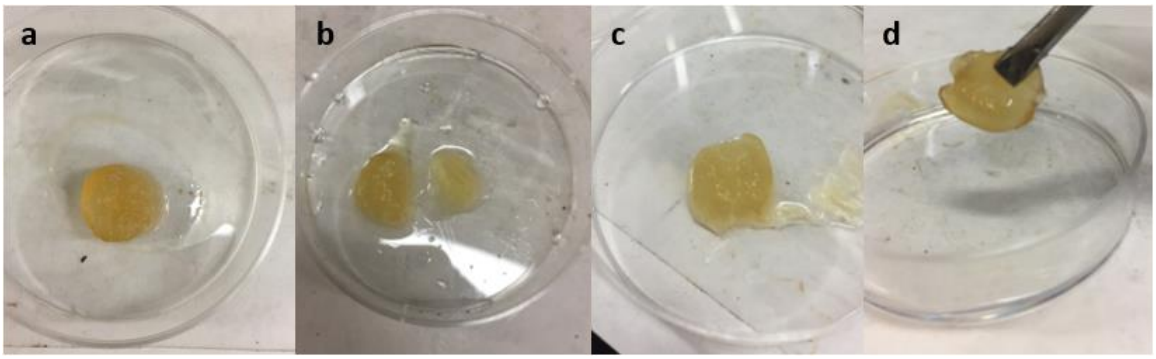

Figure 6. Self-healing behavior of OX-HPC-Chitosan hydrogel. a) hydrogel film before cutting, b) hydrogel film cut into two pieces, c) two pieces placed in contact and healed, then d) picked up.

The self-healing natures of OX-HPC-Chitosan and OX-HPD-Chitosan hydrogels were also confirmed by rheometry, using a step-strain time sweep (OX-HPC-Chitosan displayed in Figure 7). In these experiments, strain was alternated between 0.5% and 200% in 4 minute segments. Based on these results, the hydrogel remains in the gel-state at 0.5% strain, then is converted to fluid at 200% strain. In the first segment (0 – 4 m), storage modulus exceeded loss modulus, confirming the gel state. In the second segment (4-8 m), strain was increased to 200%, disrupting the hydrogel crosslinking network. As a result, the loss modulus exceeded the storage modulus, indicating the liquid state. In the third segment, the strain decreased to 0.5% and the hydrogel immediately returned to its original gel-state with a 5300 Pa storage modulus, clearly indicating the rapid self-healing property of this hydrogel. In the subsequent fourth and fifth segments the hydrogel essentially perfectly repeated its self-healing behavior, showing the durability of the hydrogel and of its self-healing behavior. These results also illustrate that the hydrogel contains a dynamic crosslinking network.

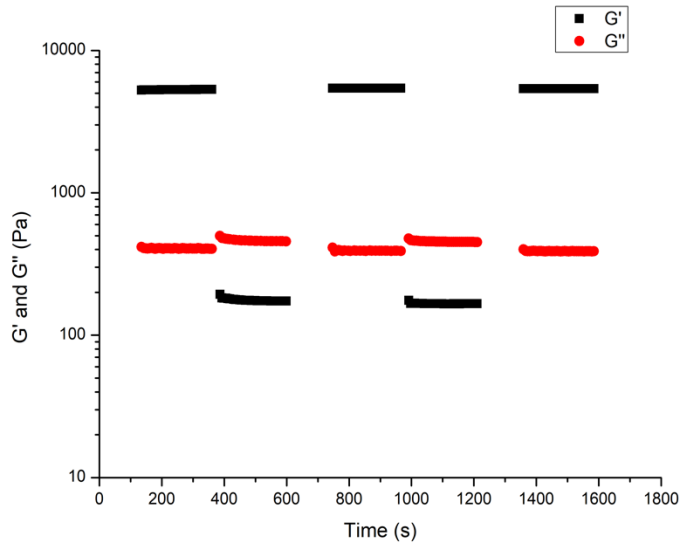

Figure 7. Step-strain time sweep of OX-HPC-Chitosan hydrogel with 0.5 Hz frequency.

We then studied whether these dynamic hydrogels could be readily injected. Dextran-based OX-HPD-Chitosan with low modulus (DS(ketone) 0.08, G' = 1000 Pa) was added into the syringe (Figure 8a). In the following step, the hydrogel was injected into a vial smoothly, without the need for excessive pressure on the plunger, where the shear of the plunger on the syringe barrel sufficed to liquefy the hydrogel. Within a minute after injection into the vial, the OX-HPD-Chitosan 'solution' reverted to a self-supporting hydrogel. Its immobility is made clear by the result of inverting the vial, in the final photograph. Thus, the rheological and self-healing properties of OX-HPD-Chitosan hydrogels appear to be ideal for ready injection, meaning that the hydrogels can be created by addition of powder to sterile water, then injected directly into the targeted area where they are needed. Notably, an OX-HPC-Chitosan with low modulus (DS(ketone) 0.066, G' = 1000 Pa) also exhibits similar ability to be injected (Figure 8b).

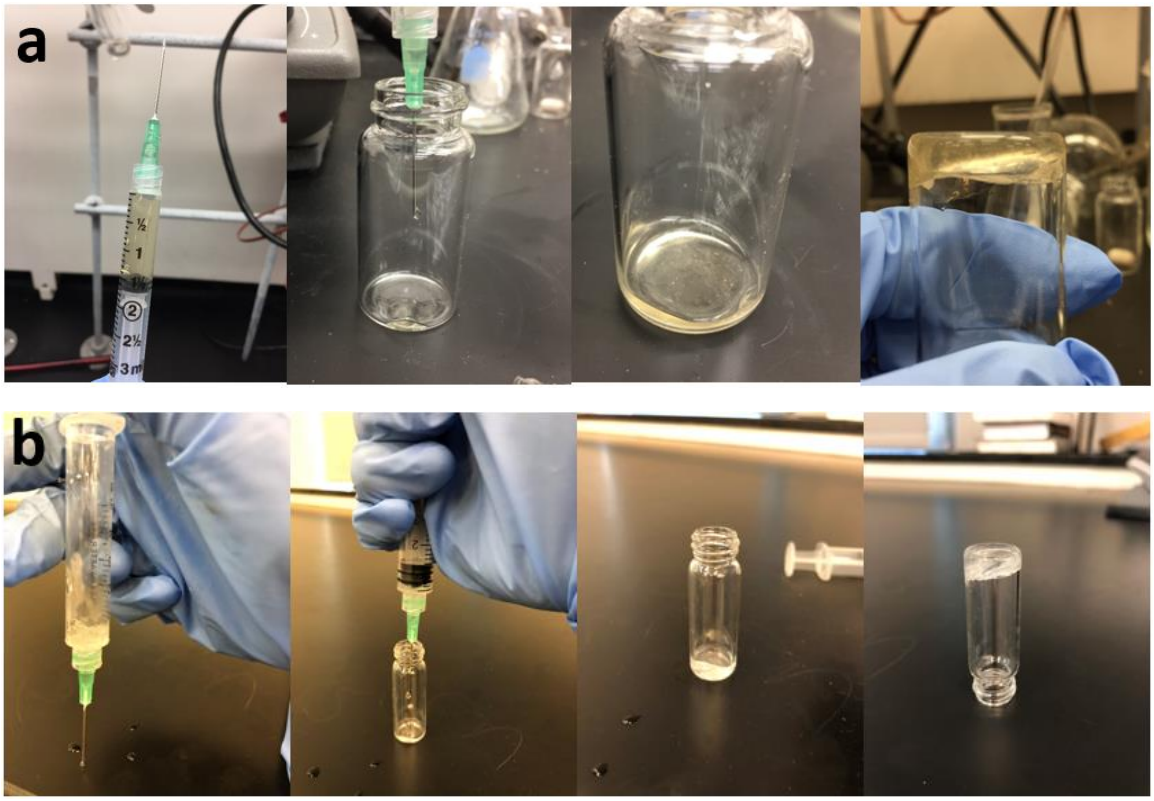

Figure 8. Injection of a) OX-HPD-Chitosan hydrogel b) OX-HPC-Chitosan hydrogel

5.5 Conclusions

We have successfully demonstrated design and preparation of OX-HPC chitosan and OX-HPD chitosan hydrogels that are crosslinked by imine bonds. Their self-healing and injectability were demonstrated on macroscopic scale and visually, and characterized rheologically, thereby confirming our original hypotheses. Oxidation of oligo(hydroxypropyl)-substituted polysaccharides afford ketone functions selectively on the terminal hydroxypropyl groups of HP polysaccharides, creating the ability to form imines with amine-containing polymers, for example chitosan. This ability to selectively impart ketone functionality and reactivity with amines creates a green, simple, controllable, efficient method for preparing *in situ* forming hydrogels, including from OX-HPC and OX-HPD. These hydrogels exhibit high swelling ratios, tunable mechanical properties, robust self-healing, and the ability to be easily injected. Based upon rheometry, hydrogel modulus can be readily tuned in the range from 300 Pa to 13.0 kPa, controlled simply by

DS(ketone) of OX-HPC or OX-HPD, which in turn is predictably adjustable by the simple expedient of changing bleach stoichiometry, for example. We expect that control by controlling the extent of chitin hydrolysis and thus DS(Ac) of the resulting chitosan should also be useful. Step-strain experiments have illustrated the rapid self-healing property of these hydrogels; upon application of strain that fluidizes the hydrogel, it can recover its modulus within 2 minutes after strain release. This family of polysaccharide-based *in situ* forming hydrogels has strong potential for biomedical applications which require biocompatibility, *in vivo* degradation, injectability, and adjustable stiffness. OX-HPD-Chitosan may have particular merit for inside the body applications, since unsubstituted regions of the dextran portion should create the ability for biodegradation by amylase or other enzymes present in the body. Other oxidized HP polysaccharides, for example those based on amylose or pullulan, should also be useful for this purpose.

This method for creating new families of imine-crosslinked hydrogels, entirely devoid of potentially toxic small molecule crosslinkers, and retaining the physical properties that arise from intact monosaccharide rings, has broad application promise. In ongoing studies, we are exploring the potential of these ketone-containing polysaccharides for further chemical modification through appending bioactive molecules, which will create exciting new potential for controlled, targeted release of bioactive agents.

In order to apply these hydrogels in the biomedical field, it is of particular interest for us to study their toxicity, pH responsiveness, *in vivo* degradation rates and mechanism, and ability to encapsulate cells and support their growth. These will also be subjects of future studies in our lab. Moreover, we will further investigate the mechanism of gelation and its kinetics, so as to further enhance potential utility in biomedical and other fields.

5.6 Acknowledgements

We thank the Departments of Chemistry and of Sustainable Biomaterials, and the Institute for Critical Technologies and Applied Science (ICTAS) at Virginia Tech for facility support. We thank the National Science Foundation for partial support of this work through grant DMR-1308276. We also thank Dong Guo and Ryan Carrazzone at Virginia Tech for performing SEC analyses.

5.7 References

(1) Hennink, W. E.; van Nostrum, C. F. Novel Crosslinking Methods to Design Hydrogels. *Adv. Drug Deliv. Rev.* **2012**, *64*, 223–236. https://doi.org/10.1016/J.ADDR.2012.09.009.

(2) Nicholsa, B. L. B. Selective Oxidation of Hydroxypropyl Cellulose and Dextran: An Efficient Approach to Schiff Base Polymeric Prodrugs . *In prepration*.

(3) Wei, Z.; Yang, J. H.; Liu, Z. Q.; Xu, F.; Zhou, J. X.; Zrínyi, M.; Osada, Y.; Chen, Y. M. Novel Biocompatible Polysaccharide-Based Self-Healing Hydrogel. *Adv. Funct. Mater.* **2015**, *25* (9), 1352–1359. https://doi.org/10.1002/adfm.201401502.

(4) Wang, F.; Li, Z.; Khan, M.; Tamama, K.; Kuppusamy, P.; Wagner, W. R.; Sen, C. K.; Guan, J. Injectable, Rapid Gelling and Highly Flexible Hydrogel Composites as Growth Factor and Cell Carriers. *Acta Biomater.* **2010**, *6* (6), 1978–1991. https://doi.org/10.1016/J.ACTBIO.2009.12.011.

(5) Yao, K. De; Peng, T.; Goosen, M. F. A.; Min, J. M.; He, Y. Y. PH-Sensitivity of Hydrogels Based on Complex Forming Chitosan: Polyether Interpenetrating Polymer Network. *J. Appl. Polym. Sci.* **1993**, *48* (2), 343–354. https://doi.org/10.1002/app.1993.070480218.

(6) Wei, Z.; Yang, J. H.; Zhou, J.; Xu, F.; Zrínyi, M.; Dussault, P. H.; Osada, Y.; Chen, Y. M. Self-Healing Gels Based on Constitutional Dynamic Chemistry and Their Potential Applications. *Chem. Soc. Rev.* **2014**, *43* (23), 8114–8131. https://doi.org/10.1039/C4CS00219A.

(7) Rowley, J. A.; Madlambayan, G.; Mooney, D. J. Alginate Hydrogels as Synthetic Extracellular Matrix Materials. *Biomaterials* **1999**, *20* (1), 45–53. https://doi.org/10.1016/S0142-9612(98)00107-0.

(8) Williams, D. F. There Is No Such Thing as a Biocompatible Material. *Biomaterials* **2014**, *35* (38), 10009–10014. https://doi.org/10.1016/J.BIOMATERIALS.2014.08.035.

(9) Muzzarelli, R. A. A. Human Enzymatic Activities Related to the Therapeutic Administration of Chitin Derivatives. *Cell. Mol. Life Sci.* **1997**, *53* (2), 131–140. https://doi.org/10.1007/PL00000584.

(10) Chang, C.; Zhang, L. Cellulose-Based Hydrogels: Present Status and Application Prospects. *Carbohydr. Polym.* **2011**, *84* (1), 40–53. https://doi.org/10.1016/J.CARBPOL.2010.12.023.

(11) Berger, J.; Reist, M.; Mayer, J. .; Felt, O.; Gurny, R. Structure and Interactions in Chitosan Hydrogels Formed by Complexation or Aggregation for Biomedical Applications. *Eur. J. Pharm. Biopharm.* **2004**, *57* (1), 35–52. https://doi.org/10.1016/S0939-6411(03)00160-7.

(12) Augst, A. D.; Kong, H. J.; Mooney, D. J. Alginate Hydrogels as Biomaterials. *Macromol. Biosci.* **2006**, *6* (8), 623–633. https://doi.org/10.1002/mabi.200600069.

(13) Burdick, J. A.; Prestwich, G. D. Hyaluronic Acid Hydrogels for Biomedical Applications. *Adv. Mater.* **2011**, *23* (12), H41–H56. https://doi.org/10.1002/adma.201003963.

(14) Zhang, R.; Tang, M.; Bowyer, A.; Eisenthal, R.; Hubble, J. A Novel PH- and Ionic-Strength-Sensitive Carboxy Methyl Dextran Hydrogel. *Biomaterials* **2005**, *26* (22), 4677–4683. https://doi.org/10.1016/J.BIOMATERIALS.2004.11.048.

(15) Jin, R.; Hiemstra, C.; Zhong, Z.; Feijen, J. Enzyme-Mediated Fast in Situ Formation of Hydrogels from Dextran–Tyramine Conjugates. *Biomaterials* **2007**, *28* (18), 2791–2800. https://doi.org/10.1016/J.BIOMATERIALS.2007.02.032.

(16) Peng, H. T.; Shek, P. N. Development of in Situ-Forming Hydrogels for Hemorrhage Control. *J. Mater. Sci. Mater. Med.* **2009**, *20* (8), 1753–1762. https://doi.org/10.1007/s10856-009-3721-5.

(17) Boehnke, N.; Cam, C.; Bat, E.; Segura, T.; Maynard, H. D. Imine Hydrogels with Tunable Degradability for Tissue Engineering. *Biomacromolecules* **2015**, *16* (7), 2101–2108. https://doi.org/10.1021/acs.biomac.5b00519.

(18) Lueckgen, A.; Garske, D. S.; Ellinghaus, A.; Desai, R. M.; Stafford, A. G.; Mooney, D. J.; Duda, G. N.; Cipitria, A. Hydrolytically-Degradable Click-Crosslinked Alginate Hydrogels. *Biomaterials* **2018**, *181*, 189–198. https://doi.org/10.1016/J.BIOMATERIALS.2018.07.031.

(19) Ravi Kumar, M. N. . A Review of Chitin and Chitosan Applications. *React. Funct. Polym.* **2000**, *46* (1), 1–27. https://doi.org/10.1016/S1381-5148(00)00038-9.

(20) Francis Suh, J.-K.; Matthew, H. W. . Application of Chitosan-Based Polysaccharide Biomaterials in Cartilage Tissue Engineering: A Review. *Biomaterials* **2000**, *21* (24), 2589–2598. https://doi.org/10.1016/S0142-9612(00)00126-5.

(21) Zhang, H.; Neau, S. H. In Vitro Degradation of Chitosan by a Commercial Enzyme Preparation: Effect of Molecular Weight and Degree of Deacetylation. *Biomaterials* **2001**, *22* (12), 1653–1658. https://doi.org/10.1016/S0142-9612(00)00326-4.

(22) Roy, K.; Mao, H.-Q.; Huang, S.-K.; Leong, K. W. Oral Gene Delivery with Chitosan–DNA Nanoparticles Generates Immunologic Protection in a Murine Model of Peanut Allergy. *Nat. Med.* **1999**, *5* (4), 387–391. https://doi.org/10.1038/7385.

(23) Peh, K.; Khan, T.; Ch'ng, H. Mechanical, Bioadhesive Strength and Biological Evaluations of Chitosan Films for Wound Dressing. *J. Pharm. Pharm. Sci. 3* (3), 303–311.

(24) Zhu, K.; Duan, J.; Guo, J.; Wu, S.; Lu, A.; Zhang, L. High-Strength Films Consisted of Oriented Chitosan Nanofibers for Guiding Cell Growth. *Biomacromolecules* **2017**, *18* (12), 3904–3912.

https://doi.org/10.1021/acs.biomac.7b00936.

(25) Heinze, T.; Liebert, T.; Heublein, B.; Hornig, S. Functional Polymers Based on Dextran. In *Polysaccharides II*; Springer Berlin Heidelberg, 2006; pp 199–291. https://doi.org/10.1007/12_100.

(26) Hahn, R. G.; Lyons, G. The Half-Life of Infusion Fluids: An Educational Review. *Eur. J. Anaesthesiol.* **2016**, *33* (7), 475. https://doi.org/10.1097/EJA.0000000000000436.

(27) Arca, H. C.; Mosquera-Giraldo, L. I.; Bi, V.; Xu, D.; Taylor, L. S.; Edgar, K. J. Pharmaceutical Applications of Cellulose Ethers and Cellulose Ether Esters. *Biomacromolecules* **2018**, *19* (7), 2351–2376. https://doi.org/10.1021/acs.biomac.8b00517.

(28) Harsh, D. C.; Gehrke, S. H. Controlling the Swelling Characteristics of Temperature-Sensitive Cellulose Ether Hydrogels. *J. Control. Release* **1991**, *17* (2), 175–185. https://doi.org/10.1016/0168-3659(91)90057-K.

(29) Rowan, S. J.; Cantrill, S. J.; Cousins, G. R. L.; Sanders, J. K. M.; Stoddart, J. F. Dynamic Covalent Chemistry. *Angew. Chemie Int. Ed.* **2002**, *41* (6), 898–952. https://doi.org/10.1002/1521-3773(20020315)41:6<898::AID-ANIE898>3.0.CO;2-E.

(30) Lehn, J.-M. Dynamers: Dynamic Molecular and Supramolecular Polymers. *Prog. Polym. Sci.* **2005**, *30* (8–9), 814–831. https://doi.org/10.1016/J.PROGPOLYMSCI.2005.06.002.

(31) Wang, Q.; Mynar, J. L.; Yoshida, M.; Lee, E.; Lee, M.; Okuro, K.; Kinbara, K.; Aida, T. High-Water-Content Mouldable Hydrogels by Mixing Clay and a Dendritic Molecular Binder. *Nature* **2010**, *463* (7279), 339–343. https://doi.org/10.1038/nature08693.

(32) Shu, X. Z.; Liu, Y.; Palumbo, F.; Prestwich, G. D. Disulfide-Crosslinked Hyaluronan-Gelatin Hydrogel Films: A Covalent Mimic of the Extracellular Matrix for in Vitro Cell Growth. *Biomaterials* **2003**, *24* (21), 3825–3834. https://doi.org/10.1016/S0142-9612(03)00267-9.

(33) Nimmo, C. M.; Owen, S. C.; Shoichet, M. S. Diels−Alder Click Cross-Linked Hyaluronic Acid Hydrogels for Tissue Engineering. *Biomacromolecules* **2011**, *12* (3), 824–830. https://doi.org/10.1021/bm101446k.

(34) Sreenivasachary, N.; Lehn, J.-M. Gelation-Driven Component Selection in the Generation of Constitutional Dynamic Hydrogels Based on Guanine-Quartet Formation. *Proc. Natl. Acad. Sci. U. S. A.* **2005**, *102* (17), 5938–5943. https://doi.org/10.1073/pnas.0501663102.

(35) Wang, T.; Turhan, M.; Gunasekaran, S. Selected Properties of PH-Sensitive, Biodegradable Chitosan–Poly(Vinyl Alcohol) Hydrogel. *Polym. Int.* **2004**, *53* (7), 911–918. https://doi.org/10.1002/pi.1461.

(36) Woodward, M. P.; Young, W. W.; Bloodgood, R. A. Detection of Monoclonal Antibodies Specific for Carbohydrate Epitopes Using Periodate Oxidation. *J. Immunol. Methods* **1985**, *78* (1), 143–153. https://doi.org/10.1016/0022-1759(85)90337-0.

(37) Boontheekul, T.; Kong, H.-J.; Mooney, D. J. Controlling Alginate Gel Degradation Utilizing Partial Oxidation and Bimodal Molecular Weight Distribution. *Biomaterials* **2005**, *26* (15), 2455–2465. https://doi.org/10.1016/J.BIOMATERIALS.2004.06.044.

(38) Liu, H.; Sui, X.; Xu, H.; Zhang, L.; Zhong, Y.; Mao, Z. Self-Healing Polysaccharide Hydrogel Based on Dynamic Covalent Enamine Bonds. *Macromol. Mater. Eng.* **2016**, *301* (6), 725–732. https://doi.org/10.1002/mame.201600042.

(39) Edgar, K. J.; Arnold, K. M.; Blount, W. W.; Lawniczak, J. E.; Lowman, D. W. Synthesis and Properties of Cellulose Acetoacetates. *Macromolecules* **1995**, *28* (12), 4122–4128. https://doi.org/10.1021/ma00116a011.

(40) Witzeman, J. S.; Nottingham, W. D. Transacetoacetylation with Tert-Butyl Acetoacetate: Synthetic Applications. *J. Org. Chem.* **1991**, *56* (5), 1713–1718.

https://doi.org/10.1021/jo00005a013.

(41) Clemens, R. J.; Hyatt, J. A. Acetoacetylation with 2,2,6-Trimethyl-4H-1,3-Dioxin-4-One: A Convenient Alternative to Diketene. *J. Org. Chem.* **1985**, *50* (14), 2431–2435. https://doi.org/10.1021/jo00214a006.

(42) Zheng, X.; Xu, D.; Edgar, K. J. Cellulose Levulinate: A Protecting Group for Cellulose That Can Be Selectively Removed in the Presence of Other Ester Groups. *Cellulose* **2015**, *22* (1), 301–311. https://doi.org/10.1007/s10570-014-0508-8.

(43) Arca, H. Ç.; Mosquera-Giraldo, L. I.; Dahal, D.; Taylor, L. S.; Edgar, K. J. Multidrug, Anti-HIV Amorphous Solid Dispersions: Nature and Mechanisms of Impacts of Drugs on Each Other's Solution Concentrations. *Mol. Pharm.* **2017**, *14* (11), 3617–3627. https://doi.org/10.1021/acs.molpharmaceut.7b00203.

(44) Stevens, R. V.; Chapman, K. T.; Weller, H. N. Convenient and Inexpensive Procedure for Oxidation of Secondary Alcohols to Ketones. *J. Org. Chem.* **1980**, *45* (10), 2030–2032. https://doi.org/10.1021/jo01298a066.

(45) Wojtecki, R. J.; Meador, M. A.; Rowan, S. J. Using the Dynamic Bond to Access Macroscopically Responsive Structurally Dynamic Polymers. *Nat. Mater.* **2011**, *10* (1), 14–27. https://doi.org/10.1038/nmat2891.

(46) Dong, Y.; Mosquera-Giraldo, L. I.; Troutman, J.; Skogstad, B.; Taylor, L. S.; Edgar, K. J. Amphiphilic Hydroxyalkyl Cellulose Derivatives for Amorphous Solid Dispersion Prepared by Olefin Cross-Metathesis. *Polym. Chem.* **2016**, *7* (30), 4953–4963. https://doi.org/10.1039/C6PY00960C.

(47) Roberts, G. A. F.; Domszy, J. G. Determination of the Viscometric Constants for Chitosan. *Int. J. Biol. Macromol.* **1982**, *4* (6), 374–377. https://doi.org/10.1016/0141-8130(82)90074-5.

(48) Rinaudo, M.; Pavlov, G.; Desbrières, J. Influence of Acetic Acid Concentration on the Solubilization of Chitosan. *Polymer (Guildf).* **1999**, *40* (25), 7029–7032. https://doi.org/10.1016/S0032-3861(99)00056-7.

(49) Mehvar, R.; Shepard, T. L. Molecular-Weight-Dependent Pharmacokinetics of Fluorescein-Labeled Dextrans in Rats. *J. Pharm. Sci.* **1992**, *81* (9), 908–912. https://doi.org/10.1002/JPS.2600810914.

(50) Park, H.; Guo, X.; Temenoff, J. S.; Tabata, Y.; Caplan, A. I.; Kasper, F. K.; Mikos, A. G. Effect of Swelling Ratio of Injectable Hydrogel Composites on Chondrogenic Differentiation of Encapsulated Rabbit Marrow Mesenchymal Stem Cells In Vitro. *Biomacromolecules* **2009**, *10* (3), 541–546. https://doi.org/10.1021/bm801197m.

Chapter 6: Thermo responsive, *in situ* forming hydrogel based on oxidized hydroxyl propyl cellulose and Jeffamine

Junyi Chen[a], *and Kevin J. Edgar*[b, c]

[a]Department of Chemistry, Virginia Tech, Blacksburg, VA 24061, United States

[b]Department of Sustainable Biomaterials, Virginia Tech, Blacksburg, VA 24061, United States

[c]Macromolecules Innovation Institute, Virginia Tech, Blacksburg, VA 24061, United States

6.1 Abstract

Oligo(hydroxypropyl)-substituted polysaccharides can be chemoselectively oxidized to introduce ketone groups at the termini of the side chains. These ketone-substituted polysaccharides, including oxidized hydroxypropyl cellulose, have been shown to be suitable components for preparation of *in situ* forming, all-polysaccharide hydrogels where chitosan is the reactive partner. This class of hydrogels exhibits several advantages including injectability, the ability to self-heal, and the absence of small molecule crosslinkers, therefore they have considerable promise for biomedical applications. Their strong potential inspires us to broaden the range of their application to include thermoresponsive hydrogels.

Herein, we design and prepare a series of oxidized hydroxypropyl cellulose hydrogels by reaction with Jeffamines. Jeffamines, polyethylene oxide-*b*-polypropylene oxide-*b*-polyethylene oxide triblock copolymers with two terminal amines, are thermally responsive with tunable lower critical solution temperatures (LCST), and are biocompatible with some tissues and under some circumstances. By using Jeffamine as the polymeric amine crosslinker, we successfully introduce thermal responsiveness to the oxidized hydroxypropyl cellulose-based hydrogel. The mechanical properties of these hydrogels were characterized by rheometry, revealing that hydrogel storage modulus could be tuned by controlling temperature and Jeffamine chain length. Furthermore, these

hydrogels display self-healing properties and high swelling ratios. Hydrogel microstructures were characterized by scanning electron microscopy. We investigate the potential for drug encapsulation in the hydrogels, as well as for thermoresponsive drug release. Overall, this study demonstrates synthesis and potential of these Jeffamine/oxidized hydroxypropyl cellulose hydrogels for *in situ* forming, thermally responsive behavior, thereby broadening the family of oxidized hydroxypropyl cellulose-based hydrogels.

6.2 Introduction

Hydrogels are crosslinked polymer networks, insoluble in water due to their very high effective molecular weights but with high water affinity, that are employed by Nature[1–3] and are also used in manufactured products[4]. They can be prepared by combining synthetic polymers, natural polymers, or both. Polysaccharides are prominent hydrogel components due to their frequent biocompatibility with living tissues[5], high swelling ratios[6], and high permeabilities to metabolites and nutrients[7]. Thus, many different types of polysaccharides, including cellulose, dextran, hyaluronic acid, and their derivatives have been employed as components of hydrogels for biomedical applications.

In situ forming hydrogels have been investigated in recent years due to certain attractive properties, including their benign natures in various biomedical applications, such as drug delivery, tissue engineering, and cell encapsulation. This class of hydrogel is usually injectable, meaning that they can be injected in the liquid state, then can recover rapidly to hydrogel form shortly after the shear force of injection ceases. Injection of an *in situ* forming hydrogel is a useful technique in the clinic as it offers great precision of location, thereby reducing off-target effects. *In situ* forming hydrogels can mimic the extracellular matrix (ECM), which provides an environment conducive to cellular growth, homeostasis, adhesion, and under the right conditions, metastasis[8]. Artificial scaffolds that

mimic the ECM nanoenvironment of the human body may have significant utility for cell studies[9,10] and therapeutic uses[11].

Several strategies have been reported for preparing self-healing hydrogels, include those that introduce dynamic covalent[12,13] and non-covalent crosslinks[14]. Dynamic chemistry including acylhydrazone bond formation[15], Diels-Alder cycloaddition, and creation of redox-responsive disulfide bonds[16] has been investigated for preparing self-healing hydrogels. However, most of these approaches involve small molecule reagents or crosslinkers, which are by definition multifunctional, capable of rapid diffusion, and thus are frequently toxic. It is also difficult or impossible to quantitatively remove unreacted crosslinker residue from the hydrogel; in combination these characteristics may severely limit the practical utility of hydrogels prepared using small molecule crosslinkers in biomedicine.

Our recent study described an *in situ* forming hydrogel that allows for injection and self-healing. This hydrogel was prepared by reaction of chitosan with oxidized oligo(hydroxypropyl)-substituted polysaccharides, which were simply derived from hydroxypropyl cellulose (HPC) and hydroxypropyl dextran (see Scheme 1). These hydrogels were crosslinked by imine bonds, formed between the primary amines of chitosan and the ketones of oxidized hydroxypropyl cellulose (OX-HPC) or oxidized hydroxypropyl dextran (OX-HPD), generating only water as a co-product[17]. This novel hydrogel preparation exhibited several advantages, including the complete absence of small molecule crosslinkers, a simple and easily controlled method of preparation, and the nature of the oxidation involved which preserves the native polysaccharide structure and thus its physical properties. Furthermore, the imine crosslinks were dynamic covalent bonds, existing in a mostly aqueous environment (the hydrogels themselves were > 97% water), able to form spontaneously between amines and ketones without the need for a catalyst[18]. Thus, these imine linkages brought

several interesting properties such like pH responsiveness, ability to self-heal, and injectability to this class of hydrogel. Having shown that oxidized oligo(hydroxypropyl)-substituted polysaccharides are valuable materials for hydrogel preparation by reaction with chitosan, we wished to further explore their potential in stimulus-responsive hydrogels.

Developing hydrogels responsive to external stimuli like pH[19], temperature[20], and electrical energy[21] has been an important topic of study because of the potential for these hydrogels for stimulus-triggered action[22]. Thermally responsive hydrogels whose physical properties can be modulated by changing temperature have potential as components of smart drug delivery systems[23]. To date, thermally responsive hydrogels have been largely prepared from synthetic polymers that show lower critical solution temperature (LCST) behavior, including poly(*N*-isopropylacrylamide) (PNIPA), poly(ethylene oxide)-*b*-poly(propylene oxide) triblock copolymers, and poly(lactic-co-glycolic acid)-*b*-poly(ethylene oxide) triblock copolymers. Among these polymers, PNIPA has received the most attention for development of temperature modulated drug delivery, as its LCST is close to human body temperature. However, most of these hydrogels do not readily biodegrade *in vivo*, limiting their therapeutic utility.

In this study, we designed a multi-responsive hydrogel. To introduce thermal responsiveness to hydrogels based on oxidized oligo(hydroxypropyl)-substituted polysaccharides, we chose bis(2-aminopropyl) polypropylene oxide-*b*-polyethylene oxide-*b*-polypropylene oxides, also known as Jeffamines, as co-components. With their amine termini, we hypothesize that Jeffamines will act as macro crosslinkers by condensing with OX-HPC ketones to form imine linkages. Jeffamines are relatively economical materials and biocompatible[24] in a number of *in vivo* situations. They comprise varying ratios of polyethylene oxide and polypropylene oxide; manipulation of the ratio permits tuning of LCST[25,26]. Jeffamine and its precursor polypropylene oxide-*b*-polyethylene-*b*-

polypropylene oxide (Pluronic) have been reported to be useful in temperature-triggered applications such as thermoresponsive nanocapsules[27], drug delivery[28], and thermoassociative hydrogels[29]. Jeffamines and Pluronics have been shown to self-assemble into multimolecular aggregates with rodlike, spherical, and lamellar architectures in aqueous solution in a temperature-dependent manner[30].

We hypothesize that OX-HPC, synthesized from hydroxypropyl cellulose by sodium hypochlorite oxidation, will readily form hydrogels by condensation with the amine termini of difunctional Jeffamines. We further hypothesize that the resulting all-polymer hydrogels will, like previous imine crosslinked oxidized oligo(hydroxypropyl)-substituted polysaccharide-based hydrogels we have reported, display self-healing, tunable modulus, and injectability. Thanks to the Jeffamine crosslinker, we further hypothesize that OX-HPC/Jeffamine hydrogels will display thermal responsiveness, permitting control of hydrogel properties and performance by controlling temperature. Herein, we report our initial attempts to confirm these hypotheses by investigating processes to prepare these hydrogels, characterizing the products, and exploring critical properties.

6.3 Experiment

6.3.1 Materials

HPC (M_n 100,000 g/mol, degree of substitution (DS) (hydroxypropyl) = 2.2, molar substitution (MS) (hydroxypropyl) = 4.4, determined by NMR[31]), and propylene oxide 99% were purchased from Acros Organics. Sodium hypochlorite aqueous solution (11-15% available chlorine) was purchased from Alfa Aesar. *O*, *O*′-Bis(2-aminopropyl) polypropylene oxide-*b*-polyethylene oxide-*b*-polypropylene oxide (M_n values 600 g/mol, 900 g/mol, and 1900 g/mol) were all purchased from Sigma-Aldrich. Sodium hydroxide and dialysis tubing (3500 molecular weight cutoff (MWCO))

were purchased from Fisher Scientific. Deionized water was prepared by ROpure ST reverse osmosis/tank system.

6.3.2 Measurements

^{1}H NMR spectra were acquired either on a Bruker Avance II spectrometer operating at 500 MHz or on an Agilent MR4 instrument operating at 400 MHz. All samples were analyzed as solutions in D_2O (ca. 10 mg/mL) at 25 °C in standard 5 mm o.d. tubes. ^{13}C NMR spectra were acquired on a Bruker Avance II 500 MHz spectrometer with a minimum of 10,000 scans in D_2O (ca. 40 mg/mL). FT-IR spectra were obtained on a Nicolet 8700 instrument using potassium bromide powder as matrix. Morphologies of OX-HPC-Jeffamine hydrogels were characterized by FEI Quanta 600 FEG Scanning Electron Microscope (SEM). The hydrogels were freeze-dried and coated with iridium (15 nm thickness) using a Cressington 208HR sputter coater.

6.3.3 Rheological characterization of hydrogels

All hydrogel samples were characterized rheologically using a TA AR2000 instrument. The test geometry employed a 25 mm ETC parallel plate. Each hydrogel sample (ca. 100 mg) was uniformly dispensed on the rheometer plate. The test geometry was moved down to the targeted gap height (1.0 mm), and excess hydrogel was removed. In strain sweep experiments, the range of strain was from 0.2% to 100%, and the experiments were conducted at 25 °C at 0.5 Hz. In frequency sweep experiments, frequency range was from 0.1 to 5.0 Hz and the experiments were conducted at 25 °C and 1% strain. In step strain sweep experiments, strain was alternated between 0.5% and 100% in 4 minute segments with 2 minute gaps between segments. Temperature and frequency were set to be 25 °C and 0.2 Hz respectively. In temperature sweep experiments, temperature was increased from 25 °C to 50 °C at 5 °C/min. The experiment was conducted at 0.5% strain and 0.5 Hz frequency.

6.3.4 Synthesis of oxidized hydroxypropyl cellulose (OX-HPC)

HPC oxidation followed a procedure recently developed by the Edgar group. HPC (4.0 g, M_n 100,000 g/mol, DS = 2.2, MS = 4.4, 31.2 mmol terminal secondary hydroxyl groups) was dissolved in 50 mL DI water, then NaOCl aqueous solution (50 mL, 146.6 mmol, 4.7 equiv.) was added slowly. Acetic acid (5 mL, 87.4 mmol, 2.8 equiv.) was then added dropwise. The solution was stirred at room temperature for 1 h. Subsequently, the solution was dialyzed in DI water for 48 h. Finally, the purified OX-HPC solution was freeze-dried to give 3.85 g product (yield: 96%).

^{1}H NMR (D_2O): δ 1.14 d, [-CH_2-CH(-C$\underline{H}_3$)-O-], δ 2.13 s, (C$\underline{H}_3$-CO-), δ 3.0 – 4.0, m, (HPC backbone), δ 3.0 – 4.2, d, [-C$\underline{H}_2$-CH(-CH_3)-O-] , δ 3.0 – 4.2, t, [-CH_2-C$\underline{H}$(-CH_3)-O-], δ 4.26, s, (-O-C$\underline{H}_2$-CO-)

^{13}C NMR (D_2O): 210 (CH_3-$\underline{C}$O-), 65-105 {cellulose backbone,□[-$\underline{C}H_2$-$\underline{C}$H(-CH_3)-O-],□(-O-C$\underline{H}_2$-CO-), 25 (C$\underline{H}_3$-CO-), 15 {C$\underline{H}_3$-CH(OH)-, [-CH_2-CH(-C$\underline{H}_3$)-O-]}

6.3.5 Preparation of OX-HPC-Jeffamine hydrogel

Jeffamine ® ED-600 (1.0 g, 600 g/mol), was added to 30 mL DI water. In a separate flask, OX-HPC (1.0 g, DS(ketone) = 1.0) was dissolved in 20 mL DI water. The solutions of OX-HPC and Jeffamine were combined and stirred overnight (12 h), then the solid product was collected by freeze drying the reaction mixture. To prepare hydrogels, 150 mg of this freeze-dried Jeffamine-OX HPC product was added to 10 mL PBS at room temperature. After 2 h, the Jeffamine/OX HPC formed a hydrogel and reached its equilibrium swelling. Hydrogels composed of Jeffamine ® ED-900 and Jeffamine ® ED-2003 were also prepared by this procedure.

6.3.6 Drug releasing study

Jeffamine (150 mg, 1900 g/mol) and OX-HPC (150 mg DS(ketone) = 1.0) were dissolved in 15 mL deionized water. Then phenylalanine (15 mg) was added to the solution with continuous stirring overnight. After 12 h, the reaction mixture was freeze-dried to afford a phenylalanine-loaded, yellow cotton-like solid. To follow phenylalanine release, hydrogel pieces (100 mg) were sealed into dialysis tubing (MWCO 3500 g/mol) and immersed in PBS (20 mL, pH 7.4). 1 mL samples of the solution were removed at predetermined times and analyzed by an Evolution 300 UV-Vis spectrophotometer. The percentage of released phenylalanine was calculated from standard calibration curves, shown in Figure S5.

6.3.7 Measurement of hydrogel swelling ratio (SR)

Jeffamine/OX-HPC hydrogels were individually lyophilized. Weighed portions of these solid products (ca. 30 mg) were added to 20 mL scintillation vials. Subsequently, 10 mL of pH 7.4 buffered phosphate solution (PBS) was added to each vial. The hydrogel samples were allowed to stand, completely immersed in PBS, for 2 h. Then the excess unabsorbed PBS was removed by glass pipet and each hydrogel sample was weighed again. The swelling ratio was determined by the following equation:

$$SR = \frac{\mathrm{W(wet)} - \mathrm{W(dry)}}{\mathrm{W(dry)}}$$

In which W(wet) represents the weight of hydrogel at equilibrium water absorption, and W(dry) represents the initial weight of dry, solid OX-HPC/Jeffamine.

6.4 Results and discussion

6.4.1 Formation of OX-HPC-Jeffamine hydrogel

In this work, we designed a method to prepare *in situ* forming hydrogels by reacting Jeffamines with the oxidation products of HPC (OX-HPC). OX-HPC was synthesized by the chemoselective

oxidation recently designed and described by the Edgar group. In this reaction (Scheme 1), household bleach (aq. NaOCl) was used to oxidize selectively the terminal secondary hydroxyl groups of the oligo(hydroxypropyl) chains at 25 °C to ketones. This method has been shown to provide an efficient, economical, green, and simple route to ketone-containing polysaccharides. Chemical structures of OX-HPCs were determined using ^{1}H NMR, ^{13}C NMR and FT-IR spectroscopic methods. The ^{1}H NMR spectra of HPC and OX-HPC are shown in Figure 1. In the ^{1}H NMR spectrum of starting HPC, the resonances from terminal methyl protons at hydroxy propyl side chain appear at 1.01 ppm. After oxidation, due to the newly formed ketones, some of the terminal methyl resonances shift to 2.00 ppm, supporting the proposed chemical structure. The DS (ketone) of OX-HPC can also be calculated based on its ^{1}H NMR spectrum, as discussed in a previous study. The OX-HPC used in this study has DS (ketone) = 1.0. ^{13}C NMR results also support the proposed structure of OX-HPC. In ^{13}C NMR spectra of HPC and OX-HPC, resonances from ketone carbonyl carbons (210 ppm) and adjacent methyl carbons (25 ppm) appeared after oxidation, supporting the formation of the terminal hydroxyacetone moieties. The FT-IR spectrum of OX-HPC is also consistent with the introduction of ketones with appearance of an absorption at 1725 cm^{-1}, corresponding to the ketone C=O stretch (Fig. S1).

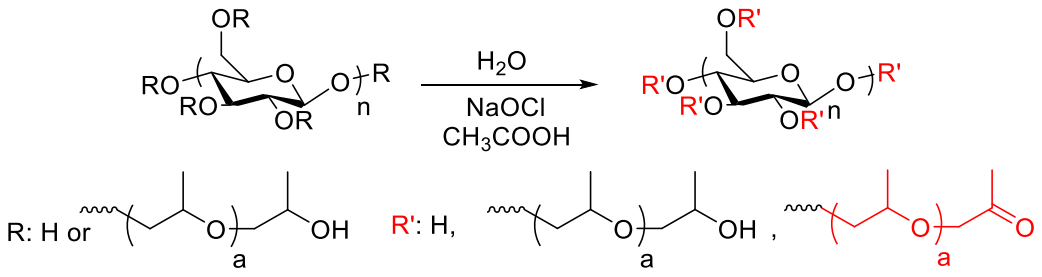

Scheme 1. HPC oxidation by sodium hypochlorite.

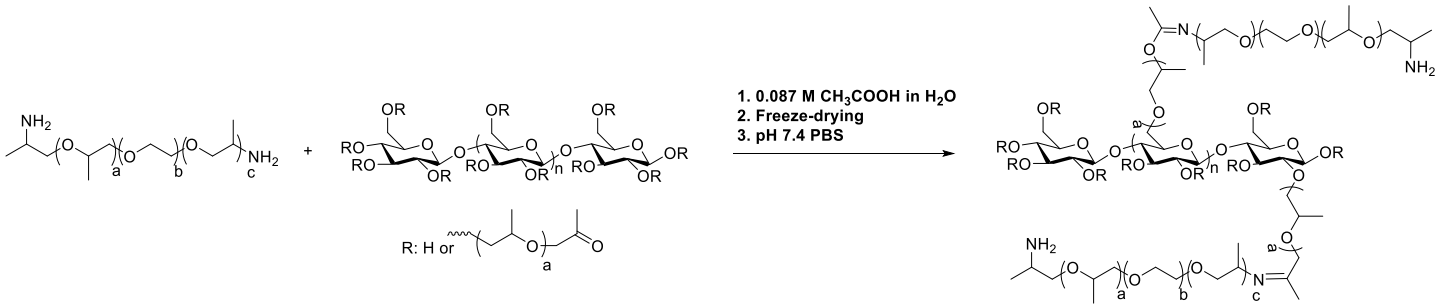

Scheme 2. Preparation of OX-HPC/Jeffamine hydrogel (product structure depicted in this way for clarity and convenience to readers, and is not meant to convey regioselectivity)

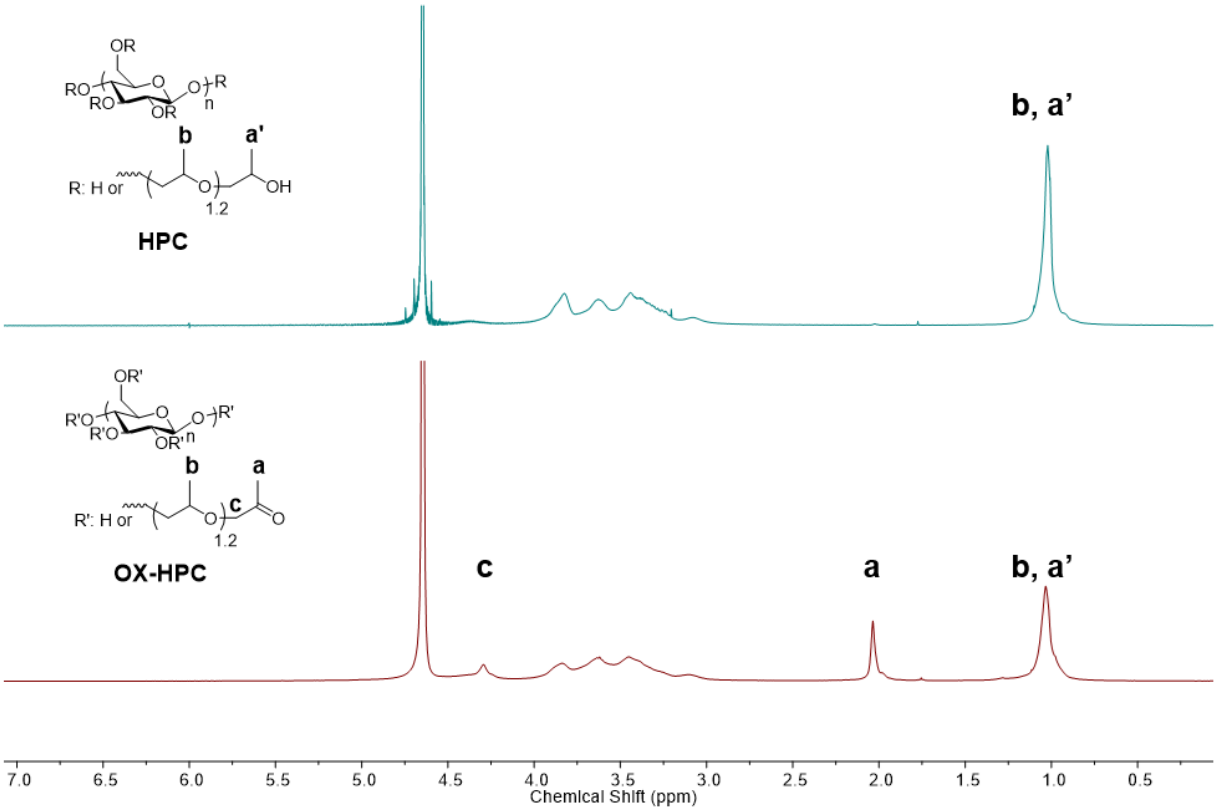

Figure 1. ^{1}H NMR spectra of HPC and OX-HPC.

OX-HPC was investigated as a hydrogel component in a previous study, and we found it is a suitable building block for preparing imine crosslinked hydrogels by reaction with multifunctional chitosan (the chitosan used had approximately one primary amine per monosaccharide). OX-HPC is soluble in water and has ketone terminated oligo(hydroxypropyl) substituents. These ketones should be able to form imine bonds by condensing with the terminal amines of ditelechelic

Jeffamines. These OX-HPC side chain terminal ketones have wider approach angles relative to ring functional groups and are therefore anticipated to be more reactive. The imine bonds that form the crosslinks and create the hydrogel are dynamic covalent bonds, that in the hydrogel (ca. 2.5% solids) exist in an environment that is very rich in water. These dynamic imine bonds can cleave and reform under the influence of external stimuli including stress and pH.

In order to introduce thermal responsiveness to OX-HPC-based hydrogels, we selected Jeffamines as the ditelechelic polymeric amine partners. There are several reasons that Jeffamines are suitable reactive polymeric partners for forming hydrogels with OX-HPC. First, the ditelechelic nature of these Jeffamines means that they can act as hydrogel crosslinkers via imine formation. Second, Jeffamines are water soluble, are biocompatible towards many tissues and situations, and are relatively inexpensive materials, positive characteristics for biomedical applications. Most importantly, Jeffamines exhibit LCST behavior, and therefore have potential for providing thermal responsiveness to the hydrogel.

While multifunctional components like OX-HPC (ca. 1 ketone/monosaccharide) and chitosan (ca. 1 amine/monosaccharide) readily react to form imine-linked hydrogels, it was unclear whether the dichelic Jeffamines would perform as well as chitosan as hydrogel amine partners. As both OX-HPC and Jeffamine are soluble in water, the most straightforward way to prepare these hydrogels would have been to mix an aqueous Jeffamine solution with one of OX-HPC. However, simply combining these two aqueous solutions only gave a clear solution with light yellow color, and did not result in formation of a visible hydrogel, as also observed in the previous study with chitosan as hydrogel partner.

Therefore, we followed the method reported in our previous study that was successful for preparation of the chitosan/OX-HPC hydrogel. We dissolved Jeffamine and OX-HPC in deionized

water to form a clear aqueous solution. Within 2 h, the solution showed a light-yellow color, which may be attributed some degree of formation of imine bonds. This solution then was freeze dried, affording a yellow cotton-like solid mixture of Jeffamine and OX-HPC. From this solid, the hydrogel could be simply prepared by adding deionized water or PBS to the solid mixture. The hydrogel formed within 1 min and became firm within 10 min. The ability to transport the two polymers as a solid mixture to the site where hydrogel formation is desired, then form the hydrogel by simple addition of water, is potentially highly useful and attractive.

To confirm hydrogel formation, the dry mixture of OX-HPC and Jeffamine was added to a scintillation vial with PBS. This material was allowed to swell for 5 minutes. Then the excess water was removed, and the scintillation vial was put on a benchtop upside down (Figure 2). OX-HPC/Jeffamine hydrogel stayed at the former bottom of the inverted vial and resisted flow, illustrating hydrogel formation. In a control experiment, HPC and Jeffamine were dissolved in deionized water, and the resulting solution was freeze dried. Subsequently, the dry mixture was added to a vial with excess deionized water. As seen in Figure S4, the white HPC/Jeffamine mixture fully dissolved in deionized water within 10 min, and could not form a hydrogel. Properties of OX-HPC/Jeffamine hydrogels were further investigated as follows.

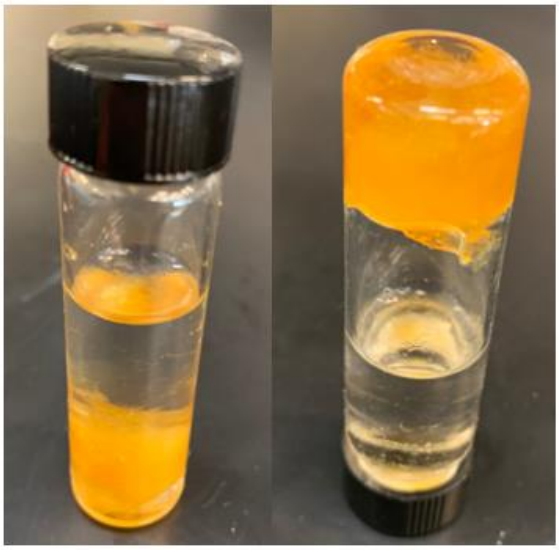

Figure 2. OX-HPC/Jeffamine (600 g/mol) hydrogel

6.4.2 Rheological properties and thermal responsiveness of OX-HPC/Jeffamine hydrogels

The range of potential applications of a particular hydrogel relies strongly on its rheological performance. We hypothesized that the physical properties of OX-HPC/Jeffamine hydrogels would be tunable by controlling various aspects, including the Jeffamine degree of polymerization (DP), ratio of OX-HPC to Jeffamine, DS (ketone) of OX-HPC, and temperature. In this study, we focused on two factors, Jeffamine DP and temperature. If the LCST behavior of the Jeffamine segments has its expected effect on the hydrogel, hydrogel modulus should vary with temperature. Jeffamine DP should influence hydrogel crosslink density, and thus afford another way to modulate hydrogel modulus. To test these hypotheses, we prepared three different hydrogels using OX-HPC and Jeffamines with molecular weights 600 g/mol, 900 g/mol, and 1900 g/mol. We subjected the resulting hydrogels to rheological testing at different temperatures. All tests were carried out at the hydrogel equilibrium swelling with pH 7.4 PBS, and rheometry was performed in parallel plate geometry.

Hydrogel behavior vs. frequency was investigated first. All hydrogel samples were subjected to frequency sweep experiments using 0.5 % strain, which is a small strain that would be unlikely to

significantly impact hydrogel structure. Figure 3 shows a frequency sweep of OX-HPC/Jeffamine (900 g/mol) hydrogel. We can observe an equilibrium G' plateau of ca. 9300 Pa, suggesting that the hydrogel remains in the gel state throughout the frequency range (0.1-5 Hz). In separate experiments hydrogels of OX-HPC with Jeffamines of other molecular weights all remained in the gel state within this frequency range. Frequency sweep data of OX-HPC/Jeffamine hydrogels are displayed in Table 1. The data illustrate the inverse relationship of hydrogel storage modulus to the length of the Jeffamine segments, with modulus increasing from 3 kPa to 20 kPa as Jeffamine molecular weight decreased from 1900 g/mol, to 900 g/mol, to 600 g/mol. This result indicates that hydrogel modulus decreases with increased crosslinker length, observed in previous hydrogel studies[32].

All hydrogel samples were further analyzed by a strain sweep experiment at 0.5 Hz frequency. The example of strain sweep analysis of OX-HPC-Jeffamine (600 g/mol) is shown in Fig. S3. This hydrogel sample displayed a storage modulus of 21,000 Pa, and a linear viscoelastic region limit of 1.6 % strain. This result supports the existence of crosslinking networks in the hydrogel. The strain sweep results of other hydrogels are listed in Table 1, indicating that the maximum strain is not significantly responsive to the Jeffamine molecular weight. All of these hydrogels exhibit similar and relatively small maximum strain (1.3% – 1.6%).

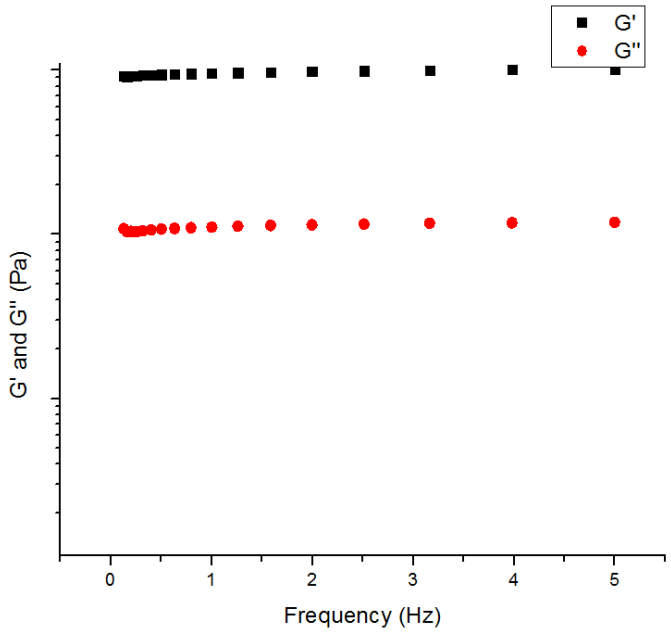

Figure 3. Frequency sweep rheometry of OX-HPC/Jeffamine (900 g/mol) hydrogel

Table 1. Mechanical properties of OX-HPC/Jeffamine hydrogels vs. Jeffamine molecular weight

Hydrogels	G' (Pa)	G'' (Pa)	Maximum strain
OX-HPC-Jeffamine (600 g/mol)	20900	1200	1.6%
OX-HPC-Jeffamine (900 g/mol)	9300	1060	1.5%
OX-HPC-Jeffamine (1900 g/mol) (wt 1:1)	4300	750	1.5%
OX-HPC-Jeffamine (1900 g/mol) (mol 1:1)	3300	620	1.3%

OX-HPC/Jeffamine hydrogels were investigated in temperature sweep experiments at 0.5 Hz frequency and 0.5% strain. An example temperature sweep using 600 g/mol Jeffamine is shown in Figure 4. The result clearly indicates the significant responsiveness of hydrogel storage modulus to temperature, with modulus decreasing from 21,000 Pa to 3300 Pa as temperature increased from 25 °C to 60 °C. This hydrogel behavior is likely caused by the thermally induced phase transition of Jeffamine from hydrophilic to hydrophobic polymer, impacting polymer arrangement in space, and resulting in the reduction of hydrogel modulus. Polymer motion also increases with increasing temperature, which suppresses interaction between polymers, and thus favors decreased modulus.

Due to the observed significant thermoresponsive behavior, we expect that these hydrogels may have potential in applications that require temperature as a trigger.

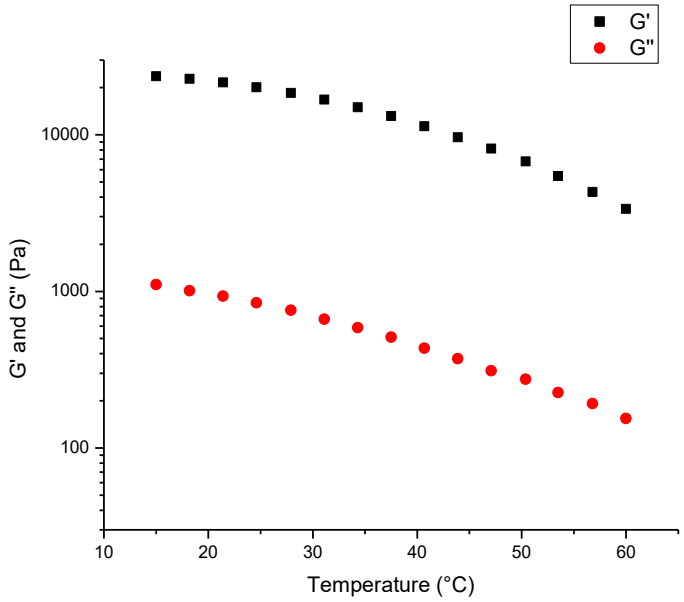

Figure 4. Temperature sweep of OX-HPC/Jeffamine (600 g/mol) hydrogel

6.4.3 Self-healing behavior

The OX-HPC/Jeffamine hydrogels are crosslinked by dynamic Schiff base linkages, reversibly breaking and reforming in the presence of water. This dynamic behavior is expected to lead to the ability of hydrogels to self-heal. To test this hypothesis, a hydrogel sample was prepared by adding pH 7.4 PBS to a dry OX-HPC-Jeffamine (900 g/mol). Then the hydrogel sample was analyzed rheologically by a step-strain time sweep. In this experiment, strain was alternated between 0.5% and 100% in 5-minute segments. An example experiment is shown in Figure 5. The OX-HPC/Jeffamine hydrogel remains in the gel-state during the first 0.5% strain period, as indicated by the fact that storage modulus exceeded loss modulus. In the second segment, a 100% strain was applied and the sample became fluid, as its loss modulus exceeded its storage modulus. The 2-min

gap between segments 2 and 3 was sufficient to allow the hydrogel to recover. Then in section 3, the hydrogel sample was exposed again to a 0.5% strain, and its storage modulus was partially restored to 4000 Pa, indicating the self-healing property of this hydrogel. This self-healing behavior also repeated in the fourth and fifth segments, illustrating that a dynamic crosslinking network existed in the hydrogel.

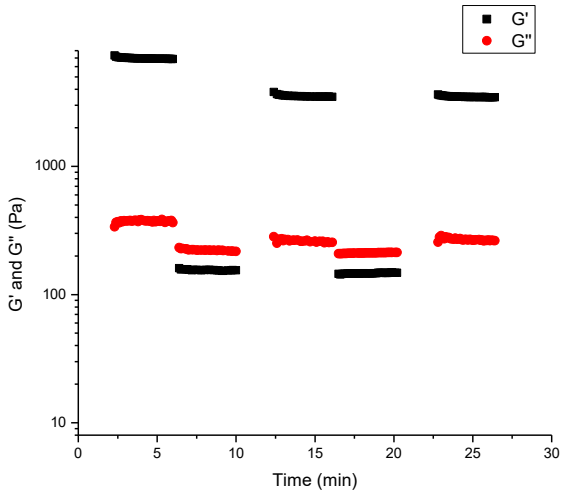

Figure 5. Step-strain time sweep of OX-HPC/Jeffamine (900 g/mol) hydrogel

6.4.4 Swelling ratios

The swelling ratio (SR) indicates the degree of water absorption of the hydrogel, which is important since it influences hydrogel properties such as cell encapsulation, modulus, and ability to support cell proliferation[33]. We investigated two factors, temperature and Jeffamine DP, which are likely to influence the SR; Measurement and calculation followed the procedure in the Experimental section. Hydrogel SR increased slightly with increasing Jeffamine DP (Table S1). OX-HPC/Jeffamine (600 g/mol) hydrogel displayed SR of 17.07 (6.2% solid content). With Jeffamine (1900 g/mol) as component, the SR of hydrogel reached 20.0 (5.0% solid content).

We also investigated the relationship between hydrogel (OX-HPC/Jeffamine (600 g/mol)) SR and temperature. Unlike hydrogel modulus which displayed significant thermoresponsiveness, the SR

decreased only slightly as the hydrogel was heated from 25 °C (SR = 17 ± 0.6) through 40 °C (SR = 15 ± 0.7) to 50 °C (SR = 15 ± 0.6). These observations likely reflect the fact that the absorbed free water (not directly bound to the hydrogel matrix) makes the major contribution to the amount of water absorbed by the hydrogel. Loss of bound water (water interacting with the polymer matrix) due to the thermally-induced transition of Jeffamine contributed only a small portion to the hydrogel SR.

6.4.5 Hydrogel drug releasing

To investigate the potential of these thermoresponsive hydrogels in drug delivery, we attempted to capture phenylalanine in a OX-HPC/Jeffamine hydrogel, and then measure its release under conditions that mimic the physiological. We chose phenylalanine as it is a precursor for many peptide-based drugs. In this experiment, 35 mg of phenylalanine was loaded into 300 mg OX-HPC/Jeffamine (1900 g/mol) hydrogel by co-dissolution, followed by freeze drying. The hydrogel was then formed and the release study was carried out in pH 7.4 PBS at 25 °C. The cumulative amount of phenylalanine release vs. time was measured by UV-Vis spectroscopy, vs. a calibration curve (Figure 7). The phenylalanine was rapidly released over 8 h, then reached a plateau. Considering the good water solubility of phenylalanine, OX-HPC/Jeffamine hydrogel prolonged its release. This drug release experiment was repeated at 37 °C to test response of release rate to temperature change (presumably impacted by response of Jeffamine shape to temperature). We discovered that the drug release vs. time curves at 25 °C and 37 °C were very similar to each other, indicating that, surprisingly, temperature did not greatly impact drug release from the hydrogel. We speculate that hydrogel pore-size and OX-HPC DS(ketone) may play decisive roles in drug release rates. In a control experiment, HPC/Jeffamine (1900 g/mol) was loaded with phenylalanine in similar fashion, and drug release was followed at 25 °C. We found the phenylalanine was fully

released within 1.5 h, supporting the assumption that the OX-HPC/Jeffamine hydrogel prolonged phenylalanine release.

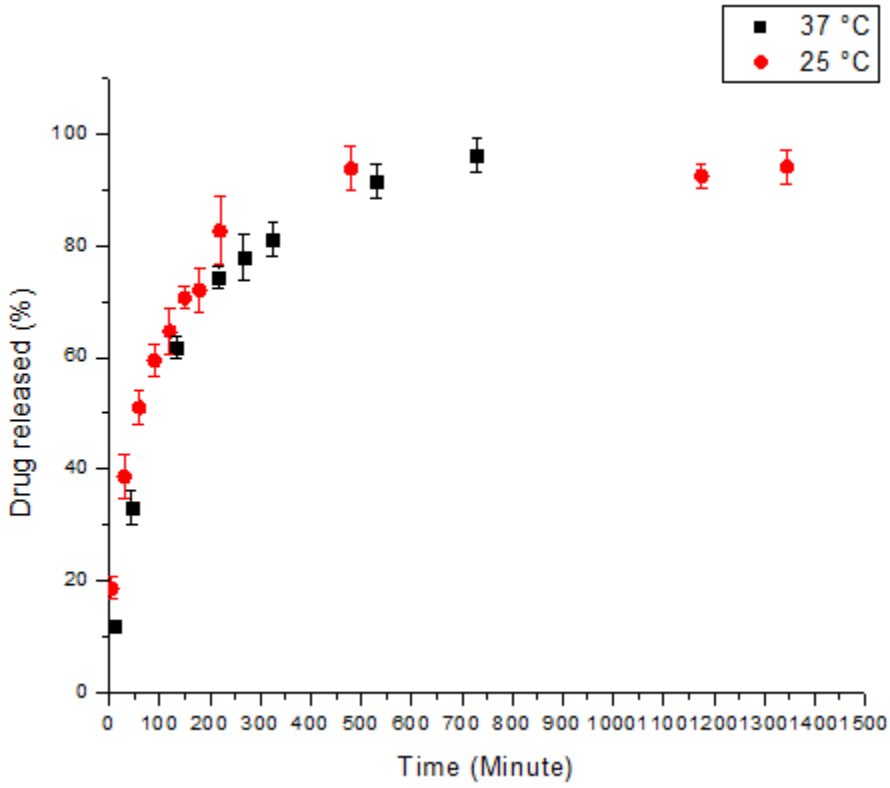

Figure 6. Phenylalanine release from OX-HPC/Jeffamine (600 g/mol) hydrogel at 25 °C and 37 °C.

6.4.6 Microstructures of OX-HPC-Jeffamine hydrogel

In order to investigate their porous structures, microstructure morphologies of freeze-dried OX-HPC/Jeffamine hydrogels were analyzed by SEM. Surface images of OX-HPC/Jeffamine (600 g/mol) and OX-HPC-Jeffamine (1900 g/mol) hydrogels are presented in Figures 7 and 8, respectively. Continuous and porous structures, contributed by the freeze drying process, were observed in both samples. OX-HPC/Jeffamine (600 g/mol) displays a multi-layer structure with pore diameters varying from 50 to 300 μm. On the other hand, OX-HPC-Jeffamine (1900 g/mol) hydrogel displayed a 3D crosslinked matrix with pore size varying from 50 to 200 μm. Crosslink density and composition of the network polymer chains would be expected to play major roles in

controlling hydrogel pore size[34]. Future studies will explore how Jeffamine length, amine/ketone ratio, DS(ketone) of OX-HPC, and freeze-drying process impact hydrogel morphology, so that it may be tailored for specific application purposes.

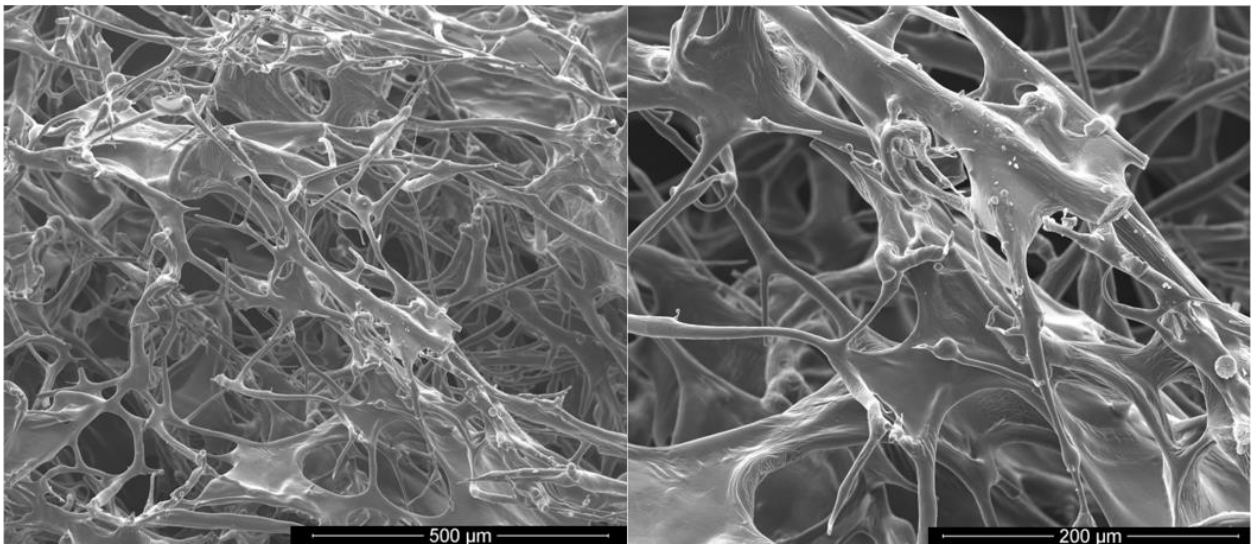

Figure 7. SEM images of OX-HPC/Jeffamine (1900 g/mol) hydrogel.

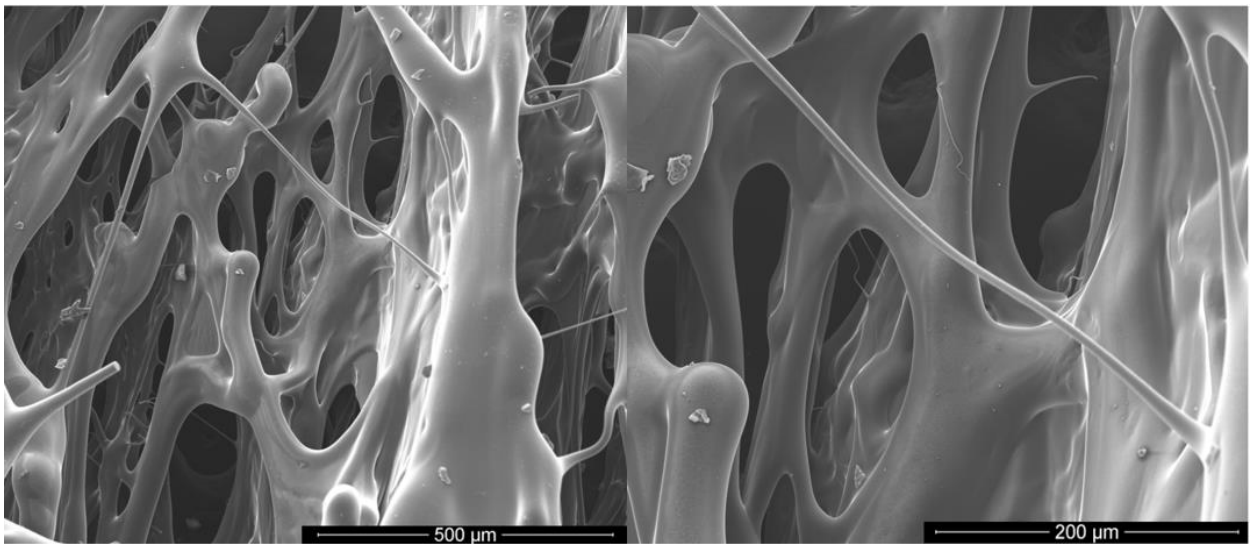

Figure 8. SEM images of OX-HPC/Jeffamine (600 g/mol) hydrogel.

6.5 Conclusion

Design and preparation of OX-HPC/Jeffamine hydrogels crosslinked by imine linkages were successfully demonstrated in this study. Their mechanical properties, ability to self-heal, and thermal responsiveness were characterized through rheometry. We demonstrate a simple process for loading drug into these hydrogels, and examine the kinetics of drug release as well as their thermal responsiveness. These results confirm our original hypotheses: OX-HPCs having ketone functions on the terminal hydroxypropyl groups are able to form imine-linked hydrogels with dichelic Jeffamine. Furthermore, introduction of Jeffamines, known LCST polymers, makes the hydrogels thermally responsive. The OX-HPC/Jeffamine hydrogels exhibited tunable mechanical properties and self-healing. Rheometric studies demonstrated that hydrogel modulus can be tuned in the range from 3 kPa to 21 kPa, controlled by temperature and the Jeffamine DP. The hydrogels were also able to prolong phenylalanine release to 8 h at physiological (blood) pH. These hydrogels have strong potential for biomedical applications (including drug delivery) that benefit from their benign components, adjustable stiffness, and injectability.

This study extends the scope of OX-HPC based imine-crosslinked hydrogels, which avoid the use of potentially toxic small molecule crosslinkers. In future studies, we will explore potential applications of these hydrogels as thermoresponsive materials, and for prolonging drug release. It is also of particular interest for us to study the toxicity, degradation rate and mechanism, ability of these hydrogels to encapsulate cells as mimics of the extracellular matrix, and the relationship of these properties to hydrogel composition. It must be noted that it should be possible to prepare hydroxypropyl derivatives of virtually any polysaccharide, and then to oxidize those oligo(hydroxypropyl) chain ends to ketones, thereby creating the potential to use a wide range of

OX-HP polysaccharides in condensation with Jeffamines to make a broad range of interesting hydrogels.

6.6 References

(1) Pawar, S. N.; Edgar, K. J. Alginate Derivatization: A Review of Chemistry, Properties and Applications. *Biomaterials* **2012**, *33* (11), 3279–3305. https://doi.org/http://dx.doi.org/10.1016/j.biomaterials.2012.01.007.

(2) Pawar, S. N.; Edgar, K. J. Chemical Modification of Alginates in Organic Solvent Systems. *Biomacromolecules* **2011**, *12* (11), 4095–4103. https://doi.org/10.1021/bm201152a.

(3) Johnson, K. L.; Gidley, M. J.; Bacic, A.; Doblin, M. S. Cell Wall Biomechanics: A Tractable Challenge in Manipulating Plant Cell Walls 'Fit for Purpose'! *Curr. Opin. Biotechnol.* **2018**, *49*, 163–171. https://doi.org/10.1016/J.COPBIO.2017.08.013.

(4) Liu, H.; Sui, X.; Xu, H.; Zhang, L.; Zhong, Y.; Mao, Z. Self-Healing Polysaccharide Hydrogel Based on Dynamic Covalent Enamine Bonds. *Macromol. Mater. Eng.* **2016**, *301* (6), 725–732. https://doi.org/10.1002/mame.201600042.

(5) Williams, D. F. There Is No Such Thing as a Biocompatible Material. *Biomaterials* **2014**, *35* (38), 10009–10014. https://doi.org/10.1016/J.BIOMATERIALS.2014.08.035.

(6) Kuang, J.; Yuk, K. Y.; Huh, K. M. Polysaccharide-Based Superporous Hydrogels with Fast Swelling and Superabsorbent Properties. *Carbohydr. Polym.* **2011**, *83* (1), 284–290. https://doi.org/10.1016/J.CARBPOL.2010.07.052.

(7) Muzzarelli, R. A. A. Human Enzymatic Activities Related to the Therapeutic Administration of Chitin Derivatives. *Cell. Mol. Life Sci.* **1997**, *53* (2), 131–140. https://doi.org/10.1007/PL00000584.

(8) Boehnke, N.; Cam, C.; Bat, E.; Segura, T.; Maynard, H. D. Imine Hydrogels with Tunable Degradability for Tissue Engineering. *Biomacromolecules* **2015**, *16* (7), 2101–2108. https://doi.org/10.1021/acs.biomac.5b00519.

(9) Rosellini, E.; Zhang, Y. S.; Migliori, B.; Barbani, N.; Lazzeri, L.; Shin, S. R.; Dokmeci, M. R.; Cascone, M. G. Protein/Polysaccharide-Based Scaffolds Mimicking Native Extracellular Matrix for Cardiac Tissue Engineering Applications. *J. Biomed. Mater. Res. Part A* **2018**, *106* (3), 769–781. https://doi.org/10.1002/jbm.a.36272.

(10) Geckil, H.; Xu, F.; Zhang, X.; Moon, S.; Demirci, U. Engineering Hydrogels as Extracellular Matrix Mimics. *Nanomedicine* **2010**, *5* (3), 469–484. https://doi.org/10.2217/nnm.10.12.

(11) Zhu, Y.; Crewe, C.; Scherer, P. E. Hyaluronan in Adipose Tissue: Beyond Dermal Filler and Therapeutic Carrier. *Sci. Transl. Med.* **2016**, *8* (323), 323ps4 LP-323ps4. https://doi.org/10.1126/scitranslmed.aad6793.

(12) Rowan, S. J.; Cantrill, S. J.; Cousins, G. R. L.; Sanders, J. K. M.; Stoddart, J. F. Dynamic Covalent Chemistry. *Angew. Chemie Int. Ed.* **2002**, *41* (6), 898–952. https://doi.org/10.1002/1521-3773(20020315)41:6<898::AID-ANIE898>3.0.CO;2-E.

(13) Lehn, J.-M. Dynamers: Dynamic Molecular and Supramolecular Polymers. *Prog. Polym. Sci.* **2005**, *30* (8–9), 814–831. https://doi.org/10.1016/J.PROGPOLYMSCI.2005.06.002.

(14) Wang, Q.; Mynar, J. L.; Yoshida, M.; Lee, E.; Lee, M.; Okuro, K.; Kinbara, K.; Aida, T. High-Water-Content Mouldable Hydrogels by Mixing Clay and a Dendritic Molecular Binder. *Nature* **2010**, *463* (7279), 339–343. https://doi.org/10.1038/nature08693.

(15) Sreenivasachary, N.; Lehn, J.-M. Gelation-Driven Component Selection in the Generation of Constitutional Dynamic Hydrogels Based on Guanine-Quartet Formation. *Proc. Natl. Acad.*

Sci. U. S. A. **2005**, *102* (17), 5938–5943. https://doi.org/10.1073/pnas.0501663102.

(16) Shu, X. Z.; Liu, Y.; Palumbo, F.; Prestwich, G. D. Disulfide-Crosslinked Hyaluronan-Gelatin Hydrogel Films: A Covalent Mimic of the Extracellular Matrix for in Vitro Cell Growth. *Biomaterials* **2003**, *24* (21), 3825–3834. https://doi.org/10.1016/S0142-9612(03)00267-9.

(17) Wojtecki, R. J.; Meador, M. A.; Rowan, S. J. Using the Dynamic Bond to Access Macroscopically Responsive Structurally Dynamic Polymers. *Nat. Mater.* **2011**, *10* (1), 14–27. https://doi.org/10.1038/nmat2891.

(18) Wang, T.; Turhan, M.; Gunasekaran, S. Selected Properties of PH-Sensitive, Biodegradable Chitosan–Poly(Vinyl Alcohol) Hydrogel. *Polym. Int.* **2004**, *53* (7), 911–918. https://doi.org/10.1002/pi.1461.

(19) Gupta, P.; Vermani, K.; Garg, S. Hydrogels: From Controlled Release to PH-Responsive Drug Delivery. *Drug Discov. Today* **2002**, *7* (10), 569–579. https://doi.org/10.1016/S1359-6446(02)02255-9.

(20) Li, Z.; Guan, J. Thermosensitive Hydrogels for Drug Delivery. *Expert Opin. Drug Deliv.* **2011**, *8* (8), 991–1007. https://doi.org/10.1517/17425247.2011.581656.

(21) D'Emanuele, A.; Staniforth, J. N. Feedback Controlled Drug Delivery Using an Electro-Diffusion Pump. *J. Control. Release* **1993**, *23* (2), 97–104. https://doi.org/10.1016/0168-3659(93)90036-5.

(22) Liu, M.; Song, X.; Wen, Y.; Zhu, J.-L.; Li, J. Injectable Thermoresponsive Hydrogel Formed by Alginate- *g* -Poly(*N* -Isopropylacrylamide) That Releases Doxorubicin-Encapsulated Micelles as a Smart Drug Delivery System. *ACS Appl. Mater. Interfaces* **2017**, *9* (41), 35673–35682. https://doi.org/10.1021/acsami.7b12849.

(23) Bae, Y. H.; Okano, T.; Hsu, R.; Kim, S. W. Thermo-sensitive Polymers as On-off Switches for Drug Release. *Die Makromol. Chemie, Rapid Commun.* **1987**, *8* (10), 481–485. https://doi.org/10.1002/marc.1987.030081002.

(24) Shachaf, Y.; Gonen-Wadmany, M.; Seliktar, D. The Biocompatibility of Pluronic®F127 Fibrinogen-Based Hydrogels. *Biomaterials* **2010**, *31* (10), 2836–2847. https://doi.org/10.1016/j.biomaterials.2009.12.050.

(25) Agut, W.; Brûlet, A.; Taton, D.; Lecommandoux, S. Thermoresponsive Micelles from Jeffamine-b-Poly(l-Glutamic Acid) Double Hydrophilic Block Copolymers. *Langmuir* **2007**, *23*, 11526–11533. https://doi.org/10.1021/LA701482W.

(26) Lu, A.; Petit, E.; Li, S.; Wang, Y.; Su, F.; Monge, S. Novel Thermo-Responsive Micelles Prepared from Amphiphilic Hydroxypropyl Methyl Cellulose-Block-JEFFAMINE Copolymers. *Int. J. Biol. Macromol.* **2019**, *135*, 38–45. https://doi.org/10.1016/J.IJBIOMAC.2019.05.087.

(27) Seung Ho Choi, †; Ji-Hwan Lee, ‡; Sung-Min Choi, ‡ and; Tae Gwan Park*, †. Thermally Reversible Pluronic/Heparin Nanocapsules Exhibiting 1000-Fold Volume Transition. **2006**. https://doi.org/10.1021/LA052549N.

(28) Kabanov, A. V; Batrakova, E. V; Alakhov, V. Y. Pluronic® Block Copolymers as Novel Polymer Therapeutics for Drug and Gene Delivery. *J. Control. Release* **2002**, *82* (2–3), 189–212. https://doi.org/10.1016/S0168-3659(02)00009-3.

(29) Mocanu, G.; Souguir, Z.; Picton, L.; Le Cerf, D. Multi-Responsive Carboxymethyl Polysaccharide Crosslinked Hydrogels Containing Jeffamine Side-Chains. *Carbohydr. Polym.* **2012**, *89* (2), 578–585. https://doi.org/10.1016/J.CARBPOL.2012.03.052.

(30) Nagarajan, R. Solubilization of Hydrocarbons and Resulting Aggregate Shape Transitions in Aqueous Solutions of Pluronic® (PEO–PPO–PEO) Block Copolymers. *Colloids Surfaces B Biointerfaces* **1999**, *16* (1–4), 55–72. https://doi.org/10.1016/S0927-7765(99)00061-2.

(31) Dong, Y.; Edgar, K. J. Imparting Functional Variety to Cellulose Ethers via Olefin Cross-Metathesis. *Polym. Chem.* **2015**, *6* (20), 3816–3827. https://doi.org/10.1039/C5PY00369E.

(32) DeForest, C. A.; Sims, E. A.; Anseth, K. S. Peptide-Functionalized Click Hydrogels with Independently Tunable Mechanics and Chemical Functionality for 3D Cell Culture. *Chem. Mater.* **2010**, *22* (16), 4783–4790. https://doi.org/10.1021/cm101391y.

(33) Park, H.; Guo, X.; Temenoff, J. S.; Tabata, Y.; Caplan, A. I.; Kasper, F. K.; Mikos, A. G. Effect of Swelling Ratio of Injectable Hydrogel Composites on Chondrogenic Differentiation of Encapsulated Rabbit Marrow Mesenchymal Stem Cells In Vitro. *Biomacromolecules* **2009**, *10* (3), 541–546. https://doi.org/10.1021/bm801197m.

(34) Hoffman, A. S. Hydrogels for Biomedical Applications. *Adv. Drug Deliv. Rev.* **2012**, *64*, 18–23. https://doi.org/10.1016/J.ADDR.2012.09.010.

Chapter 7: Summary and future work

7.1 Synthesis of polysaccharide-based block copolymers via olefin cross-metathesis (CM)

Polysaccharide-based block copolymers have great potential in applications like compatibilization, adhesion, and drug delivery. However, it is challenging to prepare this novel class of materials and only a limited number of synthetic routes have been reported. In **Chapter 3**, we demonstrate the concept of olefin cross-metathesis as a coupling method for block copolymer synthesis by preparation of a series of trimethyl cellulose (TMC)-based block copolymers. The substrate (TMC-C5), TMC bearing an ω-unsaturated alkyl glycoside substituent, was prepared by solvolysis of TMC with pent-4-en-ol. We discovered that TMC-C5 was a highly efficient CM substrate, which readily reacts with Grubbs Type II olefins including small molecules and polymers. This is the first report of introduction of an ω-olefin substituent regioselectively to the reducing end anomeric position of a polysaccharide, and the first demonstration of CM of such a substrate. We expect that this synthetic strategy will be applicable to most polysaccharides. A few limitations of this approach were defined. First, it is difficult to precisely control the molecular weight of the substrate since chain cleavage in the acid-catalyzed solvolysis is random. Secondly, isolating and purifying the desired block copolymer product is an issue. It is challenging to fully remove impurities, especially the polymers, without losing the product; therefore it is important to select a target block copolymer that can be readily separated from its precursor polymers.

We envision several promising future opportunities based on this novel synthetic strategy. As the TMC-C5 CM products have a single exposed hydroxyl group at the non-reducing end, this provides a pathway for non-reducing end functionalization and provides a handle for appending another polymer block. Therefore, TMC-C5 has potential to serve as a substrate for preparing A-B-C or A-B-A triblock copolymers, greatly extending the diversity and applications of this

approach. Furthermore, it may be possible to synthesize high molecular weight diblock and triblock copolymers based on TMC-C5 and exploit their physical properties like morphology and mechanical performance.

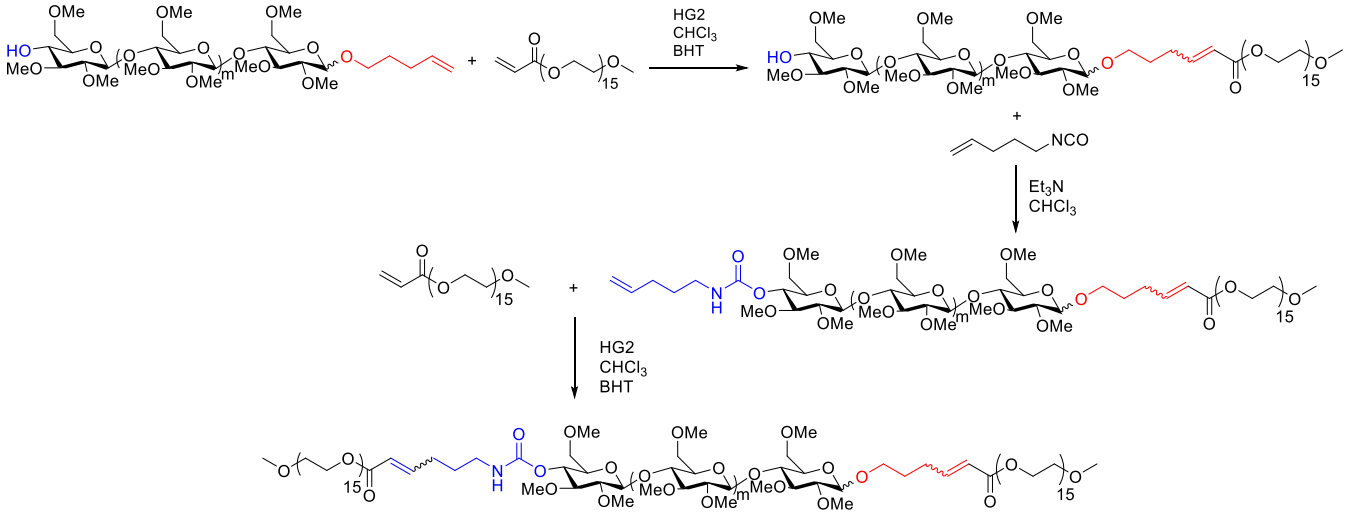

Figure 7.1 Synthesis of PEG-*b*-TMC-*b*-PEG triblock copolymer

7.2 Regioselective bromination of the dextran non-reducing end creates a pathway to dextran-based block copolymers

The few reported polysaccharide-based block copolymers have for the most part been prepared via end-functionalization at the reducing end of the polysaccharide. In **Chapter 4**, we described a unique synthetic route for preparing dextran-based block copolymers. Due to the backbone comprising α-1→6 linkages, each dextran chain has only one primary alcohol at its non-reducing end. Polysaccharide primary alcohols provide opportunities for regioselective modification. Thus, NBS bromination was applied to linear dextran, and the resulting dextran terminated at the non-reducing end by a single 6-bromo-6-deoxyglucose monosaccharide was shown to be an effective substrate for preparing block copolymers via S_N2 displacement chemistry. Three block copolymers, Dextran-*b*-PNIPA, Dextran-*b*-PEG and Dextran-*b*-Polystyrene were prepared through this simple, two-step synthetic route. This type of block copolymer displays interesting and potentially useful

properties. The morphology of dextran-*b*-polystyrene was revealed by SAXS, indicating the existence of microphase separation. Dextran-*b*-PNIPA was studied by DLS in dilute aqueous solution, showing that the hydrophilic-amphiphilic block copolymer exhibits thermally-induced micellization at 37 °C with an average micelle diameter of 170 nm. This micellization process, induced by the LCST behavior of the PNIPA block, is reversible by reducing the temperature.

These dextran-based block copolymers have their anomeric positions intact, thus affording the possibility of further regioselective and end modification. Therefore, these dextran-based diblock copolymers have potential to be elaborated into A-B-C and A-B-A triblock copolymers. In addition, we realized that Dextran-*b*-PNIPA may serve as a useful drug delivery polymer due to its thermally-induced micellization behavior. Moreover, the morphology of dextran-based block copolymers deserves further investigation. As dextrans can be readily chemically modified, we expect that the morphology of this class of block copolymer may be influenced or even controlled by appending different substituents to the dextran block.

7.3 All-polysaccharide, self-healing injectable hydrogels based on chitosan and oxidized hydroxypropyl polysaccharide

Polysaccharide-based hydrogels are useful and attractive materials for biomedical applications due to their benefits including polyfunctionality, potential for biocompatibility with living systems, biodegradability, and generally benign nature. However, preparation of polysaccharide-based hydrogels has previously required toxic small molecule crosslinkers, or periodate oxidation of the polysaccharide which fundamentally changes polymer structure, limiting application potential of these hydrogels. In **Chapter 5**, we introduced an environmentally-friendly, efficient, simple method for preparing *in situ* forming, polysaccharide-based hydrogels. In a previous study the Edgar group reported that oxidation of oligo(hydroxypropyl)-substituted polysaccharides generates ketones on the terminal hydroxypropyl groups, creating the ability to form imine

linkages with chitosan and other amine containing polymers. In this work, we prepared two different types of hydrogels: oxidized hydroxypropyl cellulose (OX-HPC)/chitosan and oxidized hydroxypropyl dextran (OX-HPD)/chitosan. These hydrogels display several impressive properties such as high swelling ratio and injectability. The hydrogel moduli are also tunable in the range of 300 Pa to 13,000 Pa simply by controlling the DS(ketone) of OX-HPC or OX-HPD, which can in turn simply be controlled by (household) bleach stoichiometry. Robust self-healing of this hydrogel was also demonstrated by rheological and macroscopic experimentation. This hydrogel preparation strategy affords new families of imine-crosslinked hydrogel, completely devoid of toxic small molecule crosslinkers, and preserving the properties that arise from the intact polysaccharide backbone.

Based on what we learned from this study, there are many aspects of work deserving further investigation. We will explore the potential of these ketone-containing polysaccharides for further chemical modification via appending drug and bioactive molecules for targeted releasing purpose. These hydrogels may have great potential for drug release over long time period. It is also particularly interesting for us to understand gelation kinetics, degradation mechanism, pH responsiveness, toxicity, and potential for cell encapsulation of these hydrogels. Moreover, as OX-HPC has free hydroxyl groups, OX-HPC/chitosan hydrogels have potential to be further chemically modified, affording doubly crosslinked hydrogels (Figure 7.1). By appending acrylate motifs to OX-HPC, UV-induced crosslinking can be introduced to the hydrogel, offering a way to greatly enhance hydrogel mechanical performances when it is desired. We expect that these hydrogels will have promising potential for 3D printing applications.

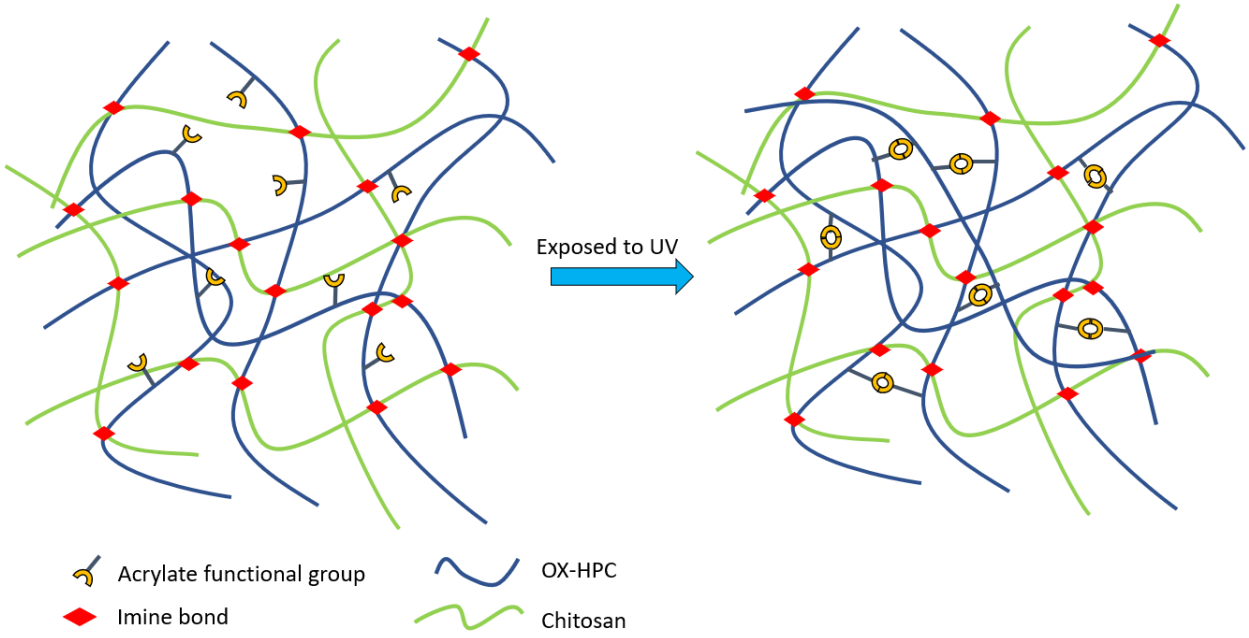

Figure 7.1 UV-induced crosslinking of acrylated OX-HPC/chitosan hydrogel.

7.4 Thermoresponsive *in situ* forming hydrogel based on oxidized hydroxypropyl cellulose and Jeffamine.

Oxidized hydroxypropyl substituted polysaccharides were discovered to be suitable materials for chitosan-based hydrogel preparation. We were greatly interested in extending the scope of this class of hydrogels, and wished to endow them with different properties. In **Chapter 6**, we designed and prepared a series of thermoresponsive, *in situ* forming hydrogels, which are composed of oxidized hydroxypropyl cellulose and polyethylene oxide-*b*-polypropylene oxide-*b*-polyethylene oxide triblock copolymers (Jeffamines) with different molecular weights. As Jeffamines display lower critical solution temperature behavior, thermoresponsiveness was successfully introduced to the hydrogel. Hydrogel moduli were tunable by controlling the temperature, covering the storage modulus (G') range from 3 kPa to 21 kPa. We also discovered that the molecular weight of Jeffamine effects the modulus of hydrogel, affording another pathway to modify hydrogel mechanical performance. Due to the imine linkages, oxidized hydroxypropyl cellulose/Jeffamine

hydrogels display self-healing properties, as revealed by rheometry. Hydrogel microstructures were characterized by Scanning Electron Microscopy, indicating that mesh sizes varied from 50 to 200 μm. In addition, drug release from the OX-HPC/Jeffamine hydrogel was investigated, and the model drug phenylalanine was released over 9 h.

This work demonstrates that oxidized hydroxypropyl polysaccharides readily form hydrogels with multifunctional amine-containing polymers like chitosan and Jeffamine. We expect that oxidized hydroxypropyl polysaccharides have potential to be prepared into many different types of hydrogels with specific properties. In future work, we will keep investigating their potential applications as thermoresponsive materials, and for prolonging drug release time. We are also interested in developing a method that can control the mesh size of hydrogel. Moreover, toxicity, cell encapsulation, and degradation of these hydrogels are worthy of further study.

Appendix A: Supplementary Information

Chapter 3: **Synthesis of polysaccharide-based block copolymer via olefin cross-metathesis**

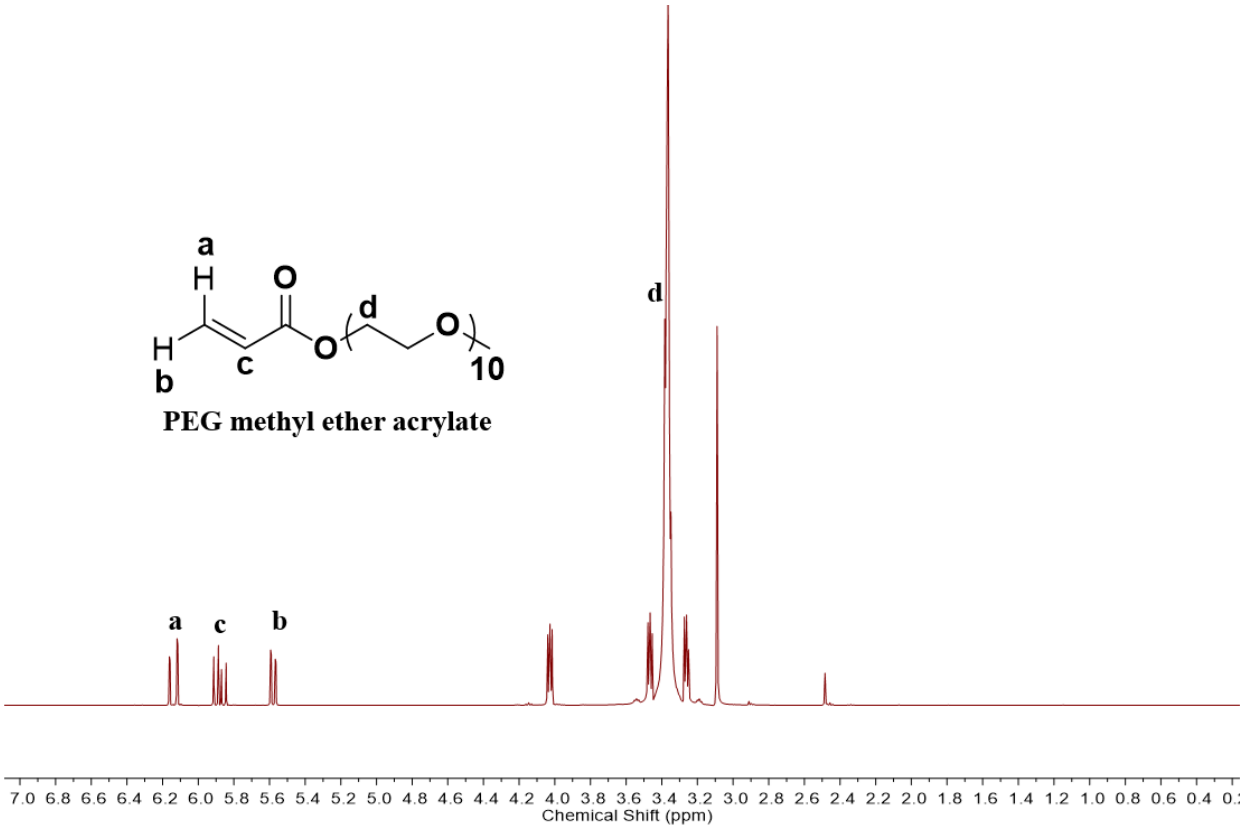

Figure S1. ^{1}H NMR spectrum of PEG methyl ether acrylate

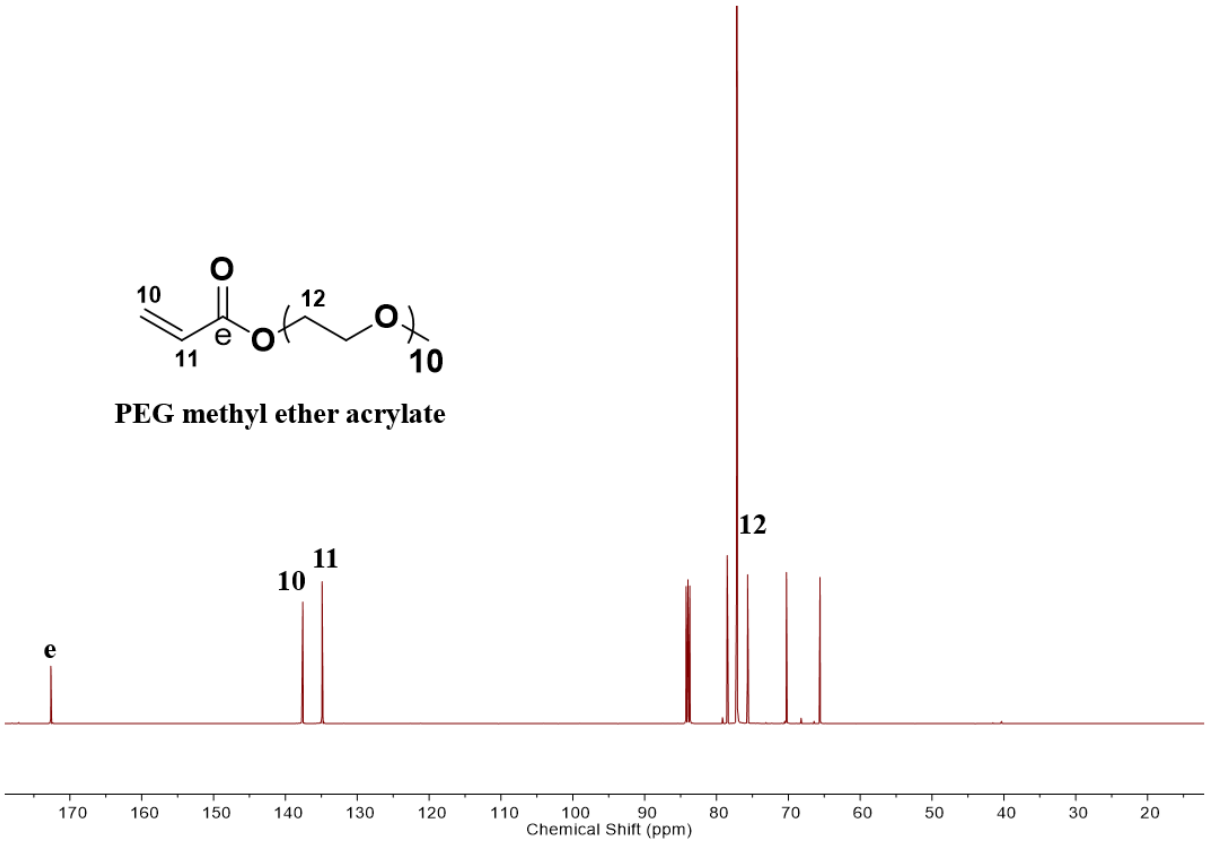

Figure S2. ^{13}C NMR spectrum of PEG methyl ether acrylate

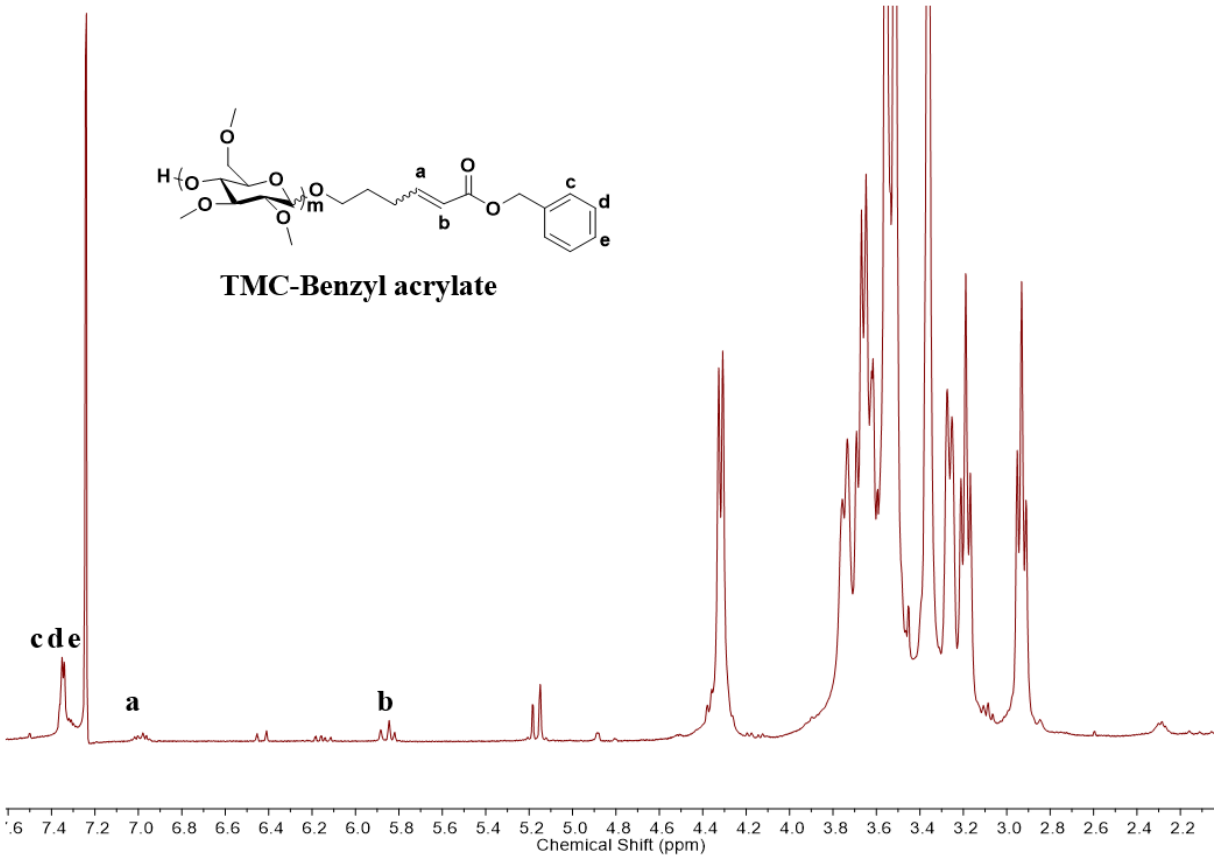

Figure S3. ^{1}H NMR spectrum of TMC-Benzyl acrylate

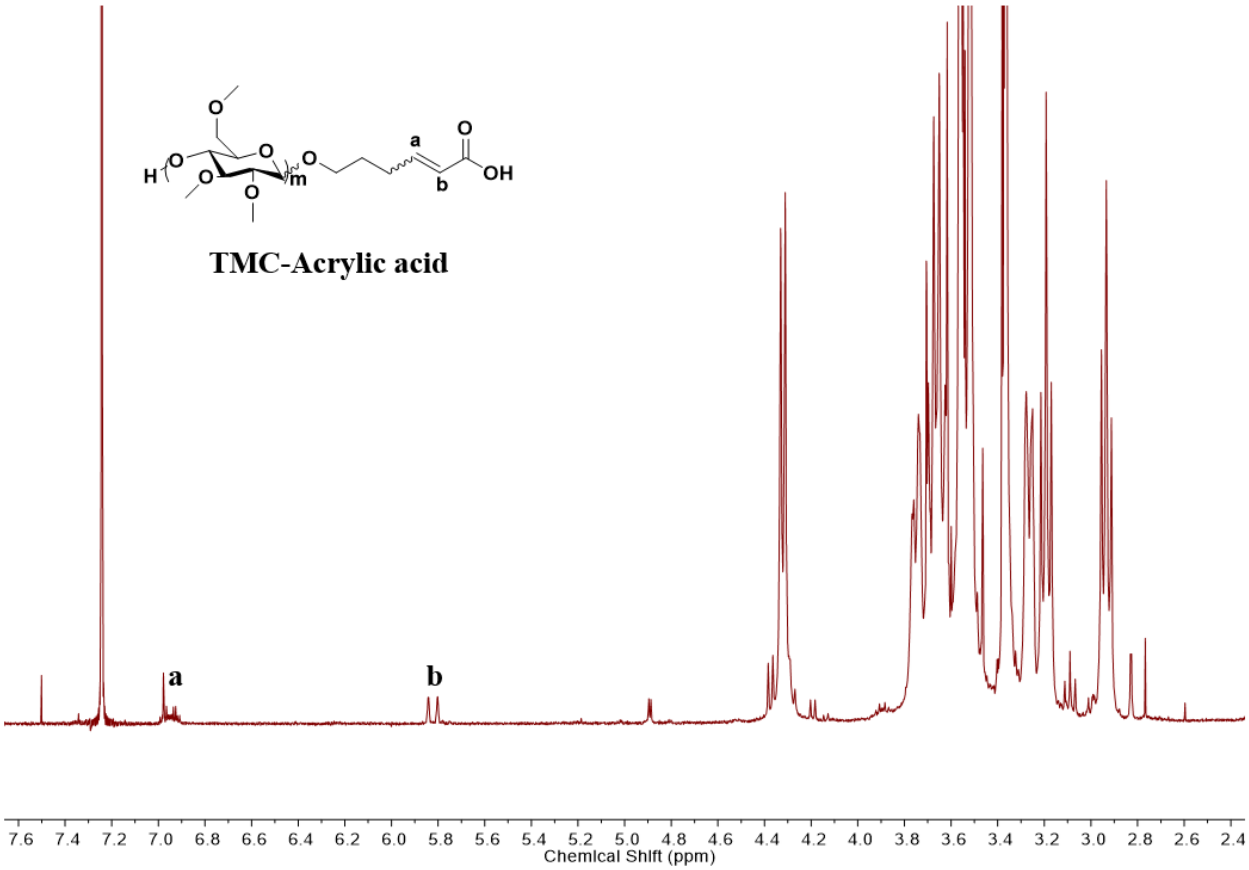

Figure S4. ^{1}H NMR spectrum of TMC-Acrylic acid

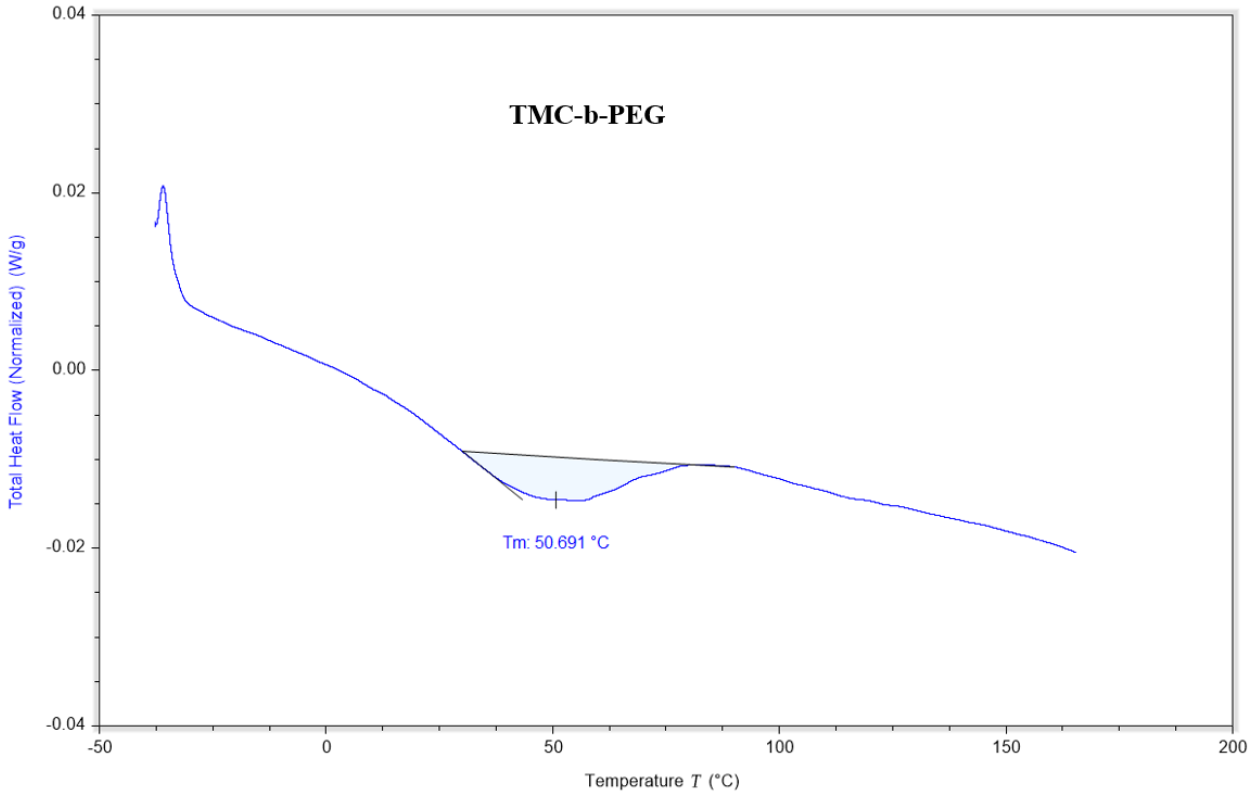

Figure S5. Modulated DSC trace (total heat flow) of TMC-*b*-PEG

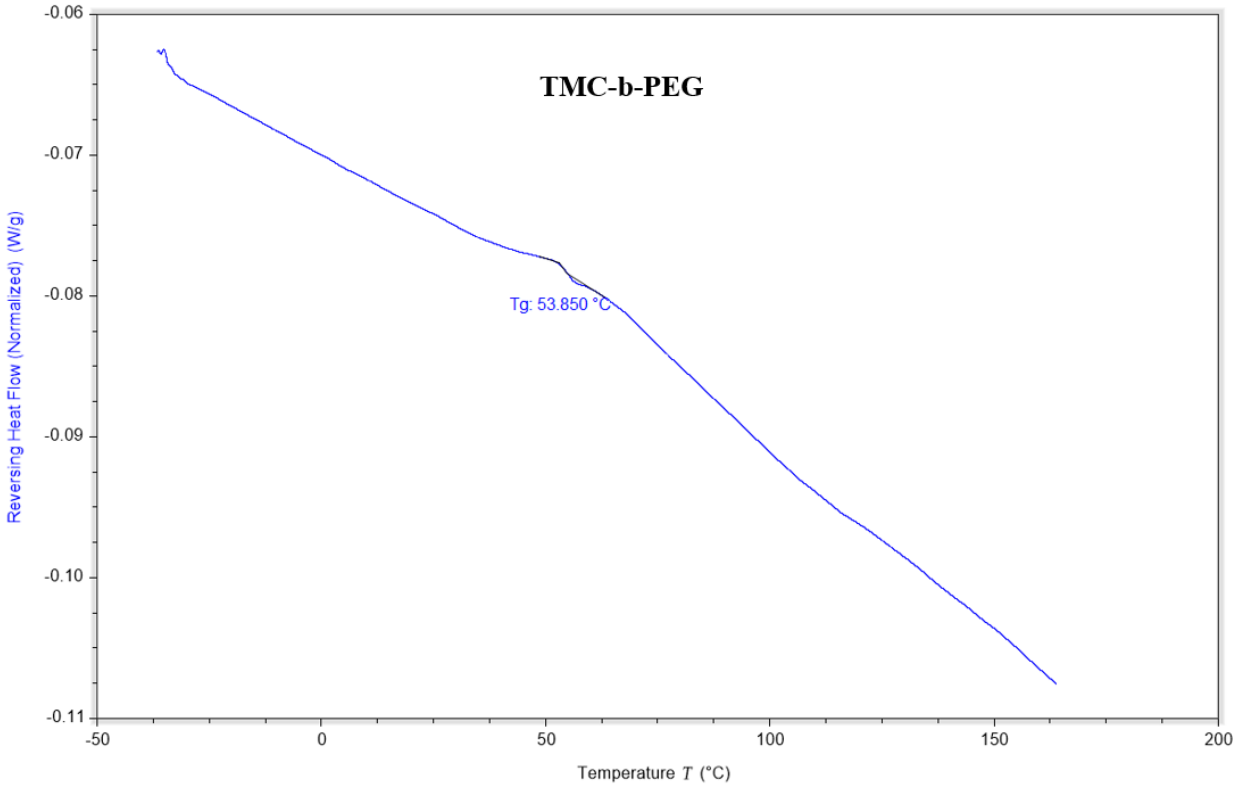

Figure S6. Modulated DSC trace (reversing heat flow) of TMC-*b*-PEG

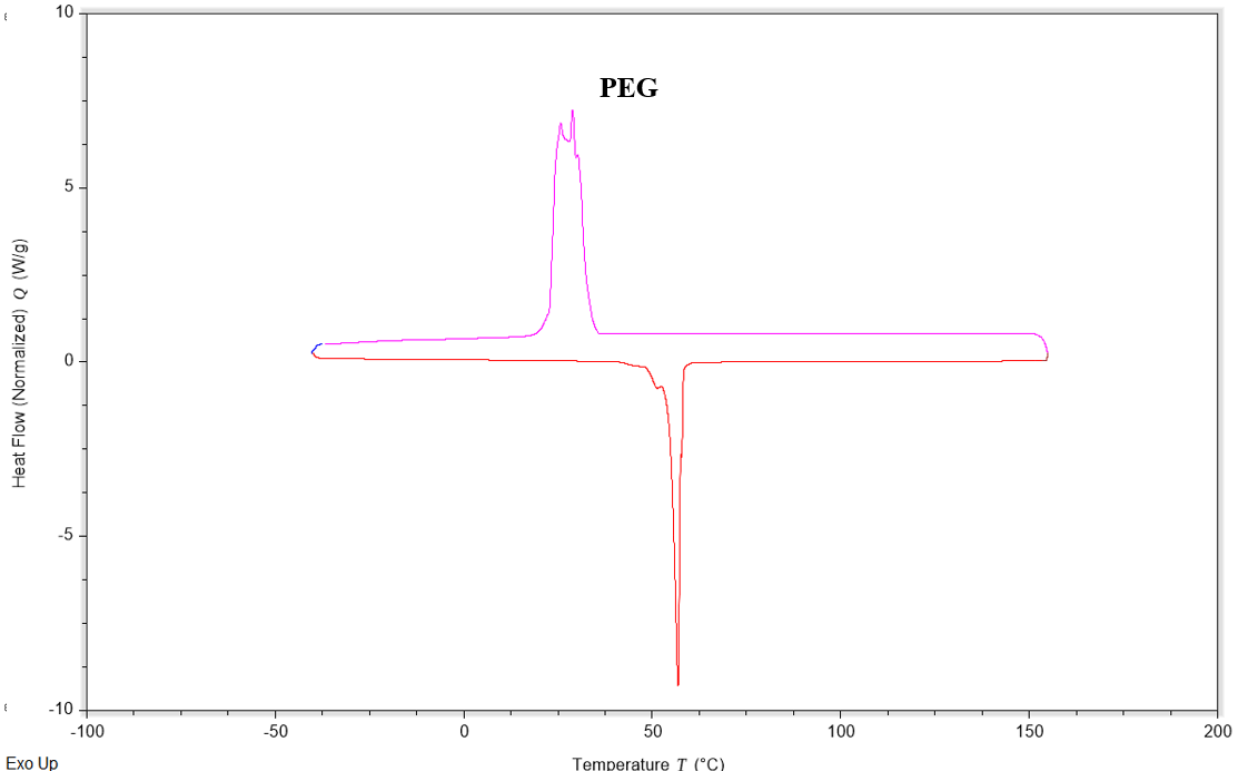

Figure S7. Conventional DSC trace of PEG

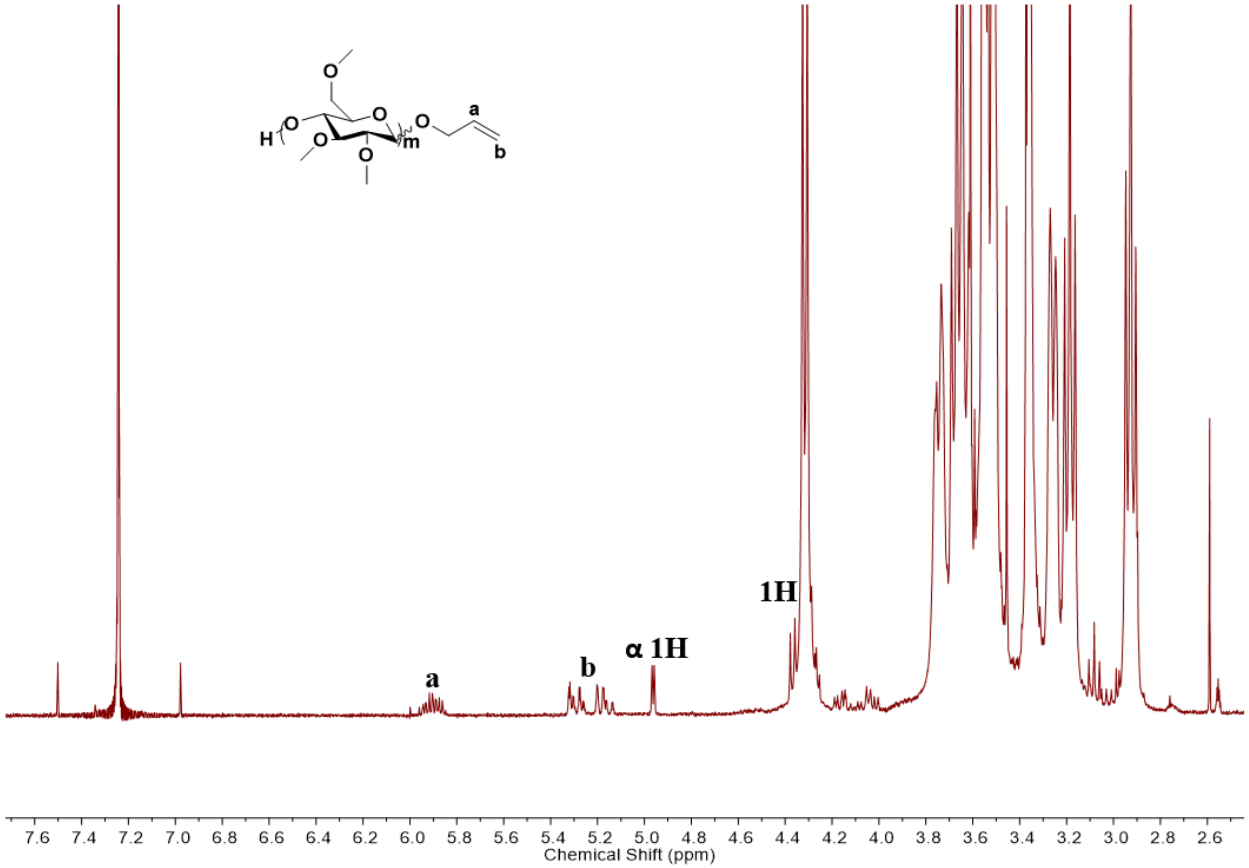

Figure S8. ^{1}H NMR spectrum of TMC-C3

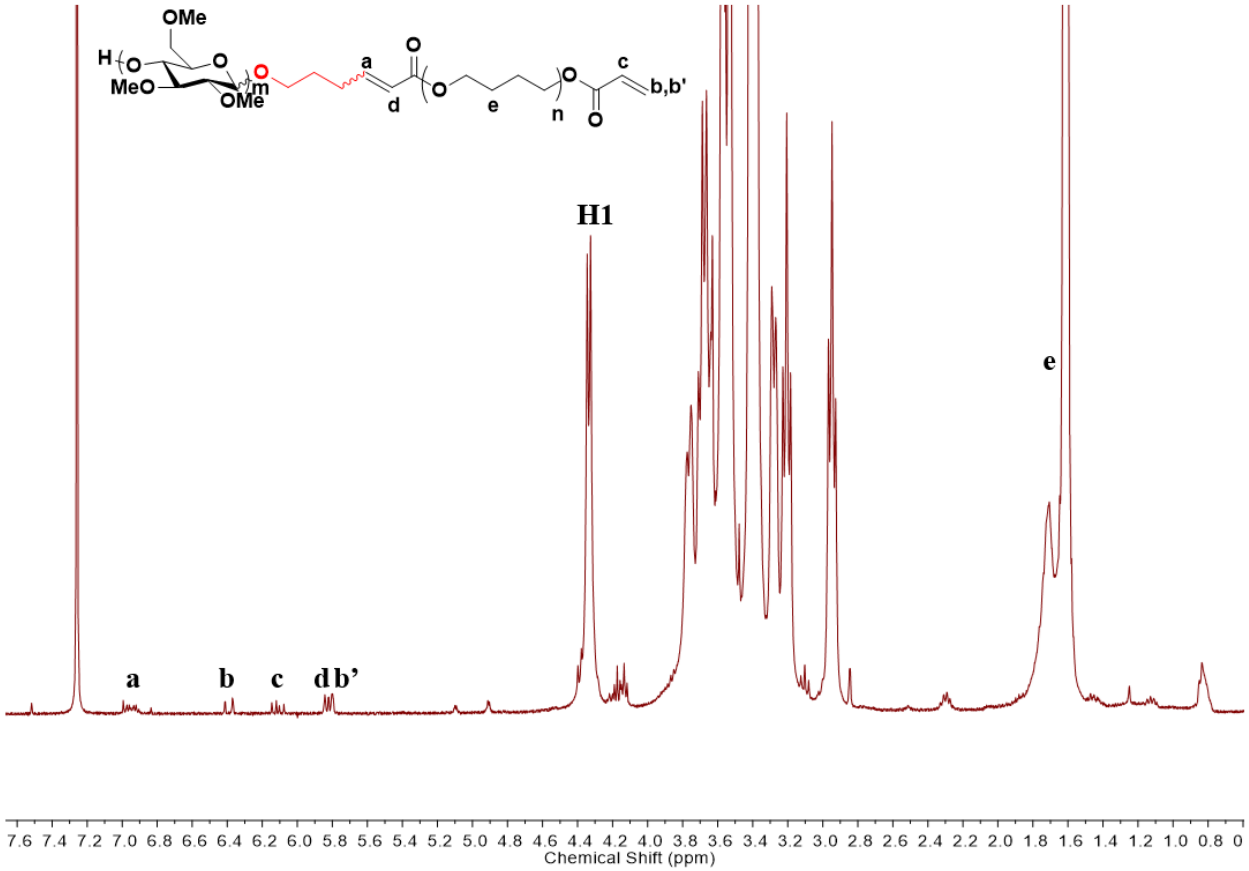

Figure S9. ^{1}H NMR spectrum of TMC-*b*-PTHF

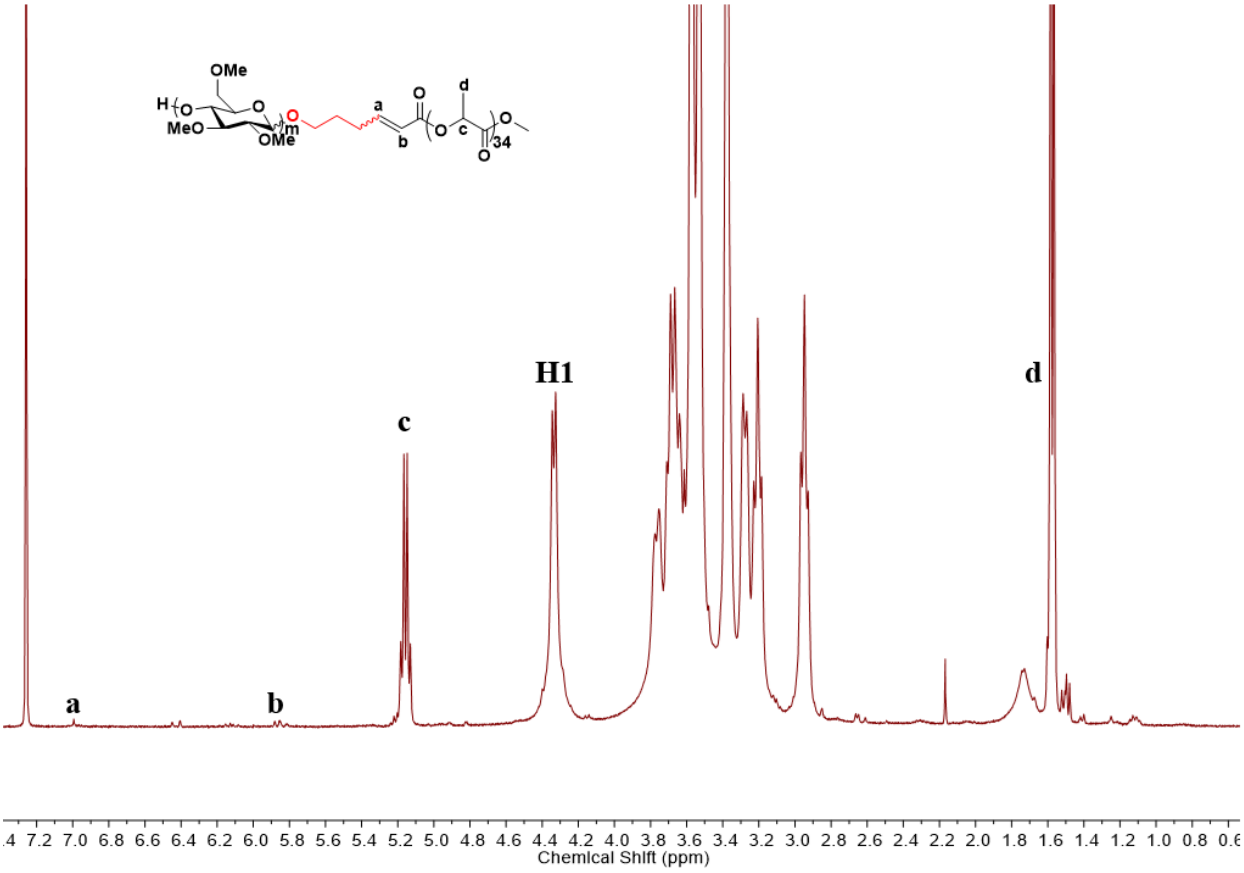

Figure S10. ^{1}H NMR spectrum of TMC-*b*-PLA

Figure S11 FT-IR spectrum of TMC

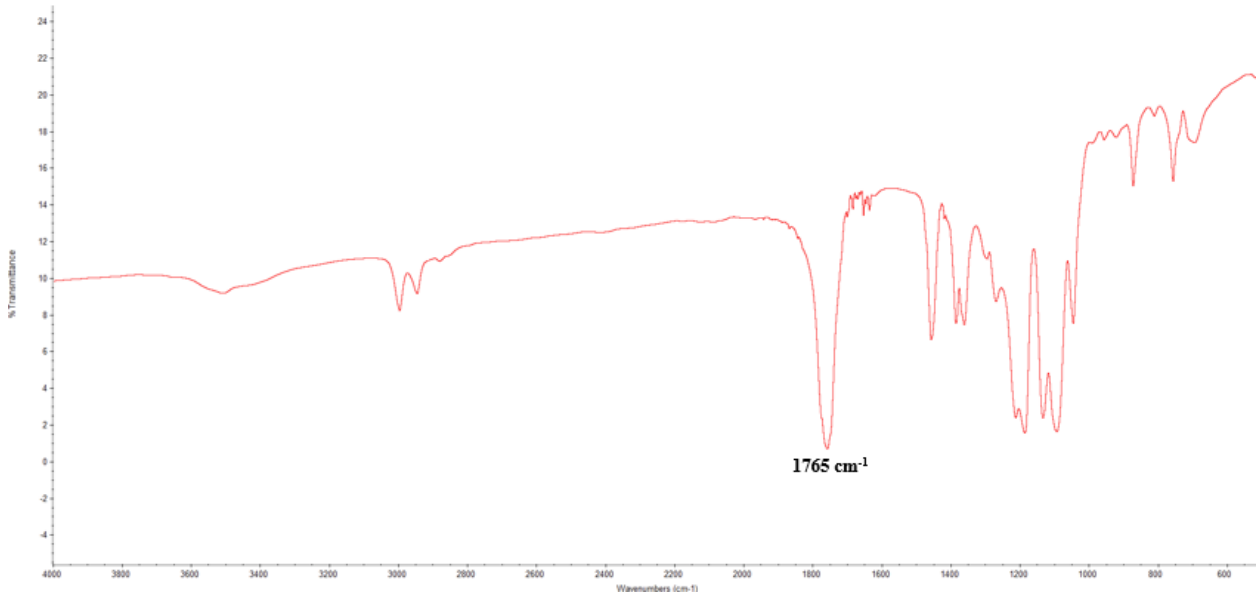

Figure S12 FT-IR spectrum of acrylate terminated PLA

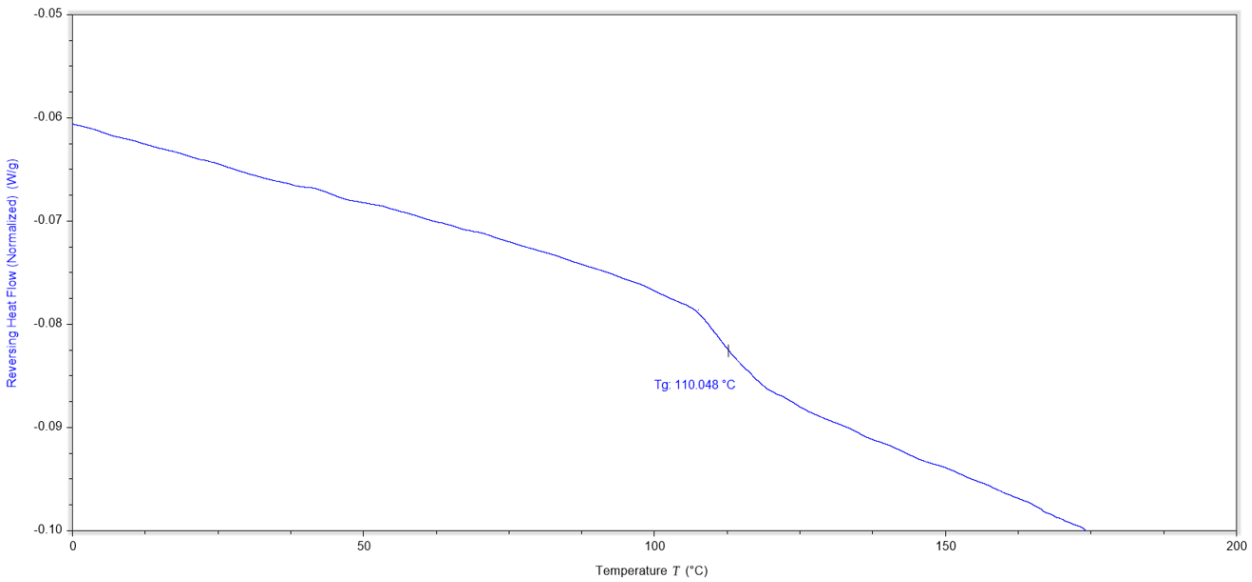

Figure S13. Modulated DSC trace (reversing heat flow) of TMC.

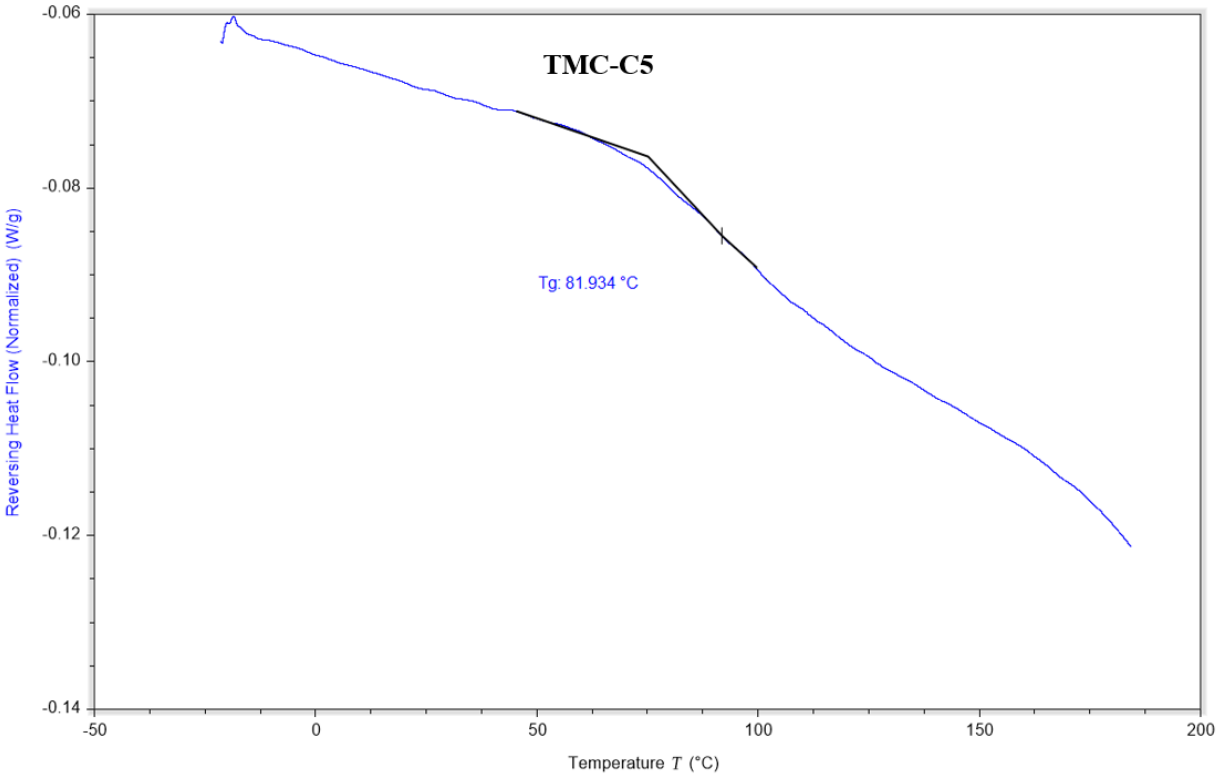

Figure S14. Modulated DSC trace (reversing heat flow) of TMC-C5

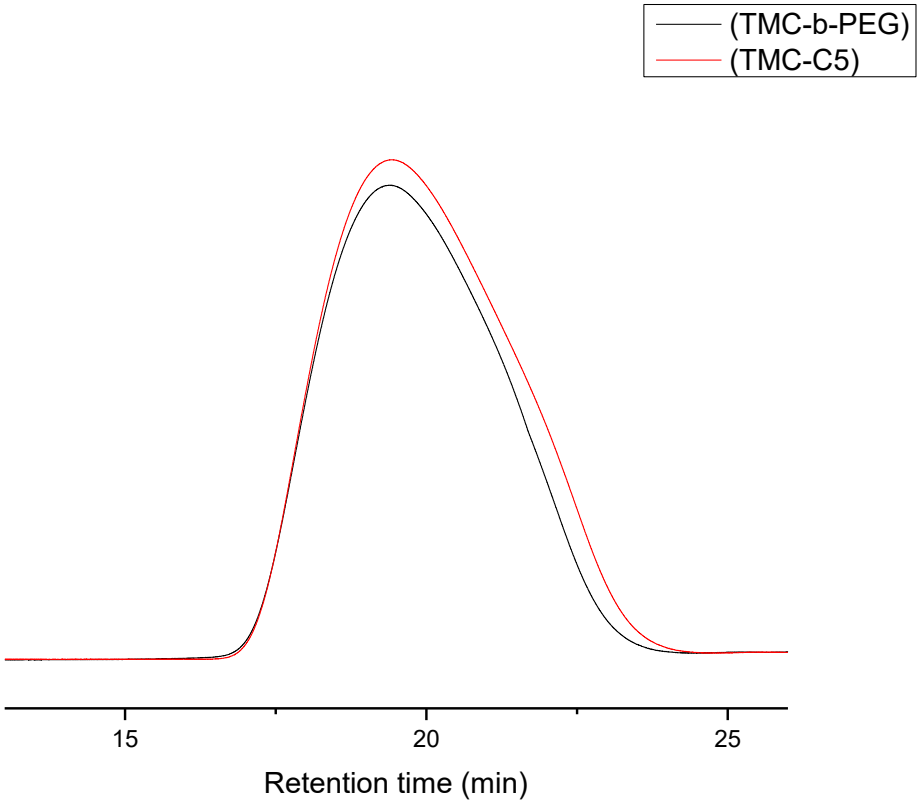

Figure S15. SEC traces (RI detector) of TMC-b-PEG (black) and TMC-C5 (Red).

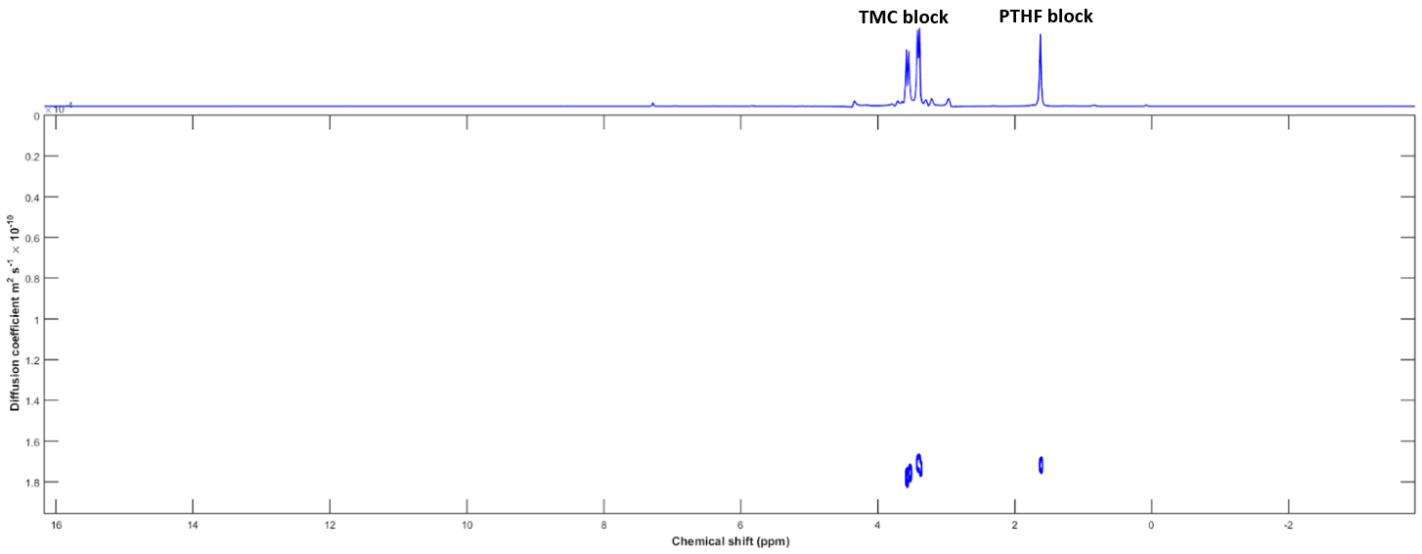

Figure S16. Diffusion-ordered spectroscopy (DOSY) NMR of TMC-*b*-PTHF

Chapter 4: **Regioselective bromination of the dextran non-reducing end creates a pathway to dextran-based block copolymers**

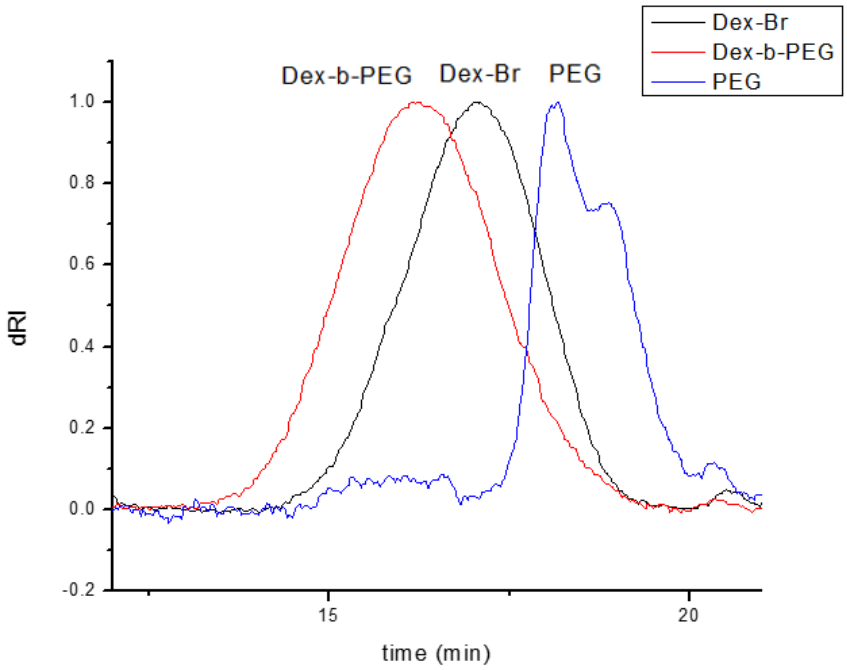

Figure S1. SEC traces of Dextran-*b*-PEG, Dex-Br and PEG-amine.

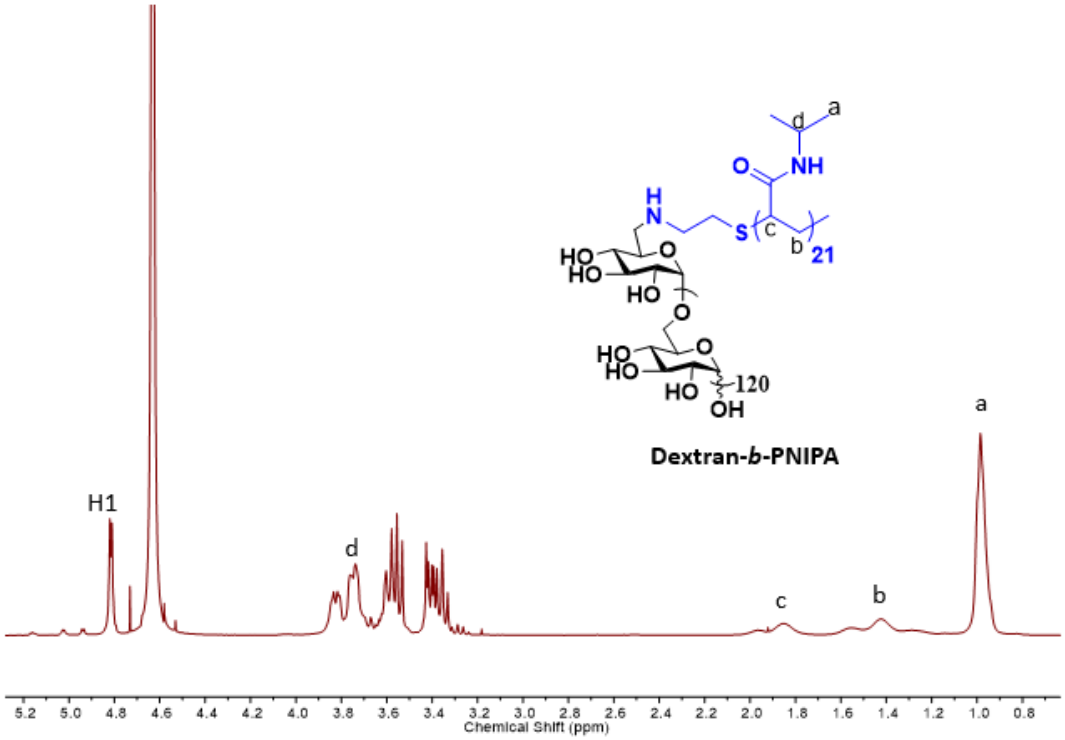

Figure S2. ^{1}H NMR spectrum of Dextran-*b*-PNIPA in D_2O.

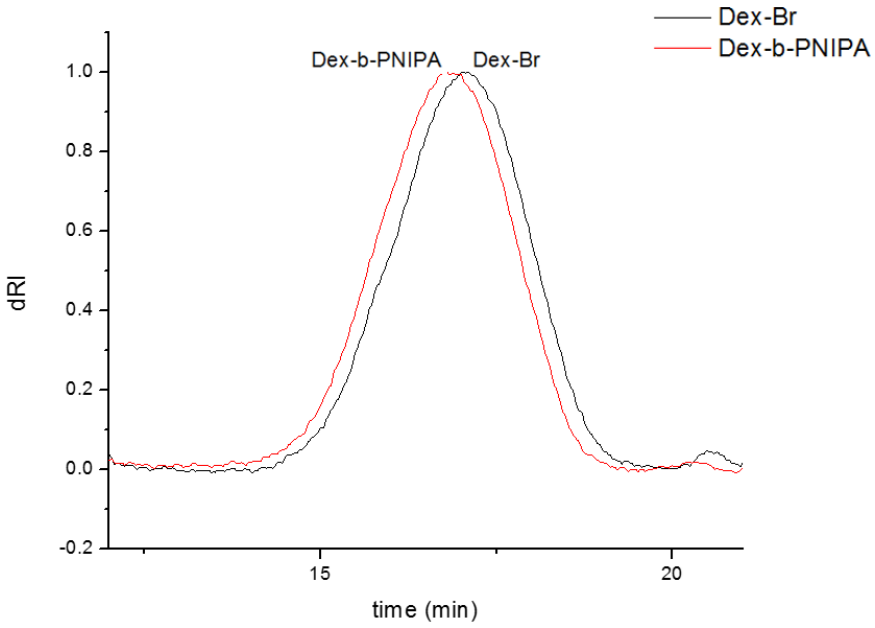

Figure S3. SEC traces of Dextran-*b*-PNIPA and Dex-Br.

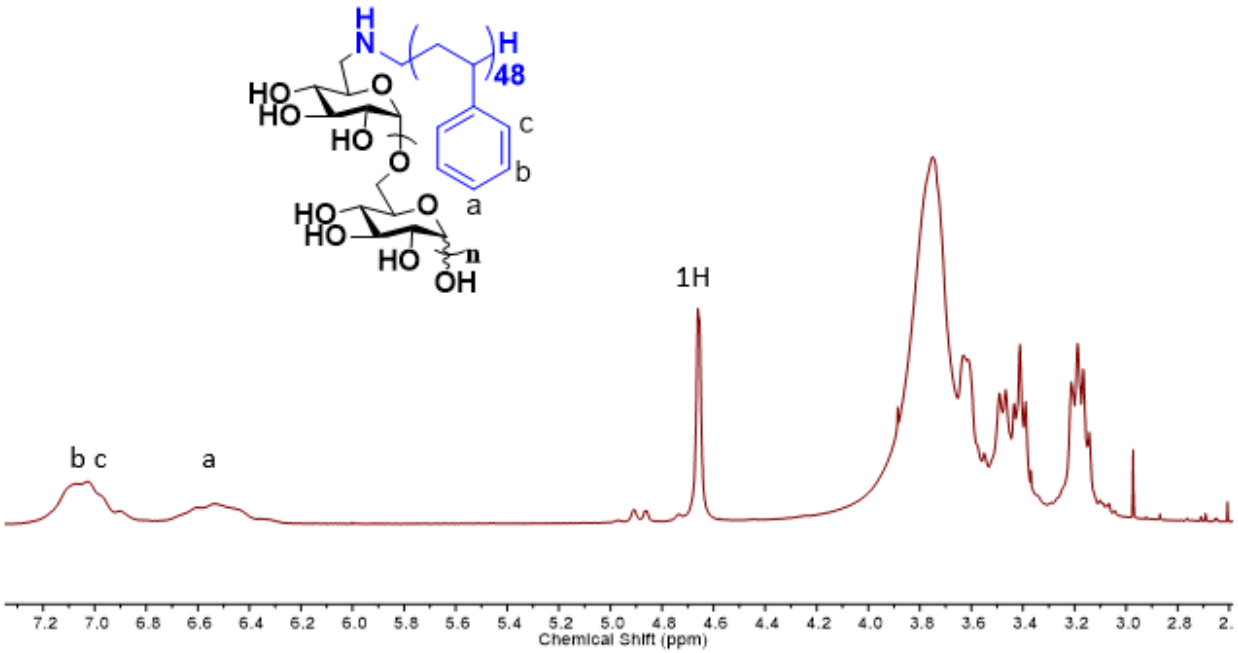

Figure S4. ^{1}H NMR spectrum of Dextran-*b*-PS in deuterated DMSO.

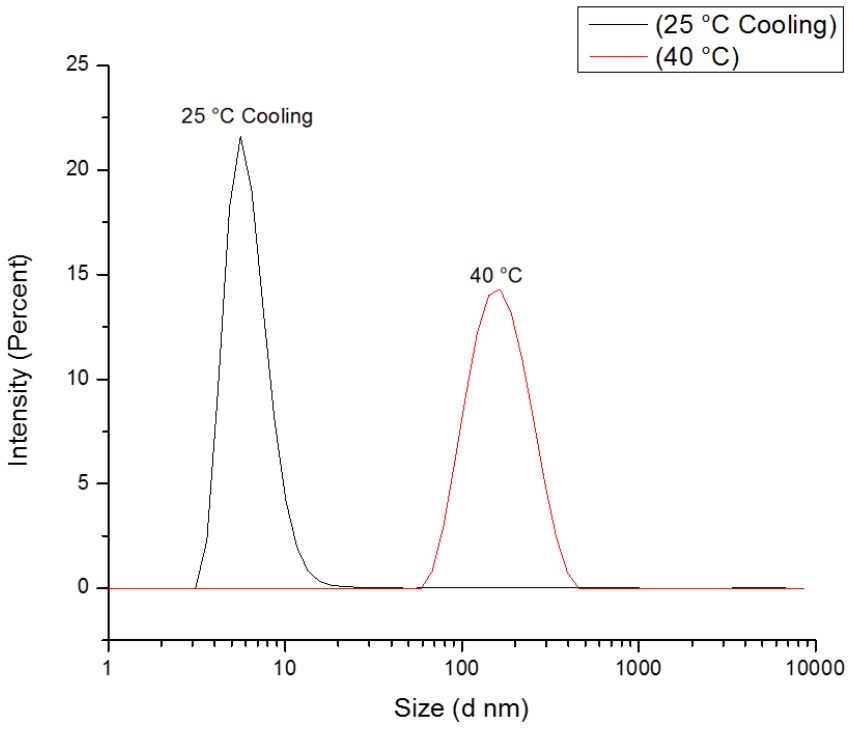

Figure S5. DLS profile of Dextran-*b*-PNIPA at 40 °C and 25 °C (Cooling).

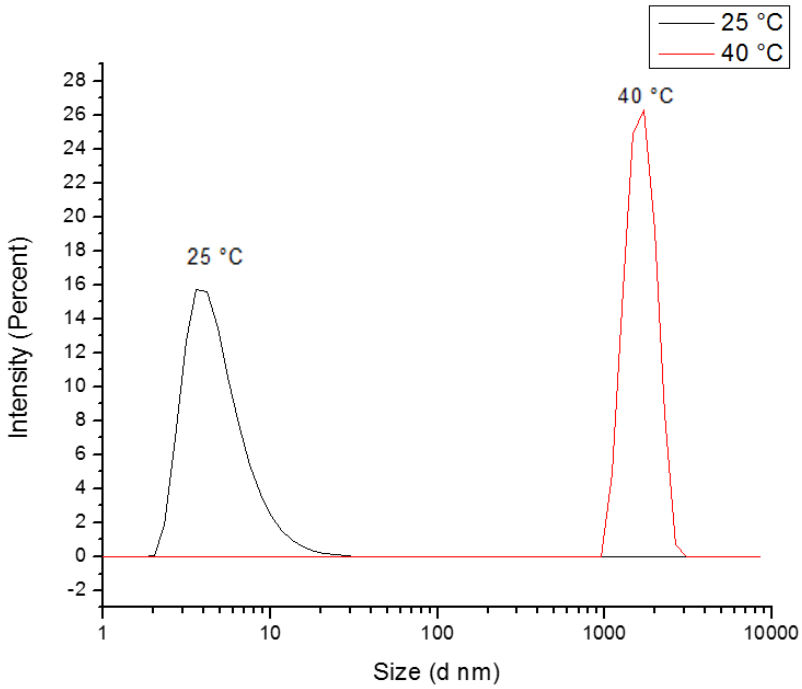

Figure S6. DLS profile of PNIPA at 25 °C and 40 °C.

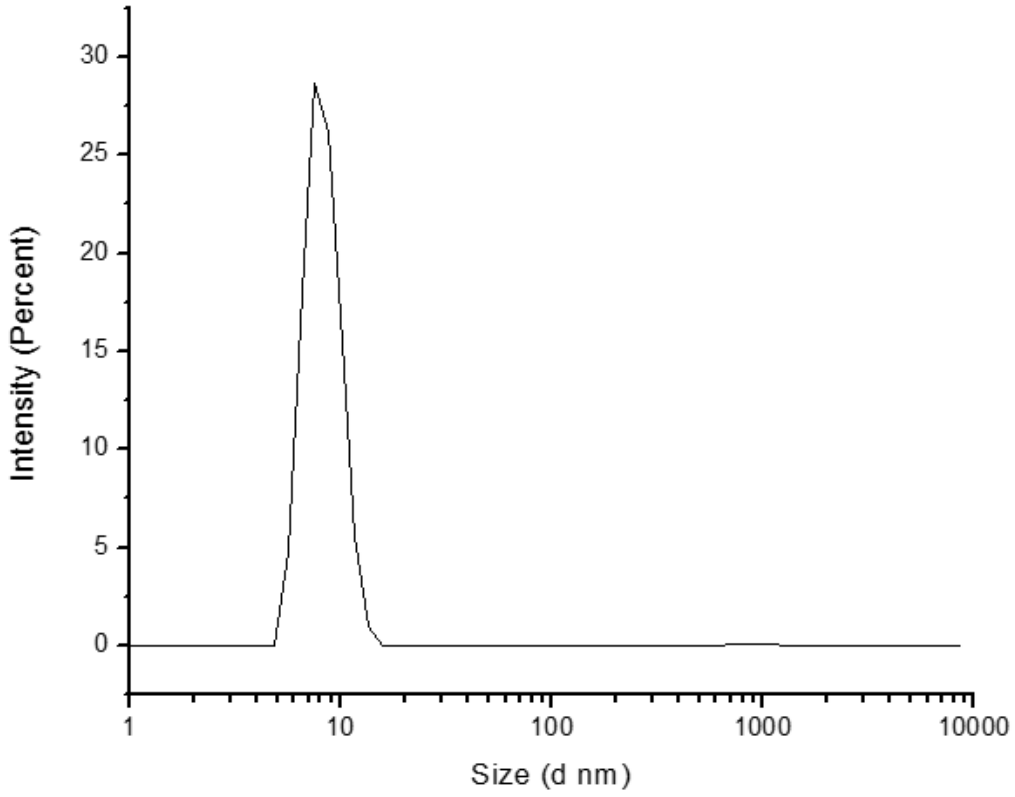

Figure S7. DLS profile of Dextran-Br at 25 °C

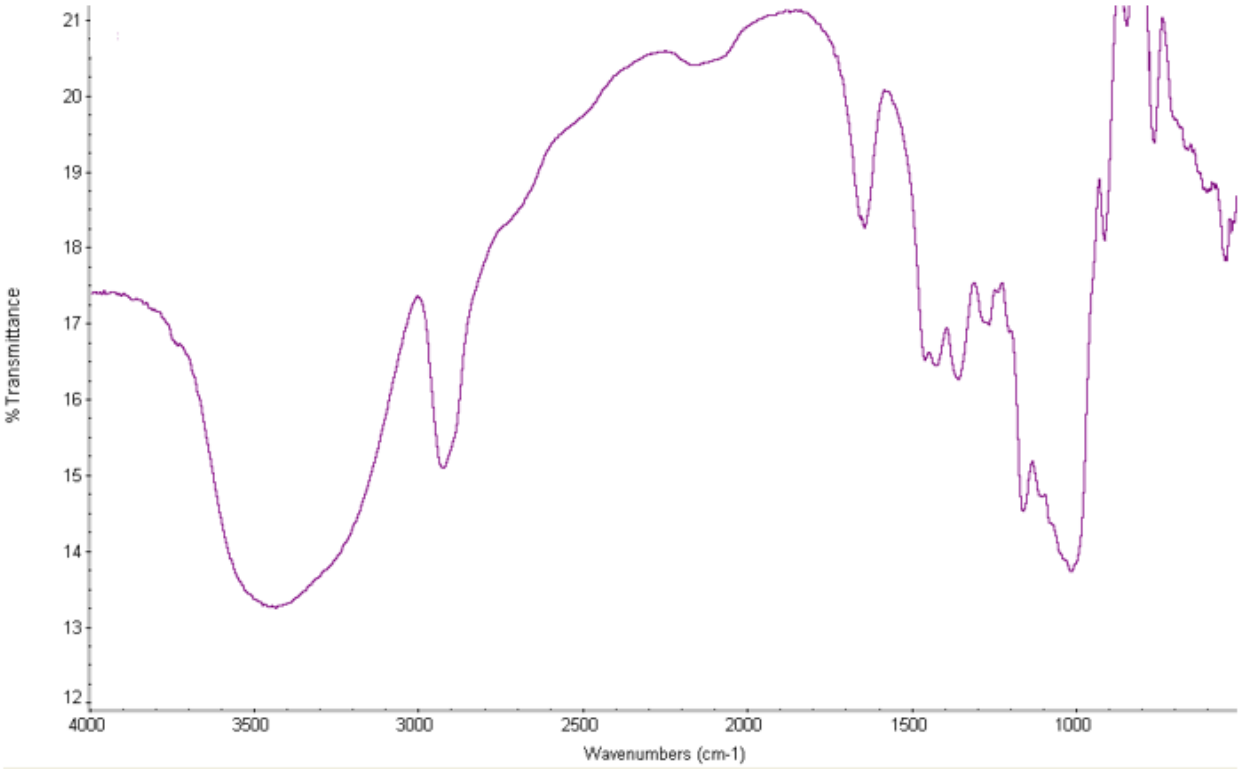

Figure S8. FT-IR spectrum of Dex-Br

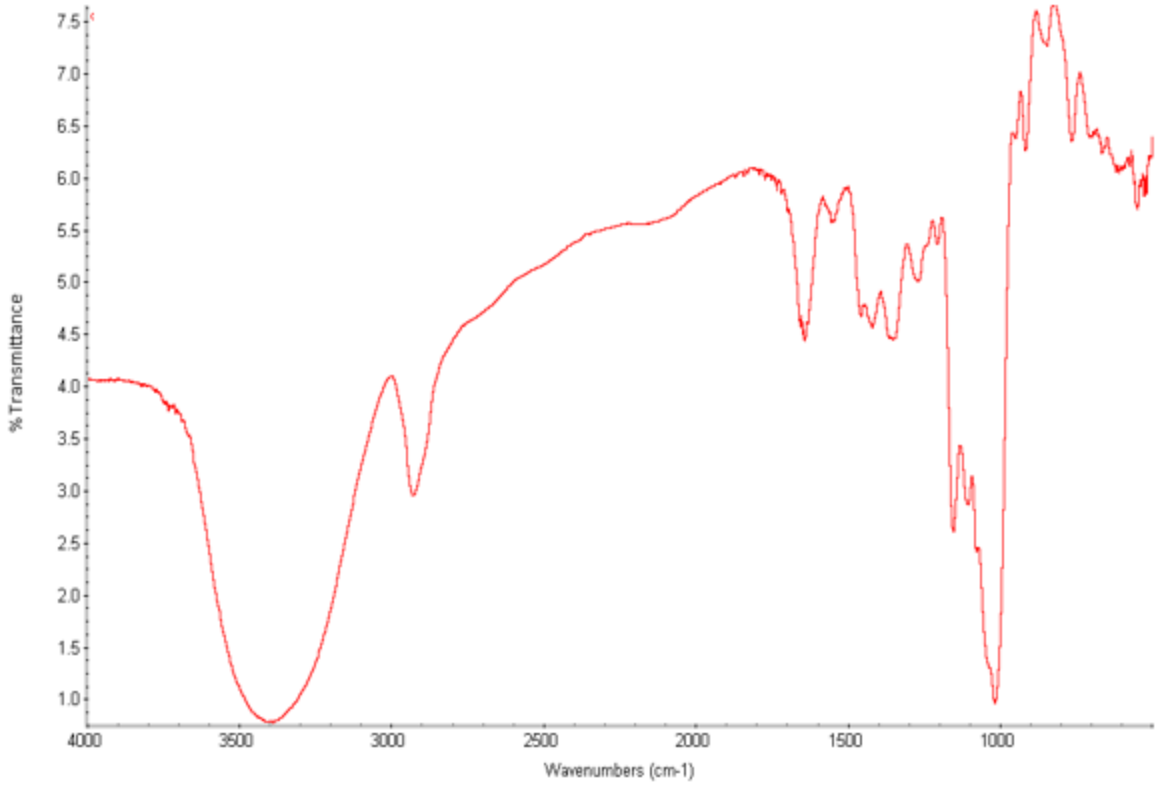

Figure S9. FT-IR spectrum of Dextran-*b*-PNIPA

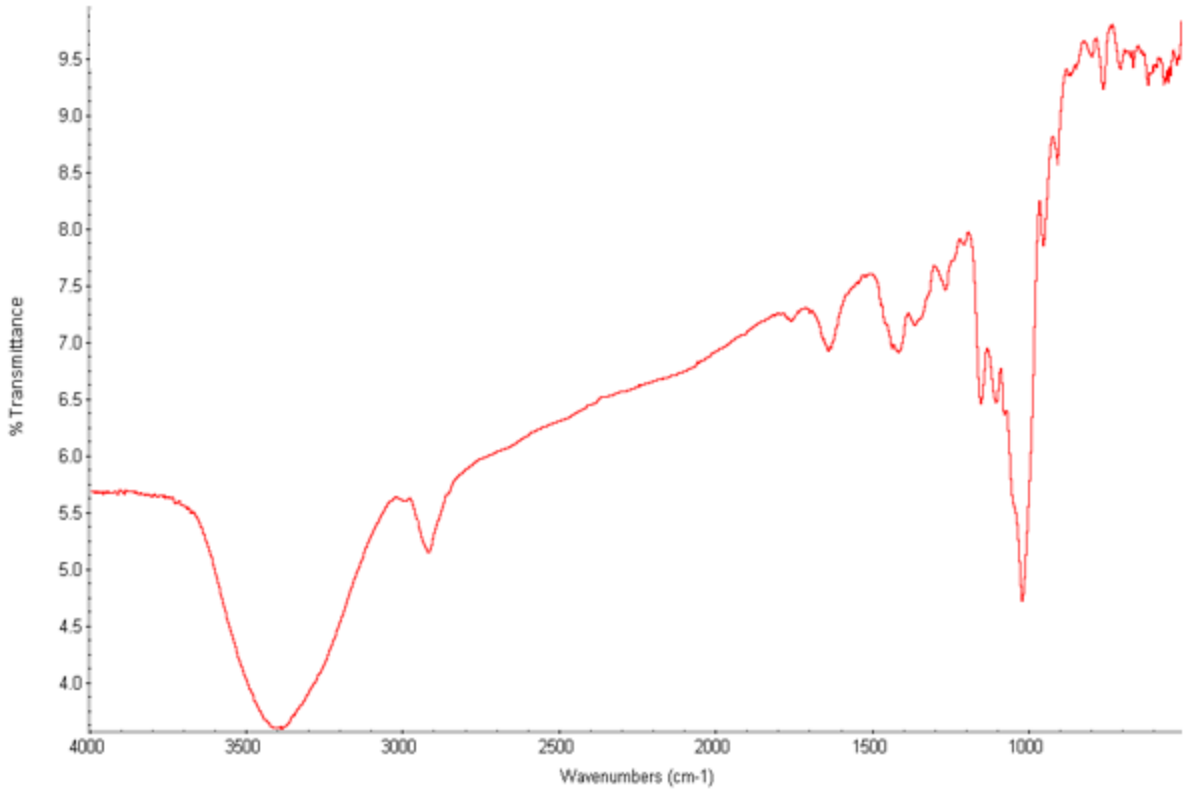

Figure S10. FT-IR spectrum of Dextran-*b*-PEG

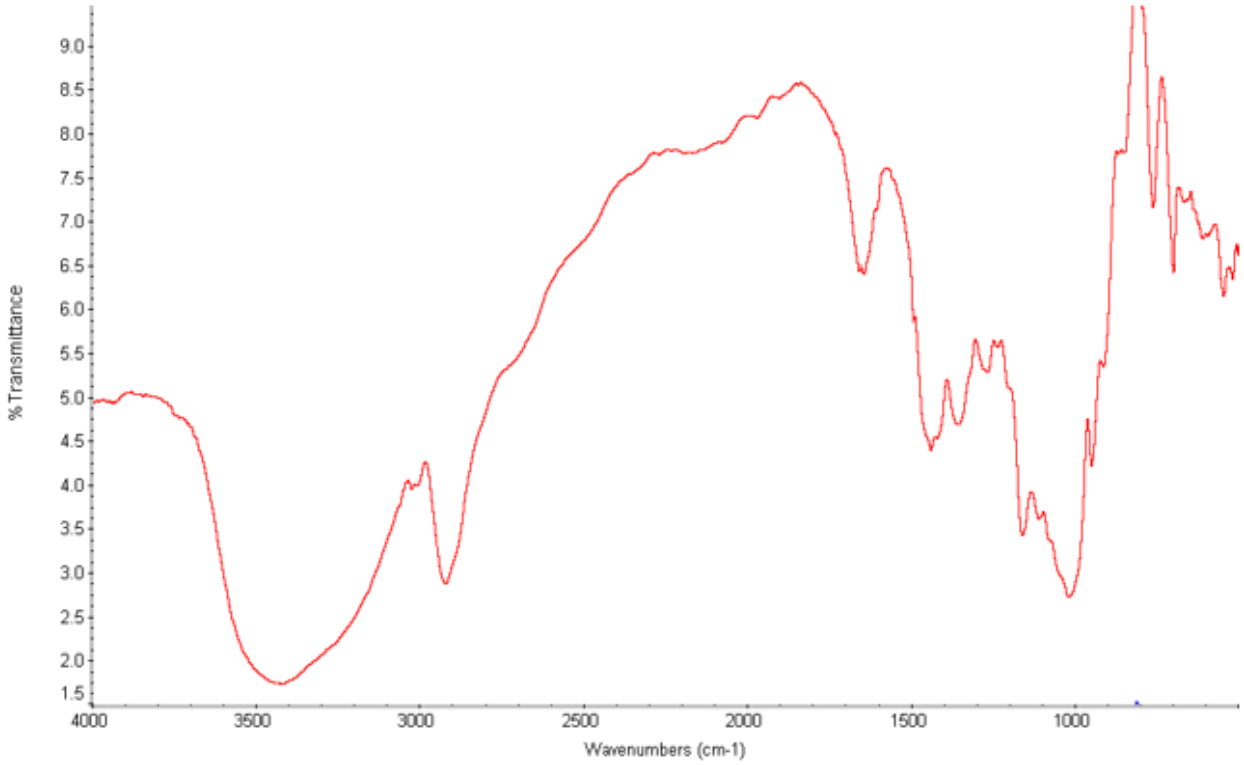

Figure S11. FT-IR spectrum of Dextran-*b*-PS

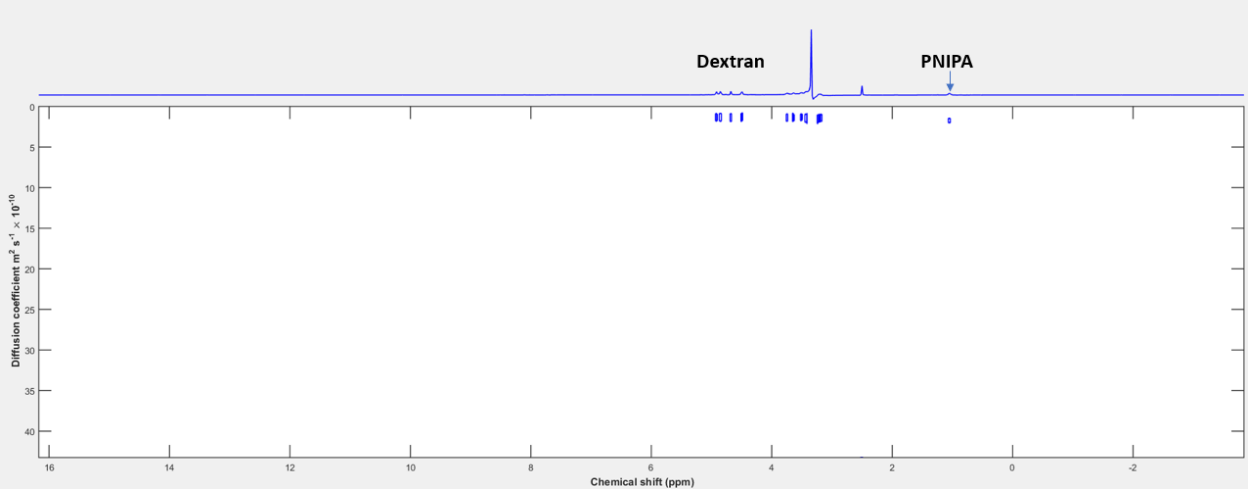

Figure S12. DOSY NMR of Dextran-*b*-PNIPA

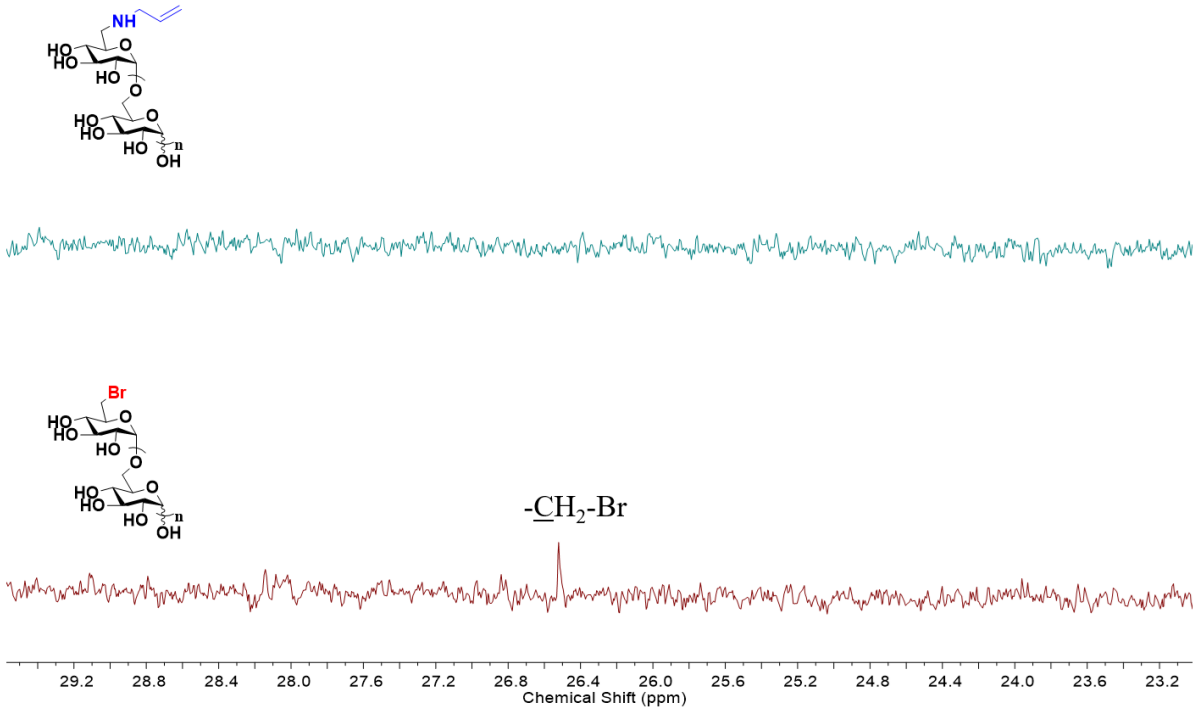

Figure S13. ^{13}C NMR spectra of dextran-Br and dextran-*N*Allyl.

Solubility Parameter Calculation

The solubility parameters were calculated by the Fedors method[1] and using a similar procedure reported by Babcock et al.[2] It considers the energy of vaporization and molar volume for the diverse chemical features.

For compounds with T_g and T_m above room temperature an additional correction must be applied to account for differences in the molar volume (Equation S1 and S2). In these equations, n is the number of main chain skeletal atoms in the smallest repeating unit 1. dextran has a value of n equal to 7 (6 atoms in the ring and the oxygen that will be bonded to the adjacent monomer). Therefore, Equation S2 is used for the molar volume correction.

$\Delta V = 4n, n < 3$ Equation S1

$\Delta V = 2n, n \geq 3$ Equation S2

To calculate the solubility parameter for dextran the structure is divided in 3: initial, middle, and end monomer, and the dextran polymer has a total of 58 repeating units. Hence, the middle type of monomer is repeated 56 times, the initial one has the substitution (OH, PEG, PNIPA, or PS), and the final group will have a hydroxyl group. Some of the groups are constant for dextran polymers including: 1 ring closure, 5 -CH, 1 -CH_2, 2 –O–, and 3 OH, therefore these groups are present in initial, middle and end monomer. In contrast, some of the substituent in the initial monomer changes depending on the polymer type, and the final monomer will have a hydroxyl group. For example, Table S1 shows the groups for the polymer Dex-b-PS, which are used for the calculation of the solubility parameter.

Table S1. Groups for Dex-*b*-PS polymer.

Group	**Number of groups**		
	a (Middle monomer) Repeated 56 times	**b (Initial monomer)**	**c (end monomer)**
Multiplier	(1/58)*56	(1/58)*1	(1/58)*1
-CH_3	0	1	0
-CH_2	1	1+1+48	1
-CH	5	5+48	5
Ring closure	1	1	1
-OH	3	3	4
-O-	2	1	2
-NH	0	1	0
-Phenyl	0	48	0

Table S2. Hildebrand solubility parameters of the polymers

Polymers	**Solubility parameter ($MPa^{1/2}$)**
Dextran	31.4[3]
PEG	20.8[4]
PNIPA	23.5[5]
PS	18.3[6]

Table S3. Fedor's solubility parameters of the polymers

Polymers	Solubility parameter ($MPa^{1/2}$)
Dextran	39.01
Dextran-*b*-PEG	30.74
Dextran-*b*-PS	31.69
Dextran-*b*-PNIPA	35.08

References

(1) Fedors, R. F. A Method for Estimating Both the Solubility Parameters and Molar Volumes of Liquids. *Polym. Eng. Sci.* **1974**, *14* (2), 147–154. https://doi.org/10.1002/pen.760140211.

(2) Pharmaceutical Compositions with Enhanced Performance. **2005**.

(3) Güner, A. The Algorithmic Calculations of Solubility Parameter for the Determination of Interactions in Dextran/Certain Polar Solvent Systems. *Eur. Polym. J.* **2004**, *40* (7), 1587–1594. https://doi.org/10.1016/J.EURPOLYMJ.2003.10.030.

(4) Adamska, K.; Voelkel, A. Hansen Solubility Parameters for Polyethylene Glycols by Inverse Gas Chromatography. *J. Chromatogr. A* **2006**, *1132* (1–2), 260–267. https://doi.org/10.1016/j.chroma.2006.07.066.

(5) Yagi, Y.; Inomata, H.; Saito, S. Solubility Parameter of an N-Isopropylacrylamide Gel. *Macromolecules* **1992**, *25* (11), 2997–2998. https://doi.org/10.1021/ma00037a034.

(6) Mieczkowski, R. The Determination of the Solubility Parameter Components of Polystyrene by Partial Specific Volume Measurements. *Eur. Polym. J.* **1988**, *24* (12), 1185–1189. https://doi.org/10.1016/0014-3057(88)90109-7.

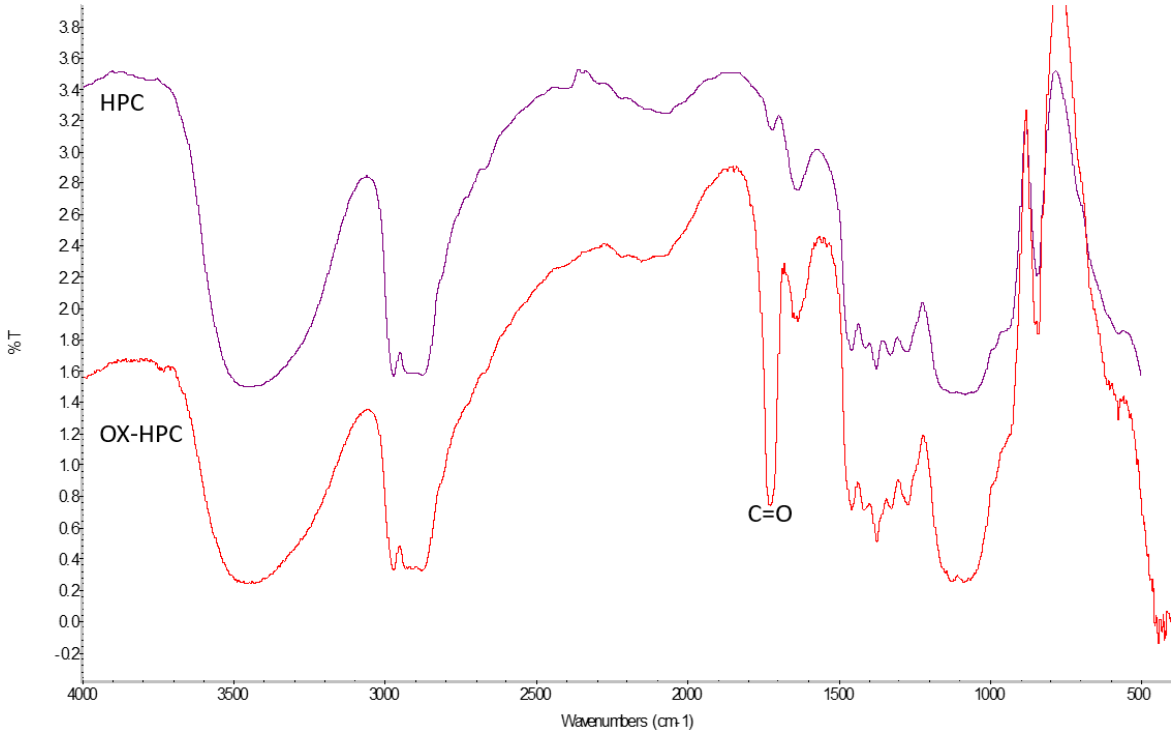

Figure S1. FTIR spectra of HPC and OX-HPC.

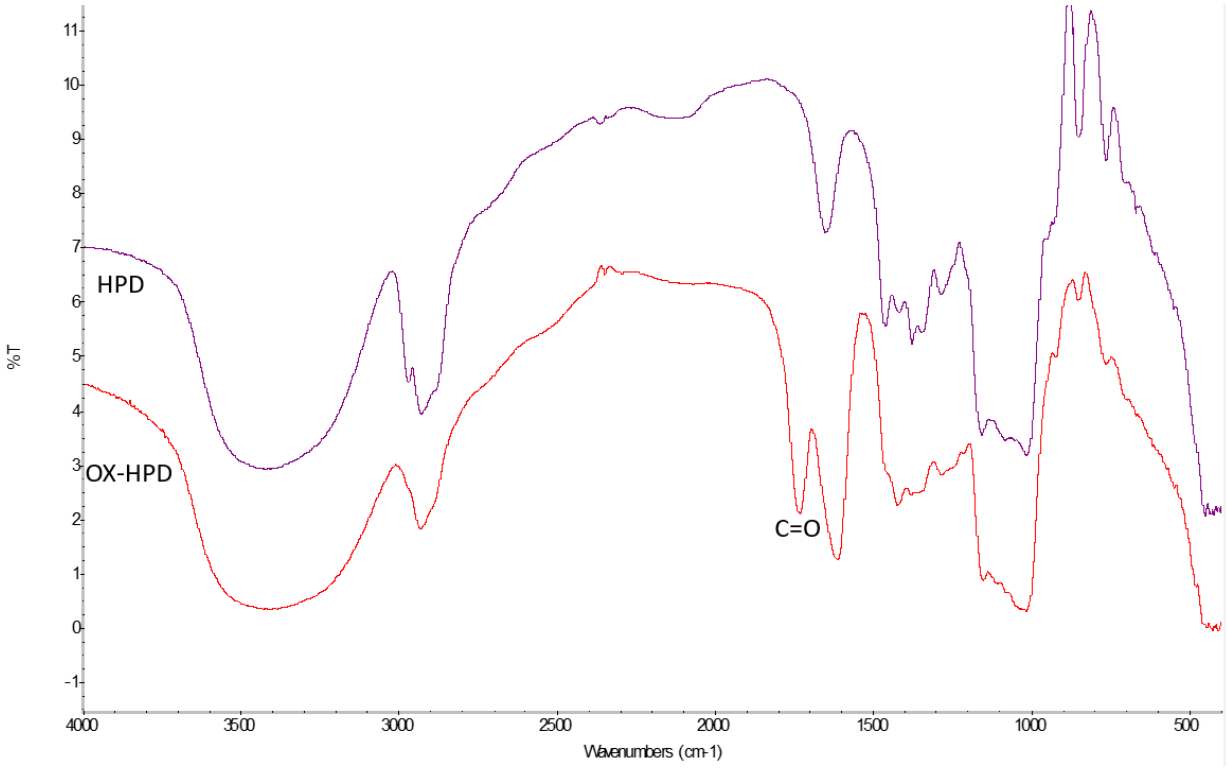

Figure S2. FTIR spectra of HPD and OX-HPD.

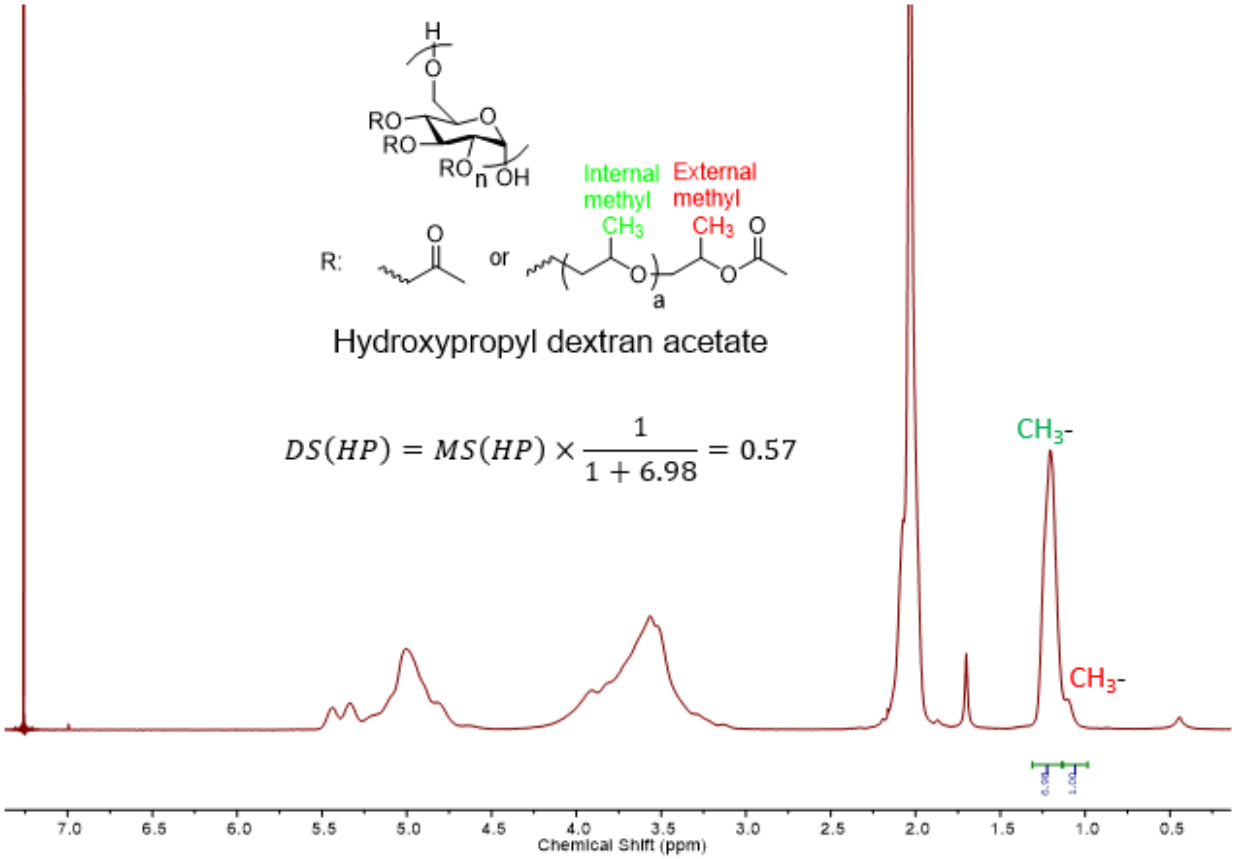

Figure S3. ^{1}H NMR spectra of hydroxypropyl dextran acetate.

The DS was determined by acetylation of HPD with acetic anhydride, where the methyl group at the terminal hydroxyl propyl group is shifted upfield due to the nearby acetyl group. The integration of two methyl peaks, from terminal methyl and internal methyl, were used to calculate the DS of HPD.

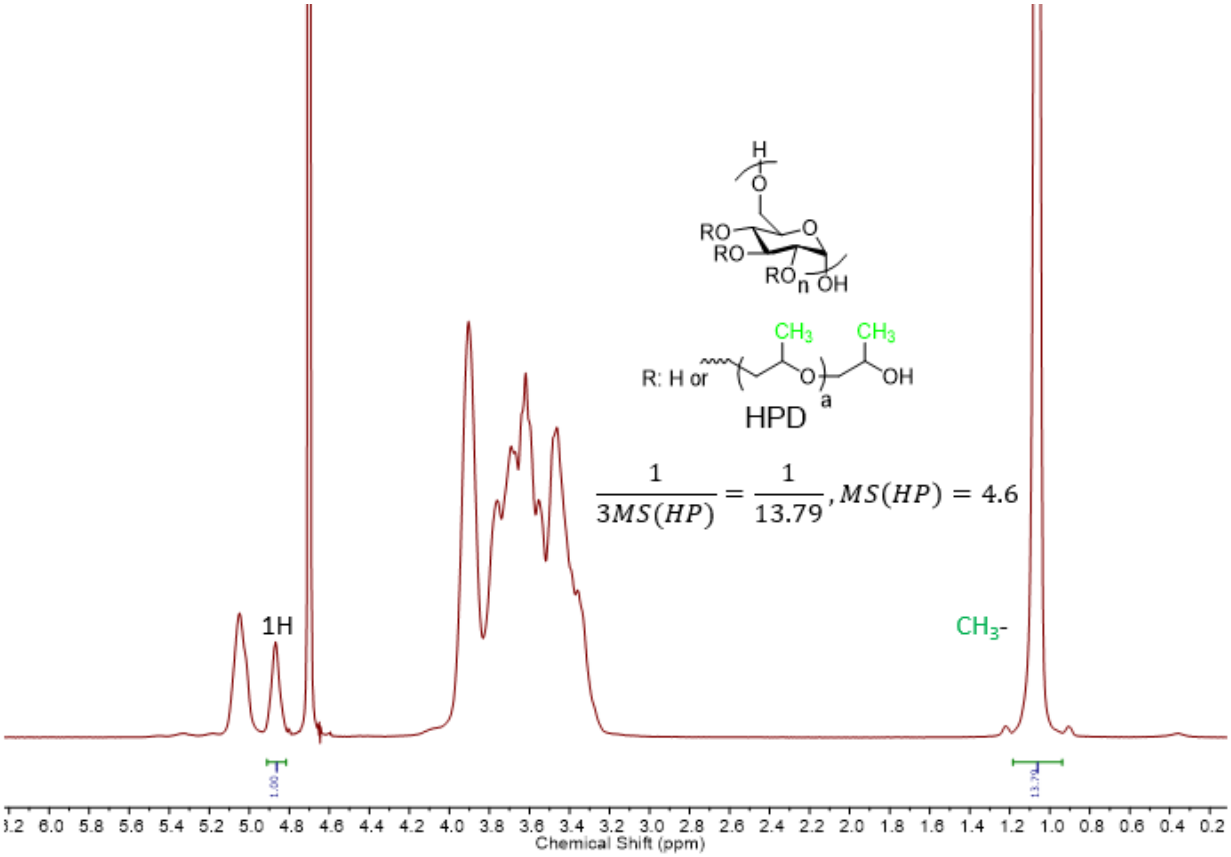

Figure S4. ^{1}H NMR spectrum of HPD

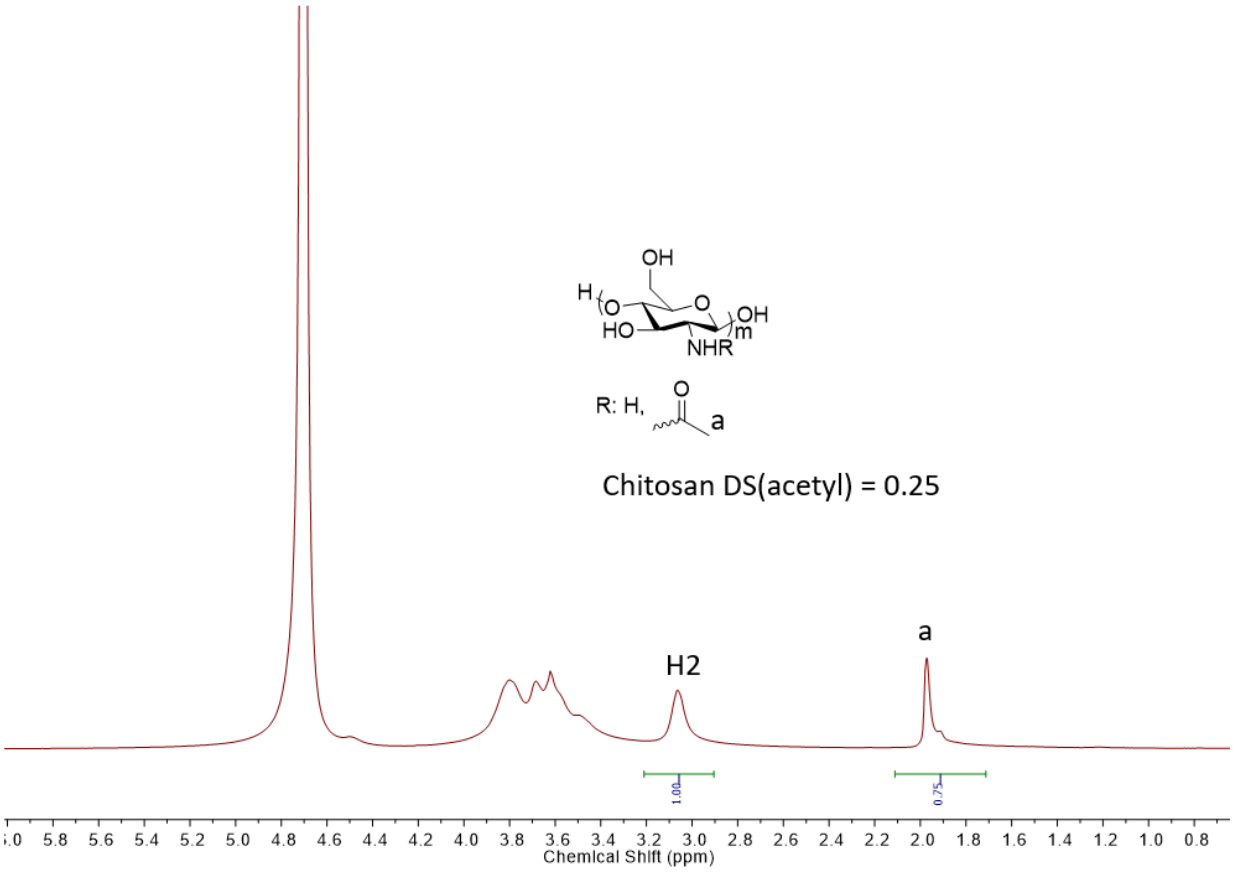

Figure S5. ^{1}H NMR spectrum of chitosan

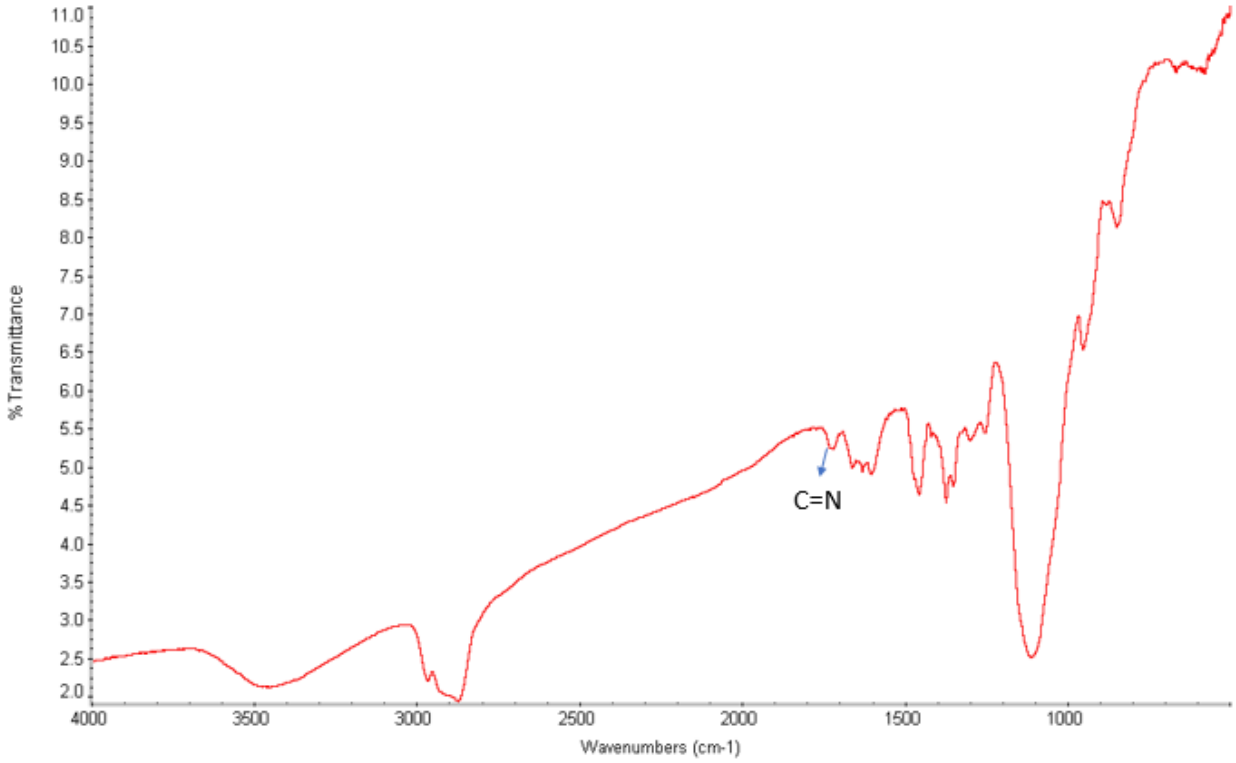

Figure S2. FT-IR spectrum of Jeffamine 600 – OX HPC hydrogel

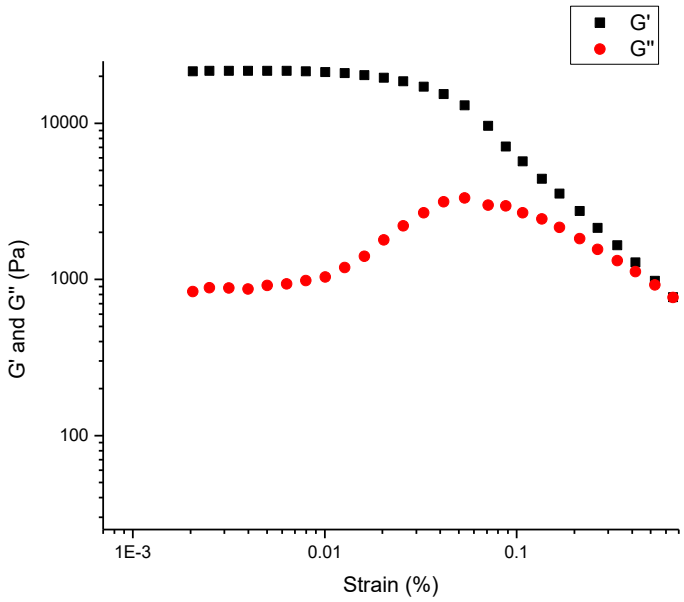

Figure S3. Strain sweep of OX-HPC-Jeffamine (600 g/mol) hydrogel with 0.5 Hz frequency.

Figure S4. Dissolution of HPC/Jeffamine mixture in water.

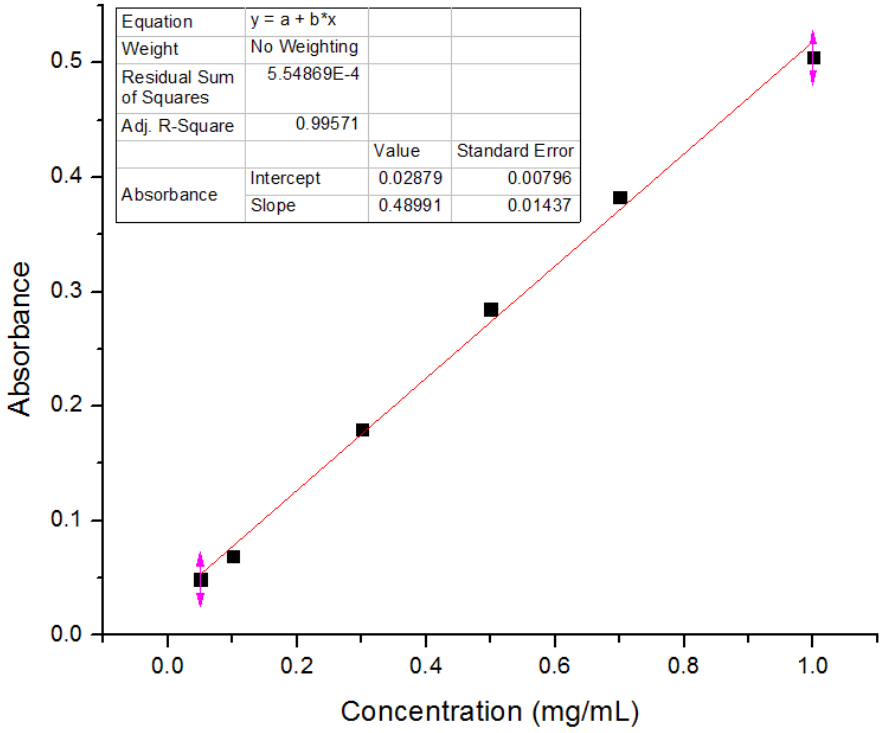

Figure S5. Calibration curve of phenylalanine.

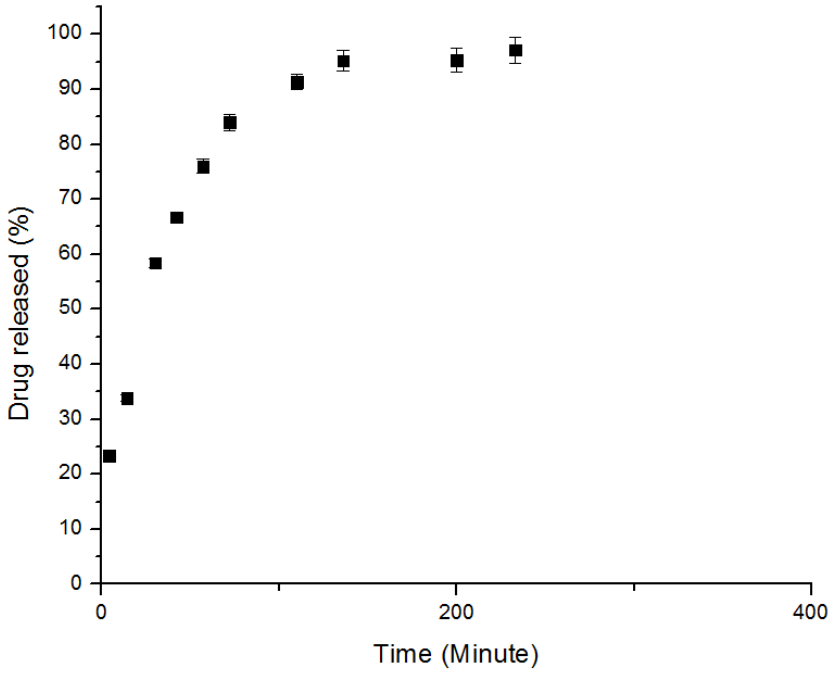

Figure S6. Phenylalanine release from HPC/Jeffamine mixture at 25 °C.

Table S1. Swelling ratio (SR) of OX-HPC/Jeffamine hydrogels.

Hydrogel Sample	SR
OX-HPC/Jeffamine (600 g/mol)	17.1
OX-HPC/Jeffamine (900 g/mol)	18.6
OX-HPC/Jeffamine(1900 g/mol)	20.0